Phenylvinylcobalamin: An alkylcobalamin with a large trans influence

-Naree Shin-

A dissertation submitted to the Faculty of Science, University of the Witwatersrand, Johannesburg, in fulfilment of the requirements for the degree of Master of Science.

May 2013

Declaration

I declare that this is my own unaided work. It is being submitted for the Degree of Master of Science at the University of the Witwatersrand, Johannesburg. It has not been submitted before for any degree or examination at any other university.

N. Shin

May 2013

ABSTRACT

The synthesis, physical characterization and properties of an alkylcobalamin, phenylvinylcobalamin, is described. Cyanocobalamin was reduced using zinc granules in a 10% acetic acid/methanol solution, before initiating an electrophilic addition reaction on the introduction of phenylacetylene into the reaction mixture under red light conditions. The product was analyzed by HPLC which showed that diastereomers were produced. These two isomers were separated using column chromatography on a C18 stationary phase and characterized by ESI-MS and NMR spectroscopy. One isomer has the phenylvinyl ligand on the upper (β) coordination site of the corrin and the other isomer has the alkyl ligand on the lower (α) coordination site. Whilst the NMR spectrum of the β isomer was virtually fully assigned, the NMR data for the α isomer was not good enough to show the nOe interactions between the phenylvinyl ligand and the corrin ring. ESI-MS strongly suggested that the second isomer was indeed the α isomer, in which the dimethylbenzimidazole (DMB) ligand was displaced from the coordination site of the metal by the alkyl ligand. Photolysis of both products yielded aquacobalamin, confirming that they are both alkylcobalamins.

The β isomer was used to achieve the main goal of this work, which was to evaluate the σ donor ability of the phenylvinyl ligand. One of the methods used to evaluate this was the determination of the pK_a for the protonation and release of the DMB ligand by a spectrophotometric titration. The greater the σ donor ability of the β axial ligand the greater the charge transferred onto the Co(III) ion; this decreases its Lewis acidity and thus the pK_a for protonation and release of the lower DMB ligand should increase. The pK_a for β-phenylvinylcobalamin was found to be 4.6(6), which is the highest value yet reported for an alkylcobalamin, confirming the large σ donor ability of phenylvinyl. The pK_a for deprotonation of H_2O trans to phenylvinyl in α-phenylvinylcobalamin, also determined by spectrophotometric titration, was found to be 13.9(1), which is typical for alkylcobalamins.

A further evaluation of the σ donor ability was done by the ligand substitution of DMB by CN^- in β-phenylvinylcobalamin and H_2O by CN^- in α-phenylvinylcobalamin. It was found that log K for substitution of H_2O by CN^- for the α isomer was 2.70 ± 0.06 and for the displacement of DMB by CN^- in the β isomer 0.7 ± 0.1. These values are compared to the values for other alkylcobalamins which are available in the literature, and enabled us to place PhVn in the trans influence order of the cobalt corrinoids.

β-Phenylvinyl was crystallized by vapour diffusion of acetone into an aqueous solution of the compound (we were unable to obtain crystals of the α isomer, presumably because of the freedom afforded the f side chain and DMB ligand once it was released from the coordination sphere of the metal). Optical microscopy was used to select a single crystal, the structure of which was determined by X-ray diffraction methods. The compound crystallized in the space group of $P2_1P2_1P2_1$ with unit cell dimensions a = 15.7783(7) Å , b = 22.3400(9) Å , c = 25.1607(14) Å with four molecules in the unit cell and a calculated density 1.319 Mg m^{-3}, The final R_1 values was 9.75%.

The axial bond length Co-NB3 to DMB was relatively long (2.225(7) Å) compared to other alkylcobalamins. This is a further indication that phenylvinyl is a powerful σ donor.

Overall, this work has allowed us to place phenylvinyl in the σ-donor order of alkyl ligands in alkylcobalmins, i.e. CN^-< CCH < $CHCH_2$ = PhVn < Me < Et.

This work in dedicated to my loving Family:

사랑하는 아빠(신동규) 엄마(김선희)

제가 이만큼 성장할수 있도록 뒷받침 해주신거

진심으로 감사드리고 사랑합니다.

My Parents: DK Shin & Sunny Kim

내 동생(신재섭), 누나 공부하는동안

늘 도와줘서 고맙고 모든일에 대박나라!!!

My Brother: Jaesup Shin

Thanks for being such an amazing friend of mine

My Bestie: Hanna Klein

Thanks to all of you for the love and support throughout the years.

Acknowledgements

I would like to express my gratitude to the following people for supporting me and giving me the opportunity to complete this thesis.

- Prof. Helder Marques, for his constant patience and invaluable help throughout the course of the project.
- Dr. Chris Perry, for his willingness to help at all times and constant advice throughout the course of the project.
- Dr. Manuel Fernandes, for his help with the crystallography.
- Mr. Richard Mampa, for his help with the 500 NMR spectrometer.
- Dr. Susan Chemaly, for her encouragement and help throughout the course of the project.
- Mrs. Marelize Ferreira, for her help with the ESI-MS data collection.

Table of Contents **Page**

Preliminaries

Abbreviations

AdoCbl	Adenosylcobalamin
AdoCbi	Adenosylcobinamide
aquaCbl	Aquacobalamin
Ado(Im)Cbl	Adenosyl imidazole cobalamin
EtCbl	Ethylcobalamin
MeCbl	Methylcobalamin
NpCbl	Neopentylcobalamin
CNCbl	Cyanocobalamin
HOCbl	Hydroxocobalamin
VnCbl	Vinylcobalamin
AdePrCbl	Adenosylpropylcobalamin
n-ButylCbl	Butylcobalamin
IsoamylCbl	Isoamylcobalamin
PhVnCbl	Phenylvinylcob(II)alamin
NMR	Nuclear magnetic resonance
ESI-MS	Electromagnetic isonization-mass spectroscopy
DMB	5,6-dimethylbenzimidazole
BzCbl	Benzylcobalamin
UV-vis	Ultraviolet-visible
HPLC	High performance liquid chromatography
Im	Imidazole
His	Histidine
IF	Intrinsic factor
COSY	COrrelation SpectroscopY

ROESY	Rotating frame nuclear Overhauser Enhancement SpectroscopY
HSQC	Heteronuclear Single Quantum Coherence
HMBC	Heteronuclear Multiple Bond Correlation

CHAPTER 1

Introduction

1.1 General overview of Inorganic Chemistry

Inorganic chemistry deals with the properties of all of the elements in the periodic table which range from highly reactive metals such as lithium to noble metals such as gold. The non-metals can be solids, liquids or gases, and range from the aggressive oxidizing agent fluorine to unreactive gases such as helium. This variety of inorganic chemistry seems very complicated, but there are trends which can help our understanding of the discipline. The reactivity, structure, and properties of the elements and their compounds provide the general landscape of the periodic table which is the foundation on which to build understanding. Inorganic compounds vary widely from ionic solids to covalent compounds and metals. The ionic solids can be described by simple applications of classical mechanics whereas the covalent compounds and metals are best described using models that have their origin in quantum mechanics. Inorganic chemistry has a strong impact on our everyday lives, especially the chemical industry which depends strongly on it. It is vital to the formulation and improvement of modern materials such as catalysts, semiconductors, optical devices, superconductors, and advanced ceramic materials.[1]

1.2 General overview of Bioinorganic Chemistry

Bioinorganic chemistry is a sub-discipline of inorganic chemistry in that its central focus is the study of the properties of metal ions in biological systems. It is therefore a cross-disciplinary endeavour, straddling inorganic chemistry and biochemistry with strong links to medicine. Bioinorganic chemistry is considered a relatively new field in science. The main focus is on metals bound to proteins and enzymes which were found in earlier centuries associated with “animal or plant tissues”.[2] In the early centuries, chemistry was still divided into either “organic” or “inorganic” chemistry where “organic” chemistry included the substances isolated from living organisms, and “inorganic” chemistry was considered as the chemistry of “dead matter”. However this distinction became meaningless after Wöhler managed to synthesize the “organic” compound urea from inorganic ammonium cyanate in 1828. This synthesis of urea dispelled the myth of a “vital force” associated with “organic” compounds which is formed inside a human body in order to neutralize the chemical force liberated, the urea. In more recent times, organic chemistry is defined as the chemistry of

carbon compounds, including hydrocarbons and their derivatives and which can also include certain heteroelements such as N, O or S without considering the origin of the material.[3] Bioinorganic chemistry deals with the interaction between inorganic substances and molecules of biological interest as it involves the role, uptake, and fate of trace elements that are essential for life. It also provides the fundamental knowledge of the understanding of the function of metal-based drugs, the synthetic production of functional compounds, the production of pharmaceutical contrast agents in medical applications, as well as the development of theoretical functional compounds.[4] Bioinorganic chemistry itself became an independent field after 1960.[5] This rapidly expanding interdisciplinary field has contributed to many other fields of science such as chemical physics (characterisation techniques), molecular biology (supply materials), pharmacology (drug-inorganic substance interactions), medicine (diagnostic aids and tumour therapy), environmental and human toxicology (toxicity of inorganic compounds), crystallography and spectroscopy (characterisation techniques) and chemistry.[2,5]

1.3 Elements vital for life

There are many inorganic elements that are essential for life and these may occur in macroscopic, microscopic or trace amounts. Some of these elements contain metals ions that are involved in life-sustaining biological systems and biochemical processes. These metals ions play a vital role in about one third of all enzymes. Ions may modify electron flow in the enzyme, which effectively controls an enzyme-catalysed reaction.

The periodic table below (Figure 1) shows the elements that are vital for life.

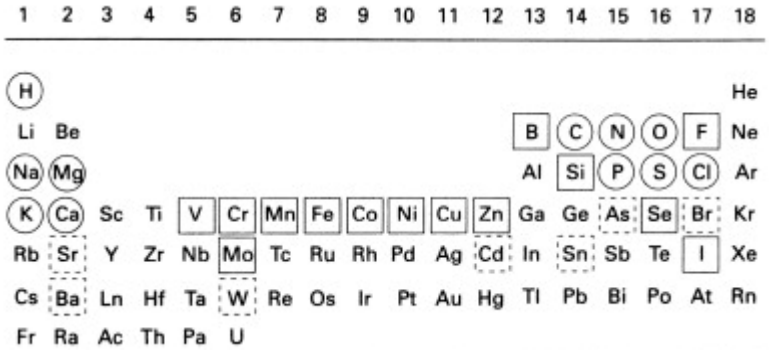

Figure 1: Periodic Table of biological elements in life[6]

Key: Circled elements = Bulk biological elements, Boxed elements = Essential trace elements, Dashed box elements = Possible trace elements showing weaker evidence for evolvement in biology

1.4 Cobalt chemistry

Cobalt is a transition metal in the first row of the periodic table and is commonly found in oxidation states from +1 to +3. This metal in the +3 oxidation state is unstable relative to the +2 state in many simple Werner-type complexes but is much more stable in complexes with stronger field ligands; the metal is then almost invariably in a low spin state.[7]

The typical geometries of cobalt complexes can range from tetrahedral to octahedral throughout the range of oxidation states.[1] Cobalt (III) is also described as being kinetically inert. The following example illustrates this statement. Hexaaqua cobalt can undergo ligand substitutions with bulk water. The rate of this reaction changes depending on the oxidation state of the cobalt ion. $[Co(H_2O)_6]^{2+}$ usually undergoes water exchange with bulk water with a rate constant of $3.2 \times 10^6\ s^{-1}$ whereas, for the same reaction, $[Co(H_2O)_6]^{3+}$ has a rate constant about ten orders of magnitude lower.[8] Therefore Co(II) is far more labile than Co(III).

The identity of the ligand system also plays a very important role in the activation of the metal ion. The rate constants for the substitution of water in the corrin, porphyrin, cobaloxime and amine complexes of the type $[Co(III)N_4X_2]$, being in the approximate ratio of $10^9:10^6:10^4:1$, where N_4 represents a four nitrogen donor system coordinating Co(III) in its equatorial plane.[8]

Therefore from these simple examples it can be seen that both the electronic configuration of the metal and the nature of its ligands can affect its lability.

1.5 Vitamin B_{12}

1.5.1 Introduction to B_{12}

Coenzyme B_{12} was identified as an organometallic derivative of B_{12} and the importance of a metal-carbon bond in enzymatic processes was revealed in the early 1960s. Vitamin B_{12} was discovered 60 years ago as a crystallisable, red complex and was revealed to be a cobalt complex with the unusual ligand, corrin, a unique member of the natural tetrapyrroles. It was described as the anti-pernicious anaemia factor by Whipple, and Minot and Murphy.[9,10] In 1937, William Castle also discovered that an "intrinsic factor", present in the gastric mucosa, was necessary for normal absorption of the "extrinsic factor" in the liver.[11] In pernicious anaemia patients this intrinsic factor was lacking. However, the functions of the extrinsic factor in the liver remained unknown until 1948. In 1948, Smith and Folkers found the cure for pernicious anaemia by administering several grams of uncooked liver to patients.[12] This anti-pernicious anaemia factor turned out to be vitamin B_{12}. Interest in this compound, the only vitamin that contains a metal, led to a great deal of research into the properties of vitamin B_{12} and the cobalt corrinoid family in general, including its biosynthesis, chemical synthesis, electrochemistry, carbon-cobalt bond chemistry, and the cloning and overexpression of numerous B_{12}-dependent enzymes.[13] This further led to the explosion of work on the enzymology of B_{12} coenzymes. The physiologically relevant vitamin B_{12} derivatives are known to be highly light-sensitive and chemically more labile than non-physiologically relevant vitamin B12 derivatives. These are known as coenzyme B_{12} (AdoCbl) and methylcobalamin (MeCbl); the "inorganic" and easily reducible B_{12} derivatives include aquacob(III)alamin and hydroxocob(III)alamin (HOCbl).

In the human body, methionine synthase and methyl malonyl-CoA mutase use methyl cobalamin (MeCbl) and AdoCbl respectively, as their B_{12} cofactors. B_{12} coenzymes are essential in the metabolic processes of a broad range of organisms. However, only microorganisms are known to have the capacity to biosynthesize B_{12} and other natural corrinoids. B_{12} derivatives are therefore "vitamins" for B_{12}-dependent organisms such as humans. The metabolic processes in humans depend on the uptake and binding of B_{12} derivatives, on their metabolic transformation into the relevant B_{12} cofactors. Transport of these and the catalysis functions are controlled by B_{12} dependant enzymes.[14,15] Therefore, B_{12} coenzymes are nature's physiologically most relevant organometallic cofactors.[16,17] Organometallic B_{12} derivatives are known to be involved in protein-activated reactions in

unique B_{12}-dependant enzymes. B_{12} cofactors depend directly upon the reactivity of the cobalt-carbon bond, and its catalysis of exceptional enzymatic reactions.[13,16] The identification of coenzyme B_{12} as corrinoid cofactors has played an important role in the better understanding of biological organometallic processes. Vitamin B_{12} (cyanocobalamin) seems to have no physical function itself and is an artefact of the isolation process in its commercial production.[18] In the last 60 years, outstanding scientific research towards the solution of some of the major "B_{12}-mysteries" has been achieved. Several books on B_{12} have been written, including the earlier ones by Pratt[19] and by Friedrich[20] more recent ones on "B_{12}", "Vitamin B_{12} and B_{12} proteins"[16] and on "Chemistry and Biochemistry of B_{12}"[17] describing the more recent findings on the chemistry of B_{12} and biological roles of the B_{12} derivatives.

1.5.2 Structure of the B_{12}

The crystal structure of vitamin B_{12} (Figure 2) and its coenzyme forms were first established by Dorothy Hodgkin and co-workers in 1956 using X-ray crystallography.[21]

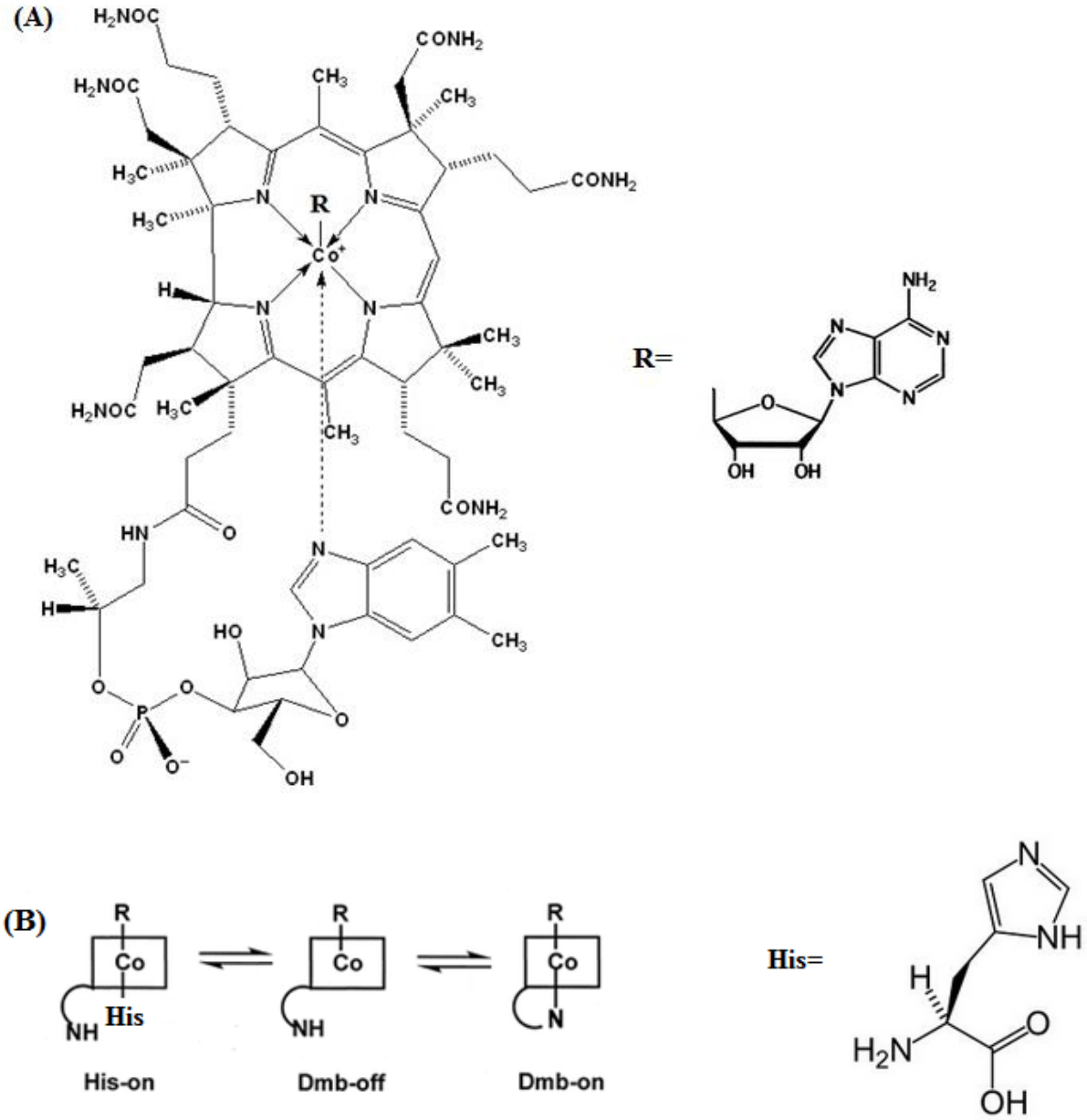

Figure 2: (A) Structure of Vitamin B_{12}[22], where R is deoxyadenosine in AdoCbl (also known as co-enzyme B_{12}), methyl in MeCbl, OH^- in hydroxocobalamin, H_2O in aquacobalamin (vitamin B_{12}) and CN^- in vitamin B_{12}. (B) In several B_{12}-dependent enzymes the cofactor exists in the His-on DMB base-off, in equilibrium with the His-off DMB-off, and the His-off DMB-on forms. The first predominates at physiological pH.

It was found that the core of the molecule is a corrin ring with various attached side-chains. The corrin ring consists of 4 pyrrole subunits, with the nitrogen atoms connected to the central atom cobalt, whose high oxidation state allows the molecule to adopt an octahedral geometry in its resting state. It is similar to a porphyrin but without one of the bridging methylene groups. However, it is

by no means a rigid structure and is fairly flexible.[21] The ring is able to bend and fold and by doing so it induces an inverse *trans* effect which appears in the case of alkyl cobalamins. This will be discussed in detail in section 1.6.

At physiological pH, the lower α axial ligand is a nitrogen atom from a dimethylbenzimidazole (DMB) base. At low pH, the nitrogen atom is protonated and the DMB substituent detaches from the corrin ring to produce a *base off* form (Figure 2). By contrast, at higher pH, the nitrogen of the DMB reattaches to the corrin ring favouring the *base on* conformation (Figure 2(B)). The change in conformations can be observed as a colour change from red (base on) to yellow (base off).[23]

The derivatives shown in Figure 2(B) are classified according to their possession of a nucleotide function into complete (nucleotide function present) and incomplete (nucleotide function absent) corrinoids. The chemical structure of the nucleotide allows for intramolecular binding to the central Co(III) ion which in turn affects the organometallic reactivity, the binding and recognition of B_{12}-binding proteins at the cobalt centre.[24] Coenzyme B_{12} or adenosylcobalamin was the first naturally-occurring compound containing an organometallic bond to be discovered. This discovery was vital in determining the biological function of the molecule, including its role in the catalysis of enzymatic reactions.[24] In many of the B_{12}-dependent enzymes the cofactor usually binds to the enzyme in the base off conformation and the DMB ligand is replaced by a histidine residue from the protein. This is known as the His-on conformation (see Figure 2(B)).[25]

1.5.3 Incomplete corrinoids

The structures of Vitamin B_{12} (CNCbl) and of coenzyme B_{12} (AdoCbl) were first established by Dorothy Hodgkin and co-workers as mentioned above. She discovered the composition of the corrin core of vitamin B_{12} and the organometallic nature of its coenzyme (AdoCbl).[26,27] These two cobalamins are known as "complete" corrinoids, in which a pseudonucleotide function is attached via an amide linkage to the corrin moiety. This combination is unique, as the B_{12}-nucleotide function may switch between the cobalt-coordinated "base on" form and the de-coordinated "base-off" form. Thus coenzyme B_{12} can be considered to be a "molecular switch".[28]

Eschenmoser and Woodward started investigating[26,27] the crystallisable "incomplete" Co(III)-corrinoids such as α-cyano-β-aqua cobyric acid[26], since it is the natural corrinoid moiety of vitamin

B_{12}.[29,30] After these times, many scientists have concentrated on obtaining detailed structural information from crystallographic work on "incomplete" Co(III)-corrinoids.

1.5.4 Complete corrinoids

The "complete" corrinoid, Vitamin B_{12}, is called a "cobalamin" or a DMB-cobamide, in which a cyanide ligand is bound at the "upper" axial coordination site (β face).[31] There are many other "cobalamins" with different ligands other than the cyanide group at the β-face of cobalamins, e.g. an organometallic group, as in coenzyme B_{12} (AdoCbl). There is another class of naturally occurring "complete" corrinoids known as purinyl-cobamides, in which a purine base is part of the nucleotide function.[16,20]

1.5.5 The "Base-on"/"Base-off" constitutional switch of "complete" corrinoids

Most cobalamins and other "complete" corrinoids can be categorized into two forms: they either have their nucleotide appendage cobalt-coordinated (in a "base-on" form) or decordinated ("base-off" form) (see Figure 3).[16]

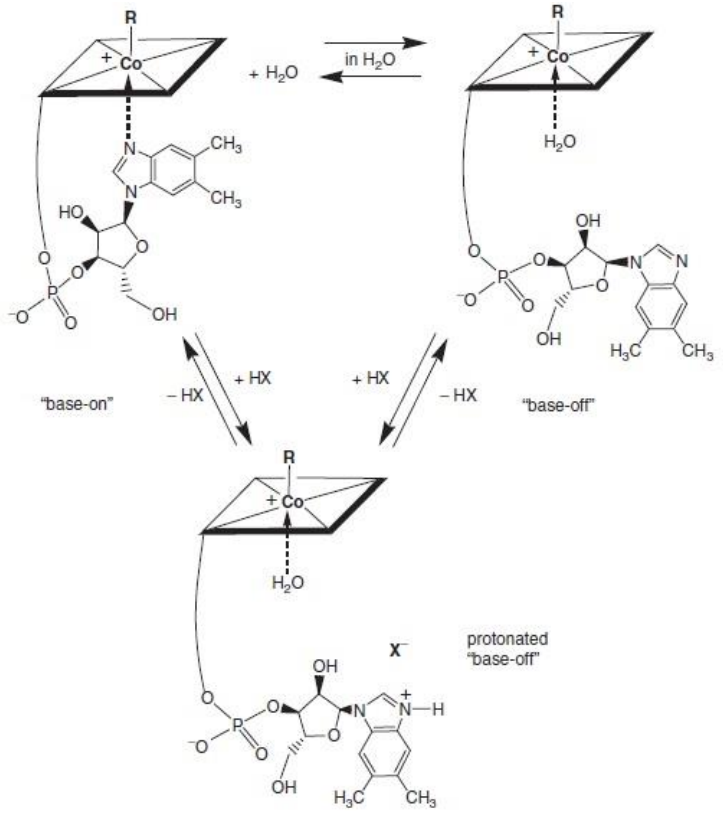

Figure 3.The B_{12} cofactors have the nucleotide base and the cobalt coordinated in the "base-on" form or de-coordinated in the ''base-off'' form; B_{12} – a constitutional ''molecular switch''[32]

In the "complete" corrinoids, both the "base-on" and "base-off" forms represent constitutional isomers that may be well structured for binding by specific B_{12} apoenzymes. Some B_{12}-derivative enzymes, such as the methyl transferases, typically bind a "base-off" form of the B_{12} cofactor.[33,34] However, coenzyme B_{12}-dependent enzymes can be categorized into two classes: one of them with a "base-on" B_{12} cofactor, the other with the B_{12} cofactor bound in a "base-off" ("His-on") form.[22] The complete structure of the nucleotide moiety is very important for the selective and tight binding by B_{12}-binding proteins.[35] An interaction in the reverse sense was recently discovered in a particular type of mRNA, for which conenzyme B_{12} (AdoCbl) is a strongly bound ligand; this part of mRNA in its untranslated region (a "B_{12} riboswitch") not only is able to bind coenzyme B_{12} (AdoCbl) tightly, but can switch upon binding of the B_{12} ligand, so as to inhibit the expression of their gene product.[36] Thus the cobalamins and related "complete" corrinoids have the capacity to switch their constitution between the "base-on" and the "base-off" forms and represent natural "molecular switches".[28] The "base-on" to "base-off" switch can also be accomplished by protonation of the nucleotide base and decordination from the corrin-bound cobalt ion.[13,16] The proton-assisted de-coordination is inhibited by strong cobalt coordination in molecules such as cyano-Co(III)corrins but is readily achieved in organic B_{12} derivatives such as AdoCbl. The associated acidity of the protonated base-off form as expressed by its pK_a value acquired quantitatively on the strength of the intramolecular coordination of the nucleotide base (Co-DMB base- on $\rightleftharpoons$ base off pK_a value).[13,16]

1.5.6 Relevant structural aspects of cobalamins

In the last decade, synchrotron X-ray sources coupled to area detectors have been used to determine various cobalamin structures accurately and the features have been reviewed.[27,37] The internal structure of the corrin ligand was found to have a π delocalized system involving the N and the sp^2 C atoms.

The four main resonance structures of the corrin moiety are shown in Figure 4(a). Accurately measured distances of the equatorial moiety indicated that they are barely affected by the kind of the X axial ligand (ligand that is bound to the centre axially). The Co–N distances involved in the five membered ring are significantly shorter than the other two equatorial Co–N distances (by about 0.02 Å). The measured C–C and C–N bond lengths within the delocalized moiety appear to have two-fold symmetries with respect to the axis passing

through Co and C10 (Figure 4(a)).[27] This trend can be easily clarified on the basis of the four main resonance structures of Figure 4(a). Indeed, linear relationships can be found between the experimental values of the C–C and C–N distances and the corresponding bond orders that are derived from the four resonance structures. The orientation of the C–C single bond lengths in the corrin ring vary from 1.508 Å of the C8–C9 bond to 1.580 Å of the C1–C2 bond reflecting the different hybridization and the number of non-H substituents at the bonded C atoms (Figure 4(a)).

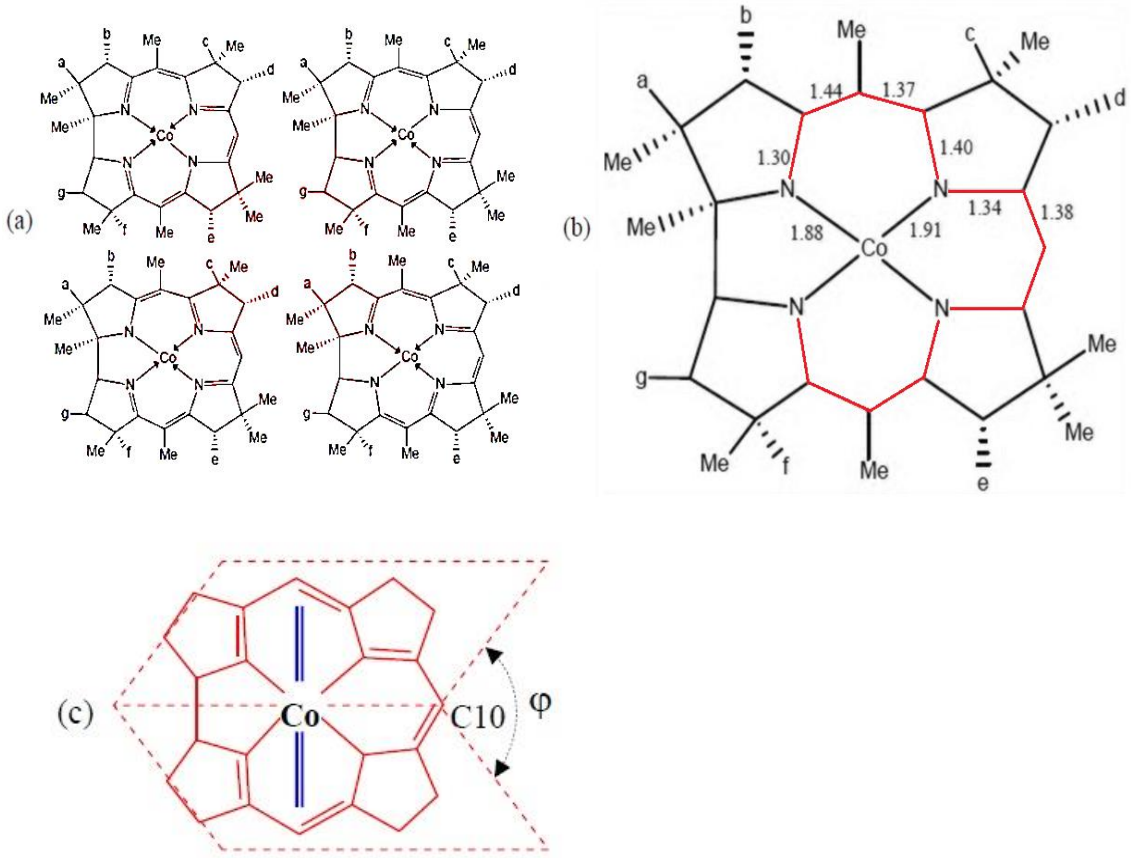

Figure 4.(a) The main four resonance structures for the delocalized corrin system; (b) mean bond lengths within the delocalised moiety of the corrin nucleus[27] (c) the folding angle φ. The double blue line represents the trace of the 5,6-benzimidazole group.[38]

The mode of deformation of the corrin ligand preferred to have a folding towards the X axial ligand with the axis approximately bisecting the C1–C19 bond and passing through C10.

The deformation is measured by the folding angle φ that is generally calculated as the dihedral angle between the planes (Figure 4(c)), passing through the atoms shown in Figure 4(b).

The benzimidazole residue on the equatorial ligand (indicated by double line in 4(c) releases its steric pressure when the Co–NB3 bond lengthens and this is due to the increase in the *trans* influencing ability of X.[27] The Co–NB3 axial distance lengthens by 0.4 Å for the complexes with X varying from H_2O to NO so that the X-Cbl distance for aquaCbl is 1.925 (2) Å and 2.349 (2) Å for NOCbl respectively. Lengthening of that Co–NB3 bond *trans* to X reflects the increase in the electron σ donating ability of X (electronic *trans*-influence) which means that NOCbl has stronger σ donor ability than aquaCbl. In comparison to the "inorganic" ligand, the alkyl groups are the stronger *trans*-influencing ligands, the order of increasing trans-influencing ability of X donor atom being O < N < S < C. Interestingly the Co-X distances do not vary when the same X donor atoms being as above (i.e. O, N, S, C) with cobaloximes and $XCo(NH_3)_5$, except when X is either H_2O (a weak electron-σ donating group) or CN^- (a good electron π-acceptor).[27,37]

This appears to be a consequence of the electronic *cis*-influence of the equatorial moiety on the axial bonds.[39] As shown in Table 1, an increase in bulkiness of the alkyl group, R in alkylcobalamins, causes the Co–C bond to become weaker due to the steric interaction of R with the corrin ring (*cis*-influence). As a matter of fact the length of the Co–NB3 bond was measured by the X-ray structural analysis of NOCbl,[39] showing that the nitroxyl ligand (with a bent Co–N–O geometry) has a significantly larger *trans* influence than an alkyl group.[40] A trend called the *inverse trans-influence* has been identified in alkyl cobalamins where both Co–NB3 and Co–C distances increase when both the bulk and the electron donating ability of X increase, in contrast to the regular *trans*-influence (when the Co–X shortens, the *trans* bond lengthens). This inverse *trans* influence is usually observed in a series of cobalamins with X = ligands containing a $S(sp^3)$ donor.[27,37] The experimental findings were confirmed by DFT calculations.[41]

Table 1: Values of $pK_{base\text{-}off}$ (at 25℃) and Co–NB3 distances for XCbl's[13,59]

X	$pK_{base\text{-}off}$	References	Co–NB3 /Å	ΔG°(kcal/mol)	References
NO	5.10	60	2.349 (2)	-15.90	61
CH_3CH_2	4.16	13	2.232 (1)	-7.42	40
$CH_3CH_2CH_2$	4.10	62		-7.84	40
Ado	3.67	63	2.236 (2)	-10.60	64-67
CH_3	2.90	68	2.17 (2)	-15.10	66,69
CF_3CH_2	2.60	70		-16.90	71
CH_2=CH	2.40	62	2.165 (6)	-18.00	23
cis ClCH=CH	2.30	23	2.144 (5)	-19.00	23
CF_2H	2.15	70	2.187 (7)	-19.50	71
$NCCH_2$	1.81	13		-21.40	72
CF_3	1.44	70	2.05 (1)	-23.50	71
CN	0.10	68	2.04 (2)	-31.10	72,66
H_2O	-2.13	68	1.925 (2)	-43.90	73

1.6 Biological Importance of B_{12}

1.6.1 General biological importance of Vitamin B_{12}

Vitamin B_{12} is soluble in both alcohol and water. It was first isolated from liver in 1948 and it was found that it can be grown by fermentation by bacteria. However, it cannot be synthesized in the human body naturally and as such, must be obtained from foods such as meat, fish and dairy products. This vitamin is necessary for us to keep a healthy body, and is essential since it is needed for the process of converting carbohydrates, fats and proteins from food into energy. It is also used to create a protective layer of all nerve cells in the body which also keeps the immune system healthy. Vitamin B_{12} cures pernicious anaemia as mentioned previously, but the vitamin itself cannot prevent the disease. It needs three soluble binding proteins, haptocorrin, instrinsic factor and transcobalamin, to be involved in the uptake and transport of cobalamins in the body. This vitamin and the glycoprotein, intrinsic factor (IF), combine to form an erythrocyte maturation factor that is required for maturation of red cells in the marrow. A lack of B_{12} affects both erythrocyte and leukocyte precursors in the bond marrow in the same way as a deficiency of folate in the blood. A very small amount of vitamin B_{12} is needed in order to prevent the symptoms of pernicious anaemia and subsequent[42] neurological change.[10,11] This vitamin is also required for the utilisation of other vitamins such as vitamin C, vitamin B5, iron, and some amino acids in the body. Methylcobalamin is biologically active and does not require any metabolic steps to be absorbed by the body. The biological activity of B_{12} derivatives involves Co–C bond

formation and cleavage which occurs due to electron transfer and organometallic reactions.[24] The oxidation-reduction reactions which involves electron transfer occur due to the reduction potential created by the different oxidation states of the central metal ion, namely Co(I), Co(II) and Co(III). The oxidation state of the metal and its nature is an important factor which determines the number of axial ligands that are able to coordinate to the central ion. As the oxidation state of the metal ion increases, the number of coordinating ligands increases; Co(I) has 4 ligands (d^8, square planar), Co(II) has 5 (low spin d^7, square pyramidal), and Co(III) has 6 (low spin d^6, octahedral). Thus the transfer of electrons between different vitamin B_{12} derivatives affects the number of attached axial ligands. These ligands with the bound nucleotide base are essential in the stabilization of the molecule against further reduction.[24]

The biological activity of the B_{12}-dependent enzymes can be traced back to the organometallic reactivity of B_{12}-derivatives.[24] There are two mechanisms that are important in the functioning of vitamin B_{12} dependent enzymes. One mechanism is a homolytic mode of cleavage of the Co–C bond, which allows coenzyme B_{12} to act as a reversible alkyl-radical carrier. The other mechanism is a heterolytic mode of cleavage that allows the respective demethylation and methylation of Co(I) and Co(III) corrins. The homolytic mode of formation/cleavage (see Figure 5) of the organometallic axial bond at the cobalt centre is important, particularly in the role of adenosylcobalamin or coenzyme B_{12} as a cofactor: coenzyme B_{12} is considered as a "reversible carrier of an alkyl radical".[24] The energy required to cleave the Co–C bond of coenzyme B_{12} has been determined to be ±30 kcal/mol. This was only affected slightly by the co-ordination of the nucleotide. The reactions of cob(II)alamin with alkyl radicals such as the 5'deoxy-5'-adenosyl radical are very fast. The radicaloid co(II)balamin acts as an efficient 'radical trap' and its reactions with radicals occur with minimal restructuring of the cobalt corrin functional group of the molecule.[16,43] The minimal rearrangement allows for rapid electron transfer as there is little rearrangement energy required.

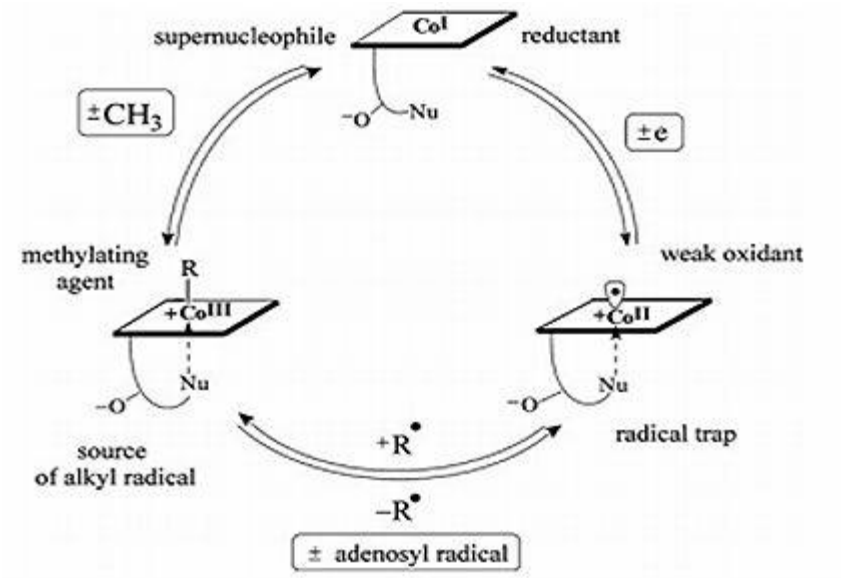

Figure 5. Homolytic and heterolytic formation[24]

In the heterolytic mode of formation, nucleophile-induced cleavage of the (Co–C) bond at the cobalt centre, which is in effect a two-electron oxidation of the metal-ion, involves the formation and cleavage of two axial bonds (see Figure 5). This mode is important in enzyme-catalysed methyl-transfer reactions and is represented by the reaction of Co(I)-corrins with alkylating agents, and also by the nucleophile-induced demethylation of methyl-Co(III)-corrins. Alkylation at the Co(I)-centre occurs via 'classical' bimolecular nucleophilic substitution (S_N2). The intramolecular coordination of dimethylbenzimidazole stabilizes 'base on' methylcobalamin by about 4 kJ mol^{-1} and this has a notable thermodynamic effect on heterolytic reactions of methylcobalamin.[25] Alkyl-Co(III)-corrins are rather resistant to proteolytic cleavage of the (Co–C) bond under physiological conditions. This is vital for the cofactor role of the B_{12}-coenzymes. However, visible light induces the cleavage of the Co–C bond of organometallic B_{12}-derivatives.

1.6.2 Co–C bond in organocorrinoids

1.6.2.1 Formation of the Co–C bond in organocorrinoids

B_{12} derivatives have a vital reactivity that is represented by the highly nucleophilic Co(I)-corrins[42] which provide the basis of the heterolytic mode of formation of the (Co–C) bond. Also this is important in methyl-corrinoids in enzyme catalysed methyl transfer reactions.[15,44] This is represented by the reaction of Co(I)-corrins with alkylating agents in the formation of the (Co–C) bond and the "nucleophile" induced demethylation of methyl Co(III)-corrins for the cleavage of the (Co–C) bond. This can be thought of as a *trans* oxidative addition of 4 coordinated Co(I) to produce 6 coordinated Co(III) (see Figure 6).[45]

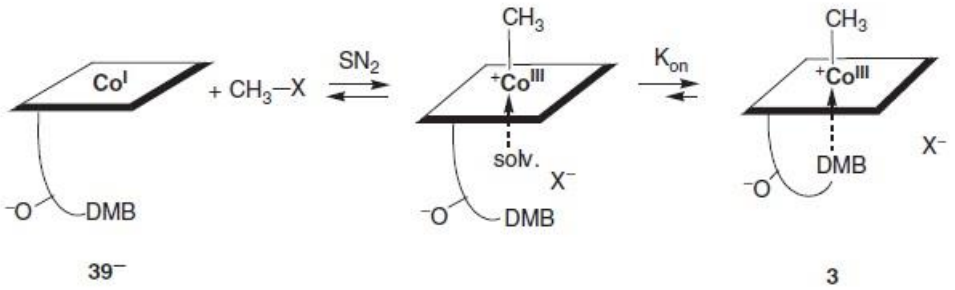

Figure 6. Methylation of cob(I)alamin by an SN2 mode is directed to the ‘‘upper’’ β-face (by both, kinetically and thermodynamically) yields MeCbl[32]

Alkylation at the corrin-bound Co(I) centre usually proceeds via the bimolecular nucleophilic substitution (S_N2) mechanism, where the Co(I)-corrin acts as a "super nucleophile".[42,44] However, the alkylation may occur via a two-step one-electron transfer path with Co(I)-corrins act as strong one-electron reducing agents and the process goes via Co(II)-corrin intermediates[46]. "Complete" corrins such as cob(I)alamin have a pathway that results in alkylation at the β face that allows the nucleotide to coordinate at the α face of alkyl cobalamins, such as MeCbl.[16,45] Only little effect on the thermodynamics of methyl transfer reaction occurs when the nucleotide base changed from a DMB base to an imidazole. Explanations of the alkylation reaction at the corrin-bound Co(I) centre via S_N2 mechanism are as follows:

(i) Co(I)-corrins: Its nucleophilicity is completely independent of the presence of the DMB nucleotide, both in its "complete" and "incomplete" states. A Co(I) centre which is very nucleophillic at the α face binds to methyl as shown in Figure 6 and leaves the X^-. The immediate product of the β-alkylation may be a penta-coordinate or already solvated and effectively hex coordinate Co_α-alkyl-Co(III)-corrin.

(ii) In aqueous solution, at room temperature the "base-on" (hexacoordinate) methylcob(II)alamin is more stable by 4 kcal mol^{-1} than the "base-off" Co_α-aqua-Co_β-methyl cob(III)alamin.[47] By NMR studies, the latter has been estimated to still be more stable in water by 7 kcal mol^{-1} than the corresponding "base-off" and dehydrated form of Co_β-methyl cob(III)alamin which has a penta-coordinate Co_β-methyl-Co(III) centre.[48]

The axial ligand at the Co(II) (corrin bound) centre is expected to direct the formation of the (Co–C) bond, which can be α-alkyl-Co(III) corrins.[46,49]

Depending on their structural requirements, the two most relevant modes of formation (cleavage) of the (Co–C) bond of the cobalt centre differ significantly (see Figure 7). The heterolytic mode of formation (and cleavage) of the (Co–C) bond tends to recognize both faces of the corrin-bound cobalt centre while the homolytic mode of formation (and cleavage) the cobalt corrin portion of complete cob(II)amides such as 2 and 3 hardly changes structure.

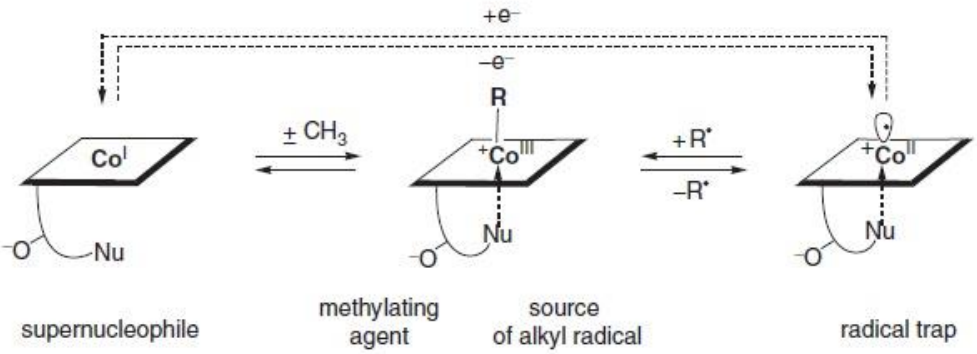

Figure 7. Redox transformations of "complete" corrinoids[32]

1.6.2.2 α/β diastereomerism of alkylcobalamins

Brown and his co-workers have done reductive alkylation of cobanamide in zinc/acetic acid with either 5'-deoxy-5'-iodoadenosine or 5'-bromo-5'-deoxyadenosine and produced a pair of diastereomeric 5'-deoxyadenosyl-cobinamides in which the deoxyadenosyl ligand is in the "upper" (β) axial ligand position (β-AdoCbi) or in the "lower" (α) axial ligand position (α-AdoCbi).[50] This work concluded that mechanisms that control the diastereomeric outcome of reductive alkylation of corrinoids are still unclear but they found a trend in which reductive alkylation favours the α-diastereomer when the alkyl group is electron withdrawing such as CF_2H, CF_3, $NCCH_2$ and CF_3CH_2, while the β diastereomer is favoured by electron- donating groups such as CH_3, CH_3CH_2 and OCH_2CH_2.[50] They revealed that α-AdoCbi and α-AdoCbl could be produced in high yields under reductive alkylation conditions given the fact that the alkylation with other bulky alkylating agent is used such as benzyl bromide and neopentyl iodide.

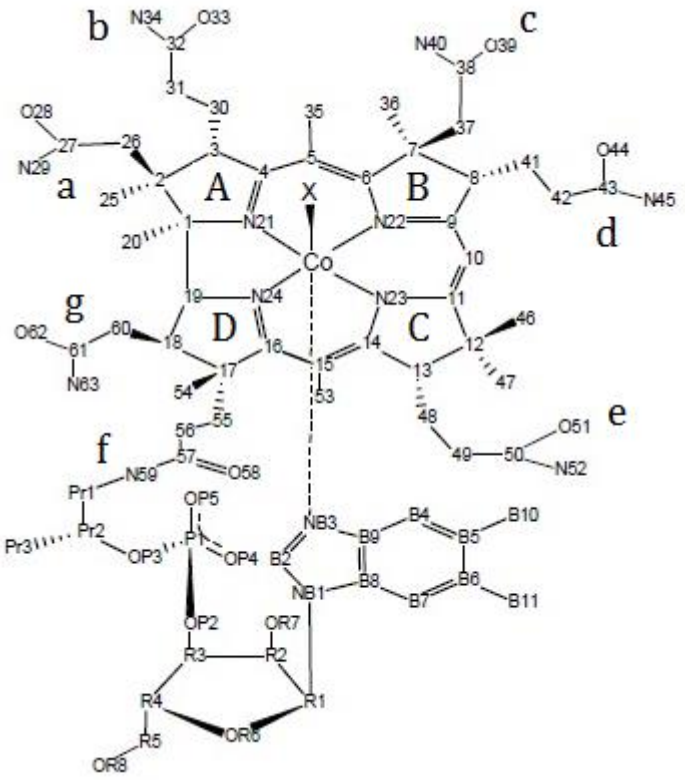

Figure 8. 'Complete' structure of X-Cbl with numbering system[17]

A year later, they synthesized α-neopentylcobinamide (α-NpCbi$^+$) and α-neopentylcobalamin (α-NpCbl) by reductive alkylation of cyanoaquacobalamin and aquacobalamin with neopentyl bromide respectively. They also discovered that these α-alkyl cobalt corrinoids can be converted thermally to their corresponding β diastereomers under anaerobic conditions but at elevated temperatures. The process involves breaking and regenerating the Co-C bond. The homolysis of Co-C bond in coenzyme B_{12} is the first unique step in the coenzyme B_{12} dependent enzymatic rearrangement reactions.[51] As mentioned, the corrin ring is sterically more crowded at the α face (due to encountering the b, d and e propionamide side chains and substituted propionamide f side chain (see Figure 8) than in the β face which only bears 3 acetamide side chains. In general, the Co-C bond in α alkyl cobalt corrinoids appears to be more labile than in the β diastereomers.[52] However its quantitative investigations of the thermolysis in α alkyl cobalt corrinoids have not been reported but they found that the rate of the homolysis of α-NpCbi$^+$ and α-NpCbl are more than 10^3-10^4 times faster than those of the corresponding β diastereomers. This in turn suggests that the steric congestion at the α face maybe relieved by an upward movement of the corrin ring leading to a weakened Co-C (α) bond thus a Co-C (α) bond is more labile than the Co-C (β).

1.6.2.3 Cleavage of the Co–C bond in organocorrinoids

The cleavage mode of a (Co–C) bond in organometallic B_{12} derivatives has been recently recognized as radical-induced substitution at the cobalt-bound carbon centre.[16,53] This type of reaction stands out due to the observation of unusual biological (C–C) bond forming reactions and methylations at inactivated carbon centres.[54,55] In certain organocorrinoids, the (Co–C) bond is cleaved homolytically by absorption of visible light and organometallic B_{12} derivatives have long been known as sensitive to visible light. Organo-cob(II)amides are also known to be labile to strong one-electron reducing agents, as it has been found only after one-electron reduction of the organo-Co(II) corrins which means (Co–C) bond is weakened. As mentioned above, this aspect suggested that it is difficult to prepare organocob(III)amides with electron-withdrawing substituents via alkylation of the strongly reducing cob(I)amides.[56]

1.7 Inorganic Chemistry of Vitamin B_{12}

1.7.1 *Cis* and *trans* influence/effect in cobalamins

The *cis* and *trans* effect (or influence, see below) can simply be recognized as the mutual interaction between ligands through the metal ion. The *cis* effect can be described as the influence of one ligand X on its neighbouring ligand Y, and the *trans* effect as the influence of X on its opposite ligand Y.[57]

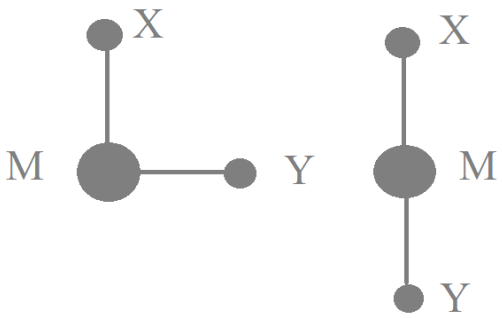

Figure 9. The *cis* effect and *trans* effect

The classical *cis* and *trans* effects are described as the effect of a ligand on the rates of the ligand substitution reactions of groups *cis* or *trans* to it and is called the kinetic, *cis*- or *trans*-effect (eq. 1). The term c*is* or *trans* influence refers to the effect on the *cis* or the *trans* ligand on the thermodynamics of ligand substitution. The ground-state influence is the effect that varying X has on the structural properties of Y in terms of the metal-Y bond length and R-metal-Y or metal-Y-R bond angles where R is another atom bonded either to the metal or to Y.

$$X\text{-}M\text{-}Y + Z \rightleftharpoons X\text{-}M\text{-}Z + Y \qquad (1)$$

1.7.2 Some structure/property relationships

The homolysis of the Co–C bond is the first step of photolysis of alkylcobalamins. The different type of R radical leads to different final products. In contrast, heterolysis of the Co–C bond (for example, by thermolysis) is observed in a displacement reaction with nucleophiles such as cyanide, the final product being the corrinoid $(CN)_2Cbl$.[13,58] According to equilibrium 1 (Figure 10), the most relevant ligand substitution reaction in cobalamins is the intramolecular dissociation of the benzimidazole ligand- "base-off" (His-on) form (protonated).

From Figure 10, K_{co} for reaction 1 can be calculated from the experimental values of $K_{base\text{-}off}$ for equilibrium 2, measured in sufficiently strong acid solution.[59] The K_{co} values obtained for XCbl for X ranging from NO to H_2O[13,59] together with the corresponding $\Delta G°$ values, the observed $K_{base\text{-}off}$ and the Co-NB3 distances is listed in the Table 1.It was shown that as the values of ΔG^o increase, the σ-donating ability of X also increases which means the increase in ΔG^o form the above ligands is linearly related to the increase in the Co–NB3 distances (Figure 10), i.e. a structural *trans*-influence.

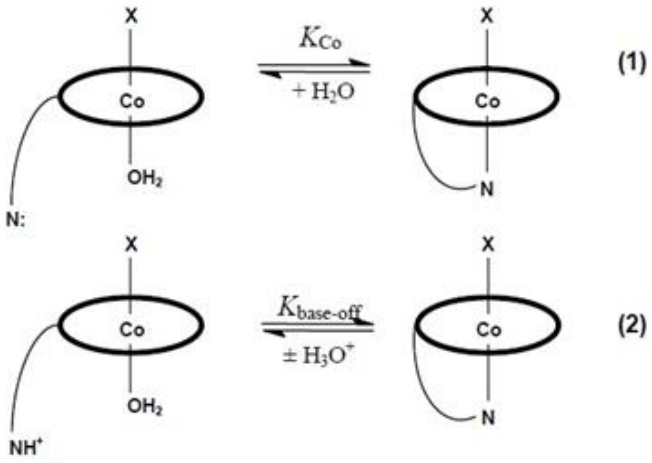

Figure 10. Dissociation equilibrium of the benzimidazole ligand to give the unprotonated (1) and protonate (2) base-off form of cobalamin[59]

Table 1: Values of $pK_{base\text{-}off}$ (at 25°C) and Co–NB3 distances for XCbl's[13,59]

X	$pK_{base\text{-}off}$	References	Co–NB3 /Å	ΔG^o(kcal/mol)	References
NO	5.10	60	2.349 (2)	-15.90	61
CH_3CH_2	4.16	13	2.232 (1)	-7.42	40
$CH_3CH_2CH_2$	4.10	62		-7.84	40
Ado	3.67	63	2.236 (2)	-10.60	64-67
CH_3	2.90	68	2.17 (2)	-15.10	66,69
CF_3CH_2	2.60	70		-16.90	71
CH_2=CH	2.40	62	2.165 (6)	-18.00	23
cis ClCH=CH	2.30	23	2.144 (5)	-19.00	23
CF_2H	2.15	70	2.187 (7)	-19.50	71
$NCCH_2$	1.81	13		-21.40	72
CF_3	1.44	70	2.05 (1)	-23.50	71
CN	0.10	68	2.04 (2)	-31.10	72,66
H_2O	-2.13	68	1.925 (2)	-43.90	73

Vinylcobalamin and chlorocobalamin provide the first examples of reported crystal structures of organocobalamins in which the carbon ligand has sp^2 hybridization. The pK_a values of these structures were significantly lower than those reported for EtCbl (4.16) and AdoCbl (3.67) and higher than those of di- and trifluorocobalamin (2.15 and 1.44, respectively). Converting the pK_a values to ΔG^o values was described by Brown and co-workers and a very good correlation between $-\Delta G^o$ and the Co–NB3 bond length for all the alkylcobobalamin structures is shown in Figure 11 (R^2= 0.85).

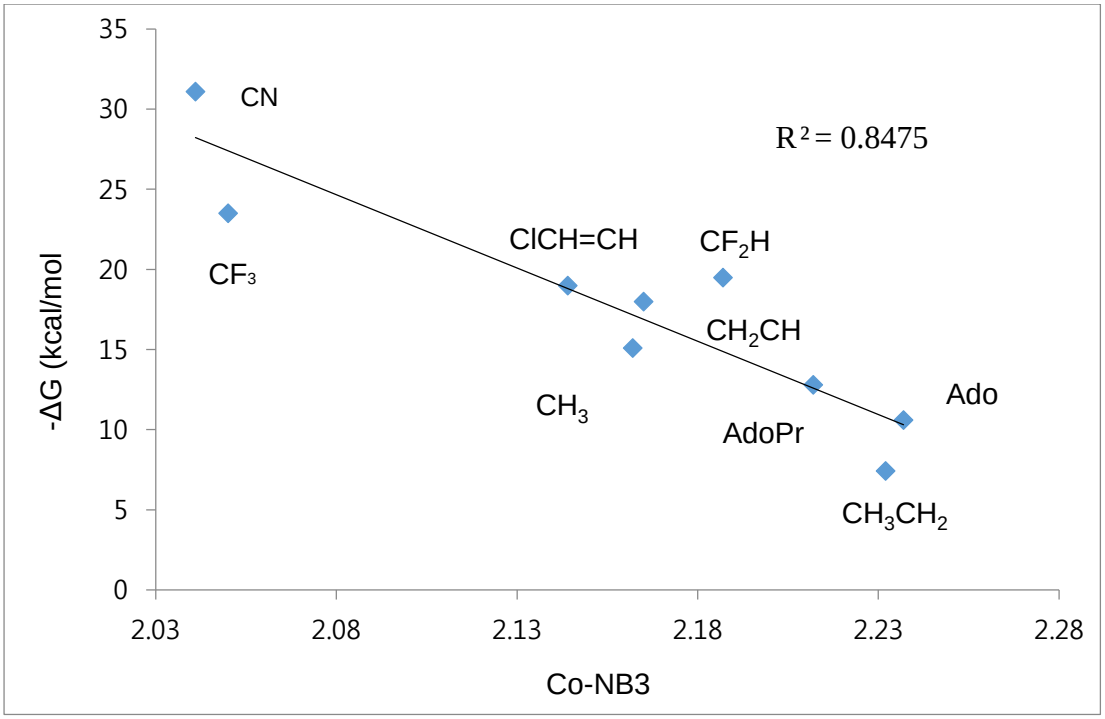

Figure 11. Empirical correlation between the Co–NB3 bond length and the free energy required for the base-on and base-off reaction in Figure 10.

1.7.3 Selected structural data for the cobalamins

Table 2 below shows selected structural data for the cobalamins, illustrating the ground-state *cis* and *trans* influence that varying the test ligand X has on both Co–N (*cis*) and Co–DMB bond lengths.

Table 2.Ground state *cis* and *trans* influence on bond lengths in alkyl cobalamins

	Co-N (*cis*)		Co-NB3 (*trans*)	References
	6-membered ring	5-membered ring		
Chlrovinyl	1.914 (3)	1.892 (4)	2.144	23
Methyl	1.92 (1)	1.87 (3)	2.16 (4)	69
Vinyl	1.915	1.880	2.164	23
Ethyl	1.910	1.870	2.232	40
n-Butyl	1.912	1.873	2.244	40
Isoamyl	1.915	1.854	2.277	74

- 6-Membered ring: Average value for the Co–N22 and Co–N23, 5-Membered ring: Average value for the Co–N21 and Co–N24

The table above shows that as the bulkiness of the ligand increases from chlorovinyl to isoamyl, its *trans* influence also increases i.e. length of the Co–NB3 increases. However there is no significant change in *cis* influence with varying the ligand which only serves a difference of 0.001 Å i.e. Chlrovinyl (1.914) - Isoamyl (1.915). Thus this implies that the *cis* influence (Co–N) does not affect the σ donor ability of alkylcobalamins.

1.8 Resonance spectroscopic methods

The complex organometallic derivatives such as pseudocoenzyme B_{12}, adenosyl-factor A and neocoenzyme B_{12} could be analyzed in a great detail using NMR spectroscopy.[75,76] This has proven to be a method that is adaptable in the detection of intra- and inter molecular H bonding. This spectroscopy enables the characterization of the pseudo-intramolecular H bonding of a specific "external" water molecule to the nucleotide structure of MeCbl [77], and also it may also be used to determine the hydration behaviour of B_{12} derivatives in aqueous solution. The protonated "base-off" forms of aquaCbl have easily been investigated by measuring nOe (nuclear Overhauser effect) interactions between the solvent. The nOe effect occurs when there is a change in population of one proton influenced by another magnetic nucleus close in space which is saturated by decoupling and this can be used to determine intra or inter molecular distances. The presence of a water molecule as the Co-axial ligand also provides the evidence for a hexacoordinated cobalt centre in the solution of organometallic cobyrinic acid (See Figure 12) derivatives.

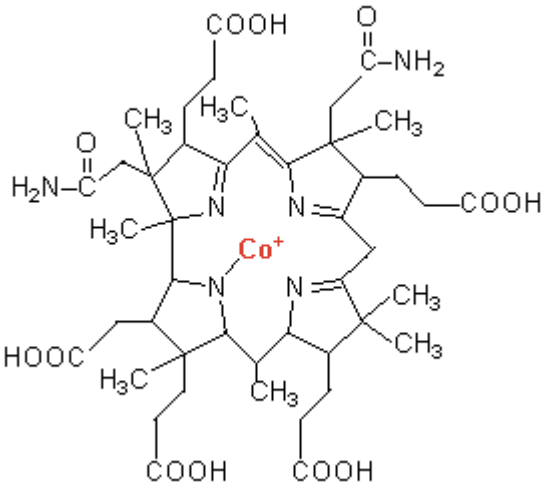

Figure 12. Schematic diagram of Cobyrinic acid

Electron spin resonance spectroscopy also provided important information on the coordination environment of Co(II)-corrins, where DMB coordination in cob(II)alamin can be detected by ESR.[17] Modern 2D-ESR techniques initiated the detection of external ligands to "incomplete" Co(II)-corrins in solution such as Co(II)cobester and in the protonated base-off form of cob(II)alamin. Application of such modern methods of absorbance spectroscopy has been important in discovering the coordination properties of corrinoids.

1.9 Aims of this project

The first aim of this project was to evaluate the σ donor ability of phenylvinyl as a ligand by determining the pK_a for the protonation and release of the DMB ligand. The greater the σ donor ability of the β axial ligand, the greater the charge transferred onto the Co(III) ion; this decreases its Lewis acidity, and hence the pK_a for protonation and release of the lower DMB ligand should increase, i.e. it requires less acid in solution to compete with the metal ion for the DMB base. The second aim of the project was to crystallize the compound in order to study the phenylvinyl Co–C bond cleavage. In AdoCbl-mediated enzymes, the enzyme increases the rate of Co–Ado bond cleavage by a factor of $10^{12;\ 78}$; this is the first step in the enzymatic reaction; but the mechanism by which the enzyme accelerates homolysis of AdoCbl is not yet fully understood. This is the reason why we chose phenylvinylcobalamin (PhVnCbl) as a model for AdoCbl since the phenylvinyl ligand should be a good radical stabilizer; it was hoped that this would provide us with an opportunity for observing a cob(II)alamin phenylvinyl radical intermediate in the solid state through radical delocalization in the phenyl ring. Even if we were unable to observe the radical intermediate (it would require the radical to move away slightly from the metal centre into a void which is often observed around the β ligand in the crystal structure of cobalamins[79]), the compound was interesting in its own right because organometallic complexes of B_{12} in which there is a Co–CH=CHR moiety are rare. A search of the Cambridge Structural Database (CSD), revealed only two structures of cobalamins with this moiety (Co-CH=CHR) (Figure 13).

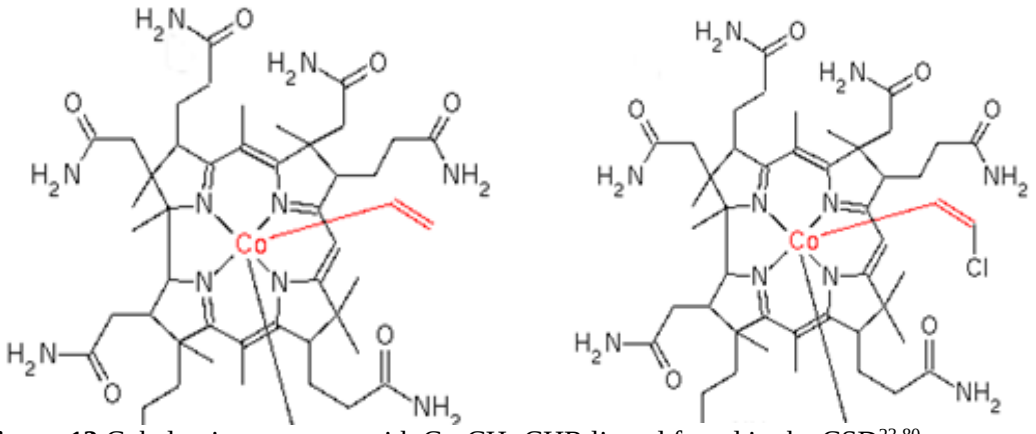

Figure 13. Cobalamin structures with Co-CH=CHR ligand found in the CSD[23,80]

However there were about 10 more structures with the Co-CH=CHR motif that are not cobalamins. The product, which is likely to be a mixture of two species, one in which the phenylvinyl ligand occupies the upper (β) coordination site and the other in which it occupied

the lower (α) coordination site, with displacement of the DMB base, was separated by column chromatography on a C18 resin. The separated compounds were characterised by 2D-NMR methods, relying on the nOe's observed between the phenylvinyl ligand and the protons of the corrin as a diagnostic tool. The reaction conditions were manipulated in order to maximise the yield of one isomer over the other.

Once we were certain that the product has formed and the desired diastereomer isolated, it was crystallized by vapour diffusion of acetone into an aqueous solution of the compound and the crystals produced were analysed by X-ray diffraction crystallography. Then we attempted to measure the bond length of Co-N (c*is*) and Co-NB3 (*trans*) to find out their *trans* and *cis* influence which in turn gave us an idea of the σ donor ability of the phenylvinyl ligand in PhVnCbl.

The σ donor power of the phenylvinyl ligand in PhVnCbl was also assessed by measuring the pK_a value of the Co-DMB base-on ⇌ base-off reaction by UV-vis titration. In addition to providing additional information on the σ donor ability of the alkyl ligand, the log K values for substitution of H_2O in the α-PhVnCbl isomer with CN^- were determined. The value of log K was compared to the values of log K for the reaction R–Co(corr)–H_2O + CN^-⇌R–Co(corr)– CN^- + H_2O for a series of R ligands, allowing the placement of the phenylvinyl moiety in the *trans* effect series in cobalt corrin chemistry.

CHAPTER 2.

Materials and Methods

Deionised water was produced by a Millipore RO unit, and further purified by reverse osmosis using a Millipore MilliQ Ultra-Pure system (18 MΩ -cm). All glassware was washed thoroughly with liquid soap, rinsed with distilled water, rinsed with commercial acetone and dried in an oven set at 100 ℃. The reagents used are listed in Table 3.

Table 3. Reagents used in this study

REAGENT	**SUPPLIER**	**GRADE**
Acetic Acid	BDH	AR
Acetone	Merck	CR
Acetonitrile	Agros-Organics	AR
Argon	Afrox	AR
Hydrochloric Acid	Saarchem	GR
Liquid Nitrogen	Afrox	CP
Methanol	BDH	AR
Nitrogen Gas	Afrox	AR
Nitric acid	Saarchem	GR
Phosphoric acid	Aldrich	AR
Potassium dihydrogen phosphate	Merck	GR
Sodium chloride	Merck	CP
Sodium cyanide	Merck	GR
Sodium hydrogen carbonate	Merck	CP
Zinc	Merck	CP
Vitamin B_{12} (cyanocobalamin)	Roussel	BP
Vitamin B_{12a} (hydroxocobalamin)	Roussel	BP

Key: AR = Analytical Reagent; **CR** = Commercial Reagent; **CP** = Chemically Pure; **GR** = General Reagent; **BP** = Biologically Pure

2.1 General methods

2.1.1 pH measurement

pH measurements were performed using a Metrohm 6.05 pH meter and a 6.0234 combination glass electrode. The instrument was calibrated against the standard buffers potassium hydrogen phthalate (pH 4.004), potassium dihydrogen phosphate/dipotassium hydrogen phosphate (pH 6.863) and borax (pH 9.183) at 25.0 ℃. The acid and base that were used to adjust the pH were HCl and NaOH, respectively. After calibration, the pH was tested with standards of known pH.

2.1.2 Buffers

Buffers used throughout the experiments were tabulated below

Table 4. Buffers commonly used in the experiments

Buffers	**pH**
Phosphate buffer	3
Sodium phosphate buffer	5.45
CAPS buffer	11

2.2 Physical techniques used in this work

2.2.1 High performance liquid chromatography

HPLC was performed using a Phenomenex 5 Micron (5µm particle size) (150 X 4.6 mm) C18 reverse phase analytical column, a Spectra-Physics SP8800 ternary gradient pump, a Linear UV-vis 200 detector (set at 410 nm), and a Varian 4290 integrator. Alternatively, a Dionex Ultimate 3000 pump and photodiode array detector was used. The compounds were separated by gradient elution on a C18 (Büchi model number 28139) reverse phase column at a constant flow rate of 1.00 ml min^{-1}. The mobile phase to be used consisted of acetonitrile, deionized water and a 25 mM phosphate buffer at pH 3. Samples of 10 µl were injected onto the column using a Rheodyne valve and eluted by using a linear gradient elution program as shown in Table 5 below.

Table 5: Gradient Elution Program.

Time	% 25mM Phosphate Buffer (pH:3)	% Deionised Water	% Acetonitrile
0	98	0	2
2	98	0	2
4	75	0	25
6	65	0	35
8	65	0	35
10	75	0	25
12	98	0	2

2.2.2 UV-vis spectroscopy

All UV-vis spectra were recorded on either a Cary 1E or a Cary 3E spectrophotometer, using quartz curvettes with a path length of 1.00 cm. The cell compartment temperature was kept constant with a water-circulating bath kept at 25.0 ± 0.1 ℃. The instruments were allowed to warm up for approximately 20 minutes prior to use to ensure optimum performance.

2.2.3 ESI-MS (Electrospray ionization-Mass spectroscopy)

This technique was used in this study to distinguish between the two different diastereomers, β-PhVnCbl and α-PhVnCbl, by analyzing the mass of the ions produced by the ionization process (Figure 14).

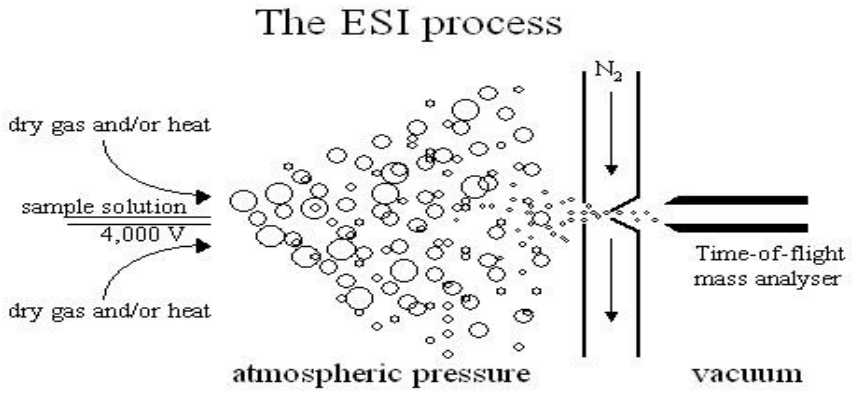

Figure 14. The ESI process[81]

The liquid which contains the analyte is pushed through a very small charged capillary needle that has a high potential difference with respect to the counter electrode. As the charges repel, the liquid pushes itself out of the needle and forms a fine aerosol of small droplets of about

10 µm diameter. The aerosol droplets are repelled from the needle towards the source sampling cone on the counter electrode. As the droplets travel between the needle tip and the cone, evaporation occurs. Due to the extensive solvent evaporation, the typical solvents for electrospray ionization must be prepared by mixing water with volatile organic compounds such as methanol or acetonitrile. As the evaporation occurs, the droplet gets smaller until the surface tension can no longer sustain the charge in a process known as Columbic fission. During the fission, the droplet loses a small percentage of its mass along with a relatively large percentage of its charge. This process is repeated until the analyte is free of solvent and becomes a lone ion which continues along to a mass analyser.

These ions are also known as quasimolecular ions that are created by the addition of a proton denoted as $[M+H]^+$ or removal of a proton $[M-H]^-$ or even by another cation such as sodium, $[M+Na]^+$.

Electrospray ionization (ESI) mass spectra were recorded at the normal scan rate on a Thermo Fischer LXQ instrument. Data were quoted in m/z value (relative abundance) with a mass in the range between 150-2000 at 4000 amu (8 kV).

2.3 NMR spectroscopic techniques

There are a number of relatively new methods in NMR spectroscopy that have proved useful in determining the structure of large and complex molecules such as PhVnCbl, the molecule under investigation in this work.

2.3.1 ROESY (Rotating-frame nuclear Overhauser Enhancement SpectroscopY)

This technique is useful for determining which signals arise from protons that are near each other in space; thus it can be used to elucidate the detailed structural interaction through space. This is used especially when the nOe effect is too weak to be detectable in the range where the rotational correlation time falls, usually with a molecular weight around 1000 Daltons.[82]

2.3.2 COSY (COrrelation SpectroscopY)

This is a useful method to determine which signals arise from neighbouring protons separated by up to 4 bonds. Correlations usually appear when there is spin-spin coupling between protons; the absence of coupling means there will be no correlation.[83]

COSY spectra are often used to determine the atom connectivity in a molecule.

2.3.3 HSQC (Heteronuclear Single Quantum Coherence)

This method is used frequently in NMR spectroscopy of organic molecules or protein molecules. The resulting spectrum is two-dimensional with one axis for ^{1}H and the other for a heteronucleus such as ^{13}C or ^{15}N. This spectrum contains a peak for each unique proton attached to the heteronucleus. Thus, if the chemical shift is known for a specific proton, its coupled heteronucleus chemical shift can also be determined, and vice versa.

2.3.4 HMBC (Heteronuclear Multiple Bond Correlation)

This technique is useful for determining the connectivity between two different nuclear species and is selective for longer range couplings (2-4 bond coupling). This method was first used to assign the non-protonated carbons in AdoCbl.[84]

2.3.5 Experimental details of 500 NMR spectrometer

One-dimensional (^{1}H, $^{13}C\{H\}$), two-dimensional proton homonuclear (COSY, ROESY) and two-dimensional heteronuclear (^{1}H-^{13}C) experiments (HSQC and HMBC) were recorded at 300 K on a Bruker Avance III 300 spectrometer operating at 500.133 MHz (^{1}H) and 125.770 MHz (^{13}C) using a 5-mm PABBO broad band probe. One-dimensional (^{1}H and ^{13}C) NMR experiments were also recorded on the Avance III 300 spectrometer at 300 K operating at 300.131 MHz (^{1}H) and 75.475 MHz (^{13}C) using a 5-mm BBI broad band probe. All NMR spectra were internally referenced to TMS. NMR spectra were processed using Bruker Topspin3.0 (Avance III 500) and Topspin2.1 (Avance III 300) software packages.

2.4 Molecular modelling

A model system based on the crystal structure of PhVnCbl was used for all calculations.

All corrin side chains were replaced by hydrogen atoms, and the α-DMB ligand was truncated to imidazole. Since no geometrical parameters are available for BzCbl, the model system was based on the PhVnCbl crystal structure, constructed by removing the vinyl group from the β-phenylvinyl ligand, and replacing it with hydrogen atoms. DFT geometry

optimizations, employing the RI-J approximation,[85,86,87,88,89] were performed using the ORCA electronic structure package.[90] Calculations were performed with the BP86 functional,[91,92] the TZVP basis set[93] and corresponding auxiliary basis set, and the empirical van der Waals correction of Grimme *et al.*[94] Frequency calculations were performed to obtain the zero-point correction to the electronic energy, as well as to confirm that all structures were at stable energy minima. Reported bond dissociation energies (*BDE*) include a correction for the zero-point vibrational energy, the dispersion energy, as well as a correction for the basis set superposition error (BSSE). The BSSE correction was obtained by performing Counterpoise[95,96] calculations in Gaussian 09 using the optimized geometries obtained from ORCA at the same level of theory. Similarly, the wavefunction files required for the analysis of the topological properties of the electron charge density using the atoms in molecules (AIM) framework of Bader[97,98] were generated in Gaussian 09 using ORCA-optimized geometries by performing a single point calculation at the same level of theory. The topological properties of the electron density (ρ) were evaluated at all the bond critical points (bcp's) using AIMALL.[99]

2.5 Methodology

2.5.1 The synthesis of PhVnCbl using zinc as a reducing agent

A few zinc granules were activated using hydrochloric acid (10 ml, 1 M) so that the zinc oxide surface layer, which forms on passivation of the metal, can be stripped off. The zinc granules were prepared by washing thoroughly with acetone and drying before being placed within a 250 ml two-necked round-bottomed flask. Argon gas was bubbled through the flask which was sealed with a rubber suba-seal with a needle inserted to allow for the escape of gas.

CNCbl (200 mg, 1.58 x 10^{-1} mmol) was dissolved in 50 ml of a 10% acetic acid /methanol solution and placed within a 100 ml two-necked, round-bottomed flask. Argon gas was bubbled through the flask which was sealed with a rubber suba-seal with a needle inserted to allow for the escape of gas. After approximately 20 minutes, the needle was removed from the flask containing the zinc chips and the red CNCbl solution was transferred into it using a metal cannula. The colour of the solution rapidly turned from red to brown to gray indicating the presence of cob(I)alamin in the solution. After reduction of the metal, phenylacetylene solution (1730 µl) was added under red light and left to react for a few hours. The product

mixture was transferred back into a round-bottomed flask using a metal cannula, leaving the zinc granules behind. The progress of the synthesis was monitored using HPLC.

2.5.2 Activation of a C18 column

Activation of a C18 column (dimensions: 230 x 15 mm) was commenced by passing 100 ml of water at a rate of 15 ml min^{-1}, 100 ml of MeCN/H_2O (50:50) at a rate of 10 ml min^{-1} and then followed by 100 ml of 0.025 M buffer (pH 3) at a rate of 15 m min^{-1}. Another 100 ml of MeCN/0.025 M buffer (50:50) was passed through the column at a rate of 10 ml min^{-1}. Finally, 200 ml of buffer was passed through at a rate of 15 ml min^{-1}. The product in methanol was inserted into the C18 column system using a 10 µl of syringe and the collected product was analyzed using HPLC.

2.5.3 Method of separation

The product solution was evaporated on a rotatory evaporator at 50 ℃ until only the product red film remained. The red film was dissolved in a small amount of methanol and filtered through cotton wool with a syringe before being separated on a C18 column.

2.5.4 Crystallography

The β-PhVnCbl was set up for crystallization using a deionized water/acetone solvent system as follows.

The product was dissolved in a small volume of deionized water and placed within a small glass vial which was in turn placed in a larger glass vial containing a small volume of acetone. The larger vial was sealed while still allowing space for the evaporation of the acetone into the product mixture. The vial was then covered with foil and placed in the fridge and left to crystallize. After two weeks, crystals formed; one was chosen by visual examination under a microscope and analyzed using X-ray diffraction. Intensity data for PhVnCbl were collected at 173(2) K on a Bruker APEX II CCD area detector diffractometer with graphite monochromated Mo K_α radiation (50 kV, 30 mA) using the APEX 2[100] data collection software. The collection method involved ω-scans of width 0.5° and 512 × 512 bit data frames. Data reduction was carried out using the program *SAINT+*[101] and multiscan absorption corrections applied using *SADABS*.[101] The crystal structure was solved by direct methods using *SHELXS-97*.[102] Non-hydrogen atoms were first refined isotropically followed

by anisotropic refinement (with the exception of the acetone molecule) by full matrix least-squares calculations based on F^2 using *SHELXL-97*.[102] Hydrogen atoms were first located in the difference map then positioned geometrically and allowed to ride on their respective parent atoms, with isotropic thermal parameters fixed at 1.2 (CH, CH_2 and NH_2) or 1.5 (CH_3 and OH) times those of their corresponding parent atoms. Oxygen O15 on the ribose group was found to be disordered and refined over two positions with the aid of SADI, DELU and SIMU restraints. The final occupancies for O15A and O15B were 0.854(12) and 0.146(12), respectively. The acetone molecule was refined isotropically with FLAT, DFIX, DELU and SIMU being used in the final refinements to restrain the molecule to a reasonable geometry. It was not possible to locate the hydrogen atoms on the water molecules. The contribution of these hydrogen atoms has, however, been accounted for in the chemical formula and related data such as crystal density and F(000).

Refinement converged as a final R_1 = 0.0975 (wR_2 = 0.2590 all data) for 9586 observed reflections [I >2σ(I)]. Figures were prepared using ORTEP-3.[103] Details of the crystallographic data are given in the Appendix A.

2.6 pK_a titration

2.6.1 β-PhVnCbl

Several drawn out capillary tubes were prepared using a Bunsen burner. The water bath was connected to the pH meter and a pump. To clean the system before use, 40 ml of a water/methanol solution (1:1) was added into the thermostat glass bottle and two pipes were placed below the level of the glass bottle. The pump was switched on and left to run for 20 minutes to clean out the system. This cleaning process was repeated several times until the system was clear. The pH meter was calibrated at 25 ℃. $NaHPO_4$ buffer (40ml, 0.025 M), was then placed in the thermostat glass bottle together with a stirrer bar, cleaned 2 pipes and the electrode. The product solution which contained a mixture of 5 ml of buffer and 1 ml of concentrated β-PhVnCbl was prepared in a small vial, while the buffer in the thermostat glass bottle was left to circulate with the cuvette inside the UV-vis spectrometer. Approximately 2 ml of the product solution was transferred into the thermostat glass bottle under red light and allowed to mix thoroughly with the buffer solution. The pH was adjusted between 8.5 and 1.5 in increments of approximately half a pH unit. At each step, a spectrum, as well as the exact pH was recorded.

2.6.2 α-PhVnCbl

Same procedure as above but in the pH range of 7-14.

2.6.3 log K titration

The UV-vis spectrophotometer was switched on 20 minutes before to ensure optimum performance. Mixture of the CAPS buffer solution (2.4 ml) and the concentrated product solution of either α-PhVnCbl or β-PhVnCbl (125 µl) were transferred into a non-reference cuvette in red light. Addition of a CN stock solution (1 M) from 1 µl to 34 µl into the product solution was monitored by UV-vis spectroscopy.

2.7 Photolysis

2.7.1 α-PhVnCbl

After α-PhVnCbl solution was separated from β-PhVnCbl via C18 column chromatography, it was desalted and evaporated to dryness in a round bottomed flask via rotatory evaporator at 50° C. A small amount of sample, reconstituted in deionized water was added to a cuvette which in turn containing 0.1 M phosphate buffer at pH 7. This cuvette was then placed on the work bench to expose in the sun light for 4 hours and monitored in the UV-Vis spectroscopy.

2.7.2 β-PhVnCbl

Same procedure as above.

Chapter 3.

Results and discussion

3.1 UV Spectroscopy and the detection of cobalt (III) corrinoids

UV-vis spectroscopy is a useful analytical tool for the study of cobalt(III) corrinoids as they exhibit a range of different colours; they also have high extinction coefficients so very little sample is required, making this technique experimentally useful for their analysis. CNCbl and H_2OCbl^+ produce what is called a "typical" cobalt corrinoid spectrum with the most prominent bands occurring above 300 nm (Figure 15).[19] The most distinguishing feature of a typical UV-vis spectrum is the γ band, which is particularly intense, occurring at around 360 nm in the case of CNCbl, and 350 nm in H_2OCbl^+. Other bands such as the α and β bands correspond to lower energy transitions are observed in the 450-600 nm range.

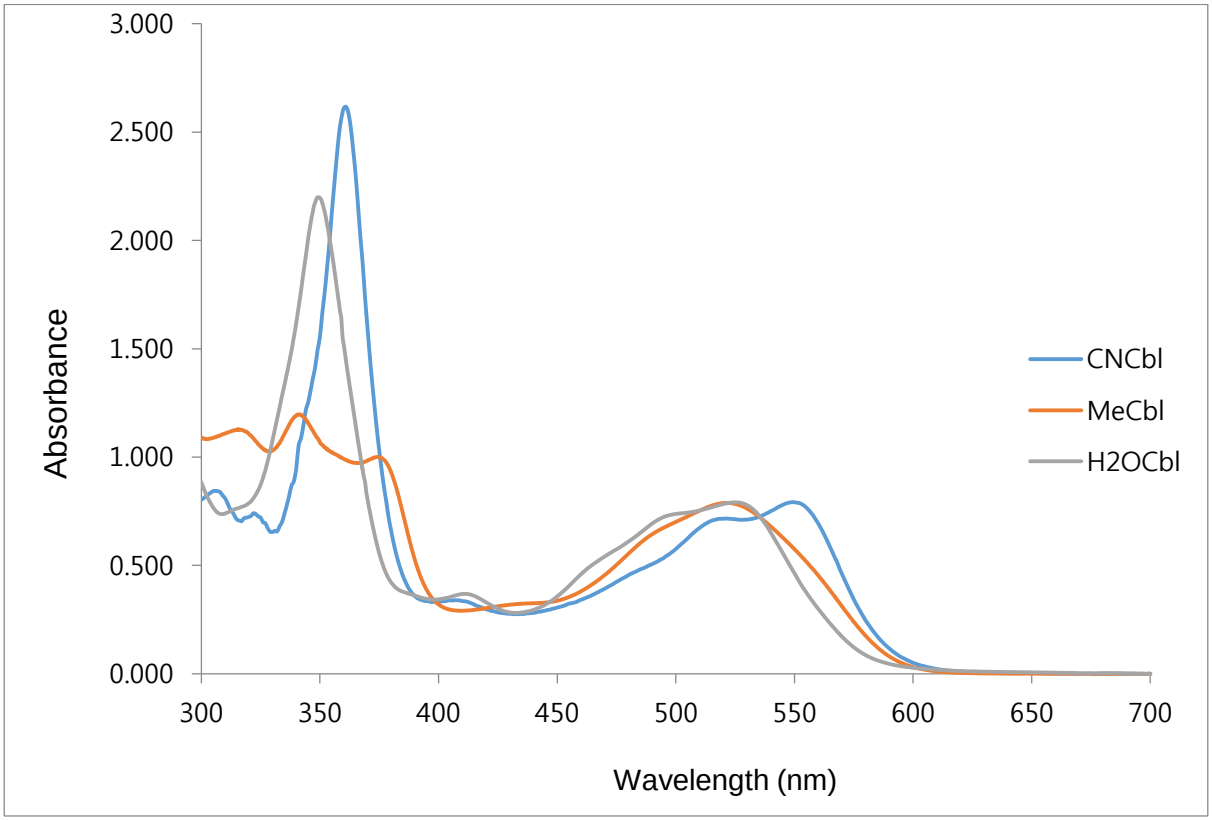

Figure 15. The "typical" UV-vis spectrum of CNCbl and H_2OCbl^+, and the "atypical" spectrum of MeCbl

In contrast, the UV spectrum of the alkylcobalamins differs considerably from that of CNCbl and H_2OCbl^+. Differences in the bands arise due to changes in the electron density of the corrin ring's nitrogen atoms which implies they are dependent on the nature of the axial ligand.[104] This can be explained by differences in the degree of configuration interaction between the "typical" and "atypical" cobalamins in Figure 15. Configuration interaction

occurs between the second electronic transition (the γ band), and the third electronic transition occurs close to 400 nm and results in two transitions: one weak and one strong. The corrin ring has 7 π orbitals that are the highest occupied π orbitals which are affected to the greatest extent by the nature of the axial ligand.[104] This implies that strong σ donors such as alkyl ligands tend to increase the degree of orbital overlap between the upper ligand axial and the cobalt metal ion. This in turn decrease the energy of the gap between the frontier orbitals, resulting in a shift of α, β and γ bands towards a longer wavelength together with a decrease in the intensity of the γ band (see Figure 15 for the spectrum of MeCbl as an example). By contrast, poor σ donor ligands such as the aqua ligand result in less orbital overlap and thus a greater gap between the frontier orbitals, which results in a shift of the α, β and γ bands towards shorter wavelengths together with an apparent increase in the intensity of the γ band as the multiple transitions that make up that band move closer together in energy (See Figure 15 for the spectrum of H_2OCbl^+).

UV-vis spectroscopy was extensively used in this study as indicated in the appropriate sections below.

3.2 Synthesis of PhVnCbl

The main objective of this project was to synthesize and characterize PhVnCbl. The synthesis of the PhVnCbl was initiated by reducing CNCbl using zinc granules in a 10% acetic acid/methanol solution under argon. The electrophilic addition of the phenylacetylenyl ligand was accomplished by addition of a 100 molar excess of phenylacetylene into the reaction mixture under red light conditions (refer to Chapter 2 for full details of experimental synthesis).

High performance liquid chromatography on a reverse phase C18 column was used to monitor the progress of the reaction. The difference in the peak areas between the reactants and products, as well as their retention times, provided insight into the progress of the reaction. The HPLC trace collected directly after the addition of phenylacetylene is shown in Figure 16.

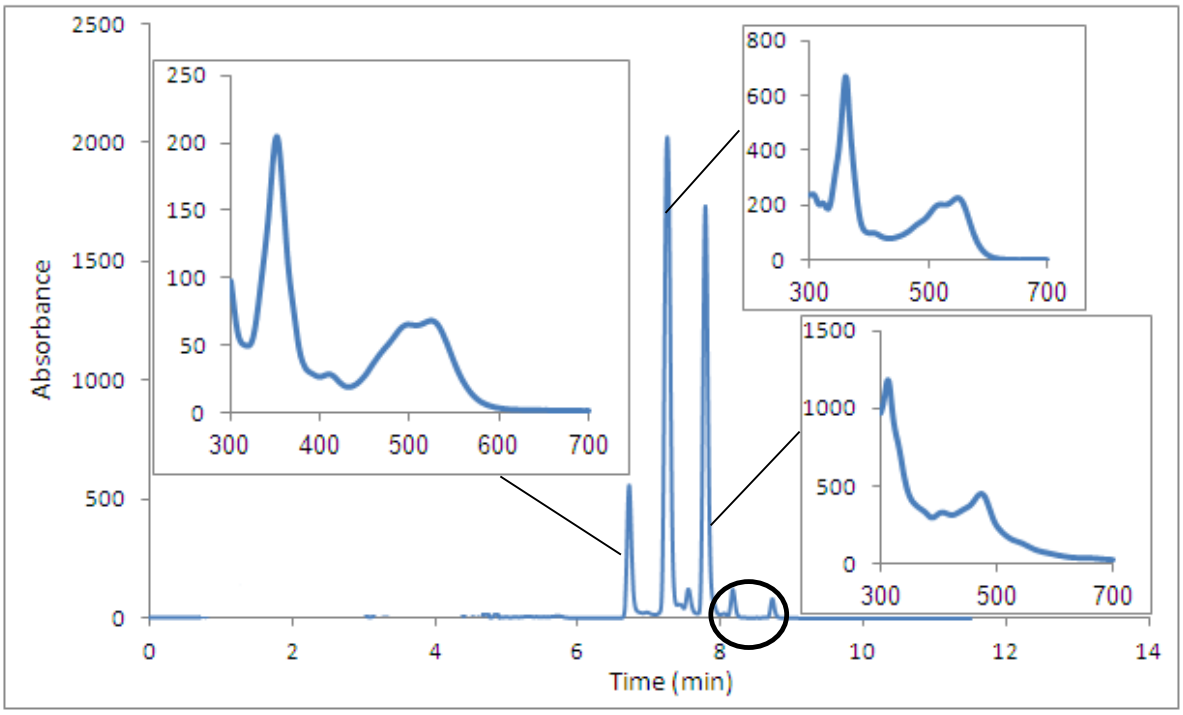

Figure 16. HPLC trace and corresponding UV-vis spectra obtained directly upon addition of phenylacetylene to a MeOH/acetic acid solution of reduced cobalamin.

The results show that initially, there are three major components. The first peak with a retention time of 6.7 minutes indicates the presence of H_2OCbl^+ (formed on the HPLC column by partial oxidation of the reduced Co(I)/Co(II) back to Co(III)). The UV-vis spectrum of the second peak (retention time = 7.3 minutes) indicates the presence of unreacted CNCbl. Finally, the third major peak, with a retention time of 7.8 minutes is unreacted cob(II)alamin. The two small peaks with retention times of 8.3, and 8.8 minutes, respectively, and highlighted by a circle in Figure 16, are assigned to the formation of the alkyl cobalamin product. Both peaks have corresponding "atypical" UV-visible spectra (shown in Figure 16) that are characteristic of alkylcobalamins. Previous studies have shown that under certain conditions, the alkyl group can substitute at both the α and β positions.[50] We thus assign these two peaks to the α- and β-phenylvinylcobalamin diastereomers (confirmation of this is provided by X-ray diffraction, NMR spectroscopy, mass spectrometry, and photolysis; see sections 3.3.1, 3.3.2, 3.3.3, and 3.3.4). The retention times of the peaks can be rationalized as follows. Non-polar compounds will have a greater affinity for the stationary phase of the column than polar compounds, and will thus elute after the latter. H_2OCbl^+, being more polar than CNCbl will elute first, and PhVnCbl, with a large non-polar alkyl ligand will have longer retention times than both H_2OCbl^+, and CNCbl..

During the course of the reaction, the intensities of the first three peaks decreased, while the two product peaks increased (Figure 17). The reaction was assumed to be complete once the first three peaks had almost disappeared. The relative height of the two product peaks was roughly 1:1.

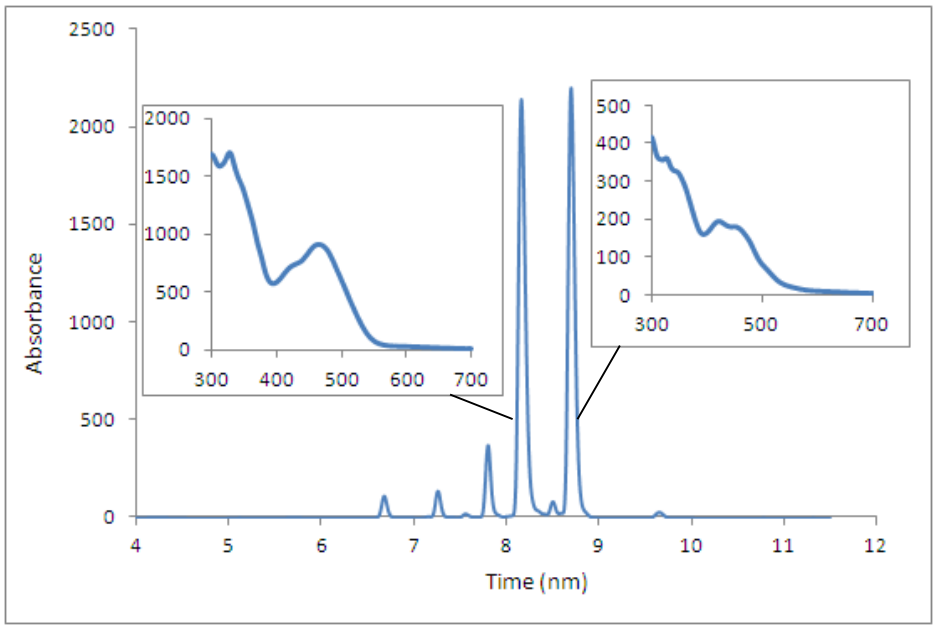

Figure 17. HPLC trace for the synthesis of PhVnCbl collected near completion of the reaction.

The UV-vis spectra corresponding to each diastereomer is indicated. In an attempt to determine if formation of one of the diastereomers could be favoured over the other, a separate experiment was conducted where a hair drier was used to heat up the reaction for about 4 hours. An HPLC trace collected upon completion of the reaction is shown in Figure 18. The relative area under the first product peak (at 8.3 min) corresponds to around 45% while the second product peak (at 8.8 min) is roughly 55%. It thus appears that the second product is thermodynamically slightly favoured upon heating.

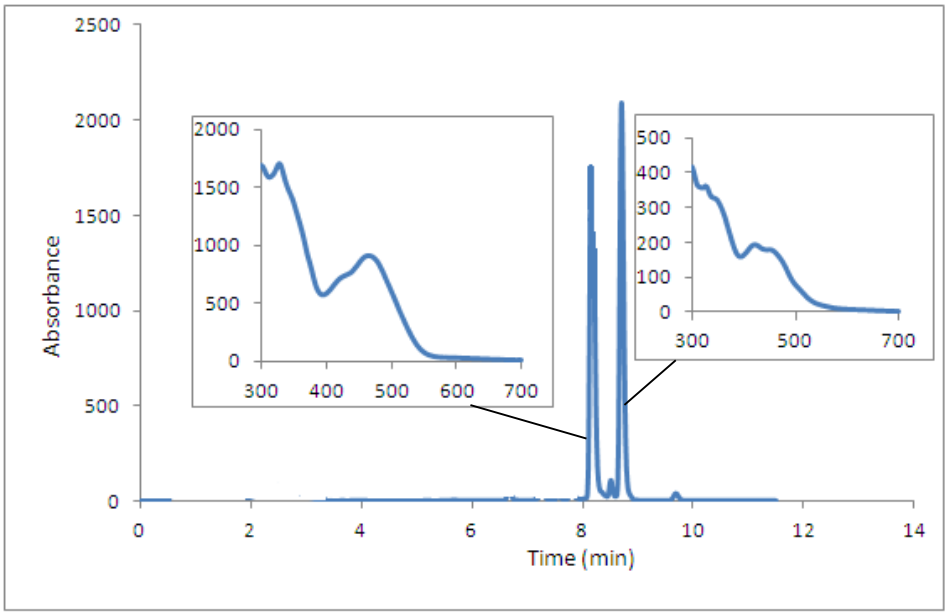

Figure 18. HPLC trace obtained after heating up the PhVnCbl synthesis reaction. The relative area under the two peaks is roughly 45% and 55%, respectively, indicating that formation of the second product is slightly favoured.

The same reaction was then repeated under reduced temperature conditions by placing the reaction vessel in an ice bath for about 4 hours. As expected, the reaction was much slower, and the HPLC trace, collected upon completion of the reaction, is shown in Figure 19.

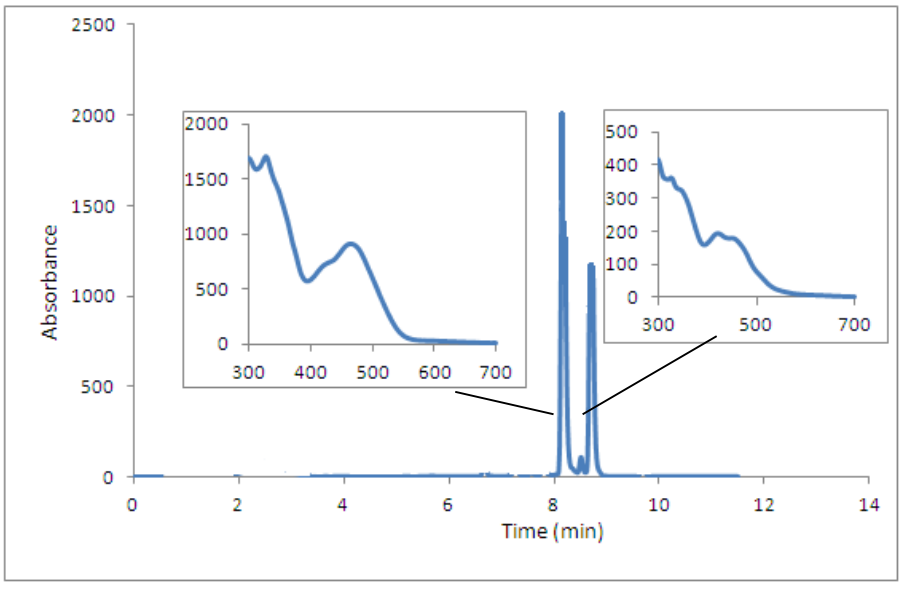

Figure 19. HPLC trace obtained at the reduced temperature of the PhVnCbl synthesis reaction. The relative area under the two peaks is roughly 65% and 35%, respectively, indicating that formation of the first product is favoured.

This time, under reduced temperature conditions, the relative area under the first product peak (65%) was bigger than the second product peak (35%) which implies that the reduced temperature favoured formation of the first product.

Separation of these two products was done by C18 column chromatography which separates compounds according to their polarity. The mobile phase was an acetonitrile/phosphate buffer (25 mM, pH 3). Activation of the C18 column was accomplished according to the procedure that was mentioned in Chapter 2. The product was dissolved in a minimum amount of water and injected with a 10 µl syringe into the C18 column system and eluted at a flow rate of 3 ml/min. The ratio of acetonitrile to the phosphate buffer was steadily increased from 0:100 up to 40:60 to effect the elution of the two main products off the column. Fractions collected off the column were analysed by HPLC, and were pooled together if they were shown to contain the same compound (Figure 20).

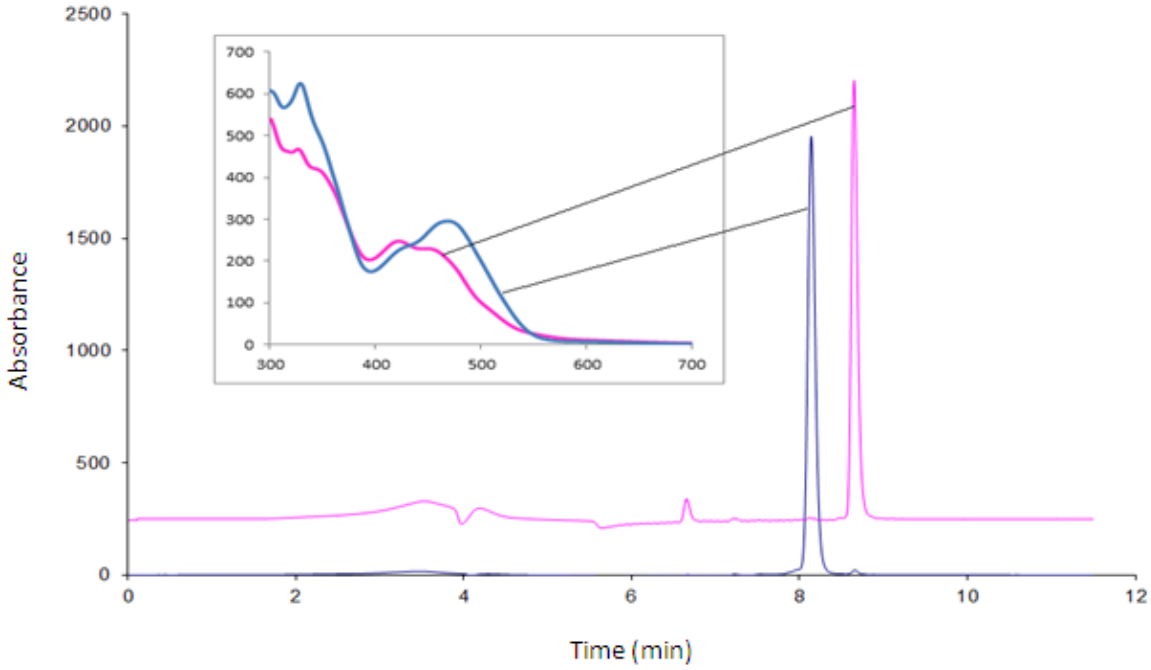

Figure 20. An overlay of the HPLC traces of the separated products. The corresponding UV-vis spectrum for each product is also shown.

The procedure used to identify which peak corresponds to the α or β diastereomer is discussed in the next section.

3.3 Product Analysis

3.3.1 X-ray Diffraction Crystallography

Once both diastereomers (α and β) had been separated, a small amount of each was prepared for crystallization. This involved dissolving the separated products in a minimum amount of deionised water, and placing each separately into a small glass vial. This vial was in turn placed into a larger glass vial which was half-filled with acetone, sealed, and placed in a refrigerator (4 ^{o}C) to allow the acetone[123] to slowly diffuse into the aqueous solution (cobalamins are soluble in aqueous media, but not in acetone). After approximately three weeks, crystals appeared for one of the isomers, but not the other; we immediately suspected that the product that crystallised was the β isomer, as to our knowledge, attempts to crystallise free α-substituted cobalamins, where the DMB base is detached, have to date been unsuccessful. X-ray data on a suitable crystal were collected, and our initial assignment was confirmed upon solving the structure. Interestingly though, at the onset of this work, we suspected that coordination of the alkyl ligand would be through the terminal alkene carbon as illustrated in Figure 21 A). However, what we found is that it coordinates through the β carbon in the manner illustrated in Figure 21 B).

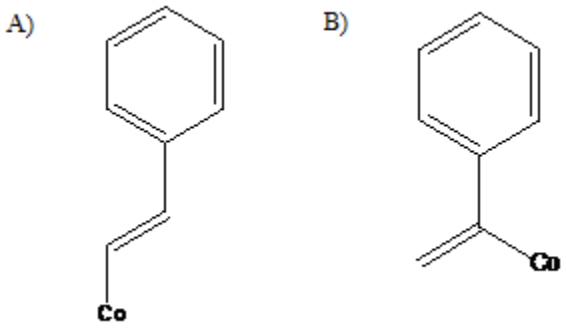

Figure 21. A) Simplified diagram indicating how we initially thought the phenylvinyl ligand would coordinate to the cobalt centre B) Simplified diagram of the actual mode of coordination of the phenylvinyl ligand as obtained by x-ray diffraction.

The ORTEP diagram in Figure 22 was obtained after solving the crystal structure. The crystallographic results are summarised in the Table 6 below.

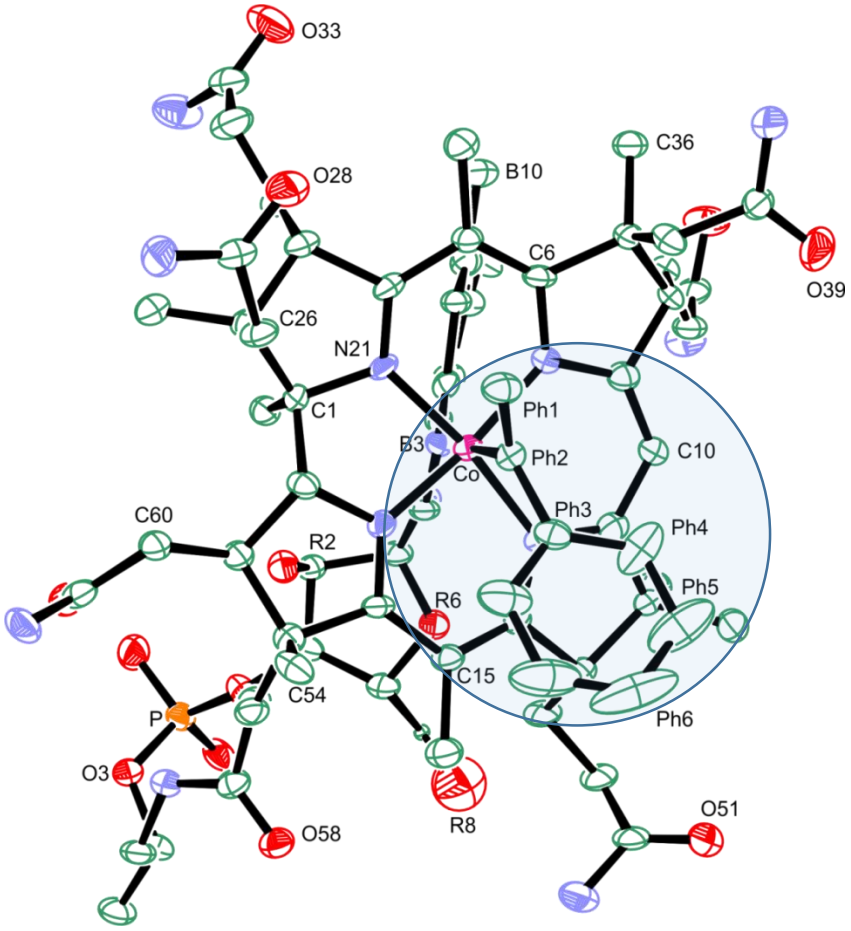

Figure 22. ORTEP diagram of β-PhVnCbl with non-H atoms drawn as 30% probability ellipsoids. For clarity, hydrogen atoms were removed.

Table 6. Crystal structure results

Empirical formula	$C_{73}H_{131}CoN_{13}O_{30}P$
Formula weight	1760.81
Temperature	173(2) K
Wavelength	0.71073 Å
Crystal system	Orthorhombic
Space group	$P2_12_12_1$
Unit cell dimensions	a = 15.7783(7) Å b = 22.3400(9) Å c = 25.1607(14) Å
Volume	8868.8(7) Å^3
Z	4
Density (calculated)	1.319 Mg m^{-3}
Absorption coefficient	0.296 mm^{-1}
F(000)	3768
Crystal size	0.48 x 0.17 x 0.15 mm^3
Theta range for data collection	1.52 to 26.00°.
Index ranges	$-18 \leq h \leq 19$, $-27 \leq k \leq 27$, $-31 \leq l \leq 13$
Reflections collected	47932
Independent reflections	17377 [R(int) = 0.0884]
Completeness to theta = 26.00°	99.9 %
Absorption correction	None
Refinement method	Full-matrix least-squares on F^2
Data / restraints / parameters	17377 / 59 / 1048
Goodness-of-fit on F^2	0.984
Final R indices [$I > 2\sigma(I)$]	R_1 = 0.0975, wR_2 = 0.2590
R indices (all data)	R_1 = 0.1652, wR_2 = 0.3001
Absolute structure parameter	0.07(3)
Largest diff. peak and hole	0.643 and -0.501 e Å^{-3}

3.3.2 Crystal packing analysis

Examination of the crystal packing reveals that the cobalamin molecules hydrogen bond to each other and to water molecules within the structure (see Figure 23). There are four molecules found in the unit cell. Removing the water molecules indicates that they fill channels as shown in Figures 23 to 26. Looking closer at the hydrogen bonding between the cobalamin molecules after removal of the water molecules shows an extensive hydrogen bonding network between these molecules. An example is illustrated in Figure 23 in which a complex hydrogen bonding network is formed in the ab plane of the unit cell by the combination of just three unique hydrogen bonds such as H10A-O5 (O5 of the amide of the *e* side chain is hydrogen bonded to N10 of a neighbouring *g* side chain amide (2.899 Å), H5A-

O4 (O4 of the *d* amide is hydrogen bonded to amide N5 of the *a* side chain of a neighbour (2.949 Å), and H9A-O1 (O1 of the *a* side chain amide hydrogen bonds to N9 of the *e* side chain amide of an neighbouring molecule (O···N = 2.987 Å). The hydrogen bonding between molecules probably templates where the channels will form, although it is likely that the solvent water occupying the voids has a structure-determining role[74] as well. The solvent channels have an approximately helical shape.

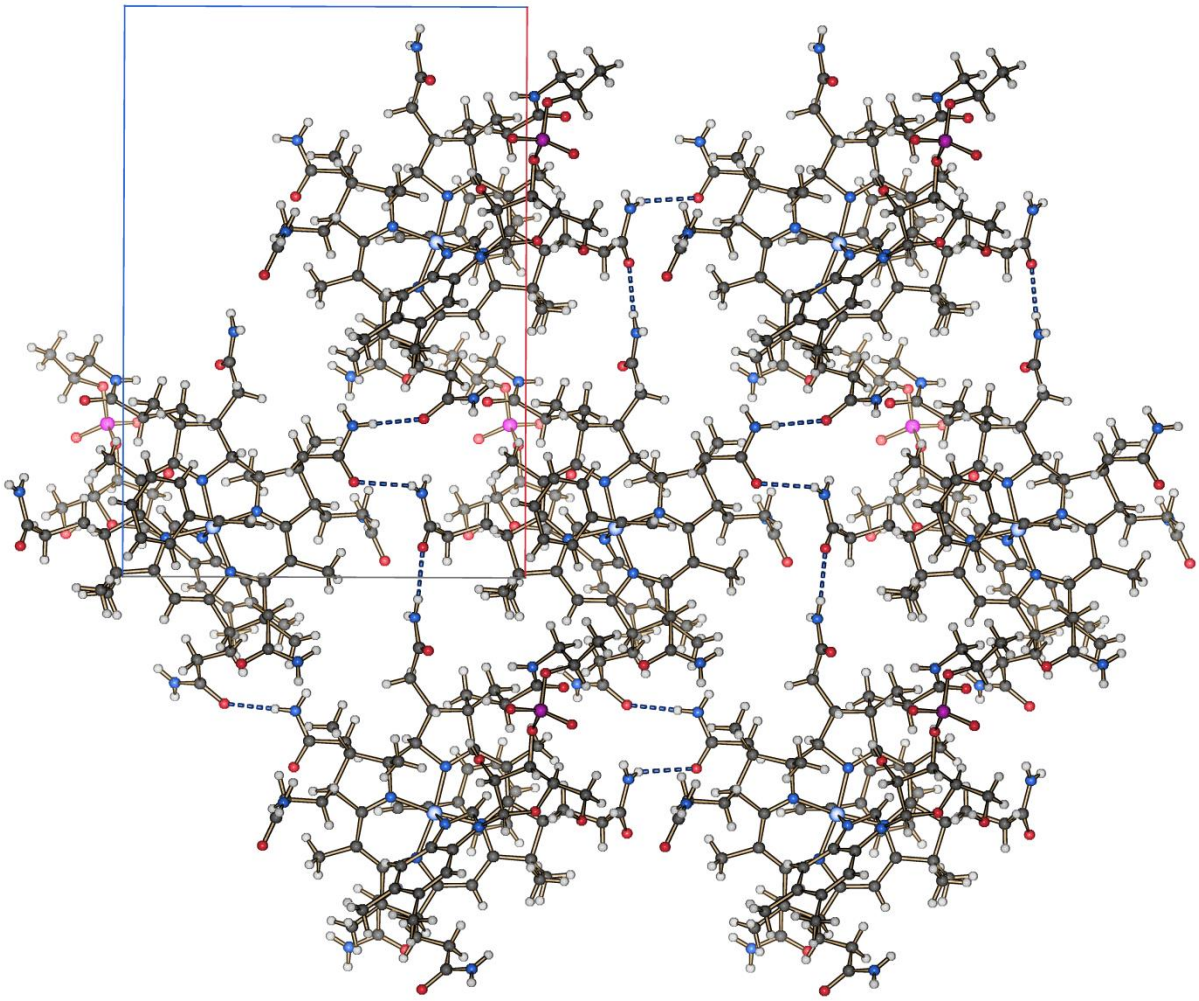

Figure 23. The solid state structure of *β*-phenylvinylcobalamin showing hydrogen bonding between cobalamin molecules. O1 of the *a* side chain amide hydrogen bonds to N9 of the *e* side chain amide of an neighbouring molecule (O···N = 2.987 Å); N7 of the *c* side chain amide hydrogen bonds to phosphate O10 of a neighbouring molecule (2.995 Å); O4 of the *d* amide is hydrogen bonded to amide N5 of the *a* side chain of a neighbour (2.949 Å); O5 of the amide of the *e* side chain is hydrogen bonded to N10 of a neighbouring *g* side chain amide (2.899 Å); and N6 of the *b* side chain is hydrogen bonded to a neighbouring phosphate O10 (2.964 Å). Also, there are many hydrogen bonds between solvent water and the ribose OH groups, and the amides of the acetamide and the propionamide side chains of the corrin.

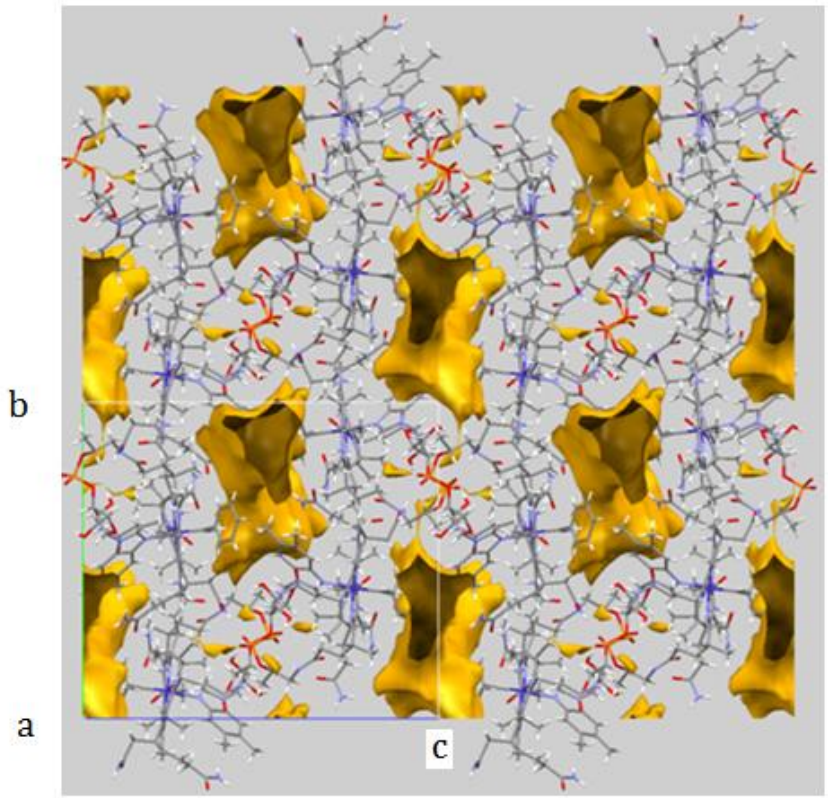

Figure 24. Channels of molecules and voids showing in the bc plane of the unit cell

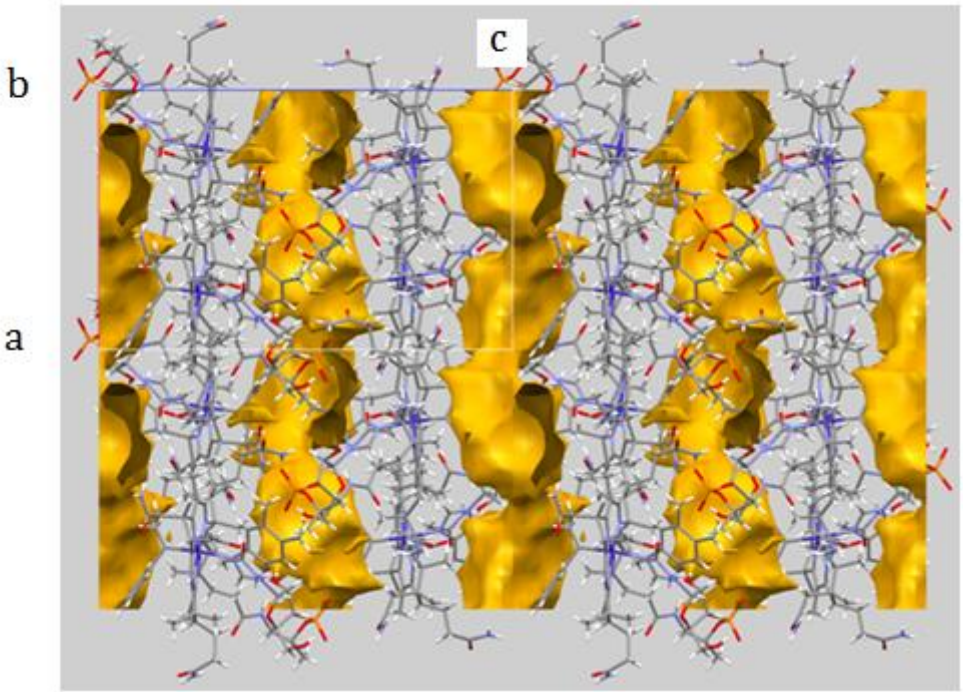

Figure 25. Channels of molecules and voids showing in the ac plane of the unit cell

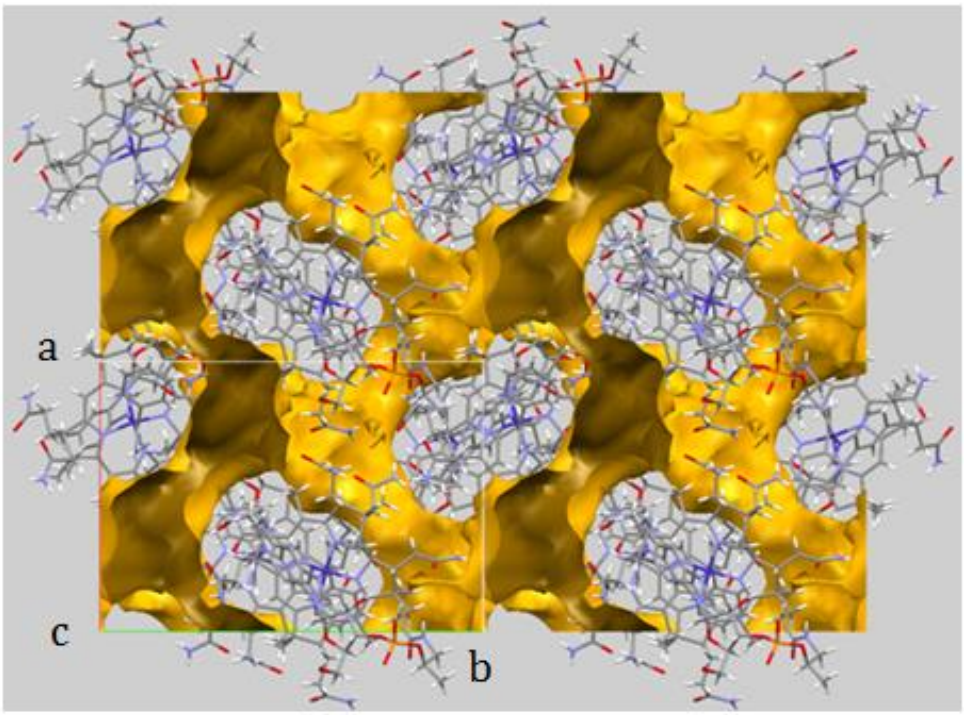

a

Figure 26. Channels of molecules and voids showing in the ab plane of the unit cell

3.3.3 Structural data for the alkyl cobalamins

Table 7. Co–C, Co–NB3, and Co–N bond lengths of various alkyl cobalamins

Alkylcoblamins	Co–C	Co–NB3	Average Co-N21 and Co-N24 bond length	Average Co-N22 and Co-N23 bond length	References
CNCbl	1.87 (4)	2.04 (2)	1.89 (1)	1.91 (1)	105,106,66,107,108,109
Chlorovinyl	1.953	2.144	1.915	1.892	23
VinylCbl	1.912	2.164	1.915	1.878	23
MeCbl	1.983 (6)	2.17 (2)	1.921	1.866	66
AdePrCbl	2.001	2.191	1.852 (7)	1.886 (7)	110
PhVnCbl	2.019 (9)	2.225 (7)	1.903	1.878	This work
EtCbl	2.023	2.232	1.910	1.870	40
AdoCbl	2.023 (6)	2.236 (2)			66,67,65
n-ButylCbl	2.031	2.244	1.912	1.873	40
IsoamylCbl	2.044	2.277	1.915	1.854	74

✧ In some instances there was more than 1 structure available from the CSD for a particular compound. In such cases, bond lengths were averaged and reported with their associated standard deviations in brackets.

The Co–C and Co–NB3 axial bond lengths of β-PhVnCbl obtained from the crystallographic analysis were found to be 2.019 (9) Å and 2.225 (7) Å, respectively. The average Co–C and Co–NB3 bond lengths for CNCbl (the starting material) are 1.87 (4) Å, and 2.04 (2) Å, respectively (see Table 7). When comparing these axial bond lengths to those for β-PhVnCbl, the latter are much longer. This is especially true for the Co–NB3 (β-PhVnCbl) bond length (0.185 Å longer) illustrating the inverse *trans* influence that is induced by the attached phenylvinyl ligand. As the bulkiness of the β ligand increases, greater steric repulsion occurs between the β ligand and the corrin ring which leads to lengthening of both the Co–β (steric *cis* influence) and the Co–NB3 bonds (steric *trans* influence).[58] Usually all alkyl cobalamins exhibit the inverse *trans* influence rather than the normal *trans* influence. This is evident from Table 7 above, and Figure 27 below. It is also clear from Table 7 that the *trans* influence of the alkyl group is much larger than the *cis* influence; the difference between the isoamylCbl (a strong σ-donor) and MeCbl (a weaker σ-donor) Co–NB3 bond lengths is 0.107 Å, whereas the difference for the average of the Co–N21 and Co–N24 bond lengths is 0.012 Å, and for the average of the Co–N22 and Co–N23 bond lengths is 0.006 Å, respectively, for the same two alkyl derivatives.

Figure 27 shows that a strong correlation (R^2 = 0.99) exists between the lengths of the upper-axial Co–C and lower-axial Co–NB3 bonds in alkylcobalamins. An increase in the bulkiness of the β-ligand results in an increase in both the Co–C and Co–NB3 bond lengths. It is clear from the table above that the three vinyl structures also fit in this trend. In fact, it is rather remarkable that PhVnCbl is even stable in aqueous solution at room temperature, because due to the bulky phenyl ligand coordinated to the Co, this should have rather long and weak axial ligands (Co-C and Co-NB3) but since the Co is also coordinated to the vinyl ligand the Co-C bond is made so much stronger. Hence the whole complex is stable.

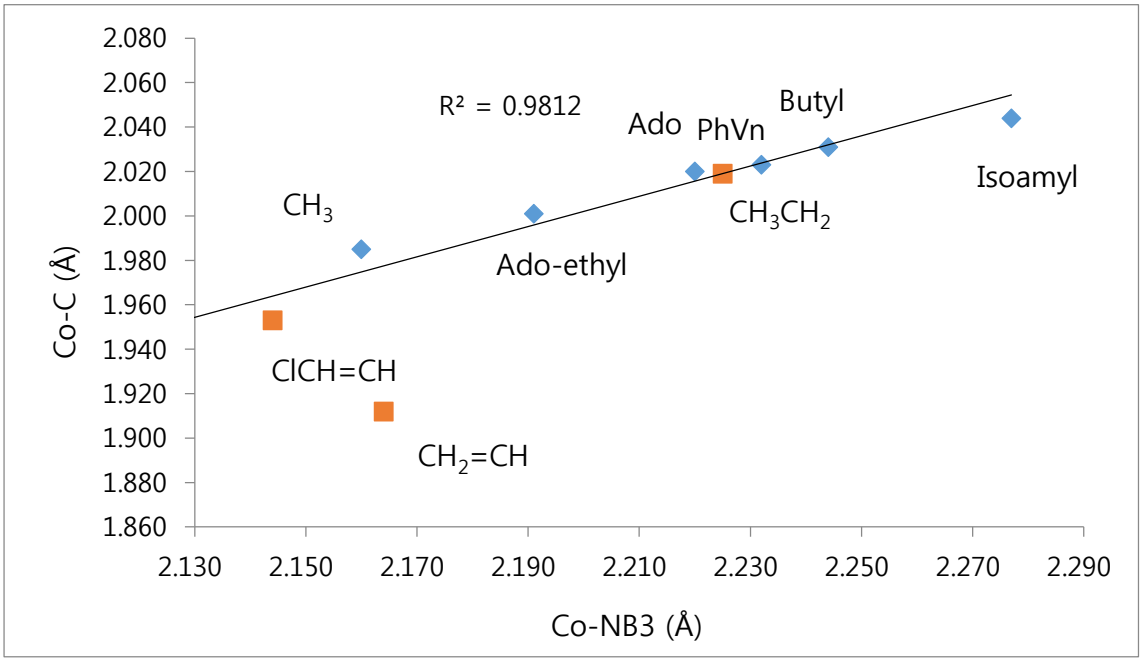

Figure 27: The relative Co–NB3 and Co–C bond lengths of alkyl cobalamins including vinyl structures such as PhVnCbl, ChlorovinylCbl and VinylCbl indicated as a square (Explanation for this is as follows)

Benzylcobalamin (structurally similar to PhVnCbl, but without the vinyl group) has been found to be very unstable at room temperature due to the postulated mechanism illustrated in Figure 28 below (the mechanism is for neopentylcobalamin, but is also applicable to benzylcobalamin).[111] Synthesis of alkylcobalamins is usually carried out under acidic conditions where the DMB base is dissociated from the Co. Coordination of the benzyl groups results in a downward folding of the corrin ring due to steric repulsion between the phenyl ring and the corrin. Under neutral conditions, the DMB base reattaches to the Co, and due to it also being bulky, causes an upward folding of the macrocycle. This in turn puts steric pressure on the β ligand, potentially causing the Co–C bond to break homolytically. The result is that benzylcobalamin has a half- life of only 5 minutes.[112]

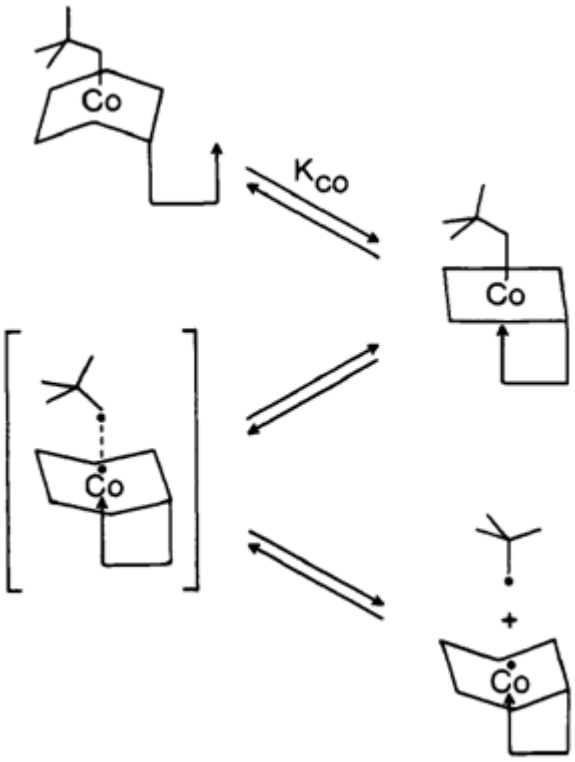

Figure 28: Schematic diagram of the corrin conformational changes in the axial base induced homolytic Co–C bond cleavage of neopentylcobalamin. (Benzylcobalamin also has the same mechanism)[111]

The vinyl group in PhVnCbl therefore appears to stabilize the molecule. It is possible that electron density from the C=C bond is transferred to the Co–C bond strengthening the latter. If this was the case, then the C=C bond length in PhVnCbl should be longer than the corresponding C=C bond length in free styrene. A CSD search for all free styrene structures returned 4 hits where the average C=C bond length was 1.292 Å and the standard deviation 0.07 Å. The C=C bond length for PhVnCbl (1.333 Å, Figure 29. A)) is not significantly different from this (although it is slightly longer than the mean C=C bond in styrene, it falls within the standard deviation range). In addition, a plot of the C=C vs the Co–C bond lengths for the three vinyl structures (Figure 30) does not indicate any clear correlation between the two (although it must be noted that there are only three points in this plot; more data points are needed to draw any definite conclusions). There does seem to be a better correlation between the lengths of the C=C and Co–DMB bonds which suggests that the Co–DMB bond gets longer as the length of the C=C bond increases. As mentioned above, inverse trans-effects are known to operate in alkyl cobalamins; both axial bonds get longer as the σ-donor ability of the β-ligand increases. Therefore, if this relationship is genuine, then perhaps the presence of the C=C bond does have an effect on the Co–C bond. Once again more cobalamin structures containing a β-vinyl group are required to verify this.

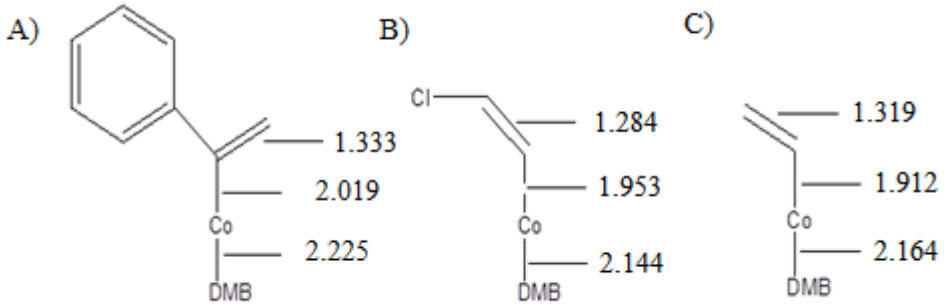

Figure 29. A) Simplified diagram of PhVnCbl indicating its vinyl, Co–C and Co–NB3 bond lengths B) ChlorovinylCbl indicating each bond lengths C) VnCbl indicating each bond lengths

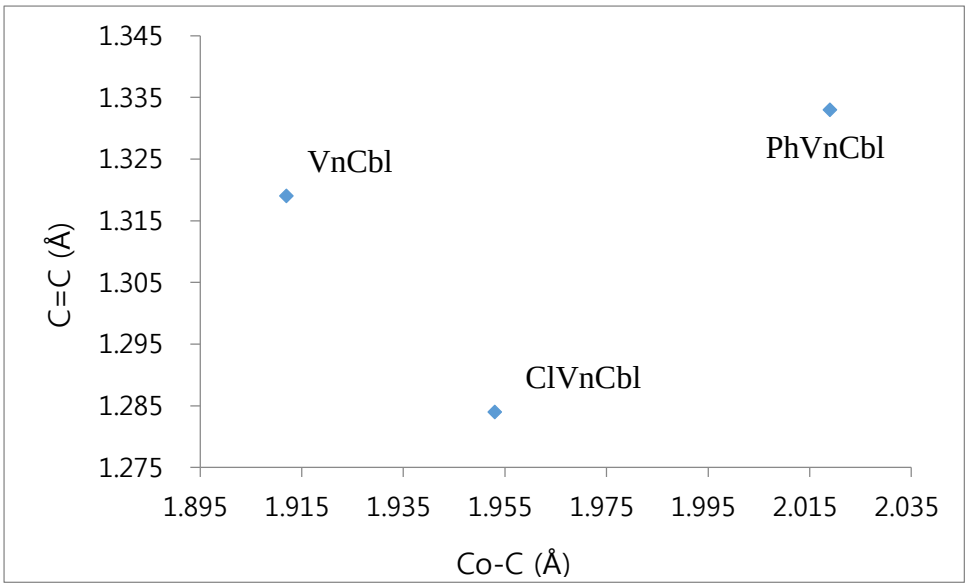

Figure 30. The relative bond lengths of all three vinyl cobalamins (C=C vs Co-C)

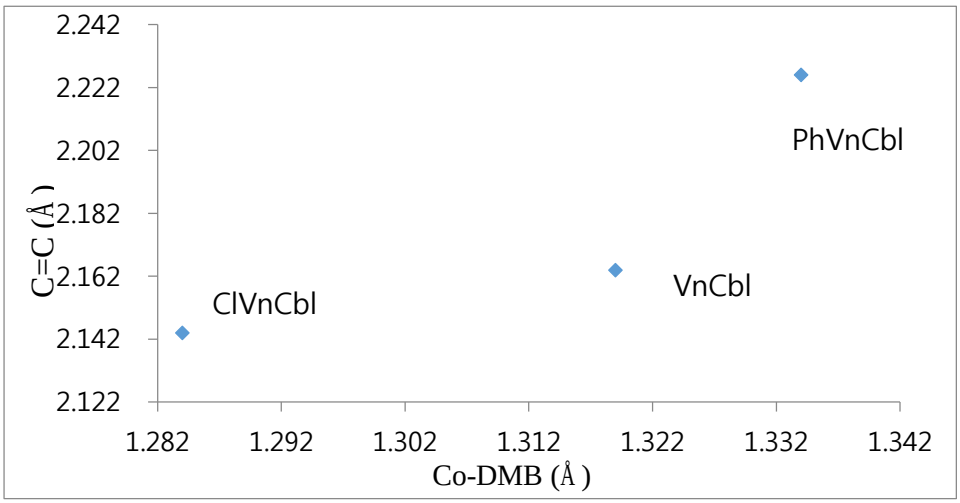

Figure 31. The relative bond lengths of all three vinyl cobalamins (C=C vs Co-DMB)

As mentioned in the introduction, the fold angle φ is indirectly proportional to the length of the Co–NB3 bond.[58] This means that as the bulkiness of the β-ligand increases, the corrin ring flattens out (and hence φ decreases), which in turn results in an increase in the length of the Co–NB3 bond. VnCbl should therefore have a larger fold angles than both PhVnCbl and ClVnCbl since it is the least sterically demanding ligand. However the data in Table 8 shows that in the solid state, the fold angle for phenylvinyl cobalamin is larger than both the remaining vinyl structures. The reason for this unexpected result may be due to: (i) the quality of our data (our R^2 value for PhVnCbl of around 10% is quite large) or (ii) the effect of crystal packing forces influencing the geometry of the corrin ring in the solid state. Removing the effects of the crystal packing forces can be accomplished by performing gas phase quantum mechanics calculations as described in the next section.

Table 8: Axial bond lengths and fold angles of the vinyl cobalamins

	Length (Å)			Fold angle (˚)	References
	Alkene	Co–C	Co–NB3		
Phenylvinyl	1.333	2.019	2.225	14.6	This work
Vinyl	1.319	1.912	2.164	12.5	23
Chloro-vinyl	1.284	1.953	2.144	5.7 (9)	23

✧ The fold angle value for Chloro-vinylCbl is an average value from 4 different structures

It is also worth noting that the conformation observed in the solid state represents only one of many possible low energy conformations that a molecule as large and flexible as vitamin B_{12} may adopt. A much better estimate of the fold angle could be obtained by performing molecular dynamics calculations (possibly even using an electrostatic potential to approximate a solvent field) to obtain an average value. Due to time constraints, this will be left for "future work".

3.4 NMR

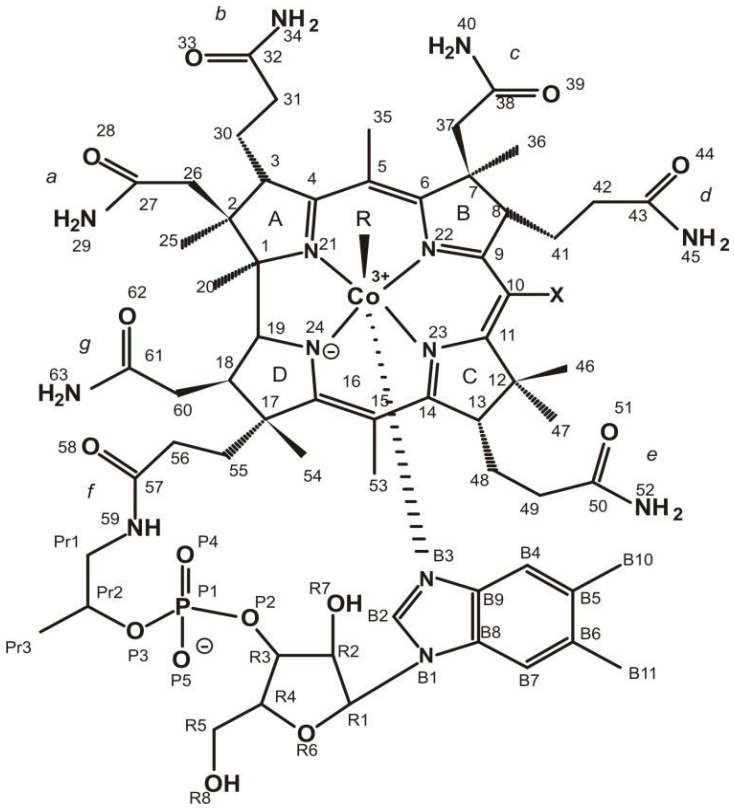

Figure 32. Standard view and numbering of the alkylcobalamins which have R = Phenylvinyl as the upper or β ligand of the corrin.[17]

NMR spectroscopy was used to confirm the identity of the β isomer, as well as to try and establish the identity of the second product. Unfortunately, the quality of the data was only good enough for full assignment of one of the isomers (the product that eluted last off the HPLC column, and previously shown by x-ray diffraction to be the β isomer). Complete assignment of all the ^{1}H and ^{13}C resonances for the corrin ring (including the side chains, the ribose moiety, and the DMB base) for this product was accomplished by using standard, previously published methods[17] and can be found in the Table 9 below.

Table 9. Complete standard assignment of all the ^{1}H and ^{13}C resonances for the corrin ring.

Data	**^{1}H**	**^{13}C**	**Data**	**^{1}H**	**^{13}C**	**Data**	**^{1}H**	**^{13}C**
B10	2.27	20.61	C36	1.82	19.95	ph1"	3.06	118.07
B11	2.25	20.43	C37'	1.72	42.99	ph2	-	143.24
B2	7.61	143.24	C37"	2.35	42.99	ph3	-	148.93
B4	6.82	119.52	C4	-	178.60	ph4	6.04	127.39
B5	-	134.20	C41'	1.41	28.52	ph5	6.87	128.31
B6	-	132.80	C41"	2.01	28.52	ph6	7.05	127.39
B7	7.21	111.91	C42'	1.83	33.74	Pr1'	3.06	46.38
B8	-	139.73	C42"	1.94	33.74	Pr1"	3.45	46.38
B9	-	132.38	C46	0.94	31.37	Pr2	4.32	73.17
C1	-	88.39	C47	1.35	23.28	Pr3	1.18	19.99
C10	6.50	97.82	C48'	2.09	34.68	R1	6.24	87.44
C11	-	177.07	C48"	2.18	34.68	R2	4.34	71.79
C12	-	48.17	C49'	1.86	27.15	R3	4.70	75.54
C13	2.89	53.55	C49"	2.08	27.15	R4	4.18	84.13
C14	-	164.53	C5	-	109.49	R5'	3.69	62.49
C15	-	107.32	C53	2.33	16.89	R5"	3.78	62.49
C16	-	177.72	C54	1.54	19.48			
C17	-	60.14	C55'	1.86	33.88			
C18	2.83	41.03	C55"	2.50	33.88			
C19	4.40	76.10	C56'	1.98	32.56			
C2	-	47.30	C56"	2.36	32.56			
C20	0.52	23.64	C57	-	175.11			
C25	1.30	17.80	C6	-	164.85			
C26'	2.13	43.06	C60'	2.58	33.14			
C26"	2.22	43.06	C60"	2.65	33.14			
C3	4.55	56.50	C7	-	51.55			
C30'	1.87	27.62	C8	3.95	55.45			
C30"	2.02	27.62	C9	-	173.53			
C31	2.40	36.40	fH	7.95	-			
C35	2.54	16.29	ph1'	3.01	118.07			

The assignment of ^{1}H and ^{13}C resonances for the PhVn ligand will be described below. The downfield region of the ^{1}H spectrum (5.9 to 7.8 ppm), corresponding to the aromatic region, is shown in Figure 33. The signals at 6.24, 6.50, 6.82, 7.21, and 7.61 ppm have been assigned to R1, C10, B4, B7, and B2, respectively (Table 9). This leaves three signals at 6.04, 6.87, and 7.05 ppm that are unaccounted for, and are most likely due to the three aromatic protons of the phenyl group (Figure 33).

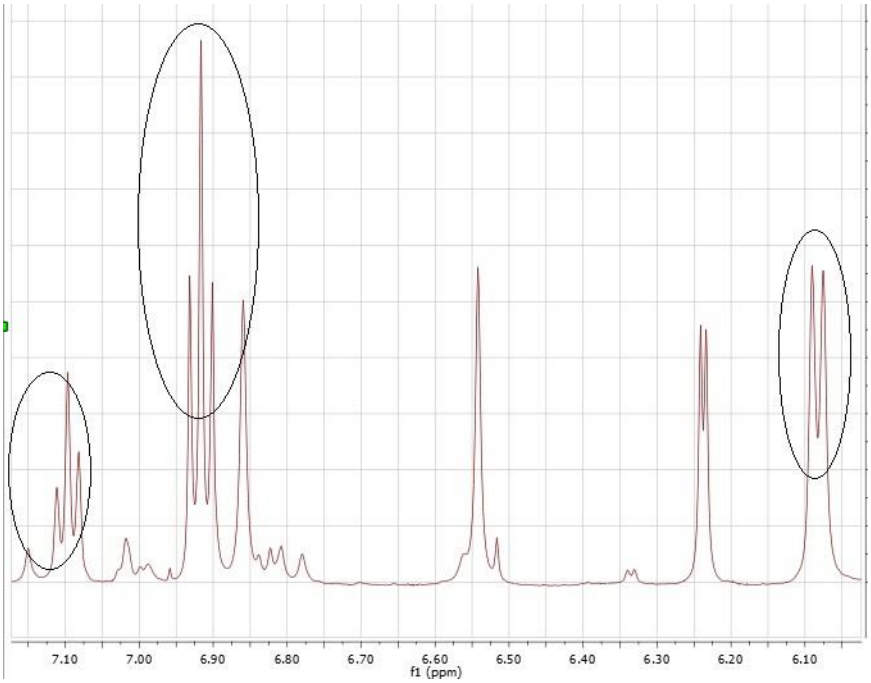

Figure 33. ^{1}H proton spectrum of the aromatic region of β-PhVnCbl. Signals highlighted in a circle are assigned to the PhVn ligand.

The COSY spectrum (see Figure 34) clearly indicates that the signal at 6.87 ppm couples strongly to the signals at 6.04 ppm and 7.05 ppm, whereas these latter two signals are only very weakly coupled to each other (the same coupling is observed in the ROESY spectrum (Figure 35). The signal at 6.87 ppm is thus assigned to ph5. Strong nOe interactions between ph5 and C46 (0.94 ppm) and C54 (1.55 ppm) are also observed, confirming that the phenylvinyl ligand is indeed coordinated to cobalt at the upper-axial position. Of the remaining two aromatic signals, 6.05 and 7.05 ppm, the former shows many more nOe interactions with groups of the upper face of the corrin ring. In fact, the signal at 7.05 ppm only shows very weak nOe interactions between C46 (0.94 ppm) and C37 (1.73 ppm). If we assume that the preferred orientation of the phenylvinyl ligands relative to the corrin ring in solution is the same at that found in the solid state, then clearly the signal at 6.05 ppm is due to ph4, and the remaining one at 7.05 ppm corresponds to ph6. Assignment of the two non-equivalent ph1 protons (3.01 and 3.06 ppm, in the alkene region of the ^{1}H spectrum) is based on the fact that one or both of them shows strong nOe interaction with ph4, C46, C54, C37, and C26.

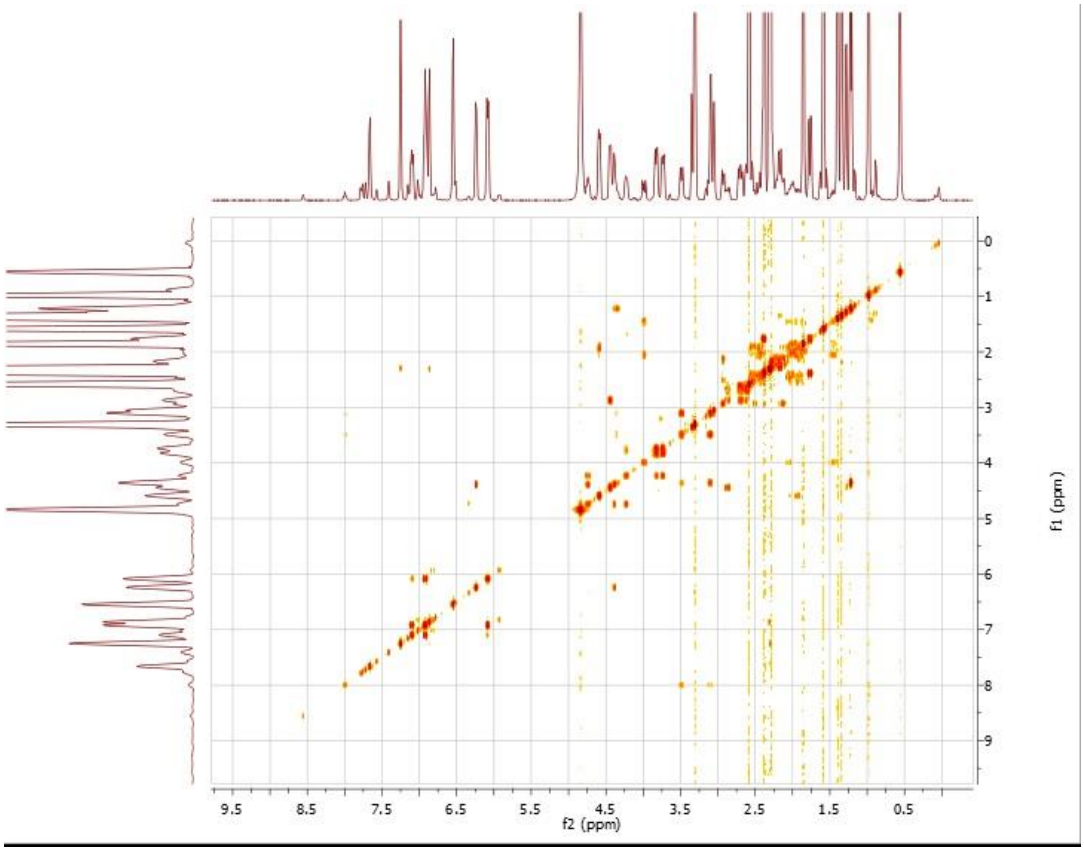

Figure 34: ^{1}H-^{1}H correlation spectrum (COSY) at 300 K on a Bruker Avance III 500 spectrometer operating at 500.133 MHz (^{1}H) and 125.770 MHz (^{13}C) using a 5-mm PABBO broad band probe.

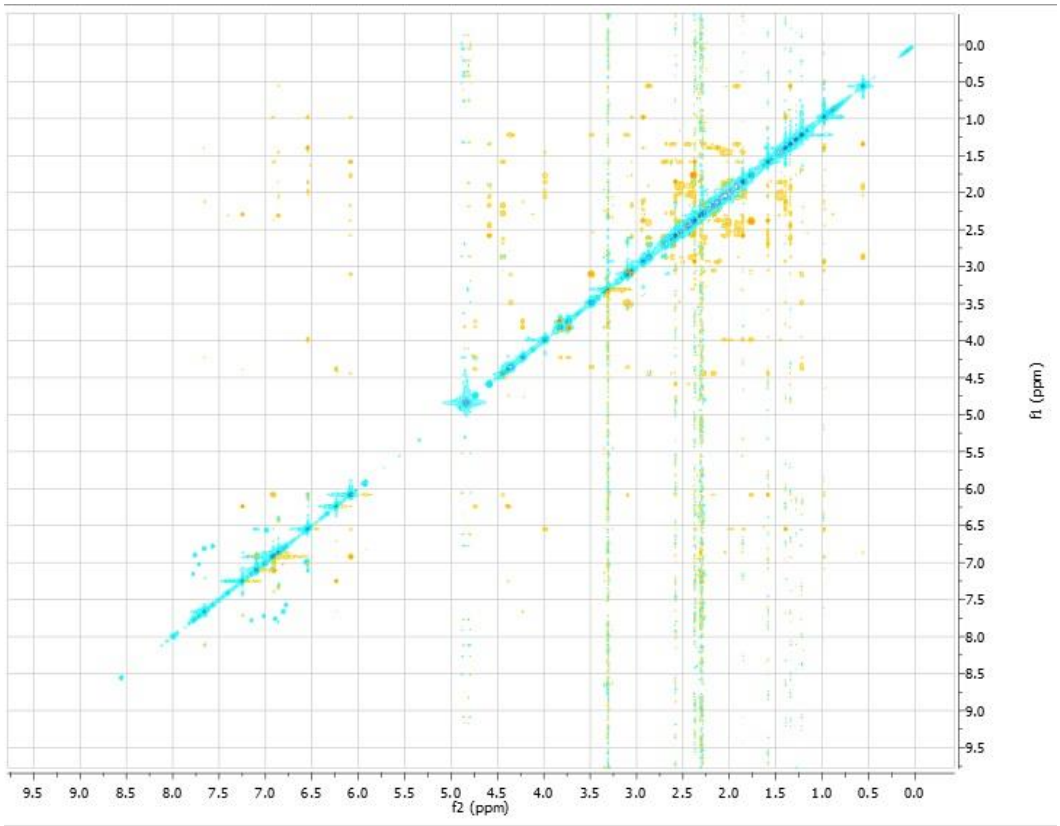

Figure 35: The correlated ^{1}H signal spectrum of β-PhVnCbl (ROESY)

^{13}C signals for the ph1, ph4, ph5, and ph6 carbons were obtained directly from the HSQC spectrum (see Figure 36) and are assigned as 118.1, 127.4, 128.3 and 127.4 ppm, respectively (the signals for ph4 and ph6 are overlapped).

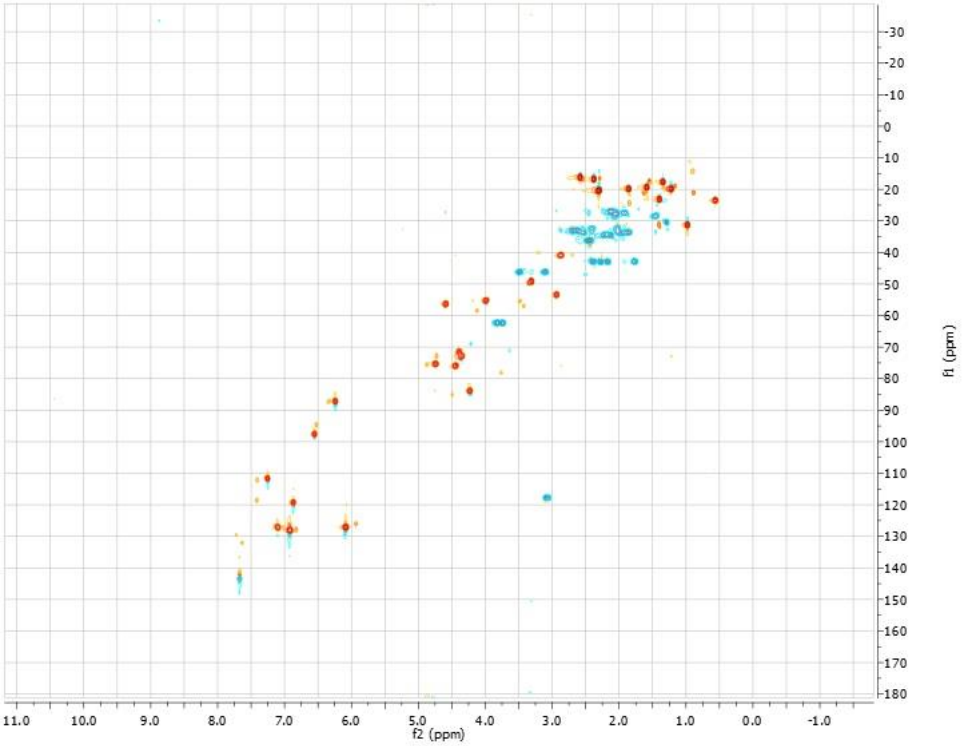

Figure 36: The correlated proton and carbon signals of β-PhVnCbl; HSQC (Heteronuclear single quantum coherence)

To assign the ph2 and ph3 resonances, the HMBC spectrum (Figure 37) was used. Both the ph5 proton and the protons on ph1 (but oddly not the ph4 proton) show a correlation to a ^{13}C signal at 148.9 ppm which we assign to ph3. Both ph1 protons, as well as the ph4 proton show a correlation with a signal at 143.2 ppm, which we assign to ph2. The NMR assignments, as well as the observed correlations for the phenylvinyl group are summarised below in Table 10.

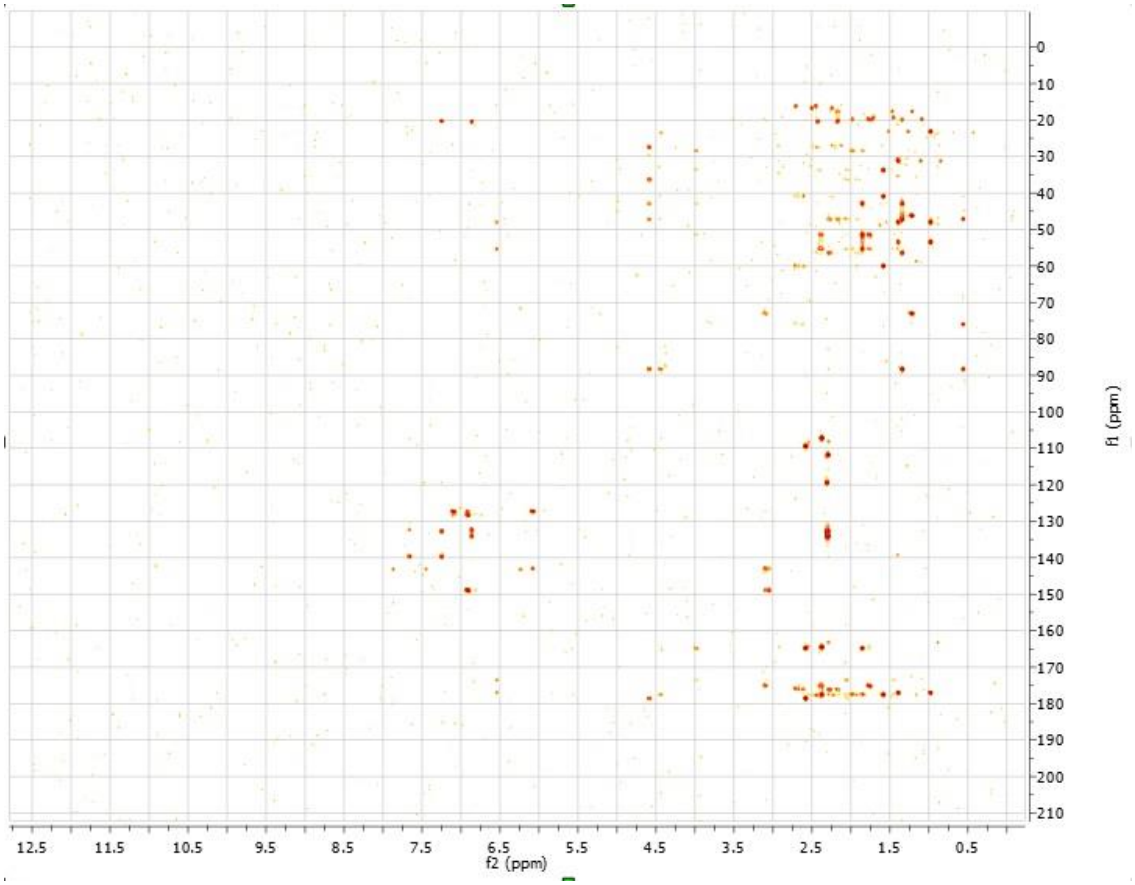

Figure 37. The correlated carbon and proton signals of β-PhVnCbl; HMBC (Heteronuclear multiple bond connectivity spectroscopy)

Table 10. ^{1}H and ^{13}C assignments and the NMR correlations for the phenylvinyl group in PhVnCbl observed by COSY, ROESY, and HMBC spectroscopies[a].

Resonance	^{1}H (ppm)	^{13}C (ppm)	COSY	ROESY	HMBC
ph1’	3.01	118.1	-	C46, C54, C37’, C26’, C35, ph1’’, C19, C10, ph4	ph2, ph3
ph1”	3.06		-	C36, C37’, ph1’, ph4	
ph2	-	143.2	-	-	-
ph3	-	148.9	-	-	-
ph4	6.05	127.4	ph5, ph6	C46, C54, C37’, C26’, C53, C35, ph1’’, C19, ph5, ph6	ph5, ph6, ph2
ph5	6.87	128.3	ph4, ph6	C46, C54, C26’’, C53, C35, ph4, ph6	ph4, ph6, ph3
ph6	7.06	127.4	ph5, ph4	C36, C37’	ph4, ph5

[a]Primes and double primes denote downfield and upfield members, respectively, of pairs of diastereotopic methylene, or in the case of ph1, geminal protons.

In the solid state, the preferred orientation of the PhVn ligand with respect to the corrin ring has the phenyl group positioned roughly over the C pyrrole ring when viewed from above This is the same solid state conformation adopted by the adenine moiety of the adenosyl group in AdoCbl.[113] It is evident however, that in solution there is at least some free rotation about the Co–C bond. One of the germinal ph1 protons shows nOe interactions with C54 and C46, which suggests that conformations where the phenyl group of the PhVn ligand occupies positions over the northern and western quadrants of the corrin ring are also accessible at room temperature. A northern conformation of the PhVn ligand would place the phenyl protons in close proximity to the C26 and C37 protons of the *a* and *c* side chains, respectively, and indeed, nOe interactions are observed between one of the diastereotopic C37 protons and ph4, as well as ph6. In addition, ph4 shows through-space interactions with one of the C26 protons. A western conformation of the PhVn ligand is confirmed by the fact that both ph4 and ph5 show nOe interactions with C54, and through-space interactions are also observed between ph4 and C26', and ph5 and C26''. Previous studies involving NMR-restrained molecular modelling on AdoCbl, and the related compound *Coβ*-5'-deoxyadenosylimidazolylcobamide (Ado(Im)Cbl, a coenzyme B_{12} analogue with an imidazole axial nucleoside) have shown that conformations of the Ado ligand other than the solid state conformation are accessible in solution at room temperature.[113,114]

3.5 Mass spectrometry

Mass spectrometry was used to further characterise the products. Mass spectrometry is used for determining the molecular mass of a compound. This method identifies a cation or anion (depending on whether the technique is run in positive or negative mode) so that if the molecule of interest is not charged it will not appear in the spectrum. The formal structure of PhVnCbl has no charge overall, thus it will not be seen in the spectrum; however ionisation in the sample chamber means its molecular ion will appear as a +1 charge by acquiring a proton. The calculated molar mass of α-PhVnCbl is 1450.53 u, whilst that of β-PhVnCbl is 1432.51 u. Figure 38 shows a peak at *m*/*z* = 1434 which is consistent with α-PhVnCbl less a water molecule plus a proton (calculated 1433). The base peak at *m*/*z* = 717 is assigned to (α-PhVnCbl.2H-H_2O)$^{2+}$. The peak at *m*/*z* = 736 is assigned to (α-PhVnCbl.K.H-H_2O)$^{2+}$;and that at 737 to (α-PhVnCbl.Na.H)$^{2+}$ Therefore the spectrum in Figure 38 is consistent with the compound being α-PhVnCbl.

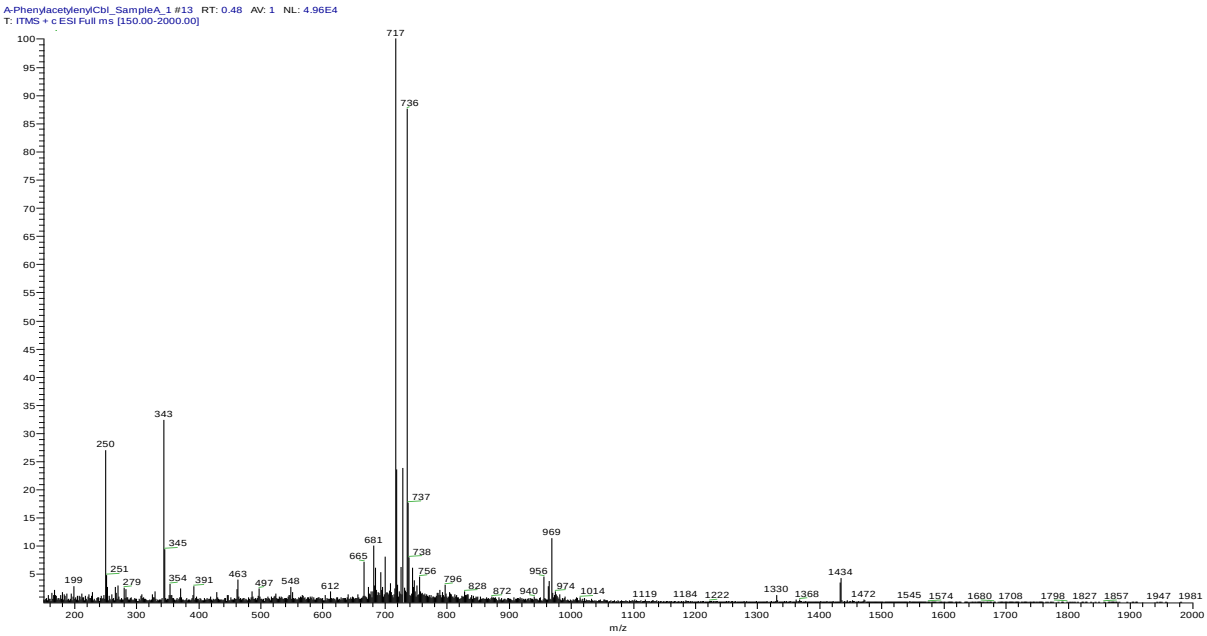

Figure 38. ESI-MS results for α-PhVnCbl

Figure 39 below shows a peak at *m*/*z*= 1433 which resulted from β-PhVnCbl plus a proton. The base peak at *m*/*z* = 729 is assigned to the (β-PhVnCbl.H.Na)$^{2+}$;. The peak at *m*/*z* = 718 resulted from (β-PhVnCbl.2H)$^{2+}$. The peak at *m*/*z* = 729 is assigned to (β-PhVnCbl.H.K)$^{2+}$MH. Therefore the spectrum in Figure 39 belongs to β-PhVnCbl.

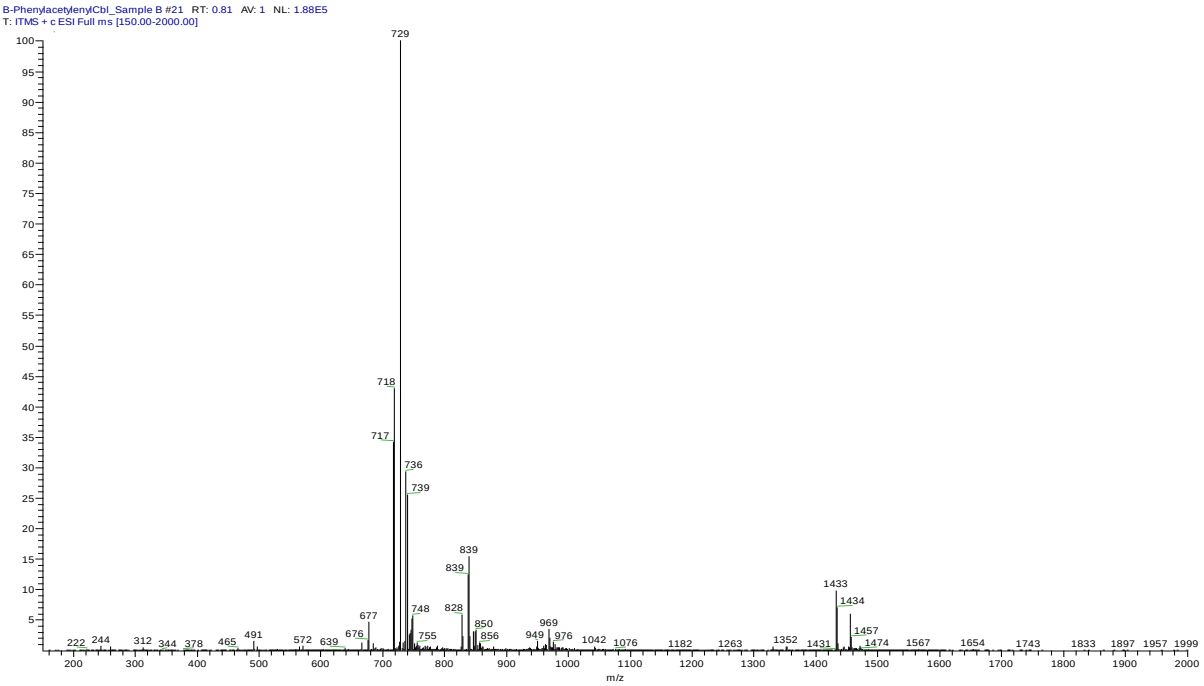

Figure 39. ESI-MS results for β-PhVnCbl

Although we were not able to assign the α-diastereomer from either X-ray diffraction or NMR, confirmation that the first peak in Figure 20 corresponding to the α-diastereomer was obtained by mass spectrometry.

Final confirmation that we have indeed obtained the α-diastereomer was obtained by performing a photolysis experiment on the product, and is detailed below.

3.6 Photolysis

Photolysis is a useful method to identify whether a particular cobalamin is an alkylcobalamin or not. This method leads to a light driven oxidation reaction of the alkylcobalamin, resulting in the alkyl group being replaced by a water ligand. The DMB base will then displace the weakly bound α-coordinated water ligand, ultimately forming aquacobalamin. Thus photolysis was used to determine whether the product that eluted off the HPLC column first (Figure 20) is indeed an alkylcobalamin.

After this product was separated from β-PhVnCbl via C18 column chromatography, it was desalted and evaporated to dryness in a round bottomed flask. A small amount of sample, reconstituted in deionized water was added to a cuvette containing 0.1 M phosphate buffer, pH 7.0. An initial UV-vis spectrum was collected, after which the sample was exposed to ambient light for 3~4 hours. The UV-vis spectrum before and after exposure to light is shown in Figure 40.

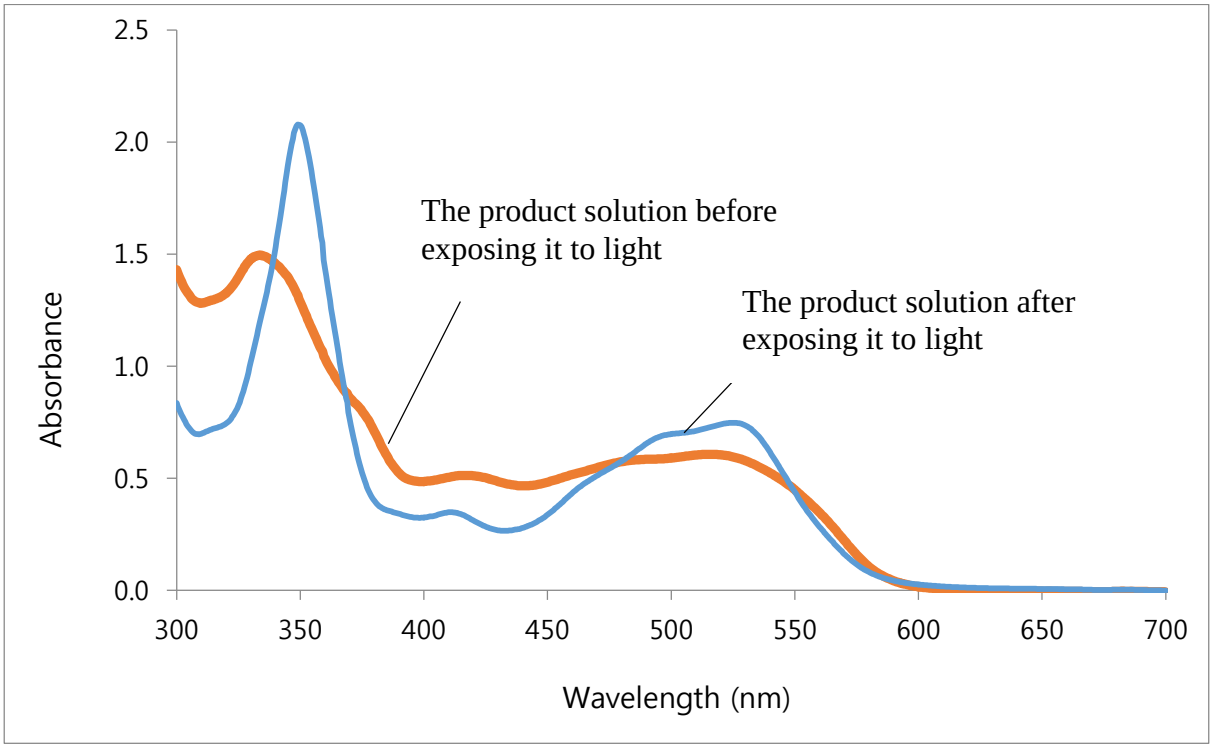

Figure 40. UV-vis spectrum of α-PhVnCbl before and after exposure to light

The UV-vis results show that the original product (which has a typical alkylcobalamin spectrum) was converted to aquacobalamin upon exposure to light. This means that it must

have been an alkylcobalamin, and hence provides more evidence that the first product eluted off the HPLC column is the α diastereomer of PhVnCbl.

3.7 pK_a titrations of the α and β forms of PhVnCbl

A measure of the *trans* σ-donor influence of the PhVn ligand can be obtained by determining the pK_a value for the DMB base-on ⇌ base-off equilibrium in β-PhVnCbl, and the pK_a for coordinated H_2O in α-PhVnCbl, as illustrated in Figure 41.

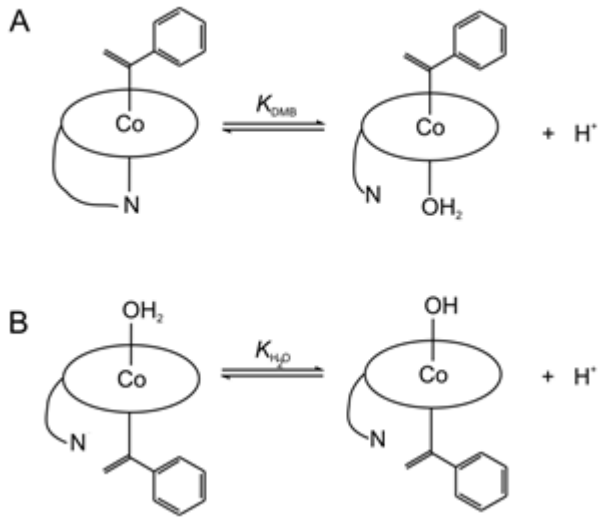

Figure 41. A) Diagram illustrating DMB base-on ⇌ base-off equilibrium in β-PhVnCbl
B) Diagram illustrating coordinated and deprotonated H_2O in α-PhVnCbl

3.7.1 pK_a titration for β-PhVnCbl

The protonation of the DMB ligands occurs upon acidification causing the "base-off" form to predominate at acidic pH. This conformational change is detected by UV-vis spectroscopy as a change in the absorbance maxima from around 425 nm in the "base-on" form to around 530 nm in the "base-off" form (see Figure 42). The pH was adjusted between 8.5 and 1.5 in increments of approximately half a pH unit. At each step, a spectrum, as well as the exact pH, was recorded. The spectral changes observed over the pH range are illustrated below (Figure 42).

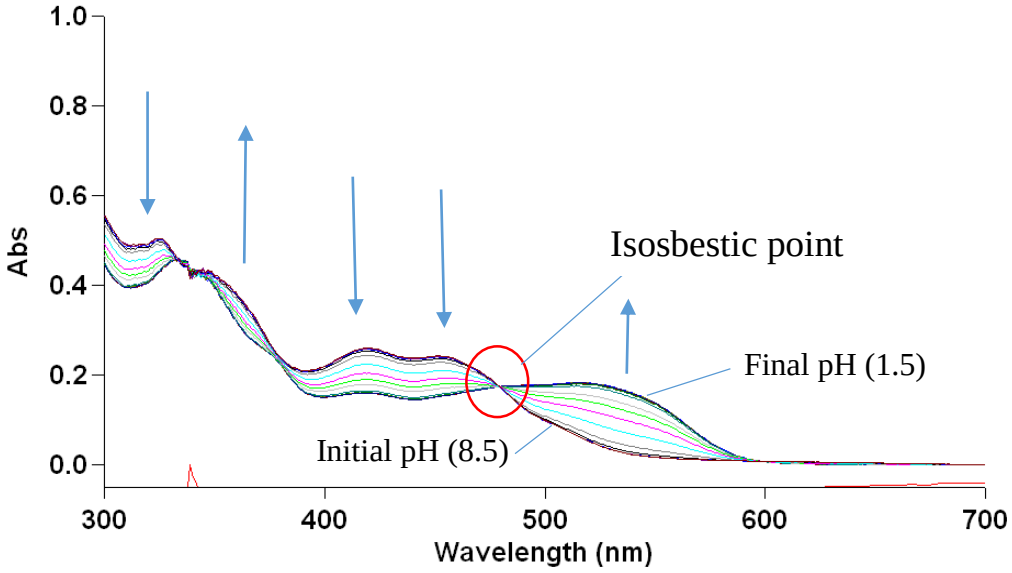

Figure 42. The UV-vis spectrum results for p$K_{base\text{-}off}$ titration for β-PhVnCbl ranged between 300-700 nm

The figure above shows that there are isosbestic points in the graph which indicate specific wavelengths at which two chemical species have the same molar absorptivity. Isosbestic points indicate that only *two* species that vary in concentration contribute to the absorbance around throughout the monitored pH range. The arrows indicate the direction which the absorbance maxima move as the pH is adjusted from 8.5 to 1.5.

Absorbance results at 4 wavelengths (see Table 11) as a function of pH were fitted to equation (3) by standard non-linear least squares methods.

$$pH_x = pK_a + \log\left(\frac{A_x - A_{AH}}{A_{A^-} - A_x}\right) \qquad (3)$$

A_x is the absorbance of the chromophore at pH_x, and A_{AH} and A_{A^-} correspond to the titration end points.

Figure 43 below shows a fit of the experimental absorbance values at 326 nm to equation (3). Titration curves for the remaining wavelengths (419, 453 and 530 nm) can be found in Appendix B. Table 11 summarises the pK_a values and standard errors obtained by fitting absorbance values above as a function of pH to equation 3.

Table 11: pK_a values at four different wavelengths

Wavelength	pKa	Standard error
326	4.34 (2)	0.02495
419	4.347(6)	0.00579
453	4.349 (6)	0.00570
530	5.54 (7)	0.07001
Average	4.6 (6)	0.59735

The average pKa value for β-PhVnCbl is 4.6 (6).

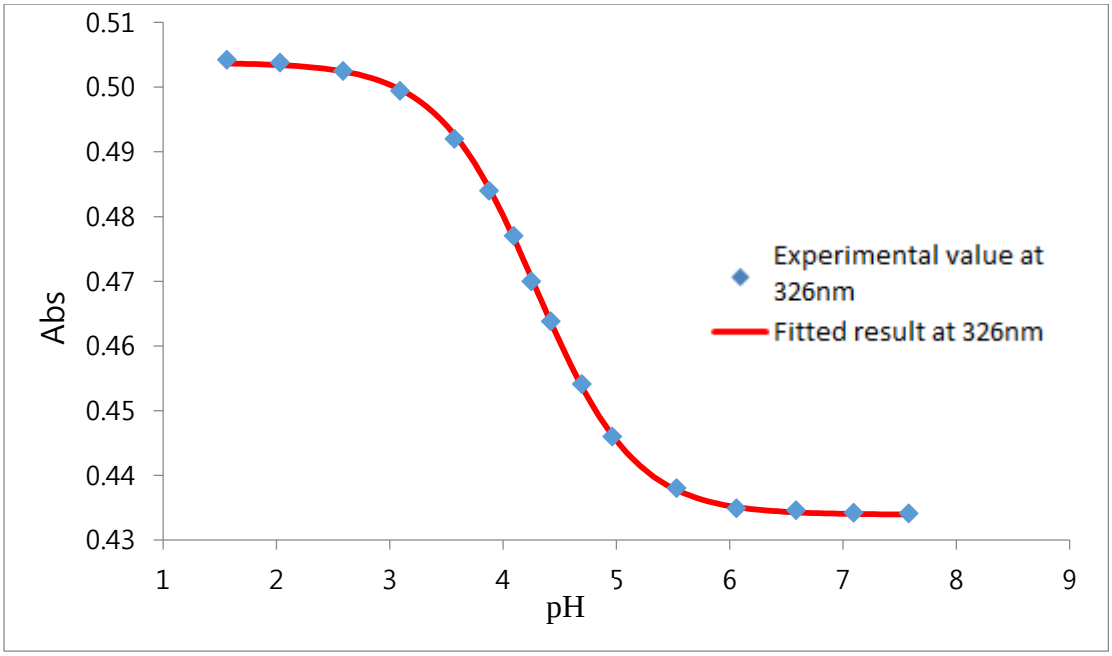

Figure 43. The p$K_{base\text{-}off}$ titration of β-PhVnCbl plot of absorbance vs pH at 326 nm

For convenience purposes, Table 1 from Chapter 1 is reproduced below.

Table 1: Values of p$K_{base\text{-}off}$ (at 25°C) and Co-NB3 distances for XCbl's[59,13]

X	p$K_{base\text{-}off}$	References	Co–NB3 /Å	References
NO	5.10	60	2.349 (2)	61
CH_3CH_2	4.16	13	2.232 (1)	40
$CH_3CH_2CH_2$	4.10	62	-	40
Ado	3.67	63	2.236 (2)	66,67,65,64
CH_3	2.90	68	2.17 (2)	66,109,115,69
CF_3CH_2	2.60	70	-	71
CH_2=CH	2.40	62	2.165 (6)	23
cis ClCH=CH	2.30	23	2.144 (5)	23
CF_2H	2.15	70	2.187 (7)	71
$NCCH_2$	1.81	13	-	72
CF_3	1.44	70	2.05 (1)	71
CN	0.10	68	2.04 (2)	72
H_2O	-2.13	68	1.925 (2)	73

The magnitude of p$K_{base\text{-}off}$ reflects the σ-donor power of the β-ligand. The effect can be explained as follows. As the β-ligand places more electron density on the Co, the latter becomes a weaker Lewis acid. This results in a weaker Lewis acid/base interaction between the Co and the N-donor ligand of the DMB base. Protonation of the DMB base subsequently requires less acid, resulting in a higher p$K_{base\text{-}off}$ value. Our p$K_{base\text{-}off}$ value of 4.60 (6) for PhVnCbl places the σ-donor power of the PhVn ligand somewhere between NO and $CH_3CH_2^-$. The strong σ-donor ability of the PhVn ligand is also reflected in the length of the Co–NB3 bond as discussed in Section 3.3.4. Figure 44 shows that a reasonably linear relationship exists between the length of the Co–NB3 bond and the p$K_{base\text{-}off}$ values for alkyl cobalamins.

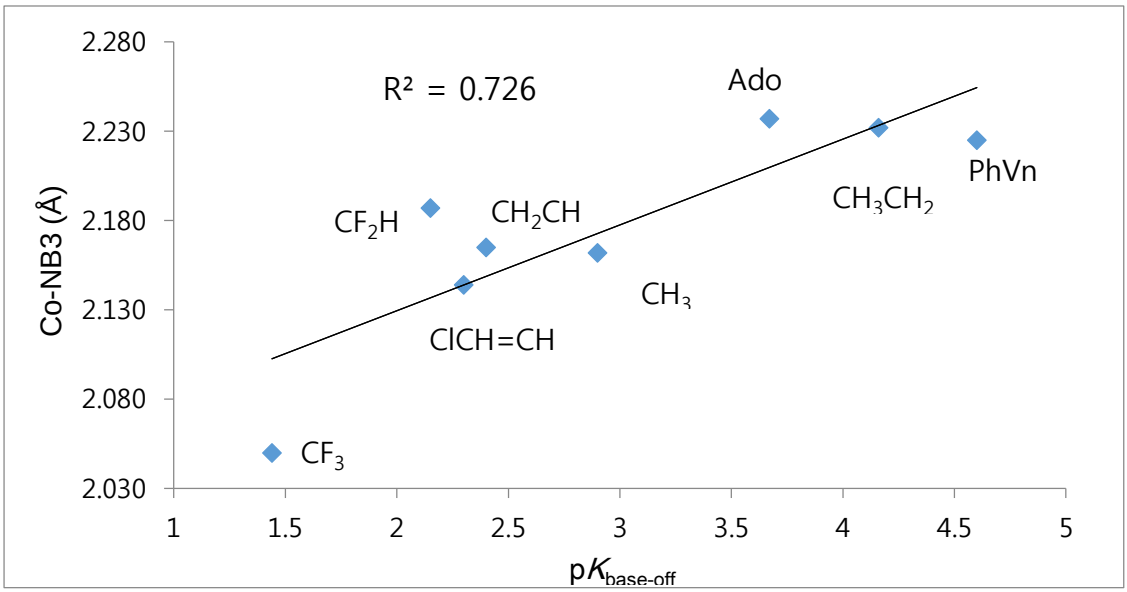

Figure 44. Correlations of p$K_{base\text{-}off}$ values to the axial bond length (Co–NB3) of alkyl cobalamins (R^2=0.7717)

As mentioned above, according to the *trans* influence, the larger the σ-donor ability of the β ligand, the longer the Co–NB3 bond. The figure shows that p$K_{base\text{-}off}$ values for the alkyl cobalamins are directly proportional to the Co–NB3 lengths. A larger p$K_{base\text{-}off}$ value implies a greater σ donor ability of the β axial ligand. From these alkyl cobalamins, PhVnCbl has the highest p$K_{base\text{-}off}$ value observed so far; thus it has the strongest σ donor ability.

A correlation (although weaker, R^2 = 0.7199) also exists between the length of the Co–C_β bond and the p$K_{base\text{-}off}$ value (Figure 45). As the length of the Co–C_β bond increases, so does the value for p$K_{base\text{-}off}$. This is not unexpected, since, as discussed in Section 3.3.4, alkylcobalamins display the inverse *trans* influence.

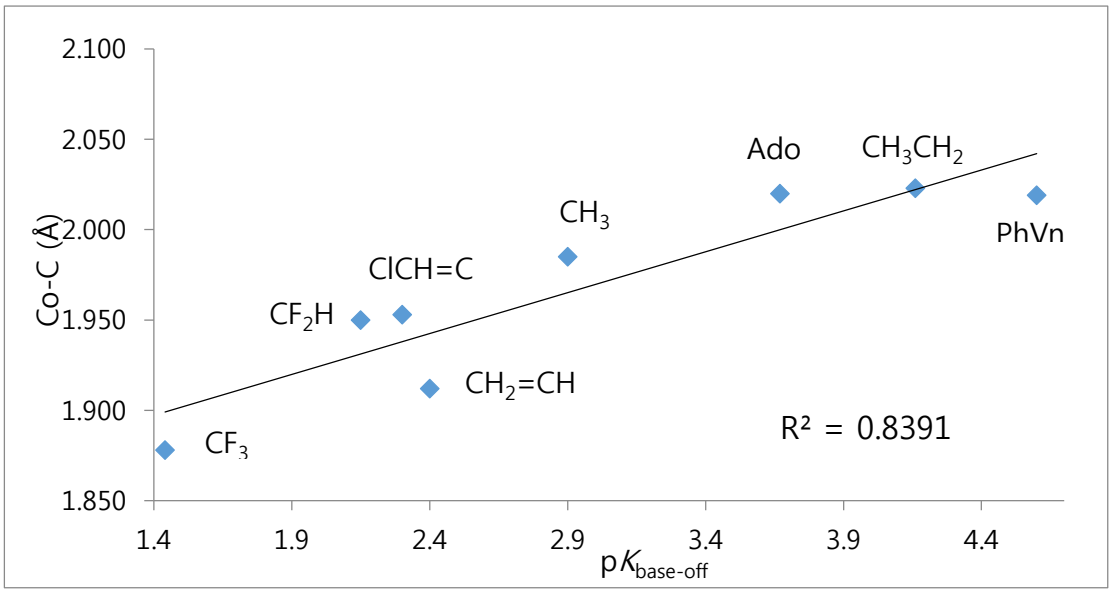

Figure 45. Correlations of p$K_{base\text{-}off}$ values to the axial bond length (Co–C) of alkyl cobalamins

3.7.2 pK_a titration for α-PhVnCbl

The deprotonation of the water ligand at the upper coordinated site occurs upon addition of concentrated base. Upward movement of electron density donated by the phenylvinyl ligand from the lower coordinated site occurs which makes the hydrogen bonding on the water ligand stronger that it needs high basicity to deprotonate the hydrogen from the water ligand. This conformational change can be observed by UV-vis spectra due to a change in the absorbance maxima from around 469 nm in the protonated form to around 530 nm in the deprotonated form of water ligand. (See Figure 46) The σ donor power of the phenylvinyl ligand in α-PhVnCbl was assessed by measuring the pK_a value of the Co-H_2O protonated from ⇌ deprotonated form by a UV-vis titrations. The range of pH used was between 7~14. However using a pH above 12 is unreliable since the calibration of pH has only been done up to 12 and also above pH 12 is too high for a glass electrode to measure its pH. Therefore this pK_a titration was used to obtain an estimate of its pK_a value.

The figure (Figure 46) below shows pK_a titration for α-PhVnCbl.

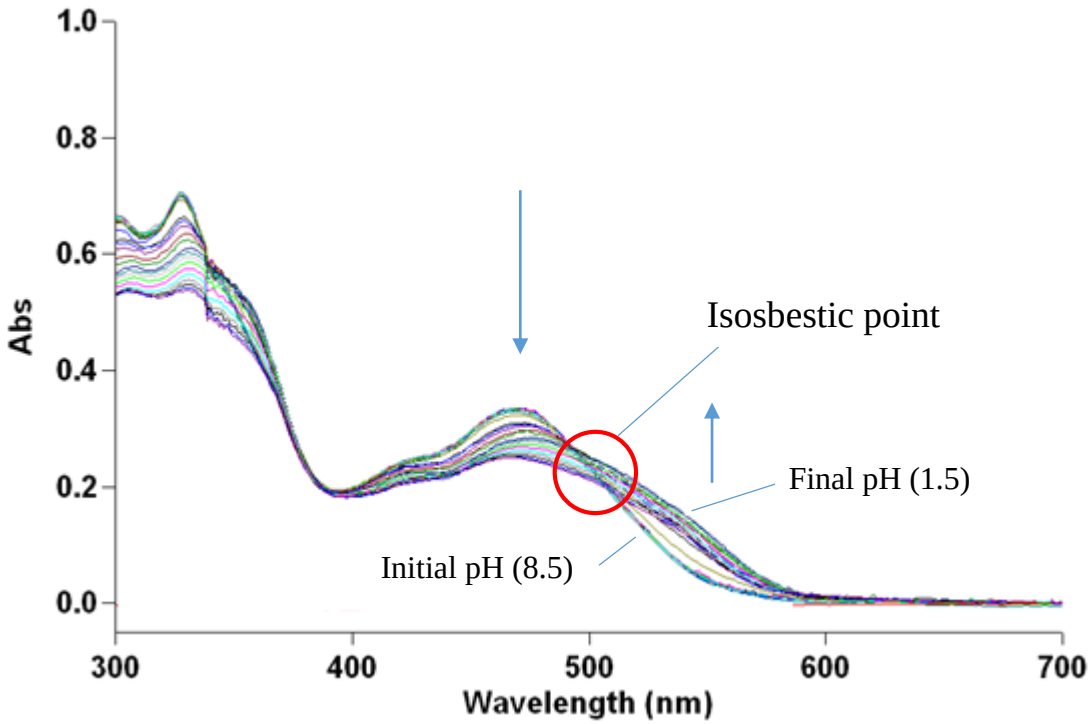

Figure 46: The UV-vis spectrum result for pK_a titration of α-PhVnCbl ranged between 300-700 nm

This figure above shows that there was a isosbetic point where deprotonation of water ligand occurs however due to titrating the solution at very high pH appeared to have an error in the spectrum.

We chose the wavelength where the maximum absorbance occurred with β-PhVnCbl to plot a graph fitted to Equation (4).

$$pH_x = pK_a + \log(|A_x - A_{AH}|/|A_{A^-} - A_x|) \quad (4)$$

where A_x: the absorbance of the chromophore at pH_x, A_{AH} and A_{A^-} : The titration end points (determined in duplicate) i.e. the absorbances at pH < pK_a -2 and pH> pK_a +2 respectively

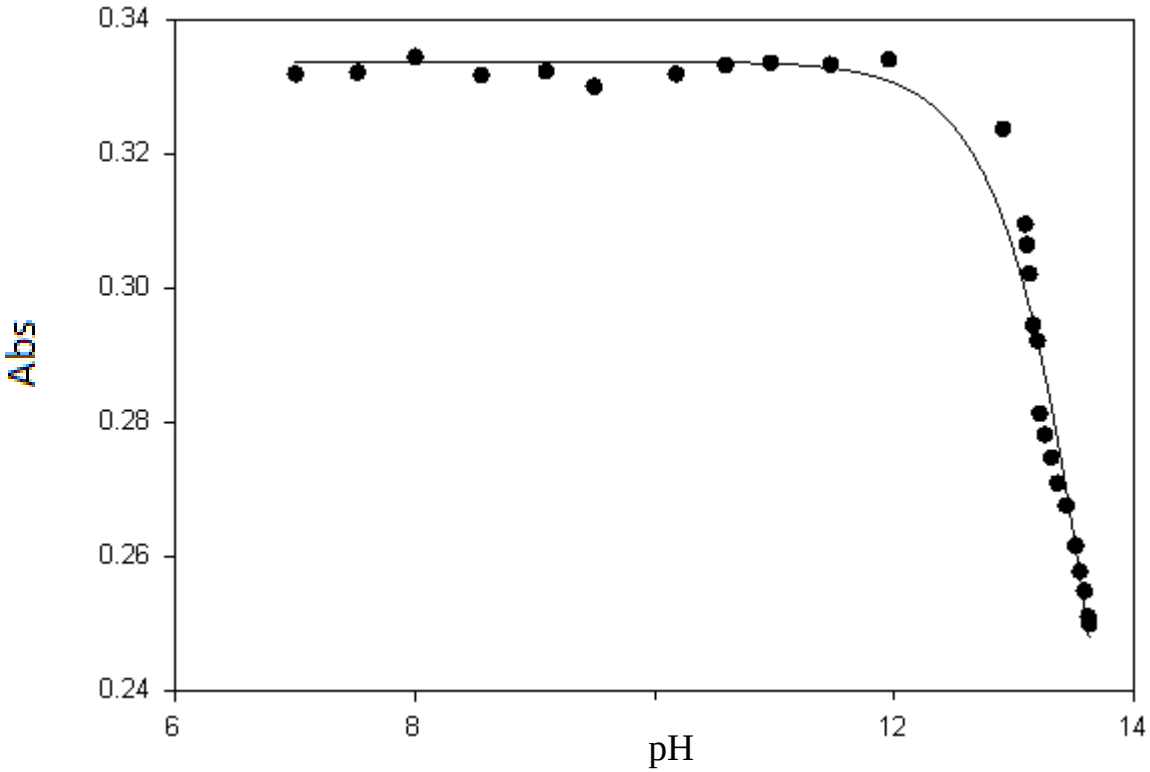

Figure 47: The pK_a titration of α-PhVnCbl plot of absorbance vs pH at 469 nm

The pK_a value for α-PhVnCbl was 13.9 ±0.1.

The accurate pH measurement was not possible because the area of the pH measurement is unreliable (>12) so it was only an estimate.

Table 12: pK_a values for alkyl cobamides

Cobamides		References
Trans-ligand	pK_a	
CN	11	19
CCH	>14	19
$CHCH_2$	>14	19
CH_3	>14	19

The pK_a value for α-PhVnCbl can be compared to these values in Table 12, since these *trans* ligands were also used to deprotonate water ligand to get the pK_a values. As seen in the table, our product α-PhVnCbl has the similar pK_a value with the methylcobinamide.

The pK_a value for our product is only an estimate since the value is too high in the pH range but this implies once again that α-PhVnCbl has a strong σ donor ability.

3.8 Determination of log K values for substitution of H_2O in the α and β substituted PhVnCbl

Measurement of the thermodynamics and kinetics of the substitution of coordinated H_2O by an exogenous probe ligand can be accomplished by accessing the *trans* influence of a ligand. We used cyanide as that probe ligand given the considerable data available.

3.8.1 Substitution of H_2O by CN^- *trans* to phenylvinyl

The σ donor power of the alkyl ligand is determined by the log K values for substitution of H_2O in the α-PhVnCbl isomer with CN^-. The value of log K was compared to the values of log K for the reaction R–Co(corr)–H_2O + CN^- ⇌ R–Co(corr)– CN^- + H_2O for a series of R ligands, thus allowing us to locate phenylvinyl ligand in the trans effect series in cobalt corrin chemistry.

A titration of *α*-PhVnCbl with a 1.000429 M CN^- stock solution (25 ºC, 0.5 M CAPS buffer, pH 11.0, well above the pK_a of HCN) gave well-defined isobestic points (see Figure 48). The spectroscopic changes between 325 nm and 640 nm were fitted to a binding isotherm for displacement of H_2O by CN^-, to yield values of the equilibrium constant, *K*.

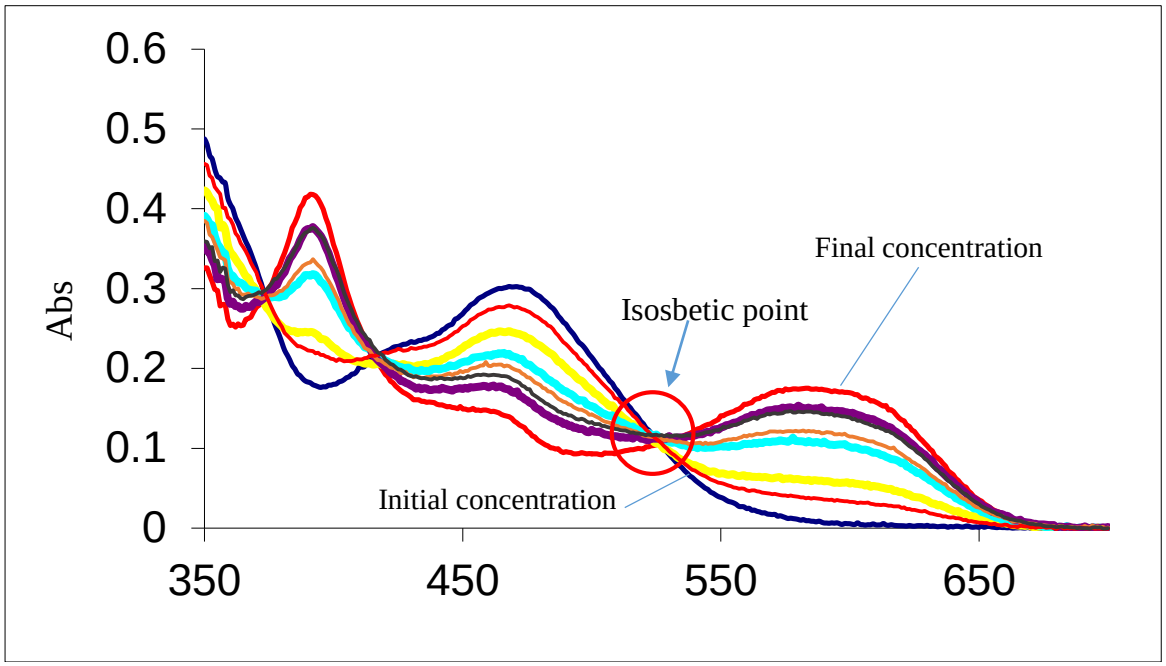

Figure 48. Plot of log K titration data of α-PhVnCbl with addition of the CN stock solution (25 ℃, μ=1 M)

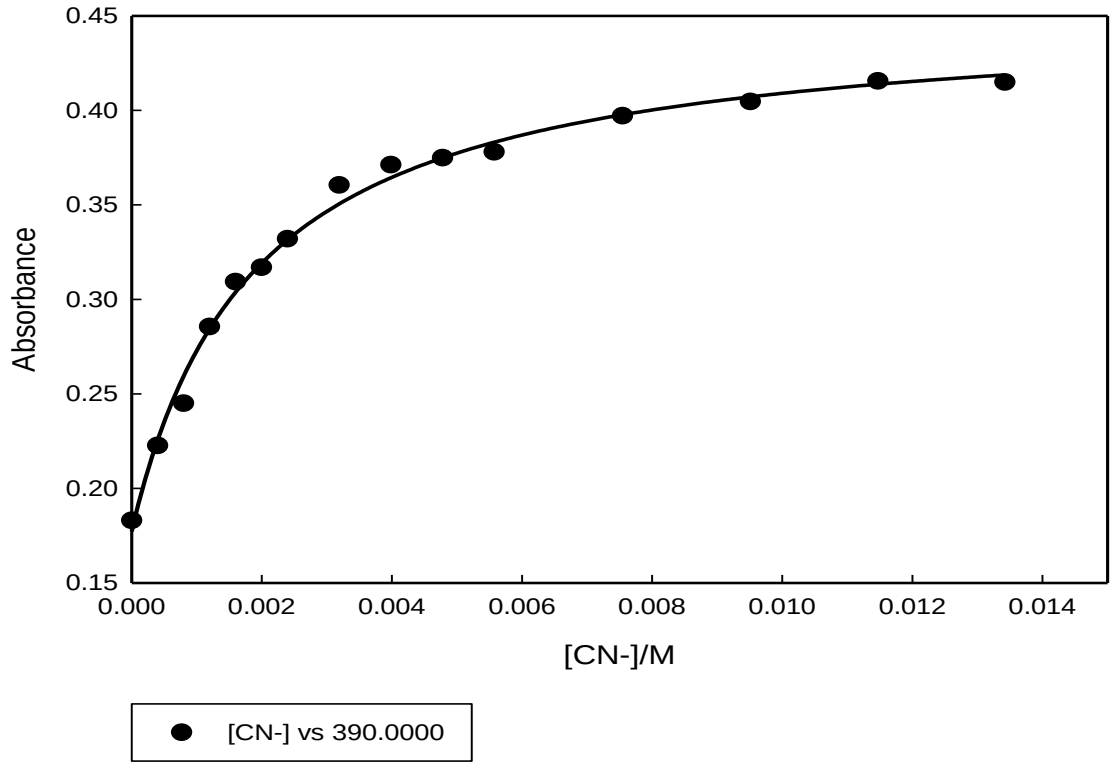

Figure 49. Plot of the log K titration data for the binding of the CN- ligand to α-PhVnCbl at 390 nm (25 ℃, μ= 1 M)

The log K value of the reaction was found from the equation fit as follows:

$A_\lambda = (A_{0+} A_1 K_{obs} [L]_{free})/ 1+ K_{obs} [L]_{free}$ (5)

A_λ is the absorbance at the absorbance monitoring wavelength, K_{obs} is the formation constant (equilibrium constant), A_0 is the initial absorbance and A_1 is the final absorbance, $[L]_{free}$ is the concentration of the free binding ligand. Since log K is relative low, it is reasonable to assume that $[L]_{free} \sim [L]_{tot}$, where $[L]_{tot}$ is the total added; ligand concentration (i.e., the fraction is bound ligand is insignificant compared to the total ligand concentration).

All fits with a correlation coefficient < 0.98 were excluded; a weighted average of *K*, weighted as the reciprocal of the standard error of each fit, yielded log $K = 2.70 \pm 0.06$.

Table 13: Some formation constants for substitution of water by cyanide with a variety of ligands in the *trans* position.

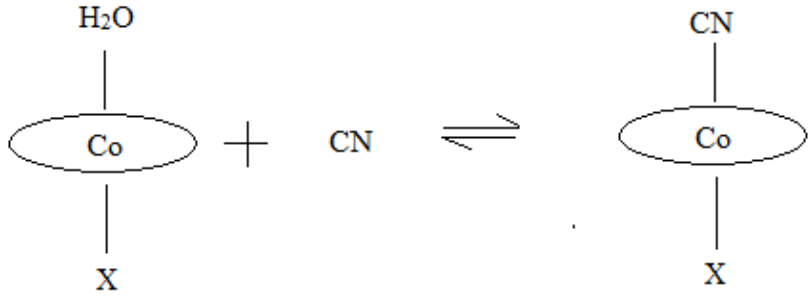

Ligand X	log *K*	References
	CN^-	
H_2O	16.6	73
Bzm	14.1	116
OH^-	11.0	117
CN^-	8.4	118
CCH	6.8≤	119
SO_3^{2-}	4.3	120
$P(OCH_3)_2O^-$	4.1	121
$CHCH_2$	2.7	122
PhVn	2.7	This work
CH_3	2.1	122
CH_2CH_3	0.6	122

Determining values of the formation constants are one of the most important factors to evaluate the *trans*-effect of the ligand in the α position as well as the effect of the nature of the incoming ligand.[123,19]

According to Pratt[123] a decrease in the log K value for cyanide results in a decrease in the Lewis acidity of the Co(III) ion that is caused by the increase in the donor power of the incoming ligand. The log K value for PhVn is the same as $CHCH_2$ according to the table above but this is probably coincidental. Comparing the values with several other alkyl ligands, PhVn has a strong *trans* influence which decreases the Lewis acidity of Co(III) such that log *K* for substitution of H_2O *trans* to it is relatively low and it has strong σ donor power.

3.8.2 Substitution of DMB by CN^- *trans* to phenylvinyl ligand

The σ donor power of the alkyl ligand was measured by determining the log K values for substitution of DMB in the β-PhVnCbl isomer with CN^-. The value of log K was compared to the values of log K for the reaction R–Co(corr)–DMB + CN^- ⇌ R–Co(corr)–CN^- + DMB for a series of R ligands, thus allowing us to locate phenylvinyl ligand in the trans effect series in cobalt corrin chemistry.

A titration of β-PhVnCbl was done with a prepared 1 M CN^- stock solution (25 ºC, 0.5 M CAPS buffer, pH 11.2, well above the pK_a of HCN).

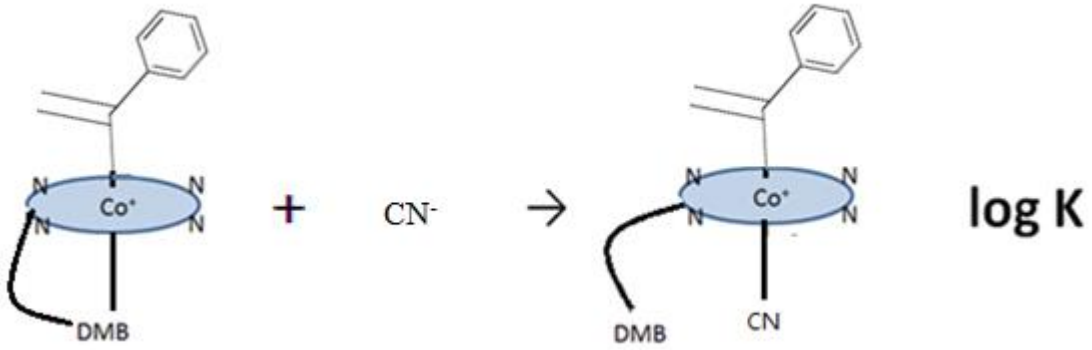

Figure 50. Binding ligand studies when L=CN (This procedure took place for log K titration of the β form)

This reaction gave log K = 0.7 ± 0.1 for β-PhVnCbl.

According to the table below, the log K value of the β form is very close to the log K value of the vinyl ligand.

Table 14: Some formation constants for substitution of DMB base by CN^- with a variety of ligands in the *trans* position.

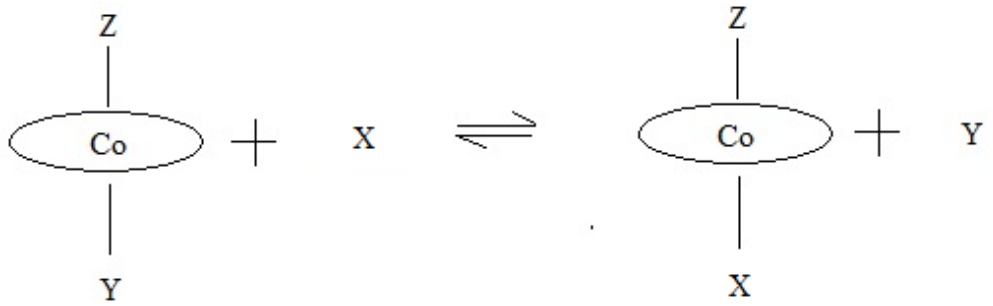

Y	X	Z	log K	Reference
Bzm	CN-	-CN	4.0	72
		-C≡CH	2.7	124
		$-CH=CH_2$	0.7	124
		PhC_2H_2	0.69	This work
		$-CH_3$	0.1	124
		$-CH_2CH_3$	<0	125

The log K value for the β-phenylvinyl ligand can be placed between the vinyl ligand and the methyl ligand as showing in the table above. Table 14 implies that the phenylvinyl ligand has a weaker σ donor ability than the methyl ligand because it has a higher log K value but the same value with the vinyl ligand which is pure coincident. This also means that β-PhVnCbl has a strong σ donor ability.

CHAPTER 4

Conclusions

The main goal of this project was to prepare a stable alkylcobalamin (RCbl, R = alkyl) containing a vinyl ligand and to evaluate its σ donor ability. Only two such compounds have been reported in the literature. The synthesis of the phenylvinylcobalamin was investigated such that cyanocobalamin was reduced using zinc granules in a 10% acetic acid (CH_3COOH)/methanol solution, before initiating the electrophilic addition reaction, on the introduction of the phenylacetylene ligand into the reaction mixture under red light conditions. The compound was synthesized in two different diastereomeric forms i.e. α-phenylvinvyl- and β-phenyvinylcobalamin. The confirmation of this product was analyzed by HPLC. These two isomers were separated using a C18 column and characterized by NMR spectroscopy. One isomer has the phenylvinyl ligand on the upper (β) coordination site and the other isomer with the ligand on the lower (α) coordination site of the corrin ring. Whilst the NMR spectrum of the β isomer was virtually fully assigned, the NMR data for the α isomer was not good enough to show the nOe interaction between the phenylvinyl ligand and the corrin ring. ESI-MS strongly suggested that the second isomer was indeed the α isomer, in which the dimethylbenzimidazole (DMB) ligand was displaced from the coordination site of the metal by the alkyl ligand. Photolysis of α isomer yielded aquacobalamin, confirming that it is an alkylcobalamin.

β-Phenylvinyl was crystallized by vapour diffusion of acetone into an aqueous solution of the compound but no crystals of the α isomer were obtained, presumably because of the freedom afforded the f side chain and DMB ligand once it was released from the coordination sphere of the metal. Optical microscopy was used to select a single crystal and the structure was determined by X-ray diffraction methods. The compound crystallized in the space group of $P2_1P2_1P2_1$ with unit cell dimentions a = 15.7783(7) Å , b = 22.3400(9) Å , c = 25.1607(14) Å with four molecules in the unit cell and a calculated density 1.319 Mg m^{-3}, The final R_1 value was 9.75%.

The axial bond length Co-NB3 to DMB was relatively long (2.225(7) Å) compared to other alkylcobalamins. This is a further indication that phenylvinyl is a powerful σ donor.

We initially anticipated that the phenylvinyl ligand would coordinate through the α-carbon of the corrin structure but it coordinated through the β-carbon. Since the crystal structures of most cobalamin compounds have the upper-axial pointing towards a solvent-filled channel that runs throughout the crystal structure, one might expect that homolysis of the Co-C bond in the solid state would lead to the stabilised alkyl radical moving away from the cob(II)alamin species, allowing for spectroscopic detection. In this case the alkyl radical species did not move away from the cob(II)alamin species. The unpaired electron on the alkyl group presumably recombine with the unpaired electron on the Co, reforming the Co–C bond. We suspect, this is why we were unable to observe the stable radical species. Also, in the case of PhVnCbl where coordination to the metal is through the β-carbon, DFT calculations showed that upon homolysis, the radical that forms on the β-carbon of the PhVn ligand is not that stable. Thus we were not able to observe the PhVn radical intermediate in the solid state.

We determined the pK_a value for the protonation and release of the DMB ligand by a spectrophotometric titration to evaluate the σ donor ability of the phenylvinyl ligand. The pK_a for β-phenylvinylcobalamin was found to be 4.6(6), which is the highest value yet reported for an alkylcobalamin, confirming the large σ donor ability of phenylvinyl. The pK_a for deprotonation of H_2O trans to phenylvinyl in α-phenylvinylcobalamin was also determined by spectrophotometric titration, and found to be 13.9(1), which is typical for alkylcobalamins. The lowest pK_a value that was reported in this thesis for alkylcobalamins was 0.1 by the CN ligand and the highest reported in this project was 4.16 by the ethyl ligand. This implies that the ligand does indeed have a strong σ donor ability. The pK_a value for α-phenylvinylcbl was estimated to be 13.9 (1) which indicated that phenylvinyl ligand was a much more powerful σ donor ability compared to DMB.

A further evaluation of the σ donor ability was done by the ligand substitution of DMB by CN^- in β-phenylvinylcbl and the log K (0.69 (1)) value for this complex was low relative to other alkylcobalamins. The highest log K value for the same substitution reaction of CN^- in CNCbl was 4 and the lowest known log K value reported was for ethylcbl which was <0. The substitution of H_2O by CN^- *trans* to phenylvinyl in α-phenylvinylcbl gave log K = 2.7 (1). This value was almost the same as the lowest log K value that was known for all the alkylcobalamins which is ethylcbl (0.6). The highest log K value reported for the same substitution reaction was by CNCbl (8.4). These results all indicate that the phenylvinyl ligand has a strong σ donor ability.

This work has allowed us to place phenylvinyl in the σ-donor order of alkyl ligands in alkylcobalmins, i.e. CN^-< CCH < $CHCH_2$ = PhVn < Me < Et.

References

(1) Shriver, D. F.; Atkins, P. W.; Langford, C. H. *Inorganic Chemistry*; Oxford University Press: Oxford, 1994.

(2) Beinert, H. *J. Biol. Chem.* **2002**, *277*, 7246.

(3) Bertini, I.; Rosate, A. *Proc. Natl. Acad. Sci.* **2003**, *100*, 3601.

(4) Williams, R. J. P. *Coord. Chem. Rev.* **1990**, *100*, 573.

(5) Kaim, W.; Schwederski, B. *Bioinorganic Chemistry: Inorganic Elements in the Chemistry of Life*; Wiley: New York, 1991.

(6) Williams, R. J. P. *J. R. Soc. Interface* **2007**, *17*, 1049.

(7) Cotton, F. A.; Wilkinson, G. *Advanced Inorganic Chemistry*; Freeman, W. H. : New York, 1988.

(8) Ducommum, Y.; Zbinden, D.; Merbach, A. E. *Helv. Chim. Acta.* **1982**, *65*, 1385.

(9) Whipple, G. H.; Robscheit-Robbins, F. S. *Am. J. Physiol.* **1926**, *72*, 408.

(10) Minot, G.; Murphy, W. *J. Am. Medic. Ass.* **1926**, *87*, 470.

(11) McDowell, L. R. *Vitamins in animal and human nutrition* New York, 2000.

(12) Zempleni, J. *Handbook of vitamins: Clinical Nutrition in Health and Disease Series*; CRC: New York, 2007.

(13) Brown, K. L. *Chem. Rev.* **2005**, *105*, 2075.

(14) Buckel, W.; Golding, B. T. *Ann. Rev. Microbiol.* **2006**, *60*, 27.

(15) Sauer, K.; Thauer, R. K.; Banerjee, R., Ed.; John Wiley & Sons: New York, 1999, p 655.

(16) Krautler, B.; Krautler, B., Arigoni, D., Golding, B. T., Eds.; Wiley-VCH Weinheim, 1998, p 3.

(17) Banerjee, R. *Chemistry and Biochemistry of B_{12}*; John Wiley & Sons: New York, 1999.

(18) Ellenbogen, L.; Cooper, B. A. *in Handbook of Vitamins, Nutritional and Clinical Aspects, Food Science and Technology*; Marcel Dekker: New York, 1984.

(19) Pratt, J. M. *Inorganic Chemistry of Vitamin B_{12}*; Academic Press: London, 1972.

(20) Friedrich, W. *in Fermente, Hormone und Vitamine*; Georg Thieme Verlag: Stuttgart, 1975.

(21) Banerjee, R. *Chem. Biol.* **1997**, *4*, 175.

(22) Buckel, W.; Kratky, C.; Golding, B. T. *Chem. Eur. J.* **2006**, *12*, 352.

(23) McCauley, K. M.; Pratt, D. A.; Wilson, S. R.; Shey, J.; Burkey, T. J.; van der Donk, W. A. *J. Am. Chem. Soc.* **2005**, *127*, 1126.

(24) Krautler, B. *Biochem. Soc. Trans.* **2005**, *33*, 806.

(25) Anderson, P. J.; Lango, J.; Carkeet, C.; Britten, A.; Krautler, B.; Hammock, B.; Roth, J. R. *J. Bacteriol* **2008**, *190*, 1160.

(26) Glusker, J. P. *in B_{12}*; John Wiley & Sons: New York, 1982; Vol. I.

(27) Randaccio, L.; Geremia, S.; Nardin, G.; Wuerges, J. *Coord. Chem. Rev.* **2006**, *250*, 1332.

(28) Gschosser, S.; Gruber, K.; Kratky, C.; Eichmuller, C.; Krautler, B. *Angew. Chem. Int. Ed.* **2005**, *44*, 2284.

(29) Eschenmoser, A.; Wintner, C. E. *Science* **1977**, *196*, 1410.

(30) Woodward, R. B. *in Vitamin B_{12}, Proceedings of the Third European Symposium on Vitamin B_{12} and Intrinsic Factor*; Walter de Gruyter: Berlin, 1979.

(31) Battersby, A. R. *in Vitamin B_{12} and B_{12}-proteins*; Wiley-VCH: Weinheim, 1998.

(32) Krautler, B. *Met. Ions. Life Sci.* **2009**, *6*, 1.

(33) Drennan, C. L.; Huang, S.; Drummond, J. T.; Mathews, R. G.; Ludwig, M. L. *Science* **1994**, *266*, 1669.

(34) Svetlitchnaia, T.; Svetlitchnyi, V.; Meyer, O.; Dobbek, H. *Proc. Nat. Acad. Sci. USA* **2006**, *103*, 14331.
(35) Stupperich, E.; Nexo, E. *Eur. J. Biochem.* **1991**, *199*, 299.
(36) Nahvi, A.; Sudarsan, N.; Ebert, M. S.; Zou, X.; Brown, K. L.; Breaker, R. R. *Chem. Biol.* **2002**, *9*, 1043.
(37) Randaccio, L.; Geremia, S.; Nardin, G.; Wuerges, J. *Trends Inorg. Chem* **2009**, *11*, 1.
(38) Randaccio, L.; Geremia, S.; Demitri, N.; Wuerges, J. *Molecules* **2010**, *15*, 3228.
(39) Hannibal, L.; Smith, C. A.; Chavez, R. A.; Jacobsen, D. W.; Brasch, N. E. *Angew. Chem. Int. Ed.* **2007**, *46*, 5140.
(40) Hannibal, L.; Smith, C. A.; Smith, J. A.; Axhemi, A.; Miller, A.; Wang, S.; Brasch, N. E.; Jacobsen, D. W. *Inorg. Chem.* **2009**, *48*, 6615.
(41) Kuta, J.; Wuerges, J.; Randaccio, L.; Kozlowski, P. M. *J. Phys. Chem* **2009**, *113*, 11604.
(42) Schrauzer, G. N.; Deutsch, E.; Windgassen, R. J. *J. Am. Chem. Soc.* **1968**, *90*, 2441.
(43) Finke, R. G. *Vitamin B_{12} and B_{12}- proteins*; Wiley-VCH: Weinheim, 1998.
(44) Schrauzer, G. N.; Deutsch, E. *J. Am. Chem. Soc.* **1969**, *91*, 3341.
(45) Krautler, B. *in The Biological Alkylation of Heavy Elements*; Royal Soc. Chem.: London, 1988.
(46) Krautler, B.; Caderas, C. *Helv. Chim. Acta.* **1984**, *67*, 1891.
(47) Krautler, B. *Helv. Chim. Acta.* **1987**, *70*, 1268.
(48) Milton, P. A.; Brown, T. L. *J. Am. Chem. Soc.* **1977**, *99*, 1390.
(49) Brown, K. L.; Zhou, L.; Zhao, D.; Cheng, S.; Xiang, Z.; Wiley-VCH: Weinheim, 1998.
(50) Brown, K. L.; Zou, X. *J. Am. Chem. Soc.* **1992**, *114*, 9643.
(51) Halpern, J. *Science*, *227*, 869.
(52) Brown, K. L.; Zou, X. *Inorg. Chem.* **1992**, *31*, 2541.
(53) Krautler, B. *in Organic Reactivity, Physical and Biological Aspects*; Royal Soc. Chem.: London, 1995.
(54) Galliker, P. K.; Grather, O.; Rummler, M.; Fitz, W.; Arigoni, D. *in Vitamin B_{12} and B_{12}-Proteins*; Wiley-VCH: Weinheim, 1998.
(55) Woodyer, R. D.; Li, G.; Zhao, H.; van der Donk, W. A. *Chem. Commun.* **2007**, 359.
(56) Tinembart, O.; Walder, L.; Scheffold, R. *Phys. Chem.* **1988**, *92*, 1225.
(57) Perry, C. *Solution, Solid state and Molecular Mechanics Investigations of Iron Porphyrins and Cobalt Corrins*; University of the Witwatersrand: South Africa, 2004.
(58) Krautler, B. *Organometallic Chemistry of B_{12} Coenzymes. In Metal Ions in Life Sciences*; Royal Society of Chemistry: Cambridge, 2009; Vol. 6.
(59) Brown, K. L. *Inorg. Chem.* **1988**, *27*, 3548.
(60) Hassanin, H. A.; Hannibal, L.; Jacobsen, D. W.; Brown, K. L.; Marques, H. M.; Brasch, N. E. *Dalton Trans.* **2009**, *3*, 424.
(61) Hassanin, H. A.; El-Shahat, M. F.; DeBeer, S.; Smith, C. A.; Brasch, N. E. *Dalton Trans.* **2010**, *39*.
(62) Hogenkamp, H. P. C. *The chemistry of cobalamins and related compounds, in Cobalamin-Biochemistry and Pathophysiology*; Babior, B. M. John Wiley and Sons: New York, 1974.
(63) Wang, R.; MacGillivray, B. C.; Macartney, D. H. *Dalton Trans.* **2009**, 3584.
(64) Sigrid, G.; Renate B, H.; Robert, K.; Karl, G.; Christian, M.; Christoph, K.; Berhard, K. *Chem. Eur. J.* **2004**, *11*, 81.
(65) Ouyang, L.; Rulis, P.; Ching, W. Y.; Nardin, G.; Randaccio, L. *Inorg. Chem.* **2004**, *43*, 1235.

(66) Mebs, S.; Henn, J.; Dittrich, B.; Paulman, C.; Luger, P. *J. Phys. Chem. A.* **2009**, *113*, 8366.
(67) Brown, K. L.; Cheng, S.; Zou, X.; Li, J.; Chen, G.; Valente, E. J.; Zubkowski, J. D.; Marques, H. M. *Biochemistry* **1998**, *37*, 9704.
(68) Brown, K. L.; Hakimi, J. M. *J. Am. Chem. Soc.* **1984**, *106*, 7894.
(69) Stefan, M.; Julian, H.; Birger, D.; Carsten, P.; Peter, L. *J. Phys. Chem. A.* **2009**, *113* 8366.
(70) Brown, K. L.; Hakimi, J. M.; Nus, D. M.; Montejano, Y. D.; Jacobsen, D. W. *Inorg. Chem.* **1984**, *23*, 1469.
(71) Wagner, T.; Afshar, C. E.; Carell, H. L.; Glusker, J. P.; Englert, U.; Hogenkamp, H. P. C. *Inorg. Chem.* **1999**, *38*, 1785.
(72) George, P.; Irvine, D. H.; Glauser, S. C. *Ann. N. Y. Acad. Sci.* **1960**, *88*, 393.
(73) Betterton, E. A.; Chemaly, S. M.; Pratt, J. M. *J. Chem. Soc. Dalton Trans.* **1985**, 1619.
(74) Perry, C. B.; Fernandes, M. A.; Marques, H. M. *Acta Crystallogr C.* **2004**, *60*, m165.
(75) Fieber, W.; Hoffmann, B.; Schimidt, W.; Stupperich, E.; Konrat, R.; Krautler, B. *Helv. Chim. Acta.* **2002**, *85*, 927.
(76) Kontaxis, G.; Riether, D.; Hannak, R.; Tollinger, M.; Krautler, B. *Helv. Chim. Acta.* **1999**, *82*, 848.
(77) Tollinger, M.; Konrat, R.; Krautler, B. *Helv. Chim. Acta.* **1999**, *82*, 1596.
(78) Frederick, B.; Elham, B.; Perry, A. *Proc. Nat. Aca. Sci.* **2004**, *101*, 15870.
(79) Sagi, I.; Wirt, M. D.; Chen, E.; Frisbie, S.; Chance, M. R. *J. Am. Chem. Soc.* **1990**, *112*, 8639.
(80) McCauley, K. M.; Wilson, S. R.; vander Donk, W. A. *J. Am, Chem. Soc.* **2003**, *125*, 4410.
(81) Cole, R. B. *Electrospray ionization mass spectrometry: fundamentals, instrumentation and applications*; Wiley: New York, 1997.
(82) Bax, A.; Davis, D. G. *J. Magn. Reson.* **1985**, *63*, 207.
(83) Baeten, V.; Manley, M.; Fernandéz Pierna, J. A.; Downey, G.; Dardenne, P. *Modern Techniques for Food Authentication*; Elsevier Inc: Oxford, 2008

(84) Bax, A.; Summers, M. F. *J. Am. Chem. Soc.* **1986**, *108*, 2093.
(85) Baerends, E. J.; Ellis, D. E.; Ros, P. *Chemical Physics* **1973**, *2*, 41.
(86) Dunlap, B. I.; Connolly, J. W. D.; Sabin, J. R. *The Journal of Chemical Physics* **1979**, *71*, 3396.
(87) Eichkorn, K.; Treutler, O.; Ö hm, H.; Häser, M.; R., A. *Chemical Physics Letters* **1995**, *240*, 283.
(88) Kendall, R. A.; Früchtl, H. A. *Theor. Chem. Acta.* **1997**, *97*, 158.
(89) Whitten, J. L. *The Journal of Chemical Physics* **1973**, *58*, 4496.
(90) Neese, F. *Wiley Interdisciplinary Reviews: Computational Molecular Science* **2012**, 73.
(91) Becke, A. D. *Physical Review A* **1988**, *38*, 3098.
(92) Perdew, J. P. *Physical Review B* **1986**, *33*, 8822.
(93) Schafer, A.; Horn, H.; Ahlrichs, R. *The Journal of Chemical Physics* **1992**, *97*, 2571.
(94) Grimme, S.; Antony, J.; Ehrlich, S.; Krieg, H. *The Journal of Chemical Physics* **2010**, *132*, 154104.
(95) Boys, S. F.; Bernardi, F. *Molecular Physics* **1970**, *19*, 553.
(96) Simon, S.; Duran, M.; Dannenberg, J. J. *The Journal of Chemical Physics* **1996**, *105*, 11024.

(97) Bader, R. F. *Atoms in Molecules: A Quantum Theory*; Oxford University Press, Oxford, 1990.
(98) Bader, R. F. W. *Acc. Chem. Res.* **1985**, *18*, 9.
(99) In *AIMAll (Version 11.12.19), 08.05.04*, http://aim.tkgristmill.com Overland Park, KS, 2011.
(100) APEX2 In *2009.1-0*; Bruker AXS Inc., Madison, Wisconsin: USA, 2005.
(101) SAINT+ In *7.60A (includes XPREP and SADABS)*; Bruker AXS Inc., Madison, Wisconsin: USA, 2005.
(102) Sheldrick, G. M. *Acta. Crystallogr.* **2008**, *A64*, 112.
(103) Farrugia, L. J. *J. Appl. Cryst.* **1997**, *30*, 565.
(104) Day, P. *Theor. Chim. Acta.* **1967**, *7*, 328.
(105) Marino, N.; Rabideau, A. E.; Doyle, R. P. *Inorg. Chem.* **2011**, *50*, 220.
(106) Fabbiani, F. P. A.; Buth, G.; Dittrich, B.; Sowa, H. *CrystEngComm.* **2010**, *12*, 2541.
(107) Krautler, B.; Konrat, R.; Stupperich, E.; Farber, G.; Gruber, K.; Kratky, C. *Inorg. Chem.* **1994**, *33*, 4128.
(108) Butler, P.; Ebert, M. O.; Lyskowski, A.; Gruber, K.; Kratky, C.; Krautler, B. *Angew. Chem. Int. Ed.*, *45*, 989.
(109) Brown, K. L.; Cheng, S.; Zou, X.; Zubkowski, J. D.; Valente, E. J.; Knapton, L.; Marques, H. M. *Inorg. Chem.* **1997**, *36*, 3666.
(110) Pagano, T. G.; Marzilli, L. G.; Flocco, M. M.; Tsai, C.; Carrell, H. L.; Glusker, J. P. *J. Am. Chem. Soc.* **1991**, *113*, 531.
(111) Schrauzer, G. N.; Grate, J. H. *J. Am. Chem. Soc.* **1981**, *103*, 541.
(112) Tucker, C. E.; Majid, T. N.; Knochel, P. *J. Am. Chem. Soc.* **1992**, *114*, 3983.
(113) Marques, H. M.; Zou, X.; Brown, K. L. *J. Mol. Struct.* **2000**, *520*, 75.
(114) Brown, K. L.; Zou, X.; Banka, R. R.; Perry, C. B.; Marques, H. M. *Inorg. Chem.* **2004**, *43*, 8130.
(115) Randaccio, L.; Furlan, M.; Geremia, S.; Slouf, M.; Srnova, I.; Toffoli, D. *Inorg. Chem.* **2000**, *39*, 3403.
(116) Lexa, D.; Savéant, J. M.; Zickler, J. *J. Am. Chem. Soc.* **1980**, *102*, 2654.
(117) Marques, H. M.; Bradley, J. C.; Brown, K. L.; Brooks, H. *Inorg. Chim. Acta.* **1993**, *209*, 161.
(118) Betterton, E. A., phD Thesis, University of the Witwatersrand, 1982.
(119) Baldwin, D. A.; Betterton, E. A.; Pratt, J. M. *J. Chem. Soc. Dalton Trans.* **1983**, 225.
(120) Firth, R. A.; Hill, H. A. O.; Pratt, J. M.; Thorp, R. G.; Williams, R. J. P. *J. Chem. Soc.* **1969**, 381.
(121) Chemaly, S. M.; Betterton, E. A.; Pratt, J. M. *J. Chem. Soc. Dalton Trans.* **1987**, 761.
(122) Firth, R. A.; Hill, H. A. O.; Pratt, J. M.; Thorp, R. G.; Williams, R. J. P. *J. Chem. Soc.* **1968**, 2428.
(123) Pratt, J. M. *Chemistry and Biochemistry of B_{12}*; Banerjee, R. John Wiley & Sons: New York, 1999.
(124) Hayward, G. C.; Hill, H. A. O.; Pratt, J. M.; Vanston, N. J.; Williams, R. J. P. *J. Chem. Soc.* **1965**, 6485.
(125) Firth, R. A.; Hill, H. A. O.; Pratt, J. M.; Thorp, R. G. *Anal. Biochem.* **1968**, *23*, 429.

APPENDICES

APPENDIX A. Crystallography

Table A1. Crystal data and structure for β–PhVnCbl

Empirical formula	C73 H131 Co N13 O30 P	
Formula weight	1760.81	
Temperature	293(2) K	
Wavelength	0.71073 Å	
Crystal system	Orthorhombic	
Space group	P2(1)2(1)2(1)	
Unit cell dimensions	a = 15.7783(7) Å	α= 90°.
	b = 22.3400(9) Å	β= 90°.
	c = 25.1607(14) Å	γ = 90°.
Volume	8868.8(7) Å^3	
Z	4	
Density (calculated)	1.319 Mg/m^3	
Absorption coefficient	0.296 mm^{-1}	
F(000)	3768	
Crystal size	0.48 x 0.17 x 0.15 mm^3	
Theta range for data collection	1.52 to 26.00°.	
Index ranges	-18<=h<=19, -27<=k<=27, -31<=l<=13	
Reflections collected	47932	
Independent reflections	17377 [R(int) = 0.0884]	
Completeness to theta = 26.00°	99.9 %	
Absorption correction	None	
Refinement method	Full-matrix least-squares on F^2	
Data / restraints / parameters	17377 / 59 / 1048	
Goodness-of-fit on F^2	0.984	
Final R indices [I>2sigma(I)]	R1 = 0.0975, wR2 = 0.2589	
R indices (all data)	R1 = 0.1651, wR2 = 0.3000	
Absolute structure parameter	0.07(3)	
Largest diff. peak and hole	0.642 and -0.500 e.Å^{-3}	

Table A2. Atomic coordinates (x 10^4) and equivalent isotropic displacement parameters (Å ^{2}x 10^3) U(eq) is defined as one third of the trace of the orthogonalized U^{ij} tensor.

	x	y	z	U(eq)
C(1)	1623(5)	6758(3)	2814(3)	42(2)
C(2)	661(5)	6917(4)	2722(4)	50(2)
C(3)	234(5)	6277(4)	2774(3)	50(2)
C(4)	955(4)	5885(4)	2567(3)	43(2)
C(5)	819(4)	5286(4)	2369(3)	44(2)
C(6)	1484(5)	4922(4)	2271(3)	47(2)
C(7)	1456(5)	4274(4)	2049(3)	49(2)
C(8)	2334(5)	4029(3)	2231(3)	49(2)
C(9)	2845(5)	4605(4)	2257(3)	52(2)
C(10)	3700(5)	4616(4)	2234(4)	56(2)
C(11)	4230(5)	5117(4)	2276(3)	47(2)
C(12)	5166(5)	5069(4)	2300(4)	51(2)
C(13)	5453(4)	5744(3)	2327(4)	48(2)
C(14)	4596(4)	6077(3)	2304(3)	43(2)
C(15)	4553(5)	6691(4)	2295(4)	48(2)
C(16)	3741(4)	6987(4)	2385(3)	44(2)
C(17)	3586(5)	7677(4)	2421(3)	47(2)
C(18)	2702(5)	7678(3)	2681(3)	47(2)
C(19)	2292(4)	7102(3)	2482(3)	46(2)
C(20)	1863(5)	6773(4)	3389(4)	52(2)
C(21)	235(5)	7374(4)	3080(4)	59(2)
C(22)	532(5)	7108(4)	2125(4)	52(2)
C(23)	-355(5)	7128(5)	1906(4)	56(2)
C(24)	-27(5)	6066(5)	3355(4)	68(3)
C(25)	-933(6)	6111(7)	3483(5)	93(4)
C(26)	-1172(6)	5782(6)	3963(5)	76(3)
C(27)	-104(5)	5097(4)	2283(5)	66(3)
C(28)	1384(6)	4335(4)	1423(4)	56(2)
C(29)	1376(6)	3741(5)	1166(4)	62(3)
C(30)	716(5)	3879(4)	2256(4)	55(2)
C(31)	2317(5)	3698(4)	2750(3)	48(2)
C(32)	3145(5)	3543(4)	2994(4)	59(2)

C(33)	3073(5)	3130(5)	3468(4)	65(2)
C(34)	5378(6)	4715(4)	2806(5)	71(3)
C(35)	5551(6)	4765(5)	1809(4)	68(3)
C(36)	5972(4)	5935(5)	2812(4)	63(2)
C(37)	6927(5)	5720(5)	2802(4)	68(3)
C(38)	7366(4)	5892(4)	2319(5)	68(3)
C(39)	5326(5)	7052(4)	2158(4)	61(2)
C(40)	3547(6)	7941(4)	1862(4)	63(3)
C(41)	2145(5)	8236(4)	2595(4)	58(2)
C(42)	2370(5)	8767(4)	2930(4)	50(2)
C(43)	4250(5)	8028(4)	2747(3)	49(2)
C(44)	4504(5)	7785(4)	3284(4)	57(2)
C(45)	5295(5)	8119(4)	3492(4)	51(2)
C(46)	5855(5)	8777(4)	4183(4)	57(2)
C(47)	6215(5)	8476(4)	4649(4)	56(2)
C(48)	6827(6)	8889(5)	4953(5)	73(3)
C(49)	5135(5)	6690(4)	4703(4)	50(2)
C(50)	4266(5)	6452(4)	4569(3)	46(2)
C(51)	4487(4)	5851(4)	4329(4)	52(2)
C(52)	5705(5)	6405(5)	4296(4)	63(2)
C(53)	6560(6)	6204(5)	4499(4)	75(3)
C(54)	3713(4)	5884(4)	3471(3)	43(2)
C(55)	1934(5)	4943(4)	3598(3)	46(2)
C(56)	1786(5)	4547(4)	3998(4)	57(2)
C(57)	2383(6)	4460(5)	4424(4)	63(2)
C(58)	3072(5)	4834(4)	4453(3)	54(2)
C(59)	3214(5)	5234(4)	4037(3)	44(2)
C(60)	2692(5)	5272(4)	3611(3)	45(2)
C(61)	984(6)	4166(6)	4003(4)	75(3)
C(62)	2249(8)	4000(5)	4841(4)	83(3)
C(63)	2613(5)	5980(4)	1601(3)	49(2)
C(64)	1850(5)	5961(5)	1374(3)	58(2)
C(65)	3349(4)	6069(3)	1268(2)	58(2)
C(66)	3836(5)	5586(3)	1101(3)	102(5)
C(67)	4551(5)	5682(5)	790(4)	147(5)
C(68)	4780(4)	6261(5)	647(3)	146(5)
C(69)	4294(6)	6744(4)	815(4)	140(5)
C(70)	3578(5)	6648(3)	1126(3)	88(3)

N(1)	1674(3)	6149(3)	2592(3)	43(2)
N(2)	2319(4)	5088(3)	2324(3)	48(2)
N(3)	3936(3)	5685(3)	2311(3)	45(2)
N(4)	3034(4)	6693(3)	2446(3)	42(1)
N(5)	-710(5)	7656(4)	1859(3)	70(2)
N(6)	-996(6)	6055(5)	4423(4)	94(3)
N(7)	650(5)	3517(4)	1031(3)	69(2)
N(8)	3696(5)	3138(4)	3818(4)	76(2)
N(9)	7581(5)	6481(4)	2265(5)	87(3)
N(10)	2257(5)	9300(3)	2713(4)	66(2)
N(11)	5181(5)	8438(3)	3928(3)	55(2)
N(12)	3871(4)	5630(3)	3944(3)	49(2)
N(13)	3029(4)	5684(3)	3244(3)	41(2)
O(1)	-738(4)	6671(3)	1762(3)	74(2)
O(2)	-1499(6)	5287(4)	3997(4)	113(3)
O(3)	2044(5)	3483(5)	1083(4)	114(4)
O(4)	2466(4)	2783(3)	3510(3)	81(2)
O(5)	7548(4)	5530(3)	1952(4)	85(2)
O(6)	2597(4)	8714(3)	3389(3)	65(2)
O(7)	5959(4)	8085(3)	3243(3)	62(2)
O(8)	5516(3)	8329(3)	5001(2)	55(2)
O(9)	6175(4)	7435(3)	5475(3)	70(2)
O(10)	4645(5)	7702(3)	5572(3)	77(2)
O(11)	5187(4)	7323(3)	4702(3)	60(2)
O(13)	5271(3)	5911(3)	4079(2)	56(1)
O(14)	3873(4)	6813(3)	4169(2)	56(2)
O(15A)	6422(5)	5769(4)	4941(3)	77(2)
O(15B)	7154(13)	6180(20)	4036(12)	77(2)
P(1)	5395(1)	7678(1)	5235(1)	52(1)
Co(1)	2762(1)	5877(1)	2392(1)	42(1)
O(1W)	7865(4)	7371(3)	5319(3)	67(2)
O(2W)	3514(4)	8728(4)	4353(3)	84(2)
O(3W)	1250(5)	8682(4)	4087(3)	82(2)
O(4W)	2026(5)	2362(4)	756(4)	102(3)
O(5W)	7192(6)	7197(4)	3195(4)	106(3)
O(6W)	2901(7)	2033(4)	4356(4)	124(3)
O(7W)	8072(7)	4332(4)	3423(5)	120(3)
O(8W)	7400(12)	5806(5)	892(5)	176(6)

O(9W)	5126(7)	3935(8)	4053(5)	164(5)
O(10W)	9318(7)	3518(5)	3398(6)	144(5)
O(11W)	6901(7)	3891(6)	4194(5)	144(4)
O(12W)	7703(14)	4918(8)	4988(9)	315(17)
O(13W)	9318(8)	5764(6)	961(6)	159(5)
O(14W)	9838(9)	5307(7)	17(6)	170(5)
O(15W)	7601(9)	2856(6)	4543(6)	163(5)
C(1A)	-752(13)	7391(10)	467(8)	155(7)
C(2A)	157(12)	7375(9)	498(7)	144(6)
C(3A)	630(20)	6882(13)	281(13)	243(13)
O(1A)	606(10)	7764(8)	715(6)	176(5)

Table A3. Bond lengths [Å] and angles [°] for

Bond Lengths

C(1)-N(1)	1.472(10)
C(1)-C(20)	1.498(12)
C(1)-C(19)	1.550(11)
C(1)-C(2)	1.576(10)
C(2)-C(21)	1.521(13)
C(2)-C(22)	1.574(12)
C(2)-C(3)	1.585(12)
C(3)-C(4)	1.528(11)
C(3)-C(24)	1.592(14)
C(3)-H(3)	1.0000
C(4)-N(1)	1.281(9)
C(4)-C(5)	1.443(12)
C(5)-C(6)	1.350(11)
C(5)-C(27)	1.534(11)
C(6)-N(2)	1.375(9)
C(6)-C(7)	1.552(12)
C(7)-C(30)	1.553(11)
C(7)-C(8)	1.558(11)
C(7)-C(28)	1.585(13)
C(8)-C(31)	1.502(12)
C(8)-C(9)	1.521(11)
C(8)-H(8)	1.0000
C(9)-C(10)	1.351(12)
C(9)-N(2)	1.373(11)
C(10)-C(11)	1.403(12)
C(10)-H(10)	0.9500
C(11)-N(3)	1.352(11)
C(11)-C(12)	1.483(11)
C(12)-C(34)	1.536(14)
C(12)-C(35)	1.537(13)
C(12)-C(13)	1.575(11)
C(13)-C(36)	1.532(13)
C(13)-C(14)	1.545(10)
C(13)-H(13)	1.0000
C(14)-N(3)	1.361(10)
C(14)-C(15)	1.373(11)
C(15)-C(16)	1.459(11)
C(15)-C(39)	1.503(12)
C(16)-N(4)	1.304(9)
C(16)-C(17)	1.564(11)
C(17)-C(40)	1.526(13)
C(17)-C(18)	1.542(11)
C(17)-C(43)	1.545(11)
C(18)-C(19)	1.525(11)
C(18)-C(41)	1.541(11)
C(18)-H(18)	1.0000
C(19)-N(4)	1.488(10)
C(19)-H(19)	1.0000
C(20)-H(20A)	0.9800
C(20)-H(20B)	0.9800
C(20)-H(20C)	0.9800
C(21)-H(21A)	0.9800

C(21)-H(21B)	0.9800
C(21)-H(21C)	0.9800
C(22)-C(23)	1.505(11)
C(22)-H(22A)	0.9900
C(22)-H(22B)	0.9900
C(23)-O(1)	1.240(11)
C(23)-N(5)	1.313(13)
C(24)-C(25)	1.469(13)
C(24)-H(24A)	0.9900
C(24)-H(24B)	0.9900
C(25)-C(26)	1.463(18)
C(25)-H(25A)	0.9900
C(25)-H(25B)	0.9900
C(26)-O(2)	1.222(14)
C(26)-N(6)	1.338(14)
C(27)-H(27A)	0.9800
C(27)-H(27B)	0.9800
C(27)-H(27C)	0.9800
C(28)-C(29)	1.478(13)
C(28)-H(28A)	0.9900
C(28)-H(28B)	0.9900
C(29)-O(3)	1.219(12)
C(29)-N(7)	1.295(11)
C(30)-H(30A)	0.9800
C(30)-H(30B)	0.9800
C(30)-H(30C)	0.9800
C(31)-C(32)	1.484(11)
C(31)-H(31A)	0.9900
C(31)-H(31B)	0.9900
C(32)-C(33)	1.511(15)
C(32)-H(32A)	0.9900
C(32)-H(32B)	0.9900
C(33)-O(4)	1.234(11)
C(33)-N(8)	1.322(12)
C(34)-H(34A)	0.9800
C(34)-H(34B)	0.9800
C(34)-H(34C)	0.9800
C(35)-H(35A)	0.9800
C(35)-H(35B)	0.9800
C(35)-H(35C)	0.9800
C(36)-C(37)	1.582(11)
C(36)-H(36A)	0.9900
C(36)-H(36B)	0.9900
C(37)-C(38)	1.452(15)
C(37)-H(37A)	0.9900
C(37)-H(37B)	0.9900
C(38)-O(5)	1.259(13)
C(38)-N(9)	1.366(13)
C(39)-H(39A)	0.9800
C(39)-H(39B)	0.9800
C(39)-H(39C)	0.9800
C(40)-H(40A)	0.9800
C(40)-H(40B)	0.9800
C(40)-H(40C)	0.9800
C(41)-C(42)	1.498(13)

C(41)-H(41A)	0.9900
C(41)-H(41B)	0.9900
C(42)-O(6)	1.217(10)
C(42)-N(10)	1.322(11)
C(43)-C(44)	1.512(12)
C(43)-H(43A)	0.9900
C(43)-H(43B)	0.9900
C(44)-C(45)	1.544(12)
C(44)-H(44A)	0.9900
C(44)-H(44B)	0.9900
C(45)-O(7)	1.224(10)
C(45)-N(11)	1.322(12)
C(46)-N(11)	1.456(11)
C(46)-C(47)	1.467(13)
C(46)-H(46A)	0.9900
C(46)-H(46B)	0.9900
C(47)-O(8)	1.453(11)
C(47)-C(48)	1.539(12)
C(47)-H(47)	1.0000
C(48)-H(48A)	0.9800
C(48)-H(48B)	0.9800
C(48)-H(48C)	0.9800
C(49)-O(11)	1.417(10)
C(49)-C(50)	1.509(11)
C(49)-C(52)	1.507(14)
C(49)-H(49)	1.0000
C(50)-O(14)	1.433(10)
C(50)-C(51)	1.512(13)
C(50)-H(50)	1.0000
C(51)-O(13)	1.393(10)
C(51)-N(12)	1.458(10)
C(51)-H(51)	1.0000
C(52)-O(13)	1.409(11)
C(52)-C(53)	1.509(14)
C(52)-H(52)	1.0000
C(53)-O(15A)	1.495(13)
C(53)-O(15B)	1.497(13)
C(53)-H(53A)	0.9900
C(53)-H(53B)	0.9900
C(53)-H(53C)	0.9700
C(53)-H(53D)	0.9700
C(54)-N(13)	1.302(9)
C(54)-N(12)	1.341(10)
C(54)-H(54)	0.9500
C(55)-C(56)	1.360(13)
C(55)-C(60)	1.405(11)
C(55)-H(55)	0.9500
C(56)-C(57)	1.442(13)
C(56)-C(61)	1.525(13)
C(57)-C(58)	1.372(12)
C(57)-C(62)	1.484(14)
C(58)-C(59)	1.394(12)
C(58)-H(58)	0.9500
C(59)-C(60)	1.355(11)
C(59)-N(12)	1.384(10)

C(60)-N(13)	1.408(10)
C(61)-H(61A)	0.9800
C(61)-H(61B)	0.9800
C(61)-H(61C)	0.9800
C(62)-H(62A)	0.9800
C(62)-H(62B)	0.9800
C(62)-H(62C)	0.9800
C(63)-C(64)	1.333(11)
C(63)-C(65)	1.445(9)
C(63)-Co(1)	2.019(9)
C(64)-H(64A)	0.9500
C(64)-H(64B)	0.9500
C(65)-C(66)	1.3900
C(65)-C(70)	1.3900
C(66)-C(67)	1.3900
C(66)-H(66)	0.9500
C(67)-C(68)	1.3900
C(67)-H(67)	0.9500
C(68)-C(69)	1.3900
C(68)-H(68)	0.9500
C(69)-C(70)	1.3900
C(69)-H(69)	0.9500
C(70)-H(70)	0.9500
N(1)-Co(1)	1.890(5)
N(2)-Co(1)	1.903(6)
N(3)-Co(1)	1.913(6)
N(4)-Co(1)	1.879(6)
N(5)-H(5A)	0.8800
N(5)-H(5B)	0.8800
N(6)-H(6A)	0.8800
N(6)-H(6B)	0.8800
N(7)-H(7A)	0.8800
N(7)-H(7B)	0.8800
N(8)-H(8A)	0.8800
N(8)-H(8B)	0.8800
N(9)-H(9A)	0.8800
N(9)-H(9B)	0.8800
N(10)-H(10A)	0.8800
N(10)-H(10B)	0.8800
N(11)-H(11)	0.8800
N(13)-Co(1)	2.224(7)
O(8)-P(1)	1.579(6)
O(9)-P(1)	1.475(7)
O(10)-P(1)	1.457(7)
O(11)-P(1)	1.591(6)
O(14)-H(14)	0.8400
O(15A)-H(53C)	0.7744
O(15A)-H(15A)	0.8400
O(15B)-H(15B)	0.8200
C(1A)-C(2A)	1.438(19)
C(1A)-H(1A)	0.9800
C(1A)-H(1B)	0.9800
C(1A)-H(1C)	0.9800
C(2A)-O(1A)	1.247(15)
C(2A)-C(3A)	1.44(2)

C(3A)-H(3A)	0.9800
C(3A)-H(3B)	0.9800
C(3A)-H(3C)	0.9800

Bond angles

N(1)-C(1)-C(20)	111.9(7)
N(1)-C(1)-C(19)	102.5(6)
C(20)-C(1)-C(19)	109.8(6)
N(1)-C(1)-C(2)	101.8(6)
C(20)-C(1)-C(2)	112.4(7)
C(19)-C(1)-C(2)	117.7(7)
C(21)-C(2)-C(22)	109.1(7)
C(21)-C(2)-C(1)	119.3(7)
C(22)-C(2)-C(1)	109.0(6)
C(21)-C(2)-C(3)	111.7(7)
C(22)-C(2)-C(3)	105.6(7)
C(1)-C(2)-C(3)	101.2(6)
C(4)-C(3)-C(2)	99.9(6)
C(4)-C(3)-C(24)	109.5(7)
C(2)-C(3)-C(24)	117.0(7)
C(4)-C(3)-H(3)	110.0
C(2)-C(3)-H(3)	110.0
C(24)-C(3)-H(3)	110.0
N(1)-C(4)-C(5)	125.2(7)
N(1)-C(4)-C(3)	112.2(7)
C(5)-C(4)-C(3)	122.6(6)
C(6)-C(5)-C(4)	120.5(6)
C(6)-C(5)-C(27)	123.1(7)
C(4)-C(5)-C(27)	116.4(7)
C(5)-C(6)-N(2)	124.3(7)
C(5)-C(6)-C(7)	127.3(6)
N(2)-C(6)-C(7)	108.4(7)
C(30)-C(7)-C(6)	115.6(7)
C(30)-C(7)-C(8)	111.7(7)
C(6)-C(7)-C(8)	101.4(6)
C(30)-C(7)-C(28)	109.2(7)
C(6)-C(7)-C(28)	106.2(7)
C(8)-C(7)-C(28)	112.6(7)
C(31)-C(8)-C(9)	112.8(7)
C(31)-C(8)-C(7)	114.3(7)
C(9)-C(8)-C(7)	100.7(6)
C(31)-C(8)-H(8)	109.5
C(9)-C(8)-H(8)	109.5
C(7)-C(8)-H(8)	109.5
C(10)-C(9)-N(2)	126.6(8)
C(10)-C(9)-C(8)	122.8(8)
N(2)-C(9)-C(8)	110.5(6)
C(9)-C(10)-C(11)	127.3(8)
C(9)-C(10)-H(10)	116.4
C(11)-C(10)-H(10)	116.4
N(3)-C(11)-C(10)	123.4(7)
N(3)-C(11)-C(12)	114.0(7)
C(10)-C(11)-C(12)	122.6(8)

C(11)-C(12)-C(34)	106.8(7)
C(11)-C(12)-C(35)	113.1(7)
C(34)-C(12)-C(35)	110.7(7)
C(11)-C(12)-C(13)	102.6(6)
C(34)-C(12)-C(13)	113.3(8)
C(35)-C(12)-C(13)	110.1(7)
C(36)-C(13)-C(14)	111.3(7)
C(36)-C(13)-C(12)	117.1(7)
C(14)-C(13)-C(12)	102.0(6)
C(36)-C(13)-H(13)	108.7
C(14)-C(13)-H(13)	108.7
C(12)-C(13)-H(13)	108.7
N(3)-C(14)-C(15)	127.2(6)
N(3)-C(14)-C(13)	111.0(6)
C(15)-C(14)-C(13)	121.7(6)
C(14)-C(15)-C(16)	119.6(7)
C(14)-C(15)-C(39)	119.9(7)
C(16)-C(15)-C(39)	120.3(7)
N(4)-C(16)-C(15)	122.7(7)
N(4)-C(16)-C(17)	110.8(6)
C(15)-C(16)-C(17)	126.4(6)
C(40)-C(17)-C(18)	110.8(7)
C(40)-C(17)-C(43)	108.7(7)
C(18)-C(17)-C(43)	112.8(7)
C(40)-C(17)-C(16)	109.5(7)
C(18)-C(17)-C(16)	99.6(6)
C(43)-C(17)-C(16)	115.1(6)
C(19)-C(18)-C(41)	113.2(6)
C(19)-C(18)-C(17)	104.0(6)
C(41)-C(18)-C(17)	117.2(7)
C(19)-C(18)-H(18)	107.3
C(41)-C(18)-H(18)	107.3
C(17)-C(18)-H(18)	107.3
N(4)-C(19)-C(18)	101.8(5)
N(4)-C(19)-C(1)	105.3(6)
C(18)-C(19)-C(1)	121.9(7)
N(4)-C(19)-H(19)	109.0
C(18)-C(19)-H(19)	109.0
C(1)-C(19)-H(19)	109.0
C(1)-C(20)-H(20A)	109.5
C(1)-C(20)-H(20B)	109.5
H(20A)-C(20)-H(20B)	109.5
C(1)-C(20)-H(20C)	109.5
H(20A)-C(20)-H(20C)	109.5
H(20B)-C(20)-H(20C)	109.5
C(2)-C(21)-H(21A)	109.5
C(2)-C(21)-H(21B)	109.5
H(21A)-C(21)-H(21B)	109.5
C(2)-C(21)-H(21C)	109.5
H(21A)-C(21)-H(21C)	109.5
H(21B)-C(21)-H(21C)	109.5
C(23)-C(22)-C(2)	118.5(7)
C(23)-C(22)-H(22A)	107.7
C(2)-C(22)-H(22A)	107.7
C(23)-C(22)-H(22B)	107.7

C(2)-C(22)-H(22B)	107.7
H(22A)-C(22)-H(22B)	107.1
O(1)-C(23)-N(5)	120.4(8)
O(1)-C(23)-C(22)	122.4(9)
N(5)-C(23)-C(22)	117.1(9)
C(25)-C(24)-C(3)	115.6(9)
C(25)-C(24)-H(24A)	108.4
C(3)-C(24)-H(24A)	108.4
C(25)-C(24)-H(24B)	108.4
C(3)-C(24)-H(24B)	108.4
H(24A)-C(24)-H(24B)	107.4
C(26)-C(25)-C(24)	113.4(11)
C(26)-C(25)-H(25A)	108.9
C(24)-C(25)-H(25A)	108.9
C(26)-C(25)-H(25B)	108.9
C(24)-C(25)-H(25B)	108.9
H(25A)-C(25)-H(25B)	107.7
O(2)-C(26)-N(6)	116.1(11)
O(2)-C(26)-C(25)	128.4(12)
N(6)-C(26)-C(25)	115.6(11)
C(5)-C(27)-H(27A)	109.5
C(5)-C(27)-H(27B)	109.5
H(27A)-C(27)-H(27B)	109.5
C(5)-C(27)-H(27C)	109.5
H(27A)-C(27)-H(27C)	109.5
H(27B)-C(27)-H(27C)	109.5
C(29)-C(28)-C(7)	111.1(8)
C(29)-C(28)-H(28A)	109.4
C(7)-C(28)-H(28A)	109.4
C(29)-C(28)-H(28B)	109.4
C(7)-C(28)-H(28B)	109.4
H(28A)-C(28)-H(28B)	108.0
O(3)-C(29)-N(7)	122.6(9)
O(3)-C(29)-C(28)	119.4(9)
N(7)-C(29)-C(28)	117.9(9)
C(7)-C(30)-H(30A)	109.5
C(7)-C(30)-H(30B)	109.5
H(30A)-C(30)-H(30B)	109.5
C(7)-C(30)-H(30C)	109.5
H(30A)-C(30)-H(30C)	109.5
H(30B)-C(30)-H(30C)	109.5
C(32)-C(31)-C(8)	117.3(7)
C(32)-C(31)-H(31A)	108.0
C(8)-C(31)-H(31A)	108.0
C(32)-C(31)-H(31B)	108.0
C(8)-C(31)-H(31B)	108.0
H(31A)-C(31)-H(31B)	107.2
C(31)-C(32)-C(33)	113.7(7)
C(31)-C(32)-H(32A)	108.8
C(33)-C(32)-H(32A)	108.8
C(31)-C(32)-H(32B)	108.8
C(33)-C(32)-H(32B)	108.8
H(32A)-C(32)-H(32B)	107.7
O(4)-C(33)-N(8)	121.8(10)
O(4)-C(33)-C(32)	120.7(8)

N(8)-C(33)-C(32)	117.5(8)
C(12)-C(34)-H(34A)	109.5
C(12)-C(34)-H(34B)	109.5
H(34A)-C(34)-H(34B)	109.5
C(12)-C(34)-H(34C)	109.5
H(34A)-C(34)-H(34C)	109.5
H(34B)-C(34)-H(34C)	109.5
C(12)-C(35)-H(35A)	109.5
C(12)-C(35)-H(35B)	109.5
H(35A)-C(35)-H(35B)	109.5
C(12)-C(35)-H(35C)	109.5
H(35A)-C(35)-H(35C)	109.5
H(35B)-C(35)-H(35C)	109.5
C(13)-C(36)-C(37)	114.3(8)
C(13)-C(36)-H(36A)	108.7
C(37)-C(36)-H(36A)	108.7
C(13)-C(36)-H(36B)	108.7
C(37)-C(36)-H(36B)	108.7
H(36A)-C(36)-H(36B)	107.6
C(38)-C(37)-C(36)	112.8(8)
C(38)-C(37)-H(37A)	109.0
C(36)-C(37)-H(37A)	109.0
C(38)-C(37)-H(37B)	109.0
C(36)-C(37)-H(37B)	109.0
H(37A)-C(37)-H(37B)	107.8
O(5)-C(38)-N(9)	119.4(10)
O(5)-C(38)-C(37)	123.5(9)
N(9)-C(38)-C(37)	117.1(11)
C(15)-C(39)-H(39A)	109.5
C(15)-C(39)-H(39B)	109.5
H(39A)-C(39)-H(39B)	109.5
C(15)-C(39)-H(39C)	109.5
H(39A)-C(39)-H(39C)	109.5
H(39B)-C(39)-H(39C)	109.5
C(17)-C(40)-H(40A)	109.5
C(17)-C(40)-H(40B)	109.5
H(40A)-C(40)-H(40B)	109.5
C(17)-C(40)-H(40C)	109.5
H(40A)-C(40)-H(40C)	109.5
H(40B)-C(40)-H(40C)	109.5
C(42)-C(41)-C(18)	115.3(7)
C(42)-C(41)-H(41A)	108.5
C(18)-C(41)-H(41A)	108.5
C(42)-C(41)-H(41B)	108.5
C(18)-C(41)-H(41B)	108.5
H(41A)-C(41)-H(41B)	107.5
O(6)-C(42)-N(10)	121.3(9)
O(6)-C(42)-C(41)	121.7(8)
N(10)-C(42)-C(41)	116.8(8)
C(44)-C(43)-C(17)	118.1(7)
C(44)-C(43)-H(43A)	107.8
C(17)-C(43)-H(43A)	107.8
C(44)-C(43)-H(43B)	107.8
C(17)-C(43)-H(43B)	107.8
H(43A)-C(43)-H(43B)	107.1

C(43)-C(44)-C(45)	110.0(7)
C(43)-C(44)-H(44A)	109.7
C(45)-C(44)-H(44A)	109.7
C(43)-C(44)-H(44B)	109.7
C(45)-C(44)-H(44B)	109.7
H(44A)-C(44)-H(44B)	108.2
O(7)-C(45)-N(11)	125.2(8)
O(7)-C(45)-C(44)	119.3(8)
N(11)-C(45)-C(44)	115.6(7)
N(11)-C(46)-C(47)	113.3(7)
N(11)-C(46)-H(46A)	108.9
C(47)-C(46)-H(46A)	108.9
N(11)-C(46)-H(46B)	108.9
C(47)-C(46)-H(46B)	108.9
H(46A)-C(46)-H(46B)	107.7
O(8)-C(47)-C(46)	107.3(7)
O(8)-C(47)-C(48)	107.9(8)
C(46)-C(47)-C(48)	111.4(8)
O(8)-C(47)-H(47)	110.0
C(46)-C(47)-H(47)	110.0
C(48)-C(47)-H(47)	110.0
C(47)-C(48)-H(48A)	109.5
C(47)-C(48)-H(48B)	109.5
H(48A)-C(48)-H(48B)	109.5
C(47)-C(48)-H(48C)	109.5
H(48A)-C(48)-H(48C)	109.5
H(48B)-C(48)-H(48C)	109.5
O(11)-C(49)-C(50)	113.8(7)
O(11)-C(49)-C(52)	112.6(7)
C(50)-C(49)-C(52)	104.0(7)
O(11)-C(49)-H(49)	108.7
C(50)-C(49)-H(49)	108.7
C(52)-C(49)-H(49)	108.7
O(14)-C(50)-C(51)	108.6(7)
O(14)-C(50)-C(49)	110.6(7)
C(51)-C(50)-C(49)	101.2(6)
O(14)-C(50)-H(50)	112.0
C(51)-C(50)-H(50)	112.0
C(49)-C(50)-H(50)	112.0
O(13)-C(51)-N(12)	108.9(7)
O(13)-C(51)-C(50)	107.4(7)
N(12)-C(51)-C(50)	114.4(7)
O(13)-C(51)-H(51)	108.7
N(12)-C(51)-H(51)	108.7
C(50)-C(51)-H(51)	108.7
O(13)-C(52)-C(53)	109.4(8)
O(13)-C(52)-C(49)	107.6(7)
C(53)-C(52)-C(49)	115.4(8)
O(13)-C(52)-H(52)	108.1
C(53)-C(52)-H(52)	108.1
C(49)-C(52)-H(52)	108.1
O(15A)-C(53)-O(15B)	130.3(18)
O(15A)-C(53)-C(52)	108.4(7)
O(15B)-C(53)-C(52)	108.0(8)
O(15A)-C(53)-H(53A)	110.0

C(52)-C(53)-H(53A)	110.0
O(15A)-C(53)-H(53B)	110.0
O(15B)-C(53)-H(53B)	87.6
C(52)-C(53)-H(53B)	110.0
H(53A)-C(53)-H(53B)	108.4
O(15B)-C(53)-H(53C)	106.3
C(52)-C(53)-H(53C)	111.8
H(53A)-C(53)-H(53C)	83.9
H(53B)-C(53)-H(53C)	128.5
O(15A)-C(53)-H(53D)	87.7
O(15B)-C(53)-H(53D)	108.6
C(52)-C(53)-H(53D)	111.9
H(53A)-C(53)-H(53D)	125.7
H(53C)-C(53)-H(53D)	110.0
N(13)-C(54)-N(12)	113.5(7)
N(13)-C(54)-H(54)	123.2
N(12)-C(54)-H(54)	123.2
C(56)-C(55)-C(60)	118.0(8)
C(56)-C(55)-H(55)	121.0
C(60)-C(55)-H(55)	121.0
C(55)-C(56)-C(57)	121.8(8)
C(55)-C(56)-C(61)	120.8(9)
C(57)-C(56)-C(61)	117.4(8)
C(58)-C(57)-C(56)	118.3(8)
C(58)-C(57)-C(62)	119.8(8)
C(56)-C(57)-C(62)	121.8(8)
C(57)-C(58)-C(59)	118.5(8)
C(57)-C(58)-H(58)	120.7
C(59)-C(58)-H(58)	120.7
C(60)-C(59)-N(12)	106.3(7)
C(60)-C(59)-C(58)	122.5(7)
N(12)-C(59)-C(58)	131.2(7)
C(59)-C(60)-C(55)	120.2(8)
C(59)-C(60)-N(13)	109.4(7)
C(55)-C(60)-N(13)	130.4(7)
C(56)-C(61)-H(61A)	109.5
C(56)-C(61)-H(61B)	109.5
H(61A)-C(61)-H(61B)	109.5
C(56)-C(61)-H(61C)	109.5
H(61A)-C(61)-H(61C)	109.5
H(61B)-C(61)-H(61C)	109.5
C(57)-C(62)-H(62A)	109.5
C(57)-C(62)-H(62B)	109.5
H(62A)-C(62)-H(62B)	109.5
C(57)-C(62)-H(62C)	109.5
H(62A)-C(62)-H(62C)	109.5
H(62B)-C(62)-H(62C)	109.5
C(64)-C(63)-C(65)	118.9(8)
C(64)-C(63)-Co(1)	121.6(6)
C(65)-C(63)-Co(1)	119.5(5)
C(63)-C(64)-H(64A)	120.0
C(63)-C(64)-H(64B)	120.0
H(64A)-C(64)-H(64B)	120.0
C(66)-C(65)-C(70)	120.0
C(66)-C(65)-C(63)	120.9(6)

C(70)-C(65)-C(63)	119.1(5)
C(65)-C(66)-C(67)	120.0
C(65)-C(66)-H(66)	120.0
C(67)-C(66)-H(66)	120.0
C(68)-C(67)-C(66)	120.0
C(68)-C(67)-H(67)	120.0
C(66)-C(67)-H(67)	120.0
C(67)-C(68)-C(69)	120.0
C(67)-C(68)-H(68)	120.0
C(69)-C(68)-H(68)	120.0
C(70)-C(69)-C(68)	120.0
C(70)-C(69)-H(69)	120.0
C(68)-C(69)-H(69)	120.0
C(69)-C(70)-C(65)	120.0
C(69)-C(70)-H(70)	120.0
C(65)-C(70)-H(70)	120.0
C(4)-N(1)-C(1)	113.4(6)
C(4)-N(1)-Co(1)	130.0(6)
C(1)-N(1)-Co(1)	116.6(4)
C(9)-N(2)-C(6)	110.8(7)
C(9)-N(2)-Co(1)	121.1(5)
C(6)-N(2)-Co(1)	127.7(6)
C(11)-N(3)-C(14)	109.9(6)
C(11)-N(3)-Co(1)	123.3(5)
C(14)-N(3)-Co(1)	126.7(5)
C(16)-N(4)-C(19)	111.8(6)
C(16)-N(4)-Co(1)	132.6(5)
C(19)-N(4)-Co(1)	114.8(4)
C(23)-N(5)-H(5A)	120.0
C(23)-N(5)-H(5B)	120.0
H(5A)-N(5)-H(5B)	120.0
C(26)-N(6)-H(6A)	120.0
C(26)-N(6)-H(6B)	120.0
H(6A)-N(6)-H(6B)	120.0
C(29)-N(7)-H(7A)	120.0
C(29)-N(7)-H(7B)	120.0
H(7A)-N(7)-H(7B)	120.0
C(33)-N(8)-H(8A)	120.0
C(33)-N(8)-H(8B)	120.0
H(8A)-N(8)-H(8B)	120.0
C(38)-N(9)-H(9A)	120.0
C(38)-N(9)-H(9B)	120.0
H(9A)-N(9)-H(9B)	120.0
C(42)-N(10)-H(10A)	120.0
C(42)-N(10)-H(10B)	120.0
H(10A)-N(10)-H(10B)	120.0
C(45)-N(11)-C(46)	123.2(7)
C(45)-N(11)-H(11)	118.4
C(46)-N(11)-H(11)	118.4
C(54)-N(12)-C(59)	106.4(6)
C(54)-N(12)-C(51)	124.8(7)
C(59)-N(12)-C(51)	127.1(7)
C(54)-N(13)-C(60)	104.4(6)
C(54)-N(13)-Co(1)	120.9(5)
C(60)-N(13)-Co(1)	133.4(5)

C(47)-O(8)-P(1)	121.8(5)
C(49)-O(11)-P(1)	120.5(6)
C(51)-O(13)-C(52)	109.5(6)
C(50)-O(14)-H(14)	109.5
C(53)-O(15A)-H(15A)	109.5
H(53C)-O(15A)-H(15A)	74.9
C(53)-O(15B)-H(15B)	103.1
O(10)-P(1)-O(9)	116.9(4)
O(10)-P(1)-O(8)	106.3(4)
O(9)-P(1)-O(8)	112.9(4)
O(10)-P(1)-O(11)	109.9(4)
O(9)-P(1)-O(11)	109.5(4)
O(8)-P(1)-O(11)	99.9(3)
N(4)-Co(1)-N(1)	82.9(3)
N(4)-Co(1)-N(2)	171.6(3)
N(1)-Co(1)-N(2)	89.4(3)
N(4)-Co(1)-N(3)	90.2(3)
N(1)-Co(1)-N(3)	168.7(3)
N(2)-Co(1)-N(3)	98.0(3)
N(4)-Co(1)-C(63)	89.3(3)
N(1)-Co(1)-C(63)	96.9(3)
N(2)-Co(1)-C(63)	88.5(3)
N(3)-Co(1)-C(63)	91.9(3)
N(4)-Co(1)-N(13)	94.3(3)
N(1)-Co(1)-N(13)	88.8(3)
N(2)-Co(1)-N(13)	88.7(3)
N(3)-Co(1)-N(13)	82.9(3)
C(63)-Co(1)-N(13)	173.6(3)
C(2A)-C(1A)-H(1A)	109.5
C(2A)-C(1A)-H(1B)	109.5
H(1A)-C(1A)-H(1B)	109.5
C(2A)-C(1A)-H(1C)	109.5
H(1A)-C(1A)-H(1C)	109.5
H(1B)-C(1A)-H(1C)	109.5
O(1A)-C(2A)-C(1A)	125(2)
O(1A)-C(2A)-C(3A)	114(2)
C(1A)-C(2A)-C(3A)	121(2)
C(2A)-C(3A)-H(3A)	109.5
C(2A)-C(3A)-H(3B)	109.5
H(3A)-C(3A)-H(3B)	109.5
C(2A)-C(3A)-H(3C)	109.5
H(3A)-C(3A)-H(3C)	109.5
H(3B)-C(3A)-H(3C)	109.5

Table A4. Anisotropic displacement parameters (Å ^{2}x 10^3)for β-PhVnCbl. The anisotropic displacement factor exponent takes the form: $-2\pi^2[h^2a^{*2}U^{11} + ... + 2 h k a^* b^* U^{12}]$

	U^{11}	U^{22}	U^{33}	U^{23}	U^{13}	U^{12}
C(1)	35(4)	38(4)	52(5)	-7(4)	0(3)	2(3)
C(2)	35(4)	50(5)	65(6)	6(4)	-3(4)	1(3)
C(3)	31(4)	65(5)	54(5)	2(4)	-1(3)	-2(4)
C(4)	24(3)	63(5)	43(4)	2(4)	2(3)	4(3)
C(5)	34(3)	52(5)	47(4)	-4(4)	-4(4)	-4(3)
C(6)	32(4)	58(5)	51(5)	-1(4)	-5(3)	-15(3)
C(7)	40(4)	56(5)	49(5)	-16(4)	5(3)	-14(4)
C(8)	43(4)	40(4)	65(5)	-21(4)	3(4)	-11(4)
C(9)	42(4)	54(5)	59(5)	-1(4)	-9(4)	-1(4)
C(10)	41(4)	48(5)	78(6)	-12(5)	2(4)	-4(4)
C(11)	43(4)	62(5)	36(4)	-5(4)	-5(3)	-1(4)
C(12)	38(4)	44(4)	72(6)	-10(4)	10(4)	0(3)
C(13)	31(3)	42(4)	71(5)	0(4)	2(4)	1(3)
C(14)	27(3)	46(4)	57(5)	-6(4)	-1(3)	4(3)
C(15)	33(4)	49(5)	62(5)	5(4)	-7(4)	0(3)
C(16)	34(3)	50(4)	48(4)	1(4)	5(4)	-14(3)
C(17)	39(4)	48(4)	52(4)	5(4)	-9(3)	4(3)
C(18)	37(4)	44(4)	61(5)	-2(4)	-5(4)	2(3)
C(19)	39(4)	42(4)	56(5)	5(4)	-10(4)	-5(3)
C(20)	43(4)	45(5)	68(6)	1(4)	-5(4)	1(4)
C(21)	41(4)	66(6)	68(6)	2(5)	4(4)	0(4)
C(22)	27(4)	62(5)	67(5)	9(5)	-4(4)	1(4)
C(23)	39(4)	72(6)	57(5)	3(5)	-2(4)	-10(5)
C(24)	43(4)	66(6)	95(7)	-9(6)	10(5)	-5(4)
C(25)	46(5)	120(11)	112(9)	-17(8)	17(6)	-10(6)
C(26)	42(5)	96(9)	89(8)	-11(7)	4(5)	-15(5)
C(27)	46(5)	56(5)	95(8)	3(6)	0(5)	3(4)
C(28)	51(5)	53(5)	63(5)	-6(4)	-10(4)	-13(4)
C(29)	44(5)	82(7)	59(5)	-34(5)	2(4)	-4(5)
C(30)	39(4)	59(5)	68(6)	2(5)	1(4)	-11(4)
C(31)	44(4)	42(4)	59(5)	-4(4)	4(4)	-8(4)
C(32)	32(4)	60(5)	84(5)	-2(4)	-7(4)	-8(4)
C(33)	37(4)	81(6)	78(6)	-6(4)	-5(4)	-3(4)

C(34)	55(5)	51(5)	107(8)	13(6)	-2(5)	8(5)
C(35)	46(5)	63(6)	95(8)	-19(6)	-4(5)	3(4)
C(36)	24(3)	65(6)	99(7)	7(5)	-11(4)	1(4)
C(37)	24(3)	74(6)	106(8)	5(6)	-4(4)	1(4)
C(38)	24(3)	60(5)	120(8)	5(7)	3(5)	-5(4)
C(39)	44(4)	60(6)	79(6)	8(5)	0(4)	-2(4)
C(40)	66(6)	42(5)	83(7)	8(5)	-14(5)	-14(4)
C(41)	38(4)	47(4)	88(6)	3(5)	-1(5)	-2(3)
C(42)	32(4)	58(5)	61(6)	16(4)	7(4)	5(4)
C(43)	42(4)	49(4)	56(5)	8(4)	7(3)	-8(3)
C(44)	46(4)	68(6)	57(5)	-11(5)	-2(4)	-3(4)
C(45)	37(4)	58(5)	59(5)	14(5)	0(4)	2(4)
C(46)	42(4)	57(5)	73(6)	3(5)	4(4)	-20(4)
C(47)	46(4)	51(5)	71(6)	-9(5)	-2(4)	-15(4)
C(48)	52(5)	71(6)	98(8)	-6(6)	-13(5)	-24(5)
C(49)	46(4)	47(5)	58(5)	6(4)	-11(4)	-8(4)
C(50)	37(4)	51(5)	51(5)	-1(4)	-2(3)	-2(3)
C(51)	35(4)	54(5)	67(5)	3(5)	-10(4)	-2(4)
C(52)	42(4)	69(6)	77(6)	-10(5)	-6(4)	-16(4)
C(53)	61(5)	71(6)	93(7)	-19(5)	5(5)	-5(5)
C(54)	26(3)	42(4)	61(5)	4(4)	2(3)	-9(3)
C(55)	36(4)	47(5)	55(5)	2(4)	0(4)	-5(3)
C(56)	49(5)	71(6)	53(5)	-8(5)	11(4)	-10(4)
C(57)	63(6)	77(6)	51(5)	4(5)	-6(4)	-20(5)
C(58)	46(4)	72(6)	44(5)	-1(5)	-6(4)	-1(4)
C(59)	37(4)	43(4)	52(5)	2(4)	-3(3)	1(3)
C(60)	33(4)	47(4)	56(5)	-4(4)	-3(4)	9(4)
C(61)	55(5)	94(8)	76(6)	0(6)	7(5)	-20(6)
C(62)	104(8)	71(6)	73(6)	10(5)	-25(6)	-45(7)
C(63)	40(4)	49(5)	59(5)	-12(4)	5(4)	-4(4)
C(64)	53(5)	77(6)	45(4)	-5(5)	-4(4)	-15(5)
C(65)	43(4)	75(5)	56(5)	-7(4)	-12(4)	-8(4)
C(66)	82(8)	143(12)	80(8)	16(8)	22(7)	49(8)
C(67)	89(8)	267(16)	85(7)	58(9)	21(7)	-10(9)
C(68)	81(7)	272(16)	83(7)	46(9)	12(6)	-35(8)
C(69)	96(8)	253(16)	69(7)	26(9)	12(6)	-56(8)
C(70)	101(8)	106(7)	55(6)	-11(6)	9(6)	-53(7)
N(1)	21(2)	58(4)	51(4)	-7(3)	2(3)	5(2)

N(2)	37(3)	47(4)	58(4)	-14(3)	1(3)	-8(3)
N(3)	28(3)	46(4)	60(4)	-10(3)	4(3)	1(3)
N(4)	32(3)	48(4)	45(4)	-6(3)	-2(3)	1(3)
N(5)	61(5)	60(5)	90(6)	-8(5)	-19(4)	14(4)
N(6)	88(6)	122(9)	73(6)	1(6)	9(5)	-43(6)
N(7)	49(4)	79(6)	79(6)	-25(5)	3(4)	-11(4)
N(8)	57(4)	88(6)	82(5)	20(5)	-10(4)	-5(4)
N(9)	66(5)	60(5)	135(8)	1(5)	14(5)	-18(4)
N(10)	64(4)	38(4)	96(6)	8(4)	-6(5)	-4(3)
N(11)	46(4)	55(4)	64(5)	-11(4)	6(4)	-10(3)
N(12)	45(4)	45(4)	55(4)	5(3)	-11(3)	-5(3)
N(13)	32(3)	34(3)	59(4)	-9(3)	-5(3)	-2(2)
O(1)	51(3)	78(5)	95(5)	1(4)	-7(4)	1(3)
O(2)	113(7)	89(6)	136(8)	-17(6)	19(6)	-49(6)
O(3)	61(5)	161(9)	121(7)	-91(7)	-1(5)	5(5)
O(4)	52(4)	88(5)	102(5)	30(4)	-23(4)	-14(4)
O(5)	63(4)	63(4)	131(7)	-17(5)	15(4)	-5(3)
O(6)	52(3)	68(4)	75(5)	1(4)	6(3)	2(3)
O(7)	43(3)	72(4)	72(4)	-9(3)	1(3)	-6(3)
O(8)	41(3)	54(3)	69(4)	-5(3)	-2(3)	-4(3)
O(9)	66(4)	58(4)	87(5)	-18(4)	-24(4)	-10(3)
O(10)	89(5)	65(4)	78(4)	1(4)	22(4)	3(4)
O(11)	68(4)	40(3)	71(4)	1(3)	-15(3)	-4(3)
O(13)	43(3)	58(3)	67(4)	-14(3)	-9(3)	-2(3)
O(14)	46(3)	56(4)	64(4)	-6(3)	-19(3)	6(3)
O(15A)	65(5)	71(5)	95(6)	-3(4)	-28(4)	3(4)
O(15B)	65(5)	71(5)	95(6)	-3(4)	-28(4)	3(4)
P(1)	48(1)	48(1)	62(1)	-2(1)	-6(1)	-4(1)
Co(1)	29(1)	46(1)	51(1)	-4(1)	-1(1)	-1(1)
O(1W)	63(4)	69(4)	70(4)	-3(3)	-15(3)	-14(3)
O(2W)	51(4)	100(5)	102(5)	-1(5)	18(4)	-3(4)
O(3W)	63(4)	93(5)	88(5)	-5(4)	20(4)	-15(4)
O(4W)	79(5)	105(6)	123(7)	12(5)	11(5)	22(5)
O(5W)	93(6)	87(5)	139(8)	-38(5)	-17(6)	23(5)
O(6W)	141(8)	98(6)	132(8)	25(6)	-10(7)	-5(6)
O(7W)	127(8)	90(6)	144(8)	-27(6)	-8(6)	-10(5)
O(8W)	289(18)	85(6)	153(10)	-3(7)	9(11)	-21(10)
O(9W)	97(7)	252(16)	143(9)	9(10)	-22(7)	-46(9)

O(10W)	117(8)	105(7)	211(13)	-51(8)	-42(8)	12(6)
O(11W)	94(7)	145(9)	192(11)	-49(9)	-16(7)	6(6)
O(12W)	330(20)	208(15)	400(30)	190(20)	290(30)	155(17)
O(13W)	146(10)	167(12)	164(11)	-27(10)	16(8)	-33(9)
O(14W)	164(12)	181(12)	166(12)	43(10)	57(9)	36(10)
O(15W)	165(11)	115(8)	209(13)	17(9)	-9(10)	13(8)

Table A5. Hydrogen coordinates (x 10^4) and isotropic displacement parameters (Å ^{2}x 10^3) for β-PhVnCbl

	x	y	z	U(eq)
H(3)	-255	6250	2536	60
H(8)	2567	3768	1954	59
H(10)	3967	4249	2185	67
H(13)	5776	5838	2005	58
H(18)	2786	7634	3065	57
H(19)	2067	7170	2124	55
H(20A)	1519	6494	3583	78
H(20B)	1776	7169	3527	78
H(20C)	2449	6665	3427	78
H(21A)	-356	7400	2993	88
H(21B)	496	7758	3031	88
H(21C)	295	7253	3445	88
H(22A)	778	7503	2081	62
H(22B)	859	6835	1906	62
H(24A)	146	5652	3399	82
H(24B)	287	6303	3611	82
H(25A)	-1078	6530	3530	111
H(25B)	-1259	5959	3186	111
H(27A)	-125	4775	2030	99
H(27B)	-423	5431	2150	99
H(27C)	-343	4966	2614	99
H(28A)	868	4548	1334	67
H(28B)	1861	4565	1291	67
H(30A)	204	3983	2072	83
H(30B)	642	3944	2630	83
H(30C)	845	3465	2194	83
H(31A)	2003	3939	3004	58
H(31B)	2002	3330	2698	58
H(32A)	3425	3909	3105	70
H(32B)	3498	3353	2728	70
H(34A)	5168	4926	3111	107
H(34B)	5981	4669	2835	107

H(34C)	5116	4327	2788	107
H(35A)	5442	4342	1823	102
H(35B)	6152	4833	1802	102
H(35C)	5299	4929	1493	102
H(36A)	5703	5778	3129	75
H(36B)	5962	6369	2836	75
H(37A)	7222	5889	3105	82
H(37B)	6942	5288	2836	82
H(39A)	5172	7366	1916	91
H(39B)	5740	6796	1994	91
H(39C)	5559	7223	2476	91
H(40A)	3459	8365	1884	95
H(40B)	3087	7761	1670	95
H(40C)	4070	7862	1680	95
H(41A)	2181	8351	2224	69
H(41B)	1560	8128	2667	69
H(43A)	4759	8061	2533	59
H(43B)	4035	8431	2799	59
H(44A)	4627	7361	3255	69
H(44B)	4040	7835	3533	69
H(46A)	5634	9164	4291	69
H(46B)	6303	8847	3926	69
H(47)	6510	8110	4540	67
H(48A)	7300	8987	4730	110
H(48B)	7025	8689	5267	110
H(48C)	6536	9250	5052	110
H(49)	5296	6543	5056	60
H(50)	3909	6411	4885	56
H(51)	4540	5557	4616	62
H(52)	5800	6696	4010	75
H(53A)	6878	6015	4214	90
H(53B)	6880	6546	4625	90
H(53C)	6538	5802	4644	90
H(53D)	6789	6479	4760	90
H(54)	4059	6175	3321	51
H(55)	1544	4995	3325	55
H(58)	3436	4820	4743	65
H(61A)	1131	3755	3942	113

H(61B)	607	4301	3729	113
H(61C)	711	4203	4343	113
H(62A)	1715	4068	5013	124
H(62B)	2697	4024	5098	124
H(62C)	2250	3610	4681	124
H(64A)	1798	6005	1008	70
H(64B)	1369	5904	1582	70
H(66)	3682	5199	1196	122
H(67)	4877	5359	677	176
H(68)	5259	6325	439	175
H(69)	4447	7131	719	168
H(70)	3253	6971	1238	105
H(5A)	-1212	7687	1728	84
H(5B)	-441	7972	1959	84
H(6A)	-1112	5882	4719	113
H(6B)	-766	6404	4422	113
H(7A)	626	3174	877	83
H(7B)	191	3712	1096	83
H(8A)	3687	2897	4084	91
H(8B)	4111	3383	3779	91
H(9A)	7838	6602	1984	104
H(9B)	7459	6731	2514	104
H(10A)	2344	9618	2898	79
H(10B)	2096	9329	2388	79
H(11)	4684	8446	4069	66
H(14)	3674	7114	4306	83
H(15A)	6580	5435	4848	116
H(15B)	7136	6518	3917	116
H(1A)	-960	7733	656	233
H(1B)	-981	7033	622	233
H(1C)	-922	7416	101	233
H(3A)	1227	6948	337	364
H(3B)	523	6851	-94	364
H(3C)	465	6517	453	364

Table A6. Torsion angles [°] for β-PhVnCbl

N(1)-C(1)-C(2)-C(21)	154.5(7)
C(20)-C(1)-C(2)-C(21)	34.6(10)
C(19)-C(1)-C(2)-C(21)	-94.5(9)
N(1)-C(1)-C(2)-C(22)	-79.4(8)
C(20)-C(1)-C(2)-C(22)	160.7(7)
C(19)-C(1)-C(2)-C(22)	31.6(9)
N(1)-C(1)-C(2)-C(3)	31.7(8)
C(20)-C(1)-C(2)-C(3)	-88.2(8)
C(19)-C(1)-C(2)-C(3)	142.7(7)
C(21)-C(2)-C(3)-C(4)	-158.9(7)
C(22)-C(2)-C(3)-C(4)	82.7(7)
C(1)-C(2)-C(3)-C(4)	-30.9(8)
C(21)-C(2)-C(3)-C(24)	-40.7(10)
C(22)-C(2)-C(3)-C(24)	-159.1(7)
C(1)-C(2)-C(3)-C(24)	87.3(8)
C(2)-C(3)-C(4)-N(1)	20.6(9)
C(24)-C(3)-C(4)-N(1)	-102.9(8)
C(2)-C(3)-C(4)-C(5)	-159.4(7)
C(24)-C(3)-C(4)-C(5)	77.0(9)
N(1)-C(4)-C(5)-C(6)	10.7(13)
C(3)-C(4)-C(5)-C(6)	-169.3(8)
N(1)-C(4)-C(5)-C(27)	-169.5(8)
C(3)-C(4)-C(5)-C(27)	10.5(11)
C(4)-C(5)-C(6)-N(2)	-3.1(13)
C(27)-C(5)-C(6)-N(2)	177.2(8)
C(4)-C(5)-C(6)-C(7)	-178.8(8)
C(27)-C(5)-C(6)-C(7)	1.5(14)
C(5)-C(6)-C(7)-C(30)	-38.3(12)
N(2)-C(6)-C(7)-C(30)	145.4(7)
C(5)-C(6)-C(7)-C(8)	-159.2(8)
N(2)-C(6)-C(7)-C(8)	24.5(8)
C(5)-C(6)-C(7)-C(28)	82.9(10)
N(2)-C(6)-C(7)-C(28)	-93.4(8)
C(30)-C(7)-C(8)-C(31)	-29.5(9)
C(6)-C(7)-C(8)-C(31)	94.2(7)
C(28)-C(7)-C(8)-C(31)	-152.7(7)

C(30)-C(7)-C(8)-C(9)	-150.8(7)
C(6)-C(7)-C(8)-C(9)	-27.2(8)
C(28)-C(7)-C(8)-C(9)	86.0(8)
C(31)-C(8)-C(9)-C(10)	79.0(11)
C(7)-C(8)-C(9)-C(10)	-158.6(9)
C(31)-C(8)-C(9)-N(2)	-98.8(8)
C(7)-C(8)-C(9)-N(2)	23.6(9)
N(2)-C(9)-C(10)-C(11)	0.2(17)
C(8)-C(9)-C(10)-C(11)	-177.2(9)
C(9)-C(10)-C(11)-N(3)	-4.6(15)
C(9)-C(10)-C(11)-C(12)	173.5(9)
N(3)-C(11)-C(12)-C(34)	116.2(8)
C(10)-C(11)-C(12)-C(34)	-62.1(11)
N(3)-C(11)-C(12)-C(35)	-121.9(8)
C(10)-C(11)-C(12)-C(35)	59.8(12)
N(3)-C(11)-C(12)-C(13)	-3.2(10)
C(10)-C(11)-C(12)-C(13)	178.4(8)
C(11)-C(12)-C(13)-C(36)	121.0(8)
C(34)-C(12)-C(13)-C(36)	6.2(10)
C(35)-C(12)-C(13)-C(36)	-118.3(8)
C(11)-C(12)-C(13)-C(14)	-0.9(8)
C(34)-C(12)-C(13)-C(14)	-115.6(7)
C(35)-C(12)-C(13)-C(14)	119.8(7)
C(36)-C(13)-C(14)-N(3)	-121.0(8)
C(12)-C(13)-C(14)-N(3)	4.7(9)
C(36)-C(13)-C(14)-C(15)	57.0(11)
C(12)-C(13)-C(14)-C(15)	-177.3(8)
N(3)-C(14)-C(15)-C(16)	10.5(14)
C(13)-C(14)-C(15)-C(16)	-167.2(8)
N(3)-C(14)-C(15)-C(39)	-165.4(8)
C(13)-C(14)-C(15)-C(39)	16.9(13)
C(14)-C(15)-C(16)-N(4)	-3.8(13)
C(39)-C(15)-C(16)-N(4)	172.1(8)
C(14)-C(15)-C(16)-C(17)	176.3(8)
C(39)-C(15)-C(16)-C(17)	-7.8(13)
N(4)-C(16)-C(17)-C(40)	-99.8(8)
C(15)-C(16)-C(17)-C(40)	80.1(10)
N(4)-C(16)-C(17)-C(18)	16.4(9)

C(15)-C(16)-C(17)-C(18)	-163.6(8)
N(4)-C(16)-C(17)-C(43)	137.3(7)
C(15)-C(16)-C(17)-C(43)	-42.7(12)
C(40)-C(17)-C(18)-C(19)	84.9(8)
C(43)-C(17)-C(18)-C(19)	-153.0(7)
C(16)-C(17)-C(18)-C(19)	-30.4(8)
C(40)-C(17)-C(18)-C(41)	-41.0(10)
C(43)-C(17)-C(18)-C(41)	81.1(9)
C(16)-C(17)-C(18)-C(41)	-156.3(7)
C(41)-C(18)-C(19)-N(4)	162.3(7)
C(17)-C(18)-C(19)-N(4)	33.9(7)
C(41)-C(18)-C(19)-C(1)	-81.0(9)
C(17)-C(18)-C(19)-C(1)	150.6(7)
N(1)-C(1)-C(19)-N(4)	-42.9(7)
C(20)-C(1)-C(19)-N(4)	76.1(7)
C(2)-C(1)-C(19)-N(4)	-153.5(7)
N(1)-C(1)-C(19)-C(18)	-157.8(6)
C(20)-C(1)-C(19)-C(18)	-38.7(9)
C(2)-C(1)-C(19)-C(18)	91.6(9)
C(21)-C(2)-C(22)-C(23)	-63.6(10)
C(1)-C(2)-C(22)-C(23)	164.6(8)
C(3)-C(2)-C(22)-C(23)	56.5(10)
C(2)-C(22)-C(23)-O(1)	-79.2(12)
C(2)-C(22)-C(23)-N(5)	102.3(10)
C(4)-C(3)-C(24)-C(25)	-144.7(9)
C(2)-C(3)-C(24)-C(25)	102.4(10)
C(3)-C(24)-C(25)-C(26)	166.0(10)
C(24)-C(25)-C(26)-O(2)	-99.3(15)
C(24)-C(25)-C(26)-N(6)	79.4(14)
C(30)-C(7)-C(28)-C(29)	-56.3(10)
C(6)-C(7)-C(28)-C(29)	178.4(7)
C(8)-C(7)-C(28)-C(29)	68.3(9)
C(7)-C(28)-C(29)-O(3)	-82.3(12)
C(7)-C(28)-C(29)-N(7)	98.4(11)
C(9)-C(8)-C(31)-C(32)	-55.4(10)
C(7)-C(8)-C(31)-C(32)	-169.8(7)
C(8)-C(31)-C(32)-C(33)	-171.0(8)
C(31)-C(32)-C(33)-O(4)	26.7(14)

C(31)-C(32)-C(33)-N(8)	-156.1(9)
C(14)-C(13)-C(36)-C(37)	-167.9(7)
C(12)-C(13)-C(36)-C(37)	75.3(10)
C(13)-C(36)-C(37)-C(38)	53.7(12)
C(36)-C(37)-C(38)-O(5)	-105.9(10)
C(36)-C(37)-C(38)-N(9)	73.5(11)
C(19)-C(18)-C(41)-C(42)	161.0(7)
C(17)-C(18)-C(41)-C(42)	-77.8(10)
C(18)-C(41)-C(42)-O(6)	-38.0(11)
C(18)-C(41)-C(42)-N(10)	146.3(8)
C(40)-C(17)-C(43)-C(44)	-170.2(8)
C(18)-C(17)-C(43)-C(44)	66.5(9)
C(16)-C(17)-C(43)-C(44)	-46.9(10)
C(17)-C(43)-C(44)-C(45)	168.3(7)
C(43)-C(44)-C(45)-O(7)	-62.6(11)
C(43)-C(44)-C(45)-N(11)	115.6(9)
N(11)-C(46)-C(47)-O(8)	-53.4(10)
N(11)-C(46)-C(47)-C(48)	-171.4(8)
O(11)-C(49)-C(50)-O(14)	37.2(10)
C(52)-C(49)-C(50)-O(14)	-85.7(8)
O(11)-C(49)-C(50)-C(51)	152.1(8)
C(52)-C(49)-C(50)-C(51)	29.2(9)
O(14)-C(50)-C(51)-O(13)	84.8(7)
C(49)-C(50)-C(51)-O(13)	-31.7(8)
O(14)-C(50)-C(51)-N(12)	-36.2(9)
C(49)-C(50)-C(51)-N(12)	-152.7(7)
O(11)-C(49)-C(52)-O(13)	-141.9(7)
C(50)-C(49)-C(52)-O(13)	-18.2(9)
O(11)-C(49)-C(52)-C(53)	95.6(9)
C(50)-C(49)-C(52)-C(53)	-140.7(8)
O(13)-C(52)-C(53)-O(15A)	-63.7(10)
C(49)-C(52)-C(53)-O(15A)	57.9(11)
O(13)-C(52)-C(53)-O(15B)	82(2)
C(49)-C(52)-C(53)-O(15B)	-157(2)
C(60)-C(55)-C(56)-C(57)	-0.2(13)
C(60)-C(55)-C(56)-C(61)	-178.7(8)
C(55)-C(56)-C(57)-C(58)	7.0(14)
C(61)-C(56)-C(57)-C(58)	-174.4(9)

C(55)-C(56)-C(57)-C(62)	-175.9(10)
C(61)-C(56)-C(57)-C(62)	2.7(15)
C(56)-C(57)-C(58)-C(59)	-7.1(14)
C(62)-C(57)-C(58)-C(59)	175.7(10)
C(57)-C(58)-C(59)-C(60)	0.7(13)
C(57)-C(58)-C(59)-N(12)	-175.5(9)
N(12)-C(59)-C(60)-C(55)	-176.7(7)
C(58)-C(59)-C(60)-C(55)	6.3(12)
N(12)-C(59)-C(60)-N(13)	1.1(9)
C(58)-C(59)-C(60)-N(13)	-176.0(7)
C(56)-C(55)-C(60)-C(59)	-6.4(12)
C(56)-C(55)-C(60)-N(13)	176.4(8)
C(64)-C(63)-C(65)-C(66)	-97.4(9)
Co(1)-C(63)-C(65)-C(66)	81.9(7)
C(64)-C(63)-C(65)-C(70)	83.8(9)
Co(1)-C(63)-C(65)-C(70)	-96.9(7)
C(70)-C(65)-C(66)-C(67)	0.0
C(63)-C(65)-C(66)-C(67)	-178.7(7)
C(65)-C(66)-C(67)-C(68)	0.0
C(66)-C(67)-C(68)-C(69)	0.0
C(67)-C(68)-C(69)-C(70)	0.0
C(68)-C(69)-C(70)-C(65)	0.0
C(66)-C(65)-C(70)-C(69)	0.0
C(63)-C(65)-C(70)-C(69)	178.8(7)
C(5)-C(4)-N(1)-C(1)	-179.7(7)
C(3)-C(4)-N(1)-C(1)	0.3(10)
C(5)-C(4)-N(1)-Co(1)	0.0(12)
C(3)-C(4)-N(1)-Co(1)	180.0(6)
C(20)-C(1)-N(1)-C(4)	99.0(8)
C(19)-C(1)-N(1)-C(4)	-143.5(7)
C(2)-C(1)-N(1)-C(4)	-21.3(9)
C(20)-C(1)-N(1)-Co(1)	-80.7(7)
C(19)-C(1)-N(1)-Co(1)	36.8(7)
C(2)-C(1)-N(1)-Co(1)	159.0(5)
C(10)-C(9)-N(2)-C(6)	173.5(9)
C(8)-C(9)-N(2)-C(6)	-8.8(10)
C(10)-C(9)-N(2)-Co(1)	0.5(13)
C(8)-C(9)-N(2)-Co(1)	178.2(5)

C(5)-C(6)-N(2)-C(9)	173.0(8)
C(7)-C(6)-N(2)-C(9)	-10.6(9)
C(5)-C(6)-N(2)-Co(1)	-14.6(12)
C(7)-C(6)-N(2)-Co(1)	161.8(6)
C(10)-C(11)-N(3)-C(14)	-175.1(8)
C(12)-C(11)-N(3)-C(14)	6.5(10)
C(10)-C(11)-N(3)-Co(1)	7.5(12)
C(12)-C(11)-N(3)-Co(1)	-170.8(6)
C(15)-C(14)-N(3)-C(11)	175.2(8)
C(13)-C(14)-N(3)-C(11)	-7.0(9)
C(15)-C(14)-N(3)-Co(1)	-7.6(13)
C(13)-C(14)-N(3)-Co(1)	170.3(6)
C(15)-C(16)-N(4)-C(19)	-174.8(7)
C(17)-C(16)-N(4)-C(19)	5.2(9)
C(15)-C(16)-N(4)-Co(1)	-5.8(13)
C(17)-C(16)-N(4)-Co(1)	174.1(5)
C(18)-C(19)-N(4)-C(16)	-24.9(8)
C(1)-C(19)-N(4)-C(16)	-153.0(7)
C(18)-C(19)-N(4)-Co(1)	164.1(5)
C(1)-C(19)-N(4)-Co(1)	35.9(7)
O(7)-C(45)-N(11)-C(46)	-2.5(14)
C(44)-C(45)-N(11)-C(46)	179.4(8)
C(47)-C(46)-N(11)-C(45)	-101.1(10)
N(13)-C(54)-N(12)-C(59)	-1.4(9)
N(13)-C(54)-N(12)-C(51)	-167.0(7)
C(60)-C(59)-N(12)-C(54)	0.1(9)
C(58)-C(59)-N(12)-C(54)	176.8(9)
C(60)-C(59)-N(12)-C(51)	165.3(7)
C(58)-C(59)-N(12)-C(51)	-18.0(14)
O(13)-C(51)-N(12)-C(54)	-53.7(10)
C(50)-C(51)-N(12)-C(54)	66.5(10)
O(13)-C(51)-N(12)-C(59)	143.7(8)
C(50)-C(51)-N(12)-C(59)	-96.2(10)
N(12)-C(54)-N(13)-C(60)	2.0(9)
N(12)-C(54)-N(13)-Co(1)	-166.8(5)
C(59)-C(60)-N(13)-C(54)	-1.9(8)
C(55)-C(60)-N(13)-C(54)	175.6(8)
C(59)-C(60)-N(13)-Co(1)	164.9(5)

C(55)-C(60)-N(13)-Co(1)	-17.7(12)
C(46)-C(47)-O(8)-P(1)	129.4(7)
C(48)-C(47)-O(8)-P(1)	-110.3(8)
C(50)-C(49)-O(11)-P(1)	116.2(7)
C(52)-C(49)-O(11)-P(1)	-125.8(7)
N(12)-C(51)-O(13)-C(52)	145.9(7)
C(50)-C(51)-O(13)-C(52)	21.5(9)
C(53)-C(52)-O(13)-C(51)	124.3(7)
C(49)-C(52)-O(13)-C(51)	-1.9(10)
C(47)-O(8)-P(1)-O(10)	179.2(6)
C(47)-O(8)-P(1)-O(9)	49.8(7)
C(47)-O(8)-P(1)-O(11)	-66.5(6)
C(49)-O(11)-P(1)-O(10)	-76.8(7)
C(49)-O(11)-P(1)-O(9)	52.9(7)
C(49)-O(11)-P(1)-O(8)	171.7(6)
C(16)-N(4)-Co(1)-N(1)	178.1(8)
C(19)-N(4)-Co(1)-N(1)	-13.1(5)
C(16)-N(4)-Co(1)-N(3)	7.0(8)
C(19)-N(4)-Co(1)-N(3)	175.8(5)
C(16)-N(4)-Co(1)-C(63)	-84.8(8)
C(19)-N(4)-Co(1)-C(63)	83.9(5)
C(16)-N(4)-Co(1)-N(13)	89.9(8)
C(19)-N(4)-Co(1)-N(13)	-101.4(5)
C(4)-N(1)-Co(1)-N(4)	165.1(8)
C(1)-N(1)-Co(1)-N(4)	-15.2(6)
C(4)-N(1)-Co(1)-N(2)	-11.7(8)
C(1)-N(1)-Co(1)-N(2)	168.0(6)
C(4)-N(1)-Co(1)-N(3)	-142.6(13)
C(1)-N(1)-Co(1)-N(3)	37.1(18)
C(4)-N(1)-Co(1)-C(63)	76.7(8)
C(1)-N(1)-Co(1)-C(63)	-103.6(6)
C(4)-N(1)-Co(1)-N(13)	-100.4(8)
C(1)-N(1)-Co(1)-N(13)	79.3(6)
C(9)-N(2)-Co(1)-N(1)	-169.7(7)
C(6)-N(2)-Co(1)-N(1)	18.6(7)
C(9)-N(2)-Co(1)-N(3)	1.7(7)
C(6)-N(2)-Co(1)-N(3)	-170.0(7)
C(9)-N(2)-Co(1)-C(63)	93.4(7)

C(6)-N(2)-Co(1)-C(63)	-78.3(7)
C(9)-N(2)-Co(1)-N(13)	-80.9(6)
C(6)-N(2)-Co(1)-N(13)	107.4(7)
C(11)-N(3)-Co(1)-N(4)	176.4(7)
C(14)-N(3)-Co(1)-N(4)	-0.5(7)
C(11)-N(3)-Co(1)-N(1)	124.6(14)
C(14)-N(3)-Co(1)-N(1)	-52.3(19)
C(11)-N(3)-Co(1)-N(2)	-5.6(7)
C(14)-N(3)-Co(1)-N(2)	177.5(7)
C(11)-N(3)-Co(1)-C(63)	-94.4(7)
C(14)-N(3)-Co(1)-C(63)	88.8(7)
C(11)-N(3)-Co(1)-N(13)	82.1(6)
C(14)-N(3)-Co(1)-N(13)	-94.8(7)
C(64)-C(63)-Co(1)-N(4)	-108.8(8)
C(65)-C(63)-Co(1)-N(4)	71.9(6)
C(64)-C(63)-Co(1)-N(1)	-26.1(8)
C(65)-C(63)-Co(1)-N(1)	154.6(6)
C(64)-C(63)-Co(1)-N(2)	63.1(8)
C(65)-C(63)-Co(1)-N(2)	-116.2(6)
C(64)-C(63)-Co(1)-N(3)	161.0(8)
C(65)-C(63)-Co(1)-N(3)	-18.3(6)
C(54)-N(13)-Co(1)-N(4)	-46.0(6)
C(60)-N(13)-Co(1)-N(4)	149.1(6)
C(54)-N(13)-Co(1)-N(1)	-128.7(6)
C(60)-N(13)-Co(1)-N(1)	66.3(6)
C(54)-N(13)-Co(1)-N(2)	141.9(6)
C(60)-N(13)-Co(1)-N(2)	-23.1(6)
C(54)-N(13)-Co(1)-N(3)	43.7(6)
C(60)-N(13)-Co(1)-N(3)	-121.3(7)

Appendix B. pK_a titration of β-PhVnCbl

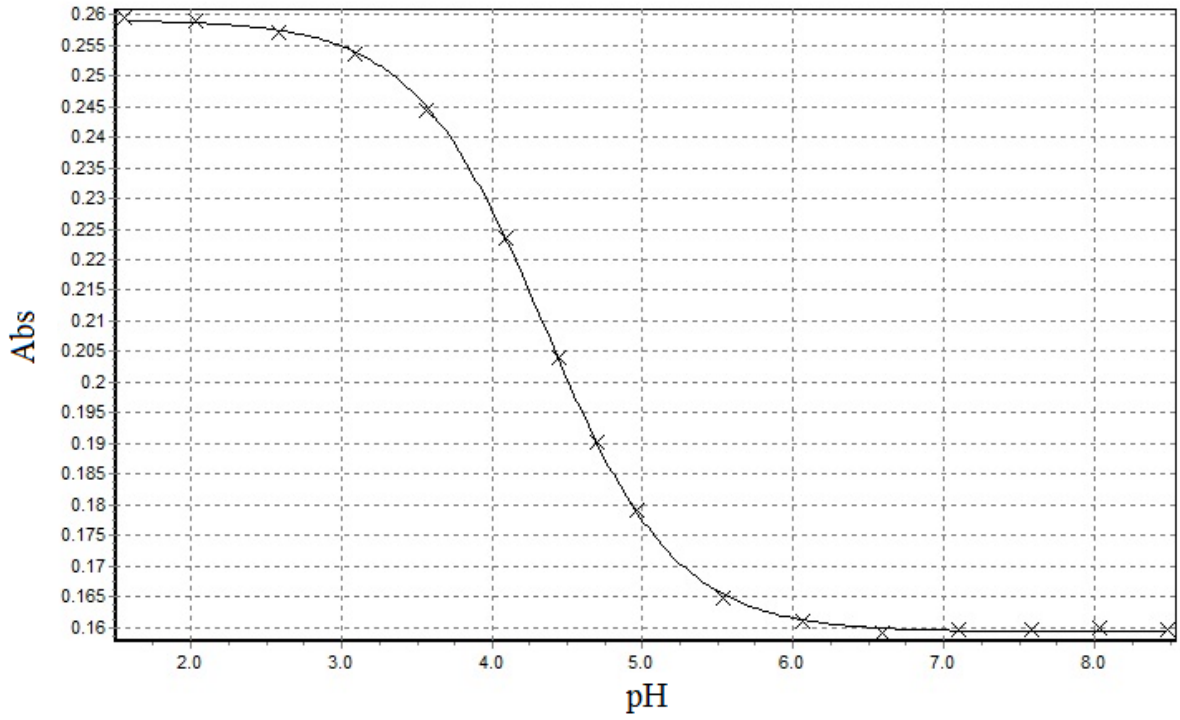

Figure 1B. The p$K_{base\text{-}off}$ titration of β-PhVnCbl plot of absorbance vs pH at 419 nm

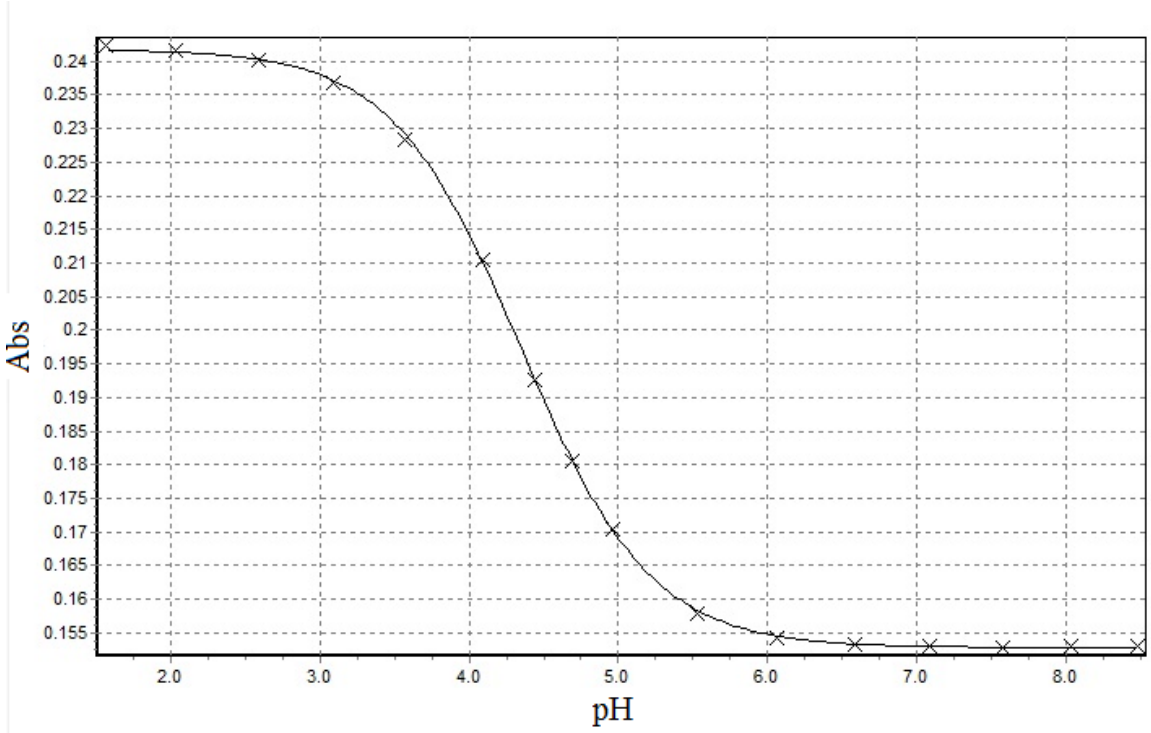

Figure 2B. The p$K_{base\text{-}off}$ titration of β-PhVnCbl plot of absorbance vs pH at 453 nm

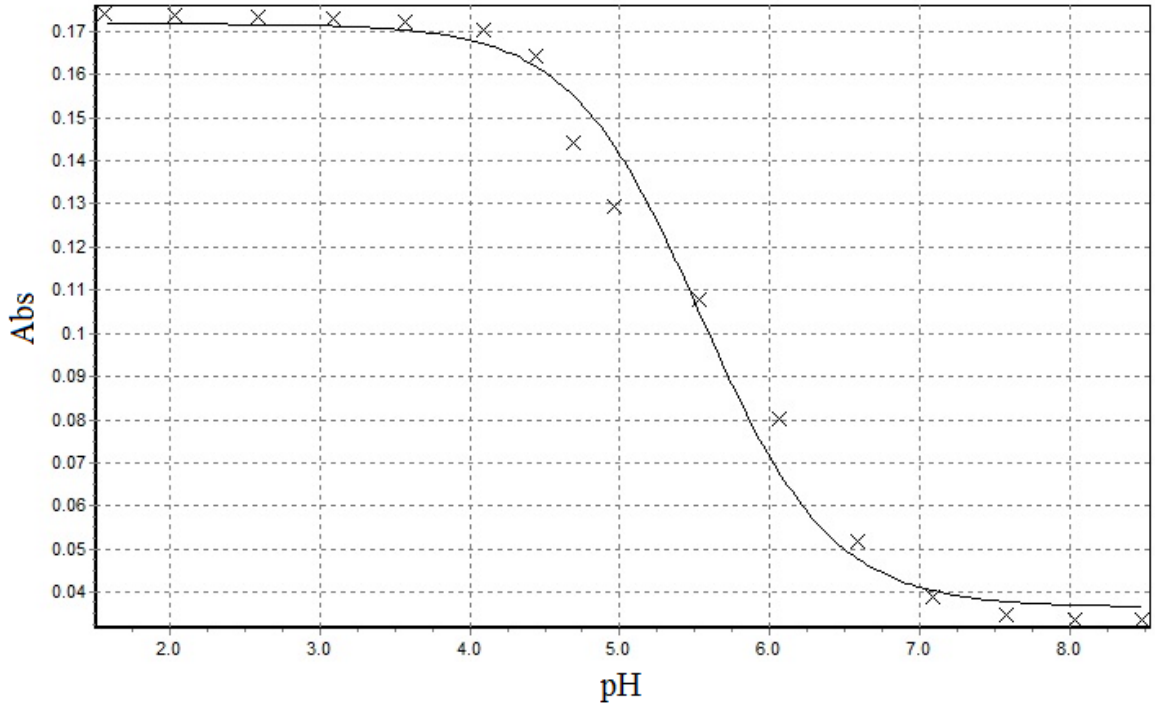

Figure 2C. The p$K_{base\text{-}off}$ titration of β-PhVnCbl plot of absorbance vs pH at 530 nm

Equation for pK_a titration

$A_T = \sum_{n=1}^{2} An\alpha n$

A_T = total solution absorbance

An= Absorbance of n^{th} species

αn= fraction of n^{th} species

Essentially a simple acid and base equilibrium:

$ImH^+ + H_2O \rightleftharpoons Im + H_3O^+$

$Keq = [Im][H_3O^+]/[ImH^+]$

We know $f(ImH^+) + f(Im) = 1$

$\therefore\ f(ImH^+) + f(keq[ImH^+]/[H_3O^+]) = 1$

$f(ImH^+)[1+Keq/[H_3O^+]] = 1$

$f(ImH^+)[[H_3O^+]+Keq/[H_3O^+]] = 1$

$[[H_3O^+]/[H_3O^+]+Keq] = f(ImH^+)$

- $pKa = -\log keq$

  $\therefore\ keq = 10^{-pka}$

- $PH = -\log[H_3O^+]\ \ \therefore\ [H_3O^+] = 10^{-Ph}$

$\therefore\ f(ImH^+) = 10^{-pH}/\ 10^{-pH} + 10^{-pKa}$

$f(Im) = 1 - f(ImH^+)$

$= 1 - (10^{-pH}/10^{-pH}+10^{-pKa})$

$\therefore\ AT = AImH^+[10^{-pH}/10^{-pH}+10^{-pKa}] + AIm[1 - (10^{-pH}/10^{-pH}+10^{-pKa})]$

APPENDIX C.

"The following manuscript based on aspects of this work has been submitted to *J. Chem. Soc. ¸Dalton Trans.*"

Phenylvinylcobalamin: An alkylcobalamin featuring a ligand with a large trans influence

Christopher B. Perry,* Naree Shin, Manuel A. Fernandes and Helder M. Marques*
Molecular Sciences Institute, School of Chemistry, University of the Witwatersrand, P.O. Wits, Johannesburg, 2050 South Africa

Abstract

Cob(I)alamin reacts with phenylacetylene to produce two diastereomers in which the alkyl ligand is coordinated to the upper (β) and lower (α) face of the corrin ring, respectively. The isomers were separated chromatographically and characterised by ESI-MS and ^{1}H and ^{13}C NMR. Only the β isomer crystallised and its molecular structure, determined by x-ray diffraction, shows that the alkyl group coordinates Co(III) through the β carbon of the phenylvinyl ligand. The Co–C bond length is 2.019(9) Å while the Co–N bond length to the trans 5,6-dimethylbenzimidazole (dmbzm) base is 2.225(7) Å, one of the longest Co–N_{dmbzm} bond lengths known in an alkylcobalamin. Unlike benzylcobalamin (BzCbl), phenylvinylcobalamin (PhVnCbl) is stableowards homolysis. DFT calculations (BP86/TZVP) on model compounds of BzCbl and PhVnCbl show that the Co—C bond dissociation energy for homolysis to Co(II) and an alkyl radical in the former is 8 kcal mol^{-1} lower than in the latter. An analysis of the electron density at the Co—C bond critical point using Bader's QTAIM approach shows that the Co—C bond in PhVnCbl is shorter, stronger and somewhat more covalent than that in BzCbl, and has some multiple bond character. Together with calculations that show that the benzyl radical is more stable than the phenylvinyl radical, this rationalises the stability of PhVnCbl compared to BzCbl. The phenylvinyl ligand has a large trans influence. The pK_a for deprotonation of dmbzm and its coordination by the metal in β-PhVnCbl is 4.60 ± 0.01, one of the highest values reported to date in cobalamin chemistry. The acid dissociation constant of H_2O trans to PhVn in α-PhVnCbl is approximately 13.9, comparable to a value of >14 for aquamethylcobinamide and significantly larger than the value of 11 reported for aquacyanocobinamide. Log *K* for

substitution of H_2O by CN^- in α-PhVnCbl is 2.70 ± 0.06 at 25 °C, a value similar to those for other alkylcobalamins. The displacement of dmbzm ligand by CN^- in β–PhVnCbl occurs with log K = 0.7 ± 0.1; the trans influence order of C-donor ligands is therefore $CN^- < CCH < CHCH_2 = PhVn < Me < Et$.

Introduction

The initial step in the coenzyme B_{12}-dependent enzymatic reactions involves homolysis of the Co–C bond between Co(III) and 5′-deoxyadenosine to produce Co(II) and the 5′-deoxyadensyl radical.[1-3] In an attempt to observe the formation of the free radical in the solid state, we prepared and crystallized the compound 1-phenylvinylcob(III)alamin (PhVnCbl) anticipating that its photolysis in the solid state would lead to a stable radical that could be observed spectroscopically. Although we were unable to find any evidence for the formation of such a stable radical species, PhVnCbl nevertheless has some interesting properties that we report in this paper. In particular we show that the phenylvinyl ligand has a particularly large trans influence, manifest in a long bond between Co and the 5,6-dimethylbenzimidazole (dmbzm) base in the solid state (Fig. 1), in the position of the base-on ⇌ base-off equilibrium, and in the stability constant for the reactions of PhVnCbl with CN^-.

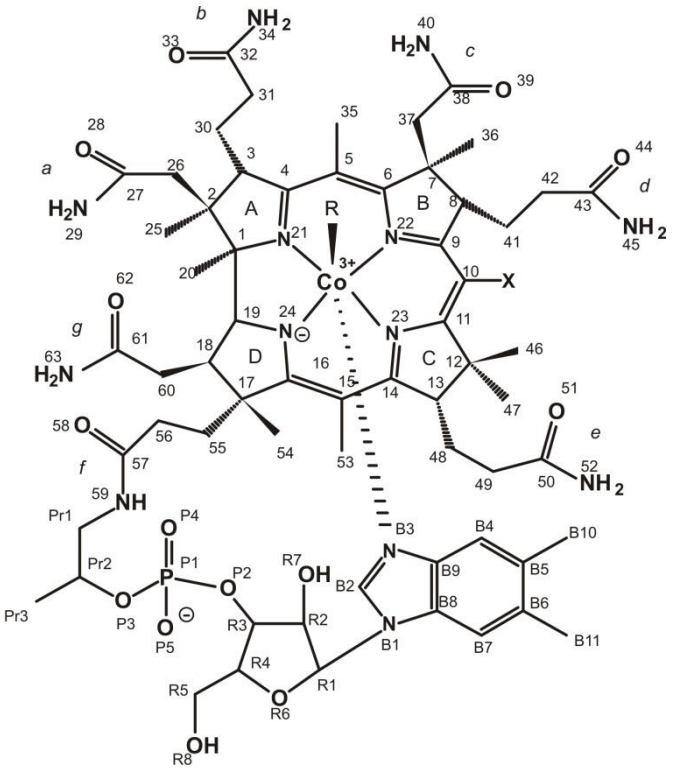

Fig. 1. Standard view and numbering of the alkylcobalamins which have R = alkyl as the upper or β ligand of the corrin. We report in this paper the molecular structure and properties of R = phenylvinyl.

Results and discussion

PhVnCbl was synthesised by the reaction of cob(I)alamin and phenylacetylene. HPLC showed the formation of two products, the ratio of which depended on the temperature of the reaction. It was anticipated[4] that alkylation of cob(I)alamin using this procedure would lead to the formation of diastereomeric alkylcobalamins with the alkyl ligand on either the upper (β) face of the corrin or on the lower (α) face; in the latter case, the dmbzm ligand is displaced from the coordination sphere of the metal.

At room temperature, two peaks of approximately equal intensity with retention times of 8.3 and 8.8 min on reverse phase HPLC emerge while a peak due to H_2OCbl^+ (from oxidation of unreacted cob(I)alamin, 6.7 min), and one due to unreacted CNCbl (7.3 min)

decrease. If the reaction proceeds with the reaction vessel in a stream of warm air, the ratio of the area of the earlier to the later eluting peak is approximately 45:55. When the reaction is carried out with the reaction vessel emerged in an ice bath the ratio becomes 65:35.

The products were separated by column chromatography on C18 and analysed by ESI-MS and ^{1}H and ^{13}C NMR. Crystallisation of the two isomers was attempted by vapour diffusion of acetone into a concentrated neutral aqueous solution of each isomer at 4 ^{o}C. After three weeks, deep red crystals of the isomer that eluted second from the column were obtained and analysed by x-ray diffraction methods.

The two compounds have slightly different uv-vis spectra. What we have shown unambiguously by XRD, confirming the ESI-MS result (see below), to be β–PhVnCbl has the γ band at 321 nm with a shoulder (which is quite prominent) at 335 nm; and the α band at 412 nm which is more intense than the β band at 440 nm. The other compound, which ESI-MS indicates to be the α diastereomer, has the γ band at 324 nm with a weak shoulder at 335 nm, and the α and β bands at 418 and 452 nm, respectively, the latter now more intense than the former.

Alkylcobalamins are light-sensitive, which cause homolysis of the Co–C bond.[5] When samples of the two products were dissolved in aqueous solution (pH 7, 0.1 M phosphate) and exposed to visible light for some 3 hours, the uv-vis spectrum of the resultant product was in each case identical to that of H_2OCbl^+.

Molecular Structure

The molecular structure of β–PhVnCbl is illustrated in Fig. 2, which gives the standard numbering scheme used for cobalt corrinoids. The crystallographic numbering is given in Fig. S1 of the Electronic Supplementary Information (ESI).

There are 4 molecules in the unit cell, hydrogen bonded to neighbouring molecules (Fig. S2 of the ESI). The hydrogen bonding results in the formation of approximately helical voids in the crystal structure that are occupied by solvent water (72 molecules were located in the unit cell) and acetone (4 molecules in the unit cell), leading to a relatively open, low density, structure (Fig. S3 of the ESI).

Contrary to our expectations, the alkyl ligand is coordinated to the metal through its β carbon rather than its α carbon. The Co–C bond length is 2.019(9) Å while the Co–N bond length to the dmbzm base is 2.225(7) Å. The fold angle of the corrin is 14.6°. (The corrin fold angle is defined as the angle between the mean planes through N21, C4, C5, C6, N22, C9, C10 and through N24, C16, C15, C14, N23, C11, C10.[6]) The structures of two other vinylcobalamins have been reported, vinylcobalamin itself (VnCbl, R = CH_2CH_2)[7] and chlorovinylcobalamin (ClVnCbl, R = CH_2CHCl).[7] The Co–C bond lengths are shorter than in the present case (1.912 and 1.953 Å, respectively), presumably because of the greater steric bulk of the Ph substituent in the present compound.

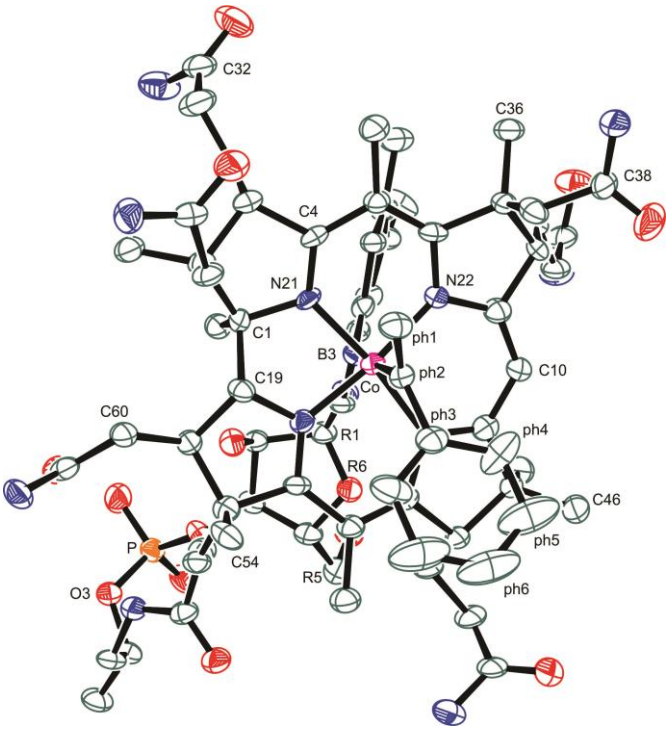

Fig. 2. The structure of β-PhVnCbl with non-H atoms drawn as 30% probability elipsoids. H atoms are omitted for clarity.

Alkylcobalamins usually exhibit an inverse trans influence[8, 9] where the Co–N bond to dmbzm increases as the Co–C bond to the β alkyl ligand increases. It is thought that this effect is primarily steric in origin and this has been verified recently by DFT calculations.[10] As the bulkiness of the β ligand increases, the steric pressure on the corrin increases (a steric cis influence) which in turn is transmitted through to the dmbzm ligand. A plot of Co–C bond length against $Co–N_{dmbzm}$ gives a strong correlation (Fig. S4 of the ESI). PhVnCbl has a relatively large trans influence with the $Co–N_{dmbzm}$ bond length, at 2.225(7) Å only some 0.05 Å shorter than the longest $Co–N_{dmbzm}$ bond length known in an alkylcobalamin, that trans to iso-amyl (2.277 Å).[11] Surprisingly, its corrin fold angle, at 14.6°, is actually larger than that in VnCbl (12.5°) and in ClVnCbl (5.7°); it might have been anticipated that the steric bulk of the PhVn ligand would have led to considerable steric pressure on the corrin, and hence a small fold angle. We suspect that crystal packing forces may have a significant effect on the corrin fold angle[12, 13] since molecular dynamics simulations have shown that the corrin ring is rather flexible.[12-17]

It is interesting to note that benzylcobalamin (BzCbl) itself is unstable towards homolysis in the dark at room temperature.[18] We found no evidence for decomposition of

PhVnCbl over several weeks which suggests that the presence of the vinyl group stabilises the complex. The C=C bond length (1.333(11) Å) is not statistically significantly longer than that of free styrenes (from a search of the Cambridge Structural Database, 1.29(7) Å, n = 4) which argues against a significant displacement of electron density from this bond to the Co–C bond.

NMR assignments

The methodology developed by Brown[4, 19-22] for assigning the NMR spectrum of cobalamins was used to assign the spectrum of β–PhVnCbl. The full assignment is given in Table S2 of the ESI. For reasons that are not obvious, the NMR data for the putative α–PhVnCbl diastereomer were unfortunately too poor for a reliable assignment.

The aromatic region (5.9 – 7.8 ppm vs TMS) of the ^{1}H NMR spectrum showed signals assigned to the R1, C10, B4, B7 and B2 protons at 6.20, 6.50, 6.82, 7.21, and 7.61 ppm, respectively (Table S1). Hence signals at 6.04, 6.87, and 7.05 ppm are due to the phenyl protons. From the COSY and ROESY spectra, the resonance at 6.87 shows strong coupling to the resonances at 6.04 and 7.05, whereas the latter two are only weakly coupled to each other. The resonance at 6.04 ppm is thus assigned to the phenyl meta H, ph5 (see Fig. S5 of the ESI for nomenclature).

Strong nOe interactions between ph5 and C46 (0.94 ppm) and C54 (1.54 ppm) are also observed, confirming that the phenylvinyl ligand is indeed coordinated to cobalt at the upper-axial position (Table S3 of the ESI). Of the remaining two aromatic signals, 6.05 and 7.05 ppm, the former shows many more nOe interactions with groups on the upper face of the corrin ring; the signal at 7.05 ppm only shows very weak nOe interactions between C46 (0.94 ppm) and C37 (1.72 ppm). If we assume that the preferred orientation of the phenylvinyl ligands relative to the corrin ring in solution is the same at that found in the solid state, then the signal at 6.05 ppm must be due to ph4, and the remaining one at 7.05 ppm corresponds to ph6.

These assignments were confirmed by observing that the multiplicities of the three signals at 6.05, 6.87, and 7.05 ppm are a doublet, and two triplets, respectively. The coupling constant for all three signals is between 7.5 and 8.0 Hz, indicating ortho-coupling (meta coupling is not observed). The only possibility for a doublet is due to ph4 coupling to ph5, as there is no proton on ph3. The doublet at 6.05 ppm is thus due to ph4. Both the ROESY and COSY spectra show that the signal at 6.05 couples much more strongly to the signal at 6.87 ppm than the one at 7.05 ppm. The former thus corresponds to ph5 and the latter to

ph6. Assignment of the two non-equivalent ph1 protons (3.01 and 3.06 ppm, in the alkene region of the ^{1}H spectrum) is based on the fact that one or both of them shows strong nOe interaction with ph4, C46, C54, C37, and C26.

^{13}C signals for the ph1, ph4, ph5, and ph6 carbon nuclei were obtained directly from the HSQC spectrum and are assigned as the resonances at 118.07, 127.39, 128.31, and 127.39 ppm, respectively (the signals for ph4 and ph6 overlap).

The HMBC spectrum was used to assign the ph2 and ph3 resonances. Both the ph5 proton and the protons on ph1 (but oddly not the ph4 proton) show a correlation to a ^{13}C signal at 148.93 ppm which we assign to ph3. Both ph1 protons, as well as the ph4 proton show a correlation with a signal at 143.24 ppm, which we assign to ph2.

In the solid state, the preferred orientation of the PhVn ligand with respect to the corrin ring has the phenyl group positioned in the "southern" quadrant of the corrin, over the C pyrrole ring when viewed from above. This is the same conformation adopted by the adenine moiety of the adenosyl group in coenzyme B_{12} (AdoCbl) in the solid state.[23] In the ROESY spectrum one of the germinal ph1 protons shows nOe interactions with C54 and C46, which suggests that conformations where the phenyl group of the PhVn ligand occupies positions over the "northern" and "western" quadrants of the corrin ring are also accessible at room temperature. There is therefore some free rotation about the Co–C bond at room temperature. A "northern" conformation of the PhVn ligand would place the phenyl protons in close proximity to the C26 and C37 protons of the *a* and *c* side chains, respectively, and indeed, nOe interactions are observed between one of the diastereotopic C37 protons and ph4, as well as ph6. In addition, ph4 shows through-space interactions with one of the C26 protons. A "western" conformation of the PhVn ligand is confirmed since both ph4 and ph5 show nOe interactions with C54, and through-space interactions are also observed between ph4 and C26′, and ph5 and C26″. Previous studies involving NMR-restrained molecular modelling of AdoCbl, and the related compound Co-*β*-5′-deoxyadenosylimidazolylcobamide (Ado(Im)Cbl, a coenzyme B_{12} analogue with an imidazole axial nucleoside) have shown that the "northern" and "western" conformations (as well as some "eastern" conformations) of the Ado ligand are accessible in solution at room temperature.[24, 25]

Molecular Modelling

To investigate the nature of the bonding in PhVnCbl, and in particular why it is significantly more stable than BzCbl, we performed DFT calculations on models of the two compounds (see Experimental Section). The Co–C bond in the PhVnCbl model was significantly shorter than in that of BzCbl (1.991 and 2.064 Å, respectively; the experimental value for the former is 2.019(9) Å, see above) which, in the absence of the substituents of the corrin, induced a normal (i.e., electronic) trans influence ($Co–N_{dmbzm}$ = 2.139 and 2.128 Å, respectively, in the PhVnCbl and BzCbl models). The Co–C–C angle in the former (115.1°) is marginally larger than in the latter (113.7°). The ph2–ph3 bond lengths were similar (1.478 Å in the PhVnCbl model; 1.474 Å in the BzCbl model) and not significantly different to that in free styrene itself (1.470 Å). The Co–C bond dissociation energy (eq. 1) for the PhVnCbl model (42.3 kcal mol^{-1}) was significantly larger than that for the BzCbl model (34.3 kcal mol^{-1}). The isodesmic reaction (eq. 2) was found to have a ΔE of -10.2 kcal mol^{-1}; thus, the benzyl is more stable than the PhVn radical.

$$\left[\mathrm{Im—Co(III)(Corrin)—R}\right]^{+} \rightarrow \left[\mathrm{Im—Co(II)(Corrin)}\right]^{+} + \mathrm{R}^{\bullet}$$

$$BDE = \left(E_{\left[\mathrm{Im—Co(II)(Corrin)}\right]^{+}} + E_{\mathrm{R}^{\bullet}}\right) - E_{\left[\mathrm{Im—Co(III)(Corrin)—R}\right]^{+}} \qquad (1)$$

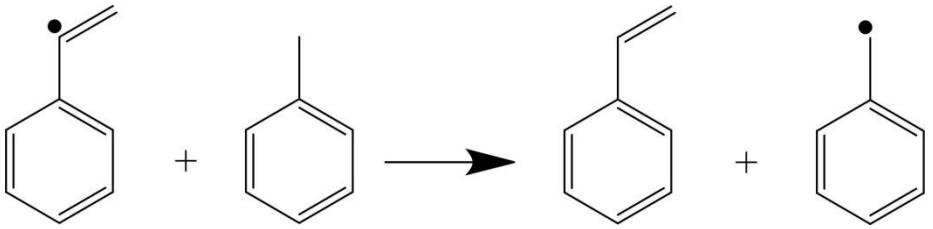

(2)

An examination of the properties of the Co–C bond using Bader's quantum theory of atoms in molecules (QTAIM)[26, 27] indicates that the electron density, ρ, at the bond critical point, which is a measure of the strength of a chemical bond,[28-31] is larger for PhVnCbl (0.109 au) than for BzCbl (0.094 au; 1 au of ρ= 6.7483 e $Å^{-3}$), consistent with the shorter bond length. The ratio of the kinetic and potential energy densities at a bond critical point, $|V_b|/G_b$ can be used to characterise the nature of a bond.[32] Interactions with $|V_b|/G_b < 1$ are characteristic of ionic interactions; those with $|V_b|/G_b > 2$ are typically covalent interactions; and $1 < |V_b|/G_b < 2$ are diagnostic of interactions of intermediate character. The values of $|V_b|/G_b$ for PhVnCbl and BzCbl are 1.649 and 1.639, respectively; the bonding in the former therefore has a somewhat more covalent character than the latter.

The ellipticity, ε_b, at a bond critical point is a function of the ratio of the rate of electron density decrease in the two directions perpendicular to the bond path at that point.[26] Values of ε_b significantly different from zero may be diagnostic of multiple bonding character.[33] For example, in the model of PhVbCbl the value of ε_b for the C–C bond in the imidazole ligand is 0.321; values for C–H bonds are typically ~ 0.01. In the case of PhVnCbl, ε_b for Co–C = 0.0375, but 0.0132 in BzCbl. This suggests there is a measure of multiple bond character between the metal and the alkyl ligand in PhVnCbl.

We conclude that the greater stability of PhVnCbl compared to BzCbl is due to stronger bonding between the metal and the β alkyl ligand, which results in a shorter, stronger, somewhat more covalent bond with some multiple bond character. The greater stability of the benzyl radical compared to the phenylvinyl radical may further explain the significantly larger *BDE* of PhVnCbl than BzCbl.

An assessment of the trans influence of the phenylvinyl ligand

The pK_a for the deprotonation of dmbzm and its coordination by the metal (to covert from the base-off to the base-on form) is a measure of the trans influence of the alkyl ligand. Titration of β–PhVnCbl from pH 8.5 to pH 1.5 causes a significant red shift in the bands of the uv-vis spectrum (Fig. S6 of the ESI) with pK_a = 4.60 ± 0.01. This is one of the highest values reported to date in cobalamin chemistry (to our knowledge only NOCbl, with a pK_a of 5.1,[34] has a higher pK_a — see Table S4 of the ESI, and Fig. 3). A spectrophotometric titration of α-PhVnCbl between pH 6.5 and 14 shows a pK_a at approximately 13.9, presumably due to the deprotonation of H_2O trans to PhVn (Fig. S7); this is comparable to a value of >14 for aquamethylcobinamide[35] and significantly larger than the value of 11 reported for aquacyanocobinamide,[35-37] attesting to the significant trans influence of the phenylvinyl ligand.

A further way of assessing the trans influence of a ligand is to measure the equilibrium constant for the substitution of coordinated H_2O by an exogenous probe ligand.[5] Given the considerable data available, we used cyanide as that probe ligand. Titration of α-PhVnCbl with aliquots of a ca. 1 M CN^- stock solution (25 ^oC, 0.5 M CAPS buffer, pH 11.0,

well above the pK_a of HCN) gave reasonably well-defined isosbestic points (Fig. S8 of the ESI). The spectroscopic changes at 170 different wavelengths (in intervals of 1 nm) between 325 and 640 nm (excluding values of 10 nm either side of each isosbestic point) were fitted to a binding isotherm to yield values of the equilibrium constant, *K*, for displacement of H_2O by CN^-. All fits with a correlation coefficient < 0.98 were excluded; a weighted average of *K*, weighted as the reciprocal of the standard error of each fit, yielded log *K* = 2.70 ± 0.06. Fig. S9 of the ESI gives examples of the fits obtained.

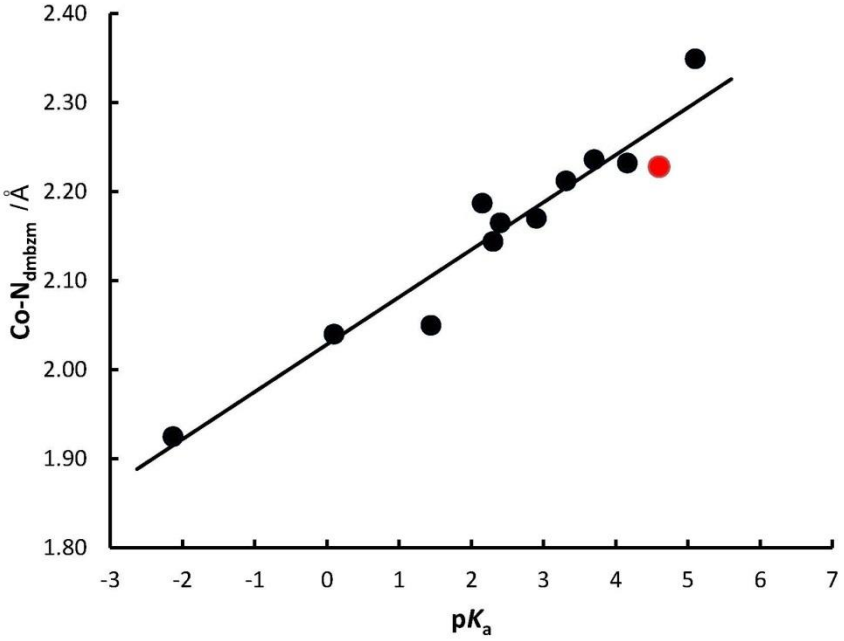

Fig. 3. Dependence of the pK_a for the deprotonation and coordination of dmbzm by Co(III) on the crystallographically-measured Co–C bond length. The red dot is for PhVnCbl. Data in Table S5 of the ESI.

The value of log *K* = 2.70 is similar to values reported for other alkycobinamides (2.7 for replacement of H_2O by CN^- trans to $CHCH_2$[38] and 2.1 trans to Me[38]; higher than a value of 0.6 for Et[38] but much lower than 6.8 reported trans to CCH[39]), significantly smaller than log *K* values when the trans ligand is a polarisable 3rd row donor (log *K* = 4.1 *trans* to $P(OCH_3)_2O^-$ [40]; 4.3 *trans* to SO_3^{2-} [41]) and very much smaller than anionic (8.4 trans to CN^- itself[42], 11 trans to OH^-[43]) or neutral ligands with 2nd row donor atoms (14.1 trans to dmbzm[44]; c. 16 trans to H_2O[45]). Thus the phenylvinyl ligand has a strong trans influence which decreases the Lewis acidity of Co(III), lowering the value of log *K* for substitution of trans H_2O.

The reaction of **β**–PhVnCbl with CN^- displaces the dmbzm ligand by CN^-. A titration at pH 11.2 (0.5 M CAPS, 25 ºC) gave log *K* = 0.7 ± 0.1. This can be compared to values of 4.0 when the **β** ligand is CN^- [36], 2.7 (CCH)[35], 0.7 ($CHCH_2$)[35], 0.1 (Me)[35] and <0 (Et)[46]. These values, together with those for the displacement of H_2O trans to an alkyl ligand, indicate that the trans influence of ligands where the donor atom is C is CN^-< CCH < $CHCH_2$ = PhVn < Me < Et.

It is interesting to note that this order only approximately parallels the trans influence order observed crystallographically as measured by the Co–N_{dmbzm} bond length: CN^-< Me < CCH_2<<PhVn< Et (Table S5 of the ESI). This could well be a consequence of crystal packing forces in the solid state perturbing the Co–N_{dmbzm} bond length and probably cautions against an over-reliance on solid state data to infer the properties of ligands in the coordination chemistry of the cobalamins.

Experimental section

Reactants and Methods

Deionised water was produced by a Millipore RO unit, and further purified by reverse osmosis using a Millipore MilliQ Ultra-Pure system (18 MΩ cm). pH measurements were performed using a Metrohm 6.05 pH meter and a 6.0234 combination glass electrode calibrated against the standard potassium hydrogen phthalate, KH_2PO_4/K_2HPO_4 and borax buffers. HPLC was performed on a Phenomenex 5μ micron (150 × 4.6 mm) C18 reverse phase analytical column, a Dionex Ultimate 3000 pump and photodiode array detector at a constant flow rate of 1.00 ml min^{-1}. The mobile phase used consisted of 25 mM phosphate buffer, pH 3, and CH_3CN with gradient elution from 98:2 to 75:25 buffer:CH_3CN over 12 minutes. All uv-vis spectra were recorded on either a Cary 1E or a Cary 3E spectrophotometer, using 1.00 cm pathlength quartz cuvettes. The cell compartment temperature was kept constant with a water-circulating bath or a Peltier device set at 25.0 ℃. ESI mass spectra were obtained using a Thermo LXQ ion trap mass spectrometer with ESI source. One-dimensional (^1H, $^{13}C\{^1H\}$ and dept135), two-dimensional proton homonuclear (COSY, TOCSY, NOESY and ROESY) and two-dimensional heteronuclear (^1H-^{13}C) experiments (HSQC and HMBC) NMR spectra were recorded on 15 mg samples dissolved in 700 μL of MeOD at 300 K on a Bruker Avance III 500 spectrometer operating at 500.133 MHz (^1H) and 125.770 MHz (^{13}C) using a 5-mm PABBO broad band probe. One-dimensional (^1H and ^{13}C) NMR experiments were also recorded on an Avance III 300 spectrometer at 300 K operating at 3000.131 MHz (^1H) and 75.475 MHz (^{13}C) using a 5-mm BBI broad band probe. All NMR spectra were internally referenced to TMS. NMR spectra were processed using Bruker Topspin3.0 (Avance III 500) and Topspin2.1 (Avance III 300) software packages. All solvents (Merck) and reagents (Sigma Aldrich) were of the highest purity available and used as received. Cyanocobalamin and hydroxocobalamin were from Roussel.

Preparation of phenylvinylcobalamin

Freshly acid-washed Zn granules (1 g) were placed in a two-necked round bottom flask through which was passed a steady stream of Ar. Cyanocobalamin (CNCbl, 200 mg, 0.15mmol) was dissolved in 50 mL of a 10% acetic acid/methanol solution in a separate flask; after deaeration (Ar), this was cannula-transferred to the flask containing the Zn metal (room temperature). The solution rapidly turned from red to brown to grey, consistent with the reduction to Co(I). After complete reduction (20 min) phenylacetylene (150 mmol) was added and left to react for three hours in the dark under Ar. The progress of the alkylation was monitored by HPLC.

All manipulations of the product were conducted under dim red light. The product mixture was cannula-transferred to a round bottom flask and rotatory evaporated to dryness (50 °C). The product was dissolved in a small amount of methanol, filtered through cotton wool, and chromatographed on a 230 x 15 mm C18 column using a Büchi Sepacore chromatographic system consisting of two C-605 pump modules, a C-615 pump manager, a C-660 fraction collector, and a C-635 UV photometer. A gradient of phosphate buffer (25 mM, pH 3) and CH_3CN from 0 to 40% CH_3CN at a flow rate of 3 ml min^{-1} was used to elute two bands from the column as well as a small amount of unreacted CNCbl

Analyses

ESI-MS of the compound that crystallised showed a peak at *m*/*z* =1433 (MH^+; relative intensity 5%, calculated 1433.59), a base peak at 729 ($MHNa^{2+}$) and a peak at 718 ($M.2H^{2+}$, 90%), proving that the compound was the β-PhVnCbl diastereomer. ESI-MS of the first product eluted from the column gave a peak at *m*/*z* = 1434 (relative intensity 5%) which is consistent with α–PhVnCbl.H^+ which has lost the H_2O ligand from the β coordination site; the base peak occurs at 717 $(M.2H–H_2O)^{2+}$. A peak at 726 is assigned to $(M.2H)^{2+}$ (27%); one at 736 to $(M.H.K–H_2O)^{2+}$ (83%); and one at 737 to $(M.H.Na)^{2+}$ (18%).

Crystallography

Intensity data for PhVnCbl were collected at 173(2) K on a Bruker APEX II CCD area detector diffractometer with graphite monochromated Mo K_α radiation (50 kV, 30 mA) using the APEX 2[47] data collection software. The collection method involved ω-scans of width 0.5° and 512 × 512 bit data frames. Data reduction was carried out using the program *SAINT+*[48]

and multiscan absorption corrections applied using *SADABS*.[48] The crystal structure was solved by direct methods using *SHELXS-97*.[49] Non-hydrogen atoms were first refined isotropically followed by anisotropic refinement (with the exception of the acetone molecule) by full matrix least-squares calculations based on F^2 using *SHELXL-97*.[49] Hydrogen atoms were first located in the difference map then positioned geometrically and allowed to ride on their respective parent atoms, with isotropic thermal parameters fixed at 1.2 (CH, CH_2 and NH_2) or 1.5 (CH_3 and OH) times those of their corresponding parent atoms. Oxygen O15 on the ribose group was found to be disordered and refined over two positions with the aid of SADI, DELU and SIMU restraints. The final occupancies for O15A and O15B were 0.854(12) and 0.146(12), respectively. The acetone molecule was refined isotropically with FLAT, DFIX, DELU and SIMU being used in the final refinements to restrain the molecule to a reasonable geometry. It was not possible to locate the hydrogen atoms on the water molecules. The contribution of these hydrogen atoms has, however, been accounted for in the chemical formula and related data such as crystal density and F(000).

Refinement converged as a final R_1 = 0.0975 (wR_2 = 0.2590 all data) for 9586 observed reflections [I >2σ(I)]. Figures were prepared using ORTEP-3.[50] Details of the crystallographic data are given in Table 1. The structure files have been deposited at the Cambridge Structural Database (deposition number 922431). A list of bond length and angles is given in Table S2 of the ESI.

Table 1. Crystallographic data for β–PhVnCbl

CCDC Deposition Code	922431
Empirical formula	$C_{73}H_{131}CoN_{13}O_{30}P$
Formula weight	1760.81
Temperature	173(2) K
Wavelength	0.71073 Å
Crystal system	Orthorhombic
Space group	$P2_12_12_1$
Unit cell dimensions	a = 15.7783(7) Å
	b = 22.3400(9) Å
	c = 25.1607(14) Å
Volume	8868.8(7) Å^3
Z	4
Density (calculated)	1.319 Mg m^{-3}
Absorption coefficient	0.296 mm^{-1}
F(000)	3768
Crystal size	0.48 x 0.17 x 0.15 mm^3
Theta range for data collection	1.52 to 26.00°.
Index ranges	$-18 \le h \le 19$, $-27 \le k \le 27$, $-31 \le l \le 13$
Reflections collected	47932
Independent reflections	17377 [R(int) = 0.0884]
Completeness to theta = 26.00°	99.9 %
Absorption correction	None
Refinement method	Full-matrix least-squares on F^2
Data / restraints / parameters	17377 / 59 / 1048
Goodness-of-fit on F^2	0.984
Final R indices [$I > 2\sigma(I)$]	R_1 = 0.0975, wR_2 = 0.2590
R indices (all data)	R_1 = 0.1652, wR_2 = 0.3001
Absolute structure parameter	0.07(3)
Largest diff. peak and hole	0.643 and -0.501 e Å^{-3}

Molecular Modelling

All calculations were conducted on a model system based on the crystal structure of PhVnCbl after suitable editing. All corrin side chains were replaced by hydrogen atoms, and the α-dmbzm ligand was truncated to imidazole. Since no geometrical parameters are available for BzCbl, the model system was based on the PhVnCbl crystal structure, constructed by removing the vinyl group from the β-phenylvinyl ligand, and replacing it with hydrogen atoms.

DFT geometry optimizations, employing the RI-J approximation,[51-57] were performed using the ORCA electronic structure package.[58] Calculations were performed with the BP86 functional,[59, 60] the TZVP basis set[61] and corresponding auxiliary basis set, and the empirical van der Waals correction of Grimme *et al.*[62] Frequency calculations were performed to obtain the zero-point correction to the electronic energy, as well as to confirm that all structures were at stable energy minima.

Reported bond dissociation energies (*BDE*) include a correction for the zero-point vibrational energy, the dispersion energy, as well as a correction for the basis set superposition error (BSSE). The BSSE correction was obtained by performing Counterpoise[63, 64] calculations in Gaussian 09 using the optimized geometries obtained from ORCA at the same level of theory. Similarly, the wavefunction files required for the analysis of the topological properties of the electron charge density using the atoms in molecules (AIM) framework of Bader[26, 27]were generated in Gaussian 09 using ORCA-optimized geometries by performing a single point calculation at the same level of theory. The topological properties of the electron density (ρ) were evaluated at all the bond critical points (bcp's) using AIMALL.[65]

Acknowledgements

Funding for this work was provided by the Department of Science and Technology/National Research Foundation South African Research Chairs Initiative, and the University of the Witwatersrand. Dr Richard Mampa is thanked for recording the NMR spectra.

References

1. T. Toraya, *Chem. Rev.*, 2003, **103**, 2095-2127.
2. W. Buckel and B. T. Golding, *Annu. Rev. Microbiol.*, 2006, **60**, 27-49.
3. E. N. Marsh, D. P. Patterson and L. Li, *Chembiochem.*, 2010, **11**, 604-621.
4. K. L. Brown and X. Zou, *J. Am. Chem. Soc.*, 1992, **114**, 9643-9651.
5. J. M. Pratt, *The Inorganic Chemistry of Vitamin B_{12}*, Academic Press, London, 1972.
6. 1982J. P. Glusker, in *B_{12}*, ed. D. Dolphin, Wiley-Interscience, New York, 1982, vol. 1, pp. 23-107.
7. K. M. McCauley, D. A. Pratt, S. R. Wilson, J. Shey, T. J. Burkey and v. d. D. W. A., *J. Am. Chem. Soc.*, 2005, **127**, 1126–1136.
8. N. Bresciani-Pahor, M. Porcolin, L. G. Marzilli, L. Randaccio, M. F. Summers and P. J. Toscano, *Coord. Chem. Rev.*, 1985, **63**, 1-125.
9. L. Randaccio, N. Bresciani-Pahor and E. Zangrando, *Chem. Soc. Rev.*, 1989, **18**, 225-250.
10. J. Kuta, J. Wuerges, L. Randaccio and P. M. Kozlowski, *J. Phys. Chem. A*, 2009, **113**, 11604-11612.
11. C. B. Perry, M. A. Fernandes and H. M. Marques, *Acta Crystallogr. Sec. C*, 2004, m165-m167.
12. K. L. Brown, X. Zou and H. M. Marques, *J. Mol. Struct. (Theochem)*, 1998, **453**, 209-224.
13. J. M. Sirovatka, A. K. Rappé and R. G. Finke, *Inorg. Chim. Acta*, 2000, **300-302**, 545-555.
14. H. M. Marques and K. L. Brown, *Coord. Chem. Rev.*, 1999, **190-192**, 127-153.
15. H. M. Marques and K. L. Brown, *J. Mol. Struct.*, 2000, **520**, 75-95.
16. K. L. Brown and H. M. Marques, *J. Inorg. Biochem.*, 2001, **83**, 121-132.
17. C. B. Perry, K. L. Brown, X. Zou and H. M. Marques, *J. Mol. Struct. (Theochem)*, 2005, **737**, 245-258.
18. G. N. Schrauzer and J. H. Grate, *J. Am. Chem. Soc,*, 1981, **103**, 541-546.
19. 1999K. L. Brown, in *Chemistry and Biochemistry of B_{12}*, ed. R. Banerjee, John Wiley & Sons, Inc., New York, 1999, pp. 197-237.
20. K. L. Brown, H. B. Brooks, B. D. Gupta, M. Victor, H. M. Marques, D. C. Scooby, W. J. Goux and R. Timkovich, *Inorg. Chem.*, 1991, **30**, 3430-3438.
21. K. L. Brown, X. Zou, G. Z. Wu, J. D. Zubkowski and E. J. Valente, *Polyhedron*, 1995, **14**, 1621-1639.
22. K. L. Brown, X. Zou, S. R. Savon and D. W. Jacobsen, *Biochemistry*, 1993, **32**, 8421-8428.
23. L. Z. Ouyang, P. Rulis, W. Y. Ching, G. Nardin and L. Randaccio, *Inorg. Chem.*, 2004, **43**, 1235-1241.
24. H. M. Marques, X. Zou and K. L. Brown, *J. Mol. Struct.*, 2000, **520**, 75-95.
25. K. L. Brown, X. Zou, R. R. Banka, C. B. Perry and H. M. Marques, *Inorg. Chem.*, 2004, **43**, 8130-8142.
26. R. F. Bader, *Atoms in Molecules: A Quantum Theory*, Oxford University Press, Oxford, 1990.
27. R. F. W. Bader, *Acc. Chem. Res.*, 1985, **18**, 9-15.
28. S. T. Howard and T. M. Krygowski, *Can. J. Chem.*, 1997, **75**, 1174-1181.
29. S. E. O'Brien and P. L. Popelier, *Can. J. Chem.*, 1999, **77**, 28-36.

30. R. F. W. Bader, C. F. Matta and F. Cortés-Guzmán, *Organometallics*, 2004, **23**.
31. I. Vidal, S. Melchor, I. Alkorta, J. Elguero, M. R. Sundberg and J. A. Dobado, *Organometallics*, 2006, **25**, 5638-5647.
32. E. Espinosa, I. Alkorta, J. Elguero and E. Molins, *J. Chem. Phys.*, 2002, **117**, 5529-5542.
33. P. R. Varadwaj, A. Varadwaj and H. M. Marques, *J. Phys. Chem. A*, 2011, **115**, 5592-5601.
34. H. A. Hassanin, M. F. El-Shahat, S. DeBeer, C. A. Smith and N. E. Brasch, *Dalton Trans.*, 2010, **39**, 10626-10630.
35. G. C. Hayward, H. A. O. Hill, J. M. Pratt, N. J. Vanston and R. J. P. Williams, *J. Chem. Soc. A*, 1965, 6485-6493.
36. P. George, D. H. Irvine and S. C. Glauser, *Ann. New York Acad. Sci.*, 1960, **88**, 393-415.
37. B. H. Offenhartz and P. George, *Biochemistry*, 1963, **2**, 142-145.
38. R. A. Firth, H. A. O. Hill, J. M. Pratt, R. G. Thorp and R. J. P. Williams, *J. Chem. Soc. A*, 1968, 2428-2433.
39. D. A. Baldwin, E. A. Betterton and J. M. Pratt, *J. Chem. Soc., Dalton Trans.*, 1983, 225-229.
40. S. M. Chemaly, E. A. Betterton and J. M. Pratt, *J. Chem. Soc. Dalton Trans.*, 1987, 761-767.
41. R. A. Firth, H. A. O. Hill, J. M. Pratt, R. G. Thorp and R. J. P. Williams, *J. Chem. Soc. (A)*, 1969, 381-386.
42. E. A. Betterton, Ph.D. Thesis, University of the Witwatersrand, 1982.
43. H. M. Marques, J. C. Bradley, K. L. Brown and H. Brooks, *Inorg. Chim. Acta*, 1993, **209**, 161-169.
44. D. Lexa, J. M. Saveant and J. Zickler, *J. Am. Chem. Soc.*, 1980, **102**, 2654-2663.
45. E. A. Betterton, S. M. Chemaly and J. M. Pratt, *J. Chem. Soc., Dalton Trans.*, 1985, 1619-1622.
46. R. A. Firth, H. A. O. Hill, J. M. Pratt and R. G. Thorp, *Anal. Biochem.*, 1968, **23**, 429-432.
47. APEX2, 2009.1-0, Bruker AXS Inc., Madison, Wisconsin, USA, 2005
48. SAINT+, 7.60A (includes XPREP and SADABS), Bruker AXS Inc., Madison, Wisconsin, USA, 2005
49. G. M. Sheldrick, *Acta Crystallogr.*, 2008, **A64**, 112-122.
50. L. J. Farrugia, *J. Appl. Cryst.*, 1997, **30**, 565-566.
51. E. J. Baerends, D. E. Ellis and P. Ros, *Chem. Phys.*, 1973, **2**, 41-51.
52. B. I. Dunlap, J. W. D. Connolly and J. R. Sabin, *J. Chem. Phys.*, 1979, **71**, 3396-3402.
53. K. Eichkorn, O. Treutler, H. Öhm, M. Häser and R. Ahlrichs, *Chem. Phys. Lett.*, 1995, **240**, 283-290.
54. K. Eichkorn, F. Weigend, O. Treutler and R. Ahlrichs, *Theor. Chem. Acc.*, 1997, **97**, 119-124.
55. R. A. Kendall and H. A. Früchtl, *Theor. Chem. Acc.*, 1997, **97**, 158-163.
56. C. Van Alsenoy, *J. Comp. Chem.*, 1988, **9**, 620-626.
57. J. L. Whitten, *J. Chem. Phys.*, 1973, **58**, 4496-4501.
58. F. Neese, *Wiley Interdisciplinary Reviews: Computational Molecular Science*, 2012, 73-78.
59. A. D. Becke, *Phys. Rev. A*, 1988, **38**, 3098-3100.
60. J. P. Perdew, *Phys. Rev. B*, 1986, **33**, 8822-8824.
61. A. Schafer, H. Horn and R. Ahlrichs, *J. Chem. Phys.*, 1992, **97**, 2571-2577.

62. S. Grimme, J. Antony, S. Ehrlich and H. Krieg, *J. Chem. Phys.*, 2010, **132**, 154104-154119.
63. S. F. Boys and F. Bernardi, *Mol. Phys.*, 1970, **19**, 553-566.
64. S. Simon, M. Duran and J. J. Dannenberg, *J. Chem. Phys.*, 1996, **105**, 11024-11031.
65. AIMAll (Version 11.12.19), 08.05.04, http://aim.tkgristmill.com, Overland Park, KS, 2011

Phenylvinylcobalamin: An alkylcobalamin featuring a ligand with a large trans influence

Christopher B. Perry,* Naree Shin, Manuel A. Fernandes and Helder M. Marques*

Molecular Sciences Institute, School of Chemistry, University of the Witwatersrand, P.O. Wits, Johannesburg, 2050 South Africa

Electronic Supplementary Information

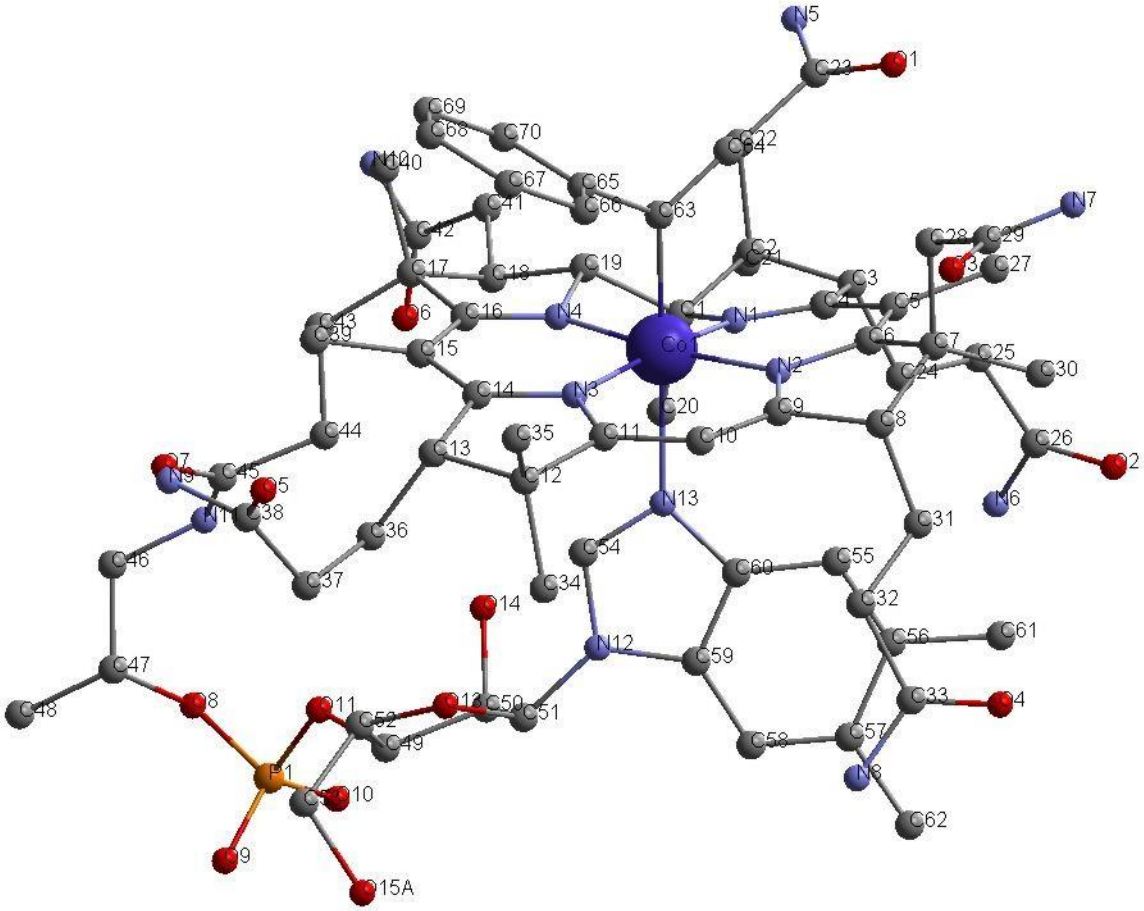

Fig S1. Crystallographic numbering scheme for PhVnCbl. There is an acetone solvent molecule in the structure. This, together with solvent water molecules and hydrogen atoms, have been omitted for clarity.

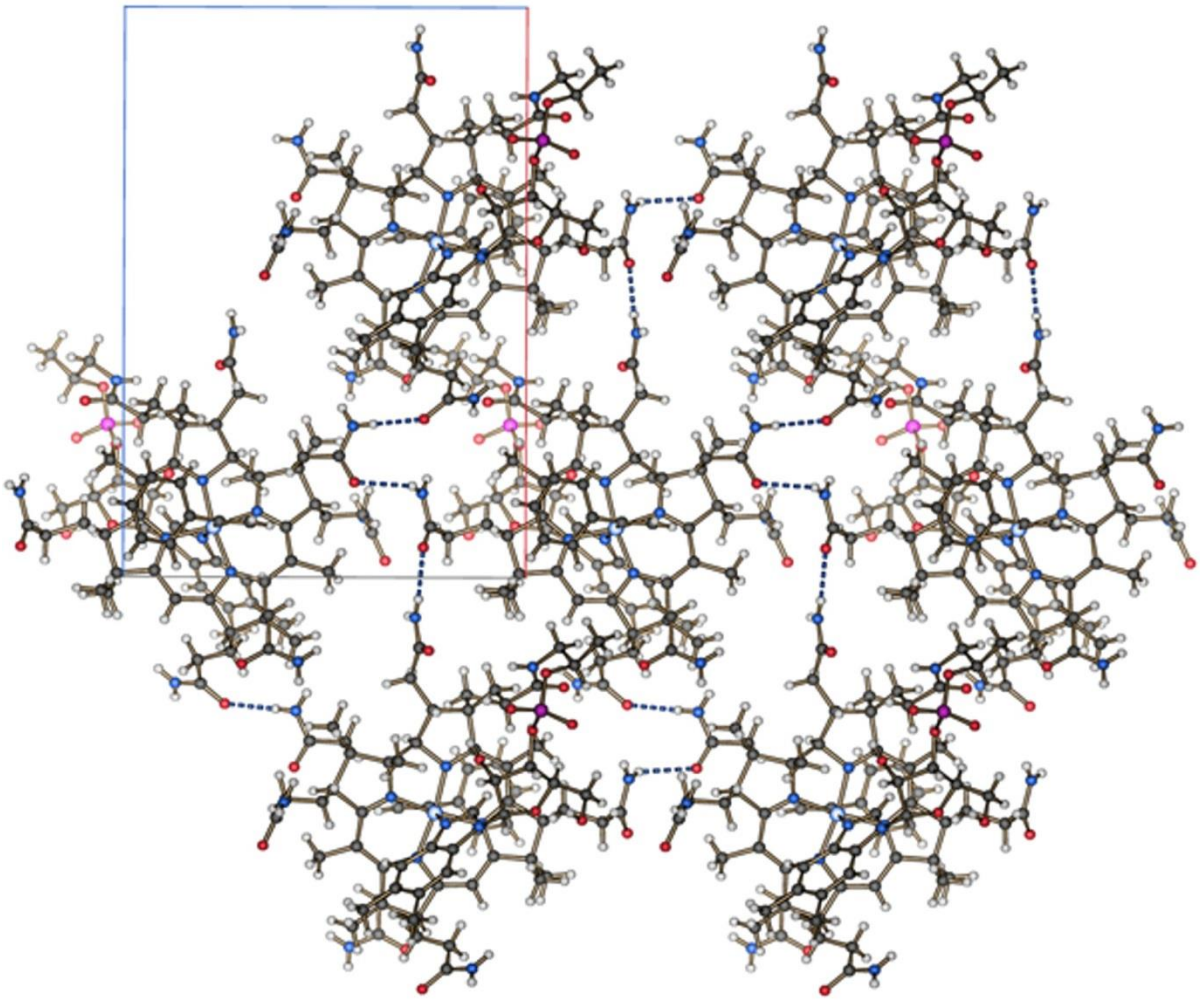

Fig. S2. Hydrogen bonding between Cobalamin molecules in the solid state structure of *β*-phenylvinylcobalamin. O1 of the *a* side chain amide hydrogen bonds to N9 of the *e* side chain amide of an neighbouring molecule (O···N = 2.987 Å); N7 of the *c* side chain amide hydrogen bonds to phosphate O10 of a neighbouring molecule (2.995 Å); O4 of the *d* amide is hydrogen bonded to amide N5 of the *a* side chain of a neighbour (2.949 Å); O5 of the amide of the *e* side chain is hydrogen bonded to N10 of a neighbouring *g* side chain amide (2.899 Å); and N6 of the *b* side chain is hydrogen bonded to a neighbouring phosphate O10 (2.964 Å). In addition, there are many hydrogen bonds between solvent water and the ribose OH groups, and the amides of the acetamide and the propionamide side chains of the corrin.

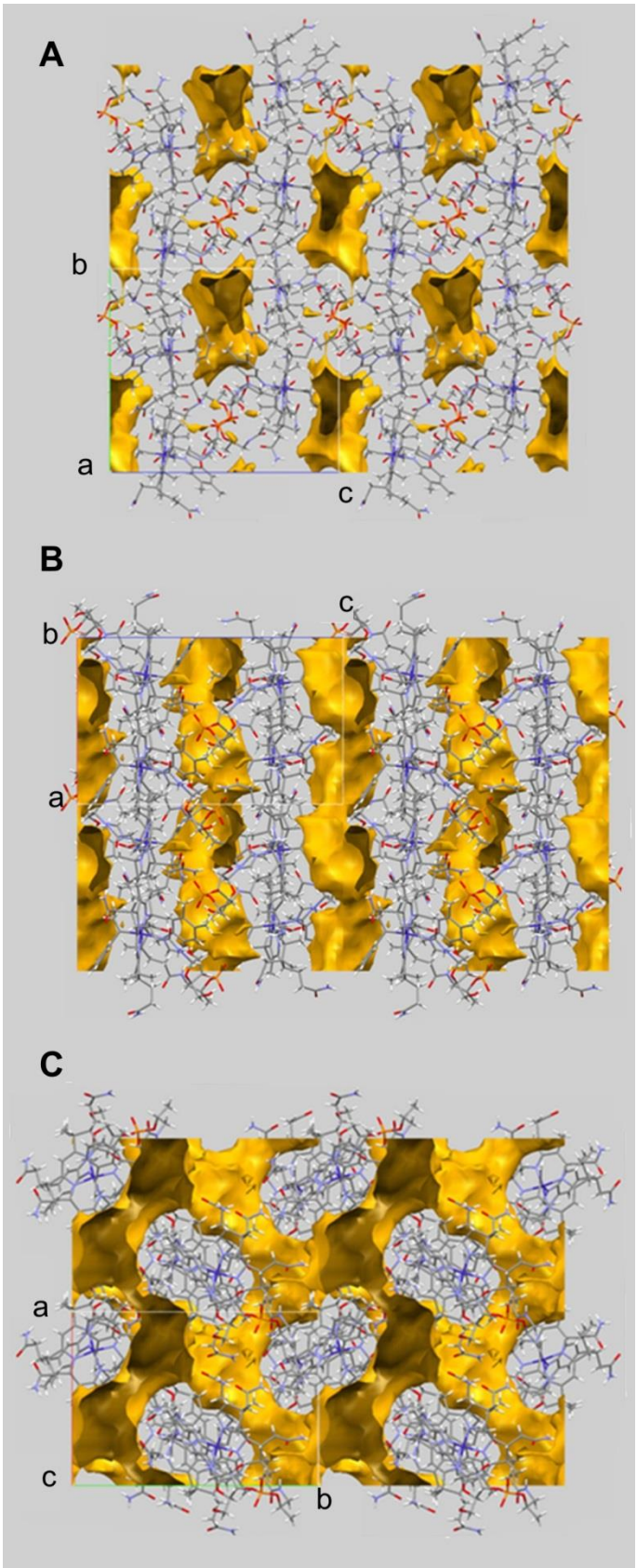

Fig. S3. Solvent voids in the structure of *β*-PACbl shown down that (A) *a*, (B) **b** and (C) *c* crystallographic axes.

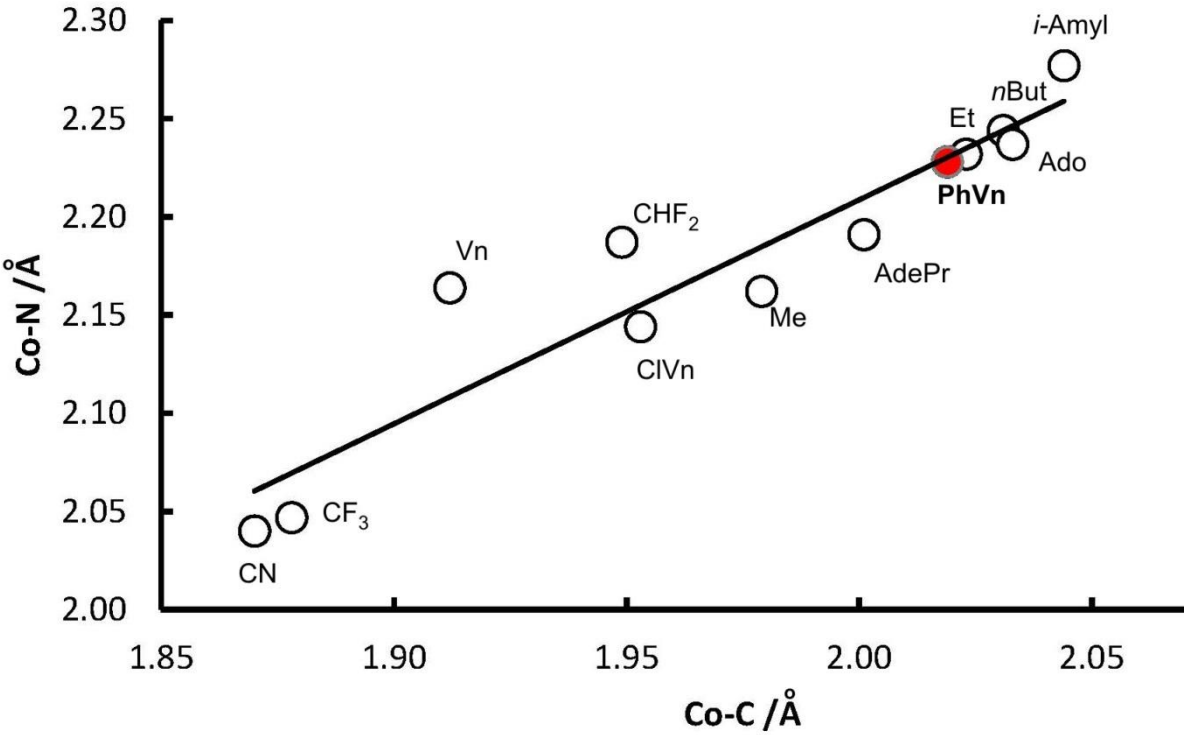

Fig. S4. The mutual dependence of the Co–C and the *trans* Co–N_{dmbzm} bond lengths in alkylcobalamins. The data are given in Table S2 of this ESI.

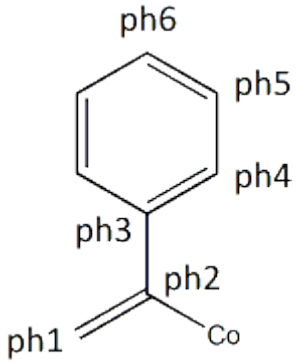

Fig. S5. Nomenclature used for the NMR assignments of the ^{1}H spectrum of the phenylvinyl ligand in *β*-PhVnCbl.

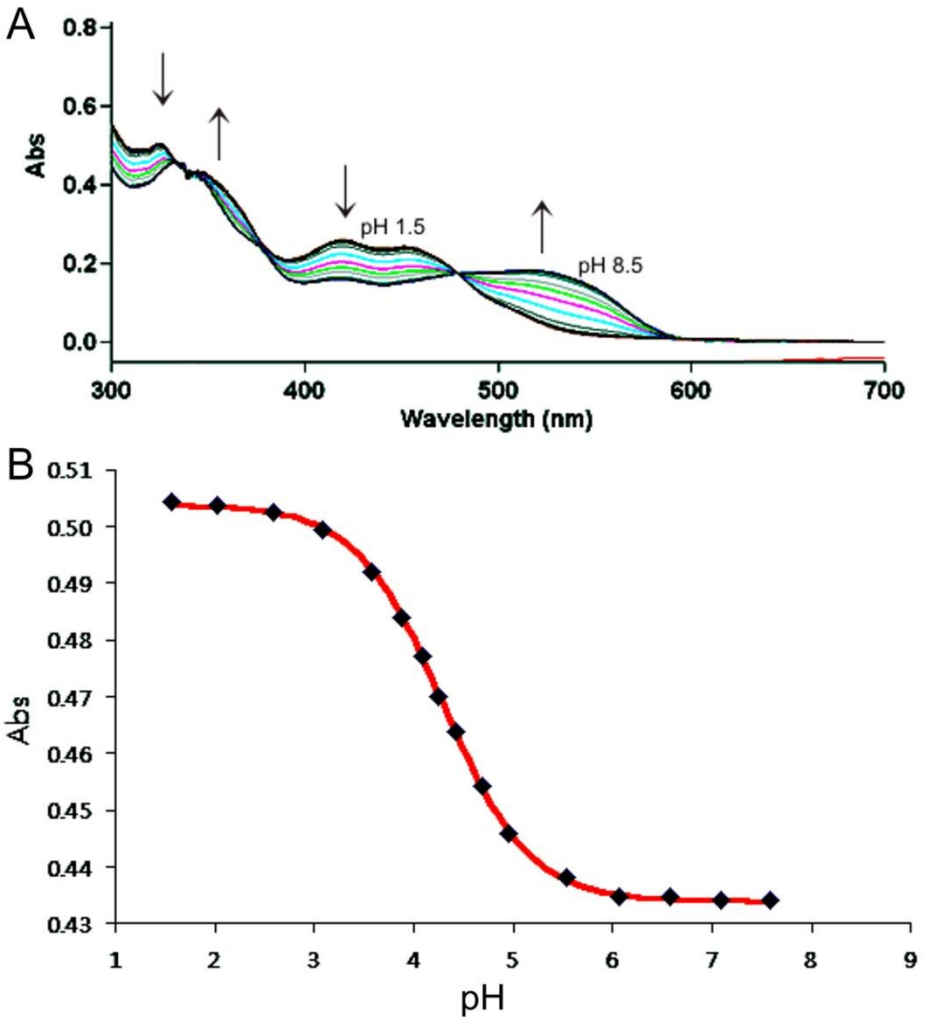

Fig. S6. Spectrophotometric titration of *β*–PhVnCbl in aqueous solution (25 mM phosphate, 25 °C). A: Spectroscopic changes observed across the uv-vis spectrum. B: Variation in absorbance at 326 nm as a function of pH. The solid line is a least squares fit to a standard ionisation isotherm $A = \frac{10^{-\mathrm{pH}} A_0 + 10^{-\mathrm{p}K_a} A_1}{10^{-\mathrm{pH}} + 10^{-\mathrm{p}K_a}}$ where A, A_0 and A_1 are the absorbance at intermediate, limiting low and limiting high pH values and pK_a is the acid dissociation constant for the deprotonation of the free dmbzm base and its coordination by Co(III).

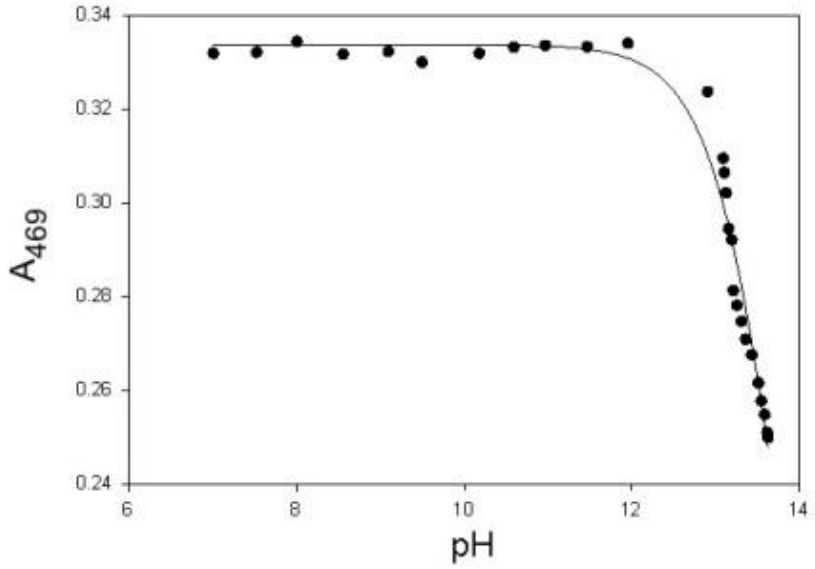

Fig. S7. Variation in absorbance at 469 nm with pH of α–PhVnCbl . The solid line, with a pK_a at 13.9, is the least squares fit of the experimental data to a ionisation isotherm (see Fig. A5).

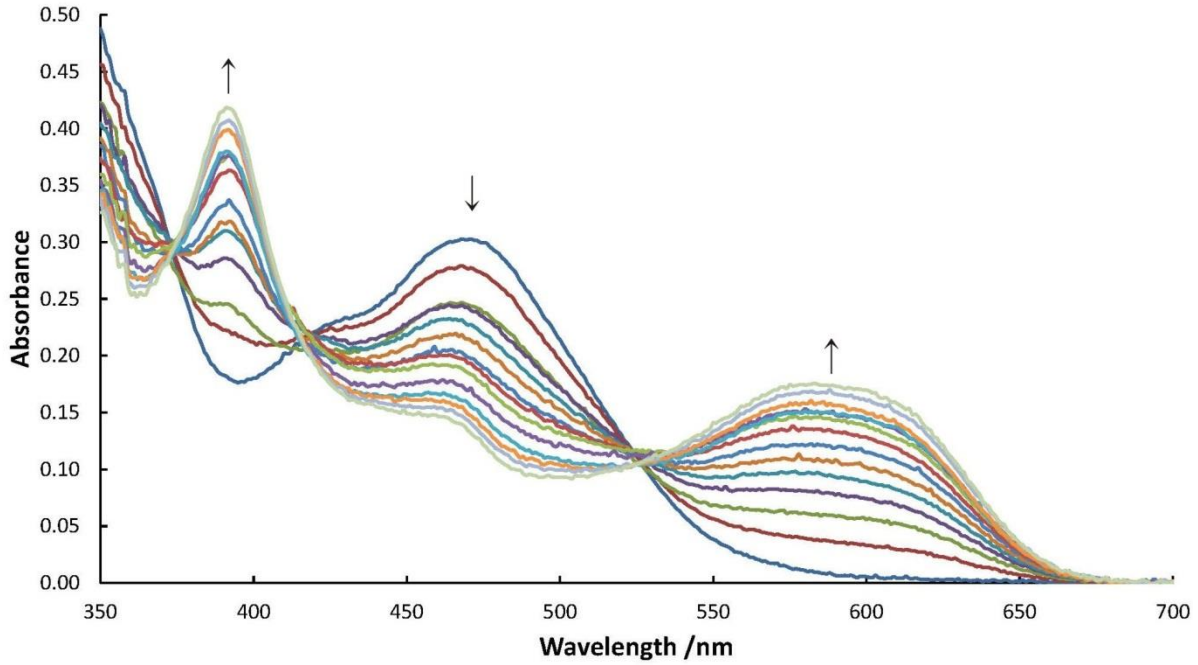

Fig. S8. Changes in the UV-vis spectrum of α-PhVnCbl as a function of cyanide concentration (up to 11.5 mM CN^-) at 25 ^oC, pH 11.0.

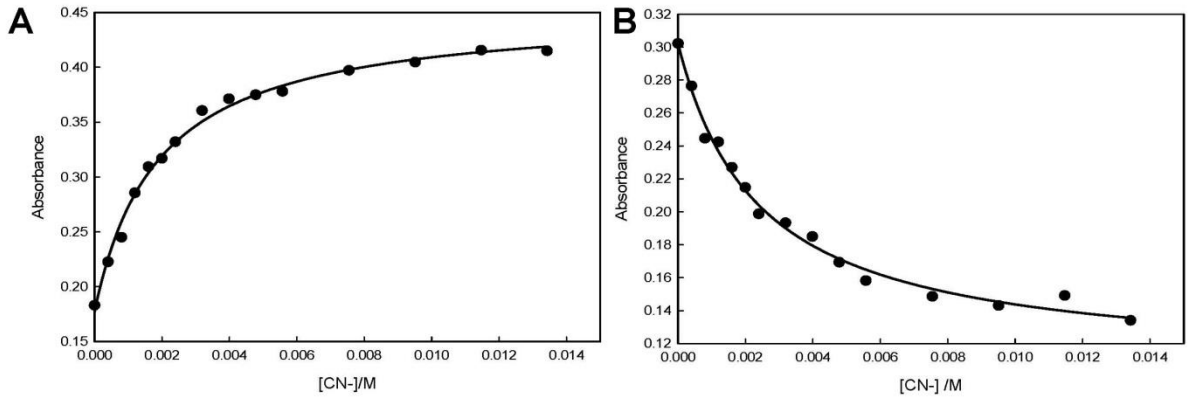

Fig. S9. Fit of the absorbance change at 390 nm (A) and 470 nm (B) with the concentration of cyanide for substitution of H_2O by CN^- in α–PhVnCbl at 25 °C, pH 11.0 (0.5 M CAPS buffer). The solid lines are least squares fits to a binding isotherm $A_\lambda = (A_0 + A_1 K[CN^-]) / (1 + K[CN^-])$ where A_λ is the absorbance at the monitoring wavelength λ, A_0 and A_1 are the limiting absorbance at 0 and 100% complex formation and K is the equilibrium constant.

Table S1. ^{1}H and ^{13}C NMR Chemical Shift Assignments for PhVnCbl.[a]

Atom[b]	^{1}H (ppm)	^{13}C (ppm)	Atom[b]	^{1}H (ppm)	^{13}C (ppm)	Atom[b]	^{1}H (ppm)	^{13}C (ppm)
C1	-	88.39	C35	2.54	16.29	Pr1″	3.45	46.38
C2	-	47.30	C36	1.82	19.95	Pr2	4.32	73.17
C3	4.55	56.50	C37′	1.72	42.99	Pr3	1.18	19.99
C4	-	178.60	C37″	2.35	42.99	R1	6.20	87.44
C5	-	109.49	C38	-	n.a.[c]	R2	4.34	71.79
C6	-	164.85	C41′	1.41	28.52	R3	4.70	75.54
C7	-	51.55	C41″	2.01	28.52	R4	4.18	84.13
C8	3.95	55.45	C42′	1.83	33.74	R5′	3.69	62.49
C9	-	173.53	C42″	1.94	33.74	R5″	3.78	62.49
C10	6.50	97.82	C43	-	n.a.[c]	B2	7.61	143.24
C11	-	177.07	C46	0.94	31.37	B4	6.82	119.52
C12	-	48.17	C47	1.35	23.28	B5	-	134.20
C13	2.89	53.55	C48′	2.09	34.68	B6	-	132.80
C14	-	164.53	C48″	2.18	34.68	B7	7.21	111.91
C15	-	107.32	C49′	1.86	27.15	B8	-	139.73
C16	-	177.72	C49″	2.08	27.15	B9	-	132.38
C17	-	60.14	C50	-	n.a.[c]	B10	2.27	20.61
C18	2.83	41.03	C53	2.33	16.89	B11	2.25	20.43
C19	4.40	76.10	C54	1.54	19.48	Ph1′	3.01	118.07
C20	0.52	23.64	C55′	1.86	33.88	Ph1″	3.06	118.07
C25	1.30	17.80	C55″	2.50	33.88	Ph2	-	143.24
C26′	2.13	43.06	C56′	1.98	32.56	Ph3	-	148.93
C26″	2.22	43.06	C56″	2.36	32.56	Ph4	6.04	127.39
C27	-	n.a.[c]	C57	-	n.a.[c]	Ph5	6.87	128.31
C30′	1.87	27.62	C60′	2.58	33.14	Ph6	7.05	127.39
C30″	2.02	27.62	C60″	2.65	33.14	*f*H	7.95	-
C31	2.40	36.40	C61	-	n.a.[c]			
C32	-	n.a.[c]	Pr1′	3.06	46.38			

[a]In MeOD, at 25 °C. Chemical shifts are relative to internal TMS. [b]Primes and double primes denote downfield and upfield members, respectively, of pairs of diastereotopic methylene, or

in the case of ph1, geminal protons. [c]Not assigned (the carbonyl carbons are clustered in a narrow region between 175 and 180 ppm, making reliable assignments problematic).

Table S2. ^{1}H and ^{13}C assignments and NMR correlations for the phenylvinyl group in PhVnCbl observed by COSY, ROESY, and HMBC spectroscopies[a].

Resonance	^{1}H (ppm)	^{13}C (ppm)	COSY	ROESY	HMBC
ph1′	3.01	118.07	-	C46, C54, C37′, C26′, C35, ph1′′, C19, C10, ph4	ph2, ph3
ph1”	3.06		-	C36, C37′, ph1′, ph4	
ph2	-	143.24	-	-	-
ph3	-	148.93	-	-	-
ph4	6.04	127.39	ph5, ph6	C46, C54, C37’, C26’, C53, C35, ph1′′, C19, C10, ph5, ph6	ph5, ph6, ph2
ph5	6.87	128.31	ph4, ph6	C46, C54, C53, ph4, ph6	ph4, ph6, ph3
ph6	7.05	127.39	ph5, ph4	C46, C37’, ph4, ph5	ph4, ph5

[a]Primes and double primes denote downfield and upfield members, respectively, of pairs of diastereotopic methylene, or in the case of ph1, geminal protons.

Table S3. Bond lengths [Å] and angles [°] for PhVnCbl

Bond Lengths

C(1)-N(1)	1.472(10)	C(21)-H(21A)	0.9800
C(1)-C(20)	1.498(12)	C(21)-H(21B)	0.9800
C(1)-C(19)	1.550(11)	C(21)-H(21C)	0.9800
C(1)-C(2)	1.576(10)	C(22)-C(23)	1.505(11)
C(2)-C(21)	1.521(13)	C(22)-H(22A)	0.9900
C(2)-C(22)	1.574(12)	C(22)-H(22B)	0.9900
C(2)-C(3)	1.585(12)	C(23)-O(1)	1.240(11)
C(3)-C(4)	1.528(11)	C(23)-N(5)	1.313(13)
C(3)-C(24)	1.592(14)	C(24)-C(25)	1.469(13)
C(3)-H(3)	1.0000	C(24)-H(24A)	0.9900
C(4)-N(1)	1.281(9)	C(24)-H(24B)	0.9900
C(4)-C(5)	1.443(12)	C(25)-C(26)	1.463(18)
C(5)-C(6)	1.350(11)	C(25)-H(25A)	0.9900
C(5)-C(27)	1.534(11)	C(25)-H(25B)	0.9900
C(6)-N(2)	1.375(9)	C(26)-O(2)	1.222(14)
C(6)-C(7)	1.552(12)	C(26)-N(6)	1.338(14)
C(7)-C(30)	1.553(11)	C(27)-H(27A)	0.9800
C(7)-C(8)	1.558(11)	C(27)-H(27B)	0.9800
C(7)-C(28)	1.585(13)	C(27)-H(27C)	0.9800
C(8)-C(31)	1.502(12)	C(28)-C(29)	1.478(13)
C(8)-C(9)	1.521(11)	C(28)-H(28A)	0.9900
C(8)-H(8)	1.0000	C(28)-H(28B)	0.9900
C(9)-C(10)	1.351(12)	C(29)-O(3)	1.219(12)
C(9)-N(2)	1.373(11)	C(29)-N(7)	1.295(11)
C(10)-C(11)	1.403(12)	C(30)-H(30A)	0.9800
C(10)-H(10)	0.9500	C(30)-H(30B)	0.9800
C(11)-N(3)	1.352(11)	C(30)-H(30C)	0.9800
C(11)-C(12)	1.483(11)	C(31)-C(32)	1.484(11)
C(12)-C(34)	1.536(14)	C(31)-H(31A)	0.9900
C(12)-C(35)	1.537(13)	C(31)-H(31B)	0.9900
C(12)-C(13)	1.575(11)	C(32)-C(33)	1.511(15)
C(13)-C(36)	1.532(13)	C(32)-H(32A)	0.9900
C(13)-C(14)	1.545(10)	C(32)-H(32B)	0.9900
C(13)-H(13)	1.0000	C(33)-O(4)	1.234(11)
C(14)-N(3)	1.361(10)	C(33)-N(8)	1.322(12)
C(14)-C(15)	1.373(11)	C(34)-H(34A)	0.9800
C(15)-C(16)	1.459(11)	C(34)-H(34B)	0.9800
C(15)-C(39)	1.503(12)	C(34)-H(34C)	0.9800
C(16)-N(4)	1.304(9)	C(35)-H(35A)	0.9800
C(16)-C(17)	1.564(11)	C(35)-H(35B)	0.9800
C(17)-C(40)	1.526(13)	C(35)-H(35C)	0.9800
C(17)-C(18)	1.542(11)	C(36)-C(37)	1.582(11)
C(17)-C(43)	1.545(11)	C(36)-H(36A)	0.9900
C(18)-C(19)	1.525(11)	C(36)-H(36B)	0.9900
C(18)-C(41)	1.541(11)	C(37)-C(38)	1.452(15)
C(18)-H(18)	1.0000	C(37)-H(37A)	0.9900
C(19)-N(4)	1.488(10)	C(37)-H(37B)	0.9900
C(19)-H(19)	1.0000	C(38)-O(5)	1.259(13)
C(20)-H(20A)	0.9800	C(38)-N(9)	1.366(13)
C(20)-H(20B)	0.9800	C(39)-H(39A)	0.9800
C(20)-H(20C)	0.9800	C(39)-H(39B)	0.9800
		C(39)-H(39C)	0.9800
		C(40)-H(40A)	0.9800

C(40)-H(40B)	0.9800	C(59)-N(12)	1.384(10)
C(40)-H(40C)	0.9800	C(60)-N(13)	1.408(10)
C(41)-C(42)	1.498(13)	C(61)-H(61A)	0.9800
C(41)-H(41A)	0.9900	C(61)-H(61B)	0.9800
C(41)-H(41B)	0.9900	C(61)-H(61C)	0.9800
C(42)-O(6)	1.217(10)	C(62)-H(62A)	0.9800
C(42)-N(10)	1.322(11)	C(62)-H(62B)	0.9800
C(43)-C(44)	1.512(12)	C(62)-H(62C)	0.9800
C(43)-H(43A)	0.9900	C(63)-C(64)	1.333(11)
C(43)-H(43B)	0.9900	C(63)-C(65)	1.445(9)
C(44)-C(45)	1.544(12)	C(63)-Co(1)	2.019(9)
C(44)-H(44A)	0.9900	C(64)-H(64A)	0.9500
C(44)-H(44B)	0.9900	C(64)-H(64B)	0.9500
C(45)-O(7)	1.224(10)	C(65)-C(66)	1.3900
C(45)-N(11)	1.322(12)	C(65)-C(70)	1.3900
C(46)-N(11)	1.456(11)	C(66)-C(67)	1.3900
C(46)-C(47)	1.467(13)	C(66)-H(66)	0.9500
C(46)-H(46A)	0.9900	C(67)-C(68)	1.3900
C(46)-H(46B)	0.9900	C(67)-H(67)	0.9500
C(47)-O(8)	1.453(11)	C(68)-C(69)	1.3900
C(47)-C(48)	1.539(12)	C(68)-H(68)	0.9500
C(47)-H(47)	1.0000	C(69)-C(70)	1.3900
C(48)-H(48A)	0.9800	C(69)-H(69)	0.9500
C(48)-H(48B)	0.9800	C(70)-H(70)	0.9500
C(48)-H(48C)	0.9800	N(1)-Co(1)	1.890(5)
C(49)-O(11)	1.417(10)	N(2)-Co(1)	1.903(6)
C(49)-C(50)	1.509(11)	N(3)-Co(1)	1.913(6)
C(49)-C(52)	1.507(14)	N(4)-Co(1)	1.879(6)
C(49)-H(49)	1.0000	N(5)-H(5A)	0.8800
C(50)-O(14)	1.433(10)	N(5)-H(5B)	0.8800
C(50)-C(51)	1.512(13)	N(6)-H(6A)	0.8800
C(50)-H(50)	1.0000	N(6)-H(6B)	0.8800
C(51)-O(13)	1.393(10)	N(7)-H(7A)	0.8800
C(51)-N(12)	1.458(10)	N(7)-H(7B)	0.8800
C(51)-H(51)	1.0000	N(8)-H(8A)	0.8800
C(52)-O(13)	1.409(11)	N(8)-H(8B)	0.8800
C(52)-C(53)	1.509(14)	N(9)-H(9A)	0.8800
C(52)-H(52)	1.0000	N(9)-H(9B)	0.8800
C(53)-O(15A)	1.495(13)	N(10)-H(10A)	0.8800
C(53)-O(15B)	1.497(13)	N(10)-H(10B)	0.8800
C(53)-H(53A)	0.9900	N(11)-H(11)	0.8800
C(53)-H(53B)	0.9900	N(13)-Co(1)	2.224(7)
C(53)-H(53C)	0.9700	O(8)-P(1)	1.579(6)
C(53)-H(53D)	0.9700	O(9)-P(1)	1.475(7)
C(54)-N(13)	1.302(9)	O(10)-P(1)	1.457(7)
C(54)-N(12)	1.341(10)	O(11)-P(1)	1.591(6)
C(54)-H(54)	0.9500	O(14)-H(14)	0.8400
C(55)-C(56)	1.360(13)	O(15A)-H(53C)	0.7744
C(55)-C(60)	1.405(11)	O(15A)-H(15A)	0.8400
C(55)-H(55)	0.9500	O(15B)-H(15B)	0.8200
C(56)-C(57)	1.442(13)	C(1A)-C(2A)	1.438(19)
C(56)-C(61)	1.525(13)	C(1A)-H(1A)	0.9800
C(57)-C(58)	1.372(12)	C(1A)-H(1B)	0.9800
C(57)-C(62)	1.484(14)	C(1A)-H(1C)	0.9800
C(58)-C(59)	1.394(12)	C(2A)-O(1A)	1.247(15)
C(58)-H(58)	0.9500	C(2A)-C(3A)	1.44(2)
C(59)-C(60)	1.355(11)	C(3A)-H(3A)	0.9800

C(3A)-H(3B)	0.9800
C(3A)-H(3C)	0.9800

Bond angles

N(1)-C(1)-C(20)	111.9(7)
N(1)-C(1)-C(19)	102.5(6)
C(20)-C(1)-C(19)	109.8(6)
N(1)-C(1)-C(2)	101.8(6)
C(20)-C(1)-C(2)	112.4(7)
C(19)-C(1)-C(2)	117.7(7)
C(21)-C(2)-C(22)	109.1(7)
C(21)-C(2)-C(1)	119.3(7)
C(22)-C(2)-C(1)	109.0(6)
C(21)-C(2)-C(3)	111.7(7)
C(22)-C(2)-C(3)	105.6(7)
C(1)-C(2)-C(3)	101.2(6)
C(4)-C(3)-C(2)	99.9(6)
C(4)-C(3)-C(24)	109.5(7)
C(2)-C(3)-C(24)	117.0(7)
C(4)-C(3)-H(3)	110.0
C(2)-C(3)-H(3)	110.0
C(24)-C(3)-H(3)	110.0
N(1)-C(4)-C(5)	125.2(7)
N(1)-C(4)-C(3)	112.2(7)
C(5)-C(4)-C(3)	122.6(6)
C(6)-C(5)-C(4)	120.5(6)
C(6)-C(5)-C(27)	123.1(7)
C(4)-C(5)-C(27)	116.4(7)
C(5)-C(6)-N(2)	124.3(7)
C(5)-C(6)-C(7)	127.3(6)
N(2)-C(6)-C(7)	108.4(7)
C(30)-C(7)-C(6)	115.6(7)
C(30)-C(7)-C(8)	111.7(7)
C(6)-C(7)-C(8)	101.4(6)
C(30)-C(7)-C(28)	109.2(7)
C(6)-C(7)-C(28)	106.2(7)
C(8)-C(7)-C(28)	112.6(7)
C(31)-C(8)-C(9)	112.8(7)
C(31)-C(8)-C(7)	114.3(7)
C(9)-C(8)-C(7)	100.7(6)
C(31)-C(8)-H(8)	109.5
C(9)-C(8)-H(8)	109.5
C(7)-C(8)-H(8)	109.5
C(10)-C(9)-N(2)	126.6(8)
C(10)-C(9)-C(8)	122.8(8)
N(2)-C(9)-C(8)	110.5(6)
C(9)-C(10)-C(11)	127.3(8)
C(9)-C(10)-H(10)	116.4
C(11)-C(10)-H(10)	116.4
N(3)-C(11)-C(10)	123.4(7)
N(3)-C(11)-C(12)	114.0(7)
C(10)-C(11)-C(12)	122.6(8)
C(11)-C(12)-C(34)	106.8(7)
C(11)-C(12)-C(35)	113.1(7)
C(34)-C(12)-C(35)	110.7(7)
C(11)-C(12)-C(13)	102.6(6)
C(34)-C(12)-C(13)	113.3(8)
C(35)-C(12)-C(13)	110.1(7)
C(36)-C(13)-C(14)	111.3(7)
C(36)-C(13)-C(12)	117.1(7)
C(14)-C(13)-C(12)	102.0(6)
C(36)-C(13)-H(13)	108.7
C(14)-C(13)-H(13)	108.7
C(12)-C(13)-H(13)	108.7
N(3)-C(14)-C(15)	127.2(6)
N(3)-C(14)-C(13)	111.0(6)
C(15)-C(14)-C(13)	121.7(6)
C(14)-C(15)-C(16)	119.6(7)
C(14)-C(15)-C(39)	119.9(7)
C(16)-C(15)-C(39)	120.3(7)
N(4)-C(16)-C(15)	122.7(7)
N(4)-C(16)-C(17)	110.8(6)
C(15)-C(16)-C(17)	126.4(6)
C(40)-C(17)-C(18)	110.8(7)
C(40)-C(17)-C(43)	108.7(7)
C(18)-C(17)-C(43)	112.8(7)
C(40)-C(17)-C(16)	109.5(7)
C(18)-C(17)-C(16)	99.6(6)
C(43)-C(17)-C(16)	115.1(6)
C(19)-C(18)-C(41)	113.2(6)
C(19)-C(18)-C(17)	104.0(6)
C(41)-C(18)-C(17)	117.2(7)
C(19)-C(18)-H(18)	107.3
C(41)-C(18)-H(18)	107.3
C(17)-C(18)-H(18)	107.3
N(4)-C(19)-C(18)	101.8(5)
N(4)-C(19)-C(1)	105.3(6)
C(18)-C(19)-C(1)	121.9(7)
N(4)-C(19)-H(19)	109.0
C(18)-C(19)-H(19)	109.0
C(1)-C(19)-H(19)	109.0
C(1)-C(20)-H(20A)	109.5
C(1)-C(20)-H(20B)	109.5
H(20A)-C(20)-H(20B)	109.5
C(1)-C(20)-H(20C)	109.5
H(20A)-C(20)-H(20C)	109.5
H(20B)-C(20)-H(20C)	109.5
C(2)-C(21)-H(21A)	109.5
C(2)-C(21)-H(21B)	109.5
H(21A)-C(21)-H(21B)	109.5
C(2)-C(21)-H(21C)	109.5
H(21A)-C(21)-H(21C)	109.5
H(21B)-C(21)-H(21C)	109.5
C(23)-C(22)-C(2)	118.5(7)
C(23)-C(22)-H(22A)	107.7
C(2)-C(22)-H(22A)	107.7
C(23)-C(22)-H(22B)	107.7
C(2)-C(22)-H(22B)	107.7
H(22A)-C(22)-H(22B)	107.1
O(1)-C(23)-N(5)	120.4(8)
O(1)-C(23)-C(22)	122.4(9)
N(5)-C(23)-C(22)	117.1(9)

C(25)-C(24)-C(3)	115.6(9)	C(12)-C(35)-H(35A)	109.5
C(25)-C(24)-H(24A)	108.4	C(12)-C(35)-H(35B)	109.5
C(3)-C(24)-H(24A)	108.4	H(35A)-C(35)-H(35B)	109.5
C(25)-C(24)-H(24B)	108.4	C(12)-C(35)-H(35C)	109.5
C(3)-C(24)-H(24B)	108.4	H(35A)-C(35)-H(35C)	109.5
H(24A)-C(24)-H(24B)	107.4	H(35B)-C(35)-H(35C)	109.5
C(26)-C(25)-C(24)	113.4(11)	C(13)-C(36)-C(37)	114.3(8)
C(26)-C(25)-H(25A)	108.9	C(13)-C(36)-H(36A)	108.7
C(24)-C(25)-H(25A)	108.9	C(37)-C(36)-H(36A)	108.7
C(26)-C(25)-H(25B)	108.9	C(13)-C(36)-H(36B)	108.7
C(24)-C(25)-H(25B)	108.9	C(37)-C(36)-H(36B)	108.7
H(25A)-C(25)-H(25B)	107.7	H(36A)-C(36)-H(36B)	107.6
O(2)-C(26)-N(6)	116.1(11)	C(38)-C(37)-C(36)	112.8(8)
O(2)-C(26)-C(25)	128.4(12)	C(38)-C(37)-H(37A)	109.0
N(6)-C(26)-C(25)	115.6(11)	C(36)-C(37)-H(37A)	109.0
C(5)-C(27)-H(27A)	109.5	C(38)-C(37)-H(37B)	109.0
C(5)-C(27)-H(27B)	109.5	C(36)-C(37)-H(37B)	109.0
H(27A)-C(27)-H(27B)	109.5	H(37A)-C(37)-H(37B)	107.8
C(5)-C(27)-H(27C)	109.5	O(5)-C(38)-N(9)	119.4(10)
H(27A)-C(27)-H(27C)	109.5	O(5)-C(38)-C(37)	123.5(9)
H(27B)-C(27)-H(27C)	109.5	N(9)-C(38)-C(37)	117.1(11)
C(29)-C(28)-C(7)	111.1(8)	C(15)-C(39)-H(39A)	109.5
C(29)-C(28)-H(28A)	109.4	C(15)-C(39)-H(39B)	109.5
C(7)-C(28)-H(28A)	109.4	H(39A)-C(39)-H(39B)	109.5
C(29)-C(28)-H(28B)	109.4	C(15)-C(39)-H(39C)	109.5
C(7)-C(28)-H(28B)	109.4	H(39A)-C(39)-H(39C)	109.5
H(28A)-C(28)-H(28B)	108.0	H(39B)-C(39)-H(39C)	109.5
O(3)-C(29)-N(7)	122.6(9)	C(17)-C(40)-H(40A)	109.5
O(3)-C(29)-C(28)	119.4(9)	C(17)-C(40)-H(40B)	109.5
N(7)-C(29)-C(28)	117.9(9)	H(40A)-C(40)-H(40B)	109.5
C(7)-C(30)-H(30A)	109.5	C(17)-C(40)-H(40C)	109.5
C(7)-C(30)-H(30B)	109.5	H(40A)-C(40)-H(40C)	109.5
H(30A)-C(30)-H(30B)	109.5	H(40B)-C(40)-H(40C)	109.5
C(7)-C(30)-H(30C)	109.5	C(42)-C(41)-C(18)	115.3(7)
H(30A)-C(30)-H(30C)	109.5	C(42)-C(41)-H(41A)	108.5
H(30B)-C(30)-H(30C)	109.5	C(18)-C(41)-H(41A)	108.5
C(32)-C(31)-C(8)	117.3(7)	C(42)-C(41)-H(41B)	108.5
C(32)-C(31)-H(31A)	108.0	C(18)-C(41)-H(41B)	108.5
C(8)-C(31)-H(31A)	108.0	H(41A)-C(41)-H(41B)	107.5
C(32)-C(31)-H(31B)	108.0	O(6)-C(42)-N(10)	121.3(9)
C(8)-C(31)-H(31B)	108.0	O(6)-C(42)-C(41)	121.7(8)
H(31A)-C(31)-H(31B)	107.2	N(10)-C(42)-C(41)	116.8(8)
C(31)-C(32)-C(33)	113.7(7)	C(44)-C(43)-C(17)	118.1(7)
C(31)-C(32)-H(32A)	108.8	C(44)-C(43)-H(43A)	107.8
C(33)-C(32)-H(32A)	108.8	C(17)-C(43)-H(43A)	107.8
C(31)-C(32)-H(32B)	108.8	C(44)-C(43)-H(43B)	107.8
C(33)-C(32)-H(32B)	108.8	C(17)-C(43)-H(43B)	107.8
H(32A)-C(32)-H(32B)	107.7	H(43A)-C(43)-H(43B)	107.1
O(4)-C(33)-N(8)	121.8(10)	C(43)-C(44)-C(45)	110.0(7)
O(4)-C(33)-C(32)	120.7(8)	C(43)-C(44)-H(44A)	109.7
N(8)-C(33)-C(32)	117.5(8)	C(45)-C(44)-H(44A)	109.7
C(12)-C(34)-H(34A)	109.5	C(43)-C(44)-H(44B)	109.7
C(12)-C(34)-H(34B)	109.5	C(45)-C(44)-H(44B)	109.7
H(34A)-C(34)-H(34B)	109.5	H(44A)-C(44)-H(44B)	108.2
C(12)-C(34)-H(34C)	109.5	O(7)-C(45)-N(11)	125.2(8)
H(34A)-C(34)-H(34C)	109.5	O(7)-C(45)-C(44)	119.3(8)
H(34B)-C(34)-H(34C)	109.5	N(11)-C(45)-C(44)	115.6(7)

N(11)-C(46)-C(47)	113.3(7)	C(52)-C(53)-H(53D)	111.9
N(11)-C(46)-H(46A)	108.9	H(53A)-C(53)-H(53D)	125.7
C(47)-C(46)-H(46A)	108.9	H(53C)-C(53)-H(53D)	110.0
N(11)-C(46)-H(46B)	108.9	N(13)-C(54)-N(12)	113.5(7)
C(47)-C(46)-H(46B)	108.9	N(13)-C(54)-H(54)	123.2
H(46A)-C(46)-H(46B)	107.7	N(12)-C(54)-H(54)	123.2
O(8)-C(47)-C(46)	107.3(7)	C(56)-C(55)-C(60)	118.0(8)
O(8)-C(47)-C(48)	107.9(8)	C(56)-C(55)-H(55)	121.0
C(46)-C(47)-C(48)	111.4(8)	C(60)-C(55)-H(55)	121.0
O(8)-C(47)-H(47)	110.0	C(55)-C(56)-C(57)	121.8(8)
C(46)-C(47)-H(47)	110.0	C(55)-C(56)-C(61)	120.8(9)
C(48)-C(47)-H(47)	110.0	C(57)-C(56)-C(61)	117.4(8)
C(47)-C(48)-H(48A)	109.5	C(58)-C(57)-C(56)	118.3(8)
C(47)-C(48)-H(48B)	109.5	C(58)-C(57)-C(62)	119.8(8)
H(48A)-C(48)-H(48B)	109.5	C(56)-C(57)-C(62)	121.8(8)
C(47)-C(48)-H(48C)	109.5	C(57)-C(58)-C(59)	118.5(8)
H(48A)-C(48)-H(48C)	109.5	C(57)-C(58)-H(58)	120.7
H(48B)-C(48)-H(48C)	109.5	C(59)-C(58)-H(58)	120.7
O(11)-C(49)-C(50)	113.8(7)	C(60)-C(59)-N(12)	106.3(7)
O(11)-C(49)-C(52)	112.6(7)	C(60)-C(59)-C(58)	122.5(7)
C(50)-C(49)-C(52)	104.0(7)	N(12)-C(59)-C(58)	131.2(7)
O(11)-C(49)-H(49)	108.7	C(59)-C(60)-C(55)	120.2(8)
C(50)-C(49)-H(49)	108.7	C(59)-C(60)-N(13)	109.4(7)
C(52)-C(49)-H(49)	108.7	C(55)-C(60)-N(13)	130.4(7)
O(14)-C(50)-C(51)	108.6(7)	C(56)-C(61)-H(61A)	109.5
O(14)-C(50)-C(49)	110.6(7)	C(56)-C(61)-H(61B)	109.5
C(51)-C(50)-C(49)	101.2(6)	H(61A)-C(61)-H(61B)	109.5
O(14)-C(50)-H(50)	112.0	C(56)-C(61)-H(61C)	109.5
C(51)-C(50)-H(50)	112.0	H(61A)-C(61)-H(61C)	109.5
C(49)-C(50)-H(50)	112.0	H(61B)-C(61)-H(61C)	109.5
O(13)-C(51)-N(12)	108.9(7)	C(57)-C(62)-H(62A)	109.5
O(13)-C(51)-C(50)	107.4(7)	C(57)-C(62)-H(62B)	109.5
N(12)-C(51)-C(50)	114.4(7)	H(62A)-C(62)-H(62B)	109.5
O(13)-C(51)-H(51)	108.7	C(57)-C(62)-H(62C)	109.5
N(12)-C(51)-H(51)	108.7	H(62A)-C(62)-H(62C)	109.5
C(50)-C(51)-H(51)	108.7	H(62B)-C(62)-H(62C)	109.5
O(13)-C(52)-C(53)	109.4(8)	C(64)-C(63)-C(65)	118.9(8)
O(13)-C(52)-C(49)	107.6(7)	C(64)-C(63)-Co(1)	121.6(6)
C(53)-C(52)-C(49)	115.4(8)	C(65)-C(63)-Co(1)	119.5(5)
O(13)-C(52)-H(52)	108.1	C(63)-C(64)-H(64A)	120.0
C(53)-C(52)-H(52)	108.1	C(63)-C(64)-H(64B)	120.0
C(49)-C(52)-H(52)	108.1	H(64A)-C(64)-H(64B)	120.0
O(15A)-C(53)-O(15B)	130.3(18)	C(66)-C(65)-C(70)	120.0
O(15A)-C(53)-C(52)	108.4(7)	C(66)-C(65)-C(63)	120.9(6)
O(15B)-C(53)-C(52)	108.0(8)	C(70)-C(65)-C(63)	119.1(5)
O(15A)-C(53)-H(53A)	110.0	C(65)-C(66)-C(67)	120.0
C(52)-C(53)-H(53A)	110.0	C(65)-C(66)-H(66)	120.0
O(15A)-C(53)-H(53B)	110.0	C(67)-C(66)-H(66)	120.0
O(15B)-C(53)-H(53B)	87.6	C(68)-C(67)-C(66)	120.0
C(52)-C(53)-H(53B)	110.0	C(68)-C(67)-H(67)	120.0
H(53A)-C(53)-H(53B)	108.4	C(66)-C(67)-H(67)	120.0
O(15B)-C(53)-H(53C)	106.3	C(67)-C(68)-C(69)	120.0
C(52)-C(53)-H(53C)	111.8	C(67)-C(68)-H(68)	120.0
H(53A)-C(53)-H(53C)	83.9	C(69)-C(68)-H(68)	120.0
H(53B)-C(53)-H(53C)	128.5	C(70)-C(69)-C(68)	120.0
O(15A)-C(53)-H(53D)	87.7	C(70)-C(69)-H(69)	120.0
O(15B)-C(53)-H(53D)	108.6	C(68)-C(69)-H(69)	120.0

C(69)-C(70)-C(65)	120.0
C(69)-C(70)-H(70)	120.0
C(65)-C(70)-H(70)	120.0
C(4)-N(1)-C(1)	113.4(6)
C(4)-N(1)-Co(1)	130.0(6)
C(1)-N(1)-Co(1)	116.6(4)
C(9)-N(2)-C(6)	110.8(7)
C(9)-N(2)-Co(1)	121.1(5)
C(6)-N(2)-Co(1)	127.7(6)
C(11)-N(3)-C(14)	109.9(6)
C(11)-N(3)-Co(1)	123.3(5)
C(14)-N(3)-Co(1)	126.7(5)
C(16)-N(4)-C(19)	111.8(6)
C(16)-N(4)-Co(1)	132.6(5)
C(19)-N(4)-Co(1)	114.8(4)
C(23)-N(5)-H(5A)	120.0
C(23)-N(5)-H(5B)	120.0
H(5A)-N(5)-H(5B)	120.0
C(26)-N(6)-H(6A)	120.0
C(26)-N(6)-H(6B)	120.0
H(6A)-N(6)-H(6B)	120.0
C(29)-N(7)-H(7A)	120.0
C(29)-N(7)-H(7B)	120.0
H(7A)-N(7)-H(7B)	120.0
C(33)-N(8)-H(8A)	120.0
C(33)-N(8)-H(8B)	120.0
H(8A)-N(8)-H(8B)	120.0
C(38)-N(9)-H(9A)	120.0
C(38)-N(9)-H(9B)	120.0
H(9A)-N(9)-H(9B)	120.0
C(42)-N(10)-H(10A)	120.0
C(42)-N(10)-H(10B)	120.0
H(10A)-N(10)-H(10B)	120.0
C(45)-N(11)-C(46)	123.2(7)
C(45)-N(11)-H(11)	118.4
C(46)-N(11)-H(11)	118.4
C(54)-N(12)-C(59)	106.4(6)
C(54)-N(12)-C(51)	124.8(7)
C(59)-N(12)-C(51)	127.1(7)
C(54)-N(13)-C(60)	104.4(6)
C(54)-N(13)-Co(1)	120.9(5)
C(60)-N(13)-Co(1)	133.4(5)
C(47)-O(8)-P(1)	121.8(5)
C(49)-O(11)-P(1)	120.5(6)
C(51)-O(13)-C(52)	109.5(6)
C(50)-O(14)-H(14)	109.5
C(53)-O(15A)-H(15A)	109.5
H(53C)-O(15A)-H(15A)	74.9
C(53)-O(15B)-H(15B)	103.1
O(10)-P(1)-O(9)	116.9(4)
O(10)-P(1)-O(8)	106.3(4)
O(9)-P(1)-O(8)	112.9(4)
O(10)-P(1)-O(11)	109.9(4)
O(9)-P(1)-O(11)	109.5(4)
O(8)-P(1)-O(11)	99.9(3)
N(4)-Co(1)-N(1)	82.9(3)
N(4)-Co(1)-N(2)	171.6(3)
N(1)-Co(1)-N(2)	89.4(3)
N(4)-Co(1)-N(3)	90.2(3)
N(1)-Co(1)-N(3)	168.7(3)
N(2)-Co(1)-N(3)	98.0(3)
N(4)-Co(1)-C(63)	89.3(3)
N(1)-Co(1)-C(63)	96.9(3)
N(2)-Co(1)-C(63)	88.5(3)
N(3)-Co(1)-C(63)	91.9(3)
N(4)-Co(1)-N(13)	94.3(3)
N(1)-Co(1)-N(13)	88.8(3)
N(2)-Co(1)-N(13)	88.7(3)
N(3)-Co(1)-N(13)	82.9(3)
C(63)-Co(1)-N(13)	173.6(3)
C(2A)-C(1A)-H(1A)	109.5
C(2A)-C(1A)-H(1B)	109.5
H(1A)-C(1A)-H(1B)	109.5
C(2A)-C(1A)-H(1C)	109.5
H(1A)-C(1A)-H(1C)	109.5
H(1B)-C(1A)-H(1C)	109.5
O(1A)-C(2A)-C(1A)	125(2)
O(1A)-C(2A)-C(3A)	114(2)
C(1A)-C(2A)-C(3A)	121(2)
C(2A)-C(3A)-H(3A)	109.5
C(2A)-C(3A)-H(3B)	109.5
H(3A)-C(3A)-H(3B)	109.5
C(2A)-C(3A)-H(3C)	109.5
H(3A)-C(3A)-H(3C)	109.5
H(3B)-C(3A)-H(3C)	109.5

Table S4. Crystallographic Co–C and Co–N_{dmbzm} bond lengths (Å) in cyanocobalamin and alkylcobalamins

β ligand	**Co–C /Å**	**Co–N_{dmbzm} /Å**	**Ref**
CN (average)	1.87	2.04	1-11
CF_3	1.878	2.047	12
Vinyl	1.912	2.164	13
CHF_2	1.949	2.187	14
cis-Chlorovinyl	1.953	2.144	13
Me	1.979	2.162	11
Adenopropyl	2.001	2.191	15
PhVn	2.008	2.228	This work
Et	2.023	2.232	16
n-Butyl	2.031	2.244	16
Ado	2.033	2.237	17
Isoamyl	2.044	2.277	18

Table S5. Available pK_a values for the deprotonation of dmbzm and its coordination by Co(III) in cobalamins

β ligand	**pK_a**	**Co–N_{dmbzm}**	**Ref**
NO	5.1	2.349(2)	19
PhVn	4.60	2.228(7)	This work
CH_3CH_2	4.16	2.232 (1)	16
$CH_3CH_2CH_2$	4.10		16
Ado	3.7	2.236 (2)	20
CH_3	2.90	2.17 (2)	21
AdoPr	3.31	2.212 (8)	15
CF_3CH_2	2.60		22
CH_2=CH	2.4	2.165 (6)	13
cis-ClCH=CH	2.30	2.144 (5)	13
CF_2H	2.15	2.187 (7)	22
$NCCH_2$	1.81		23
CF_3	1.44	2.05 (1)	22
CN	0.10	2.04 (2)	24
H_2O	-2.13	1.925 (2)	23

References

1. N. Marino, A. E. Rabideau and R. P. Doyle, *Inorg. Chem.*, 2011, **50**, 220-230.
2. F. P. A. Fabbiani, G. Buth, B. Dittrich and H. Sowa, *CrystEngComm*, 2010, **12**, 2541-2550.
3. B. Dittrich, T. Koritsanszky, A. Volkov, S. Mebs and P. Luger, *Angew. Chem., Int. Ed.*, 2007, **46**, 2935.
4. S. Mebs, J. Henn, B. Dittrich, C. Paulmann and P. Luger, *J. Phys. Chem. A* 2009, **113**, 8366–8378.
5. B. Kräutler, R. Konrat, E. Stupperich, G. Färber, K. Gruber and C. Kratky, *Inorg. Chem.*, 1994, **33**, 4128-4139.
6. K. L. Brown, D. R. Evans, J. D. Zubkowski and E. J. Valente, *Inorg. Chem.*, 1996, **35**, 415-423.
7. P. Butler, M. O. Ebert, A. Lyskowski, K. Gruber, C. Kratky and B. Krautler, *Angew. Chem. Int. Ed. Engl.*, 2006, **45**, 989-993.
8. K. L. Brown, S. Cheng, J. D. Zubkowski and E. J. Valente, *Inorg. Chem.*, 1997, **36**, 1772-1781.
9. K. L. Brown, S. Cheng, J. D. Zubkowski and E. J. Valente, *Inorg. Chem.*, 1996, **35**, 3442-3446.
10. K. L. Brown, S. Cheng, X. Zou, J. D. Zubkowski, E. J. Valente, L. Knapton and H. M. Marques, *Inorg. Chem.*, 1997, **36**, 3666-3675.
11. L. Randaccio, M. Furlan, S. Geremia, M. Šlouf, I. Srnova and D. Toffoli, *Inorg. Chem.*, 2000, **39**, 3403-3413.
12. X. Zou and K. L. Brown, *Inorg. Chim. Acta*, 1998, **267**, 305-308.
13. K. M. McCauley, D. A. Pratt, S. R. Wilson, J. Shey, T. J. Burkey and v. d. D. W. A., *J. Am. Chem. Soc.*, 2005, **127**, 1126–1136.
14. T. Wagner, C. E. Afshar, H. L. Carrell and J. P. Glusker, *Inorg. Chem.*, 1999, **38**, 1785-1794.
15. T. G. Pagano, L. G. Marzilli, M. M. Flocco, C. Tsai, H. L. Carrell and J. P. Glusker, *J. Am. Chem. Soc.*, 1991, **113**, 531-542.
16. L. Hannibal, C. A. Smith, J. A. Smith, A. Axhemi, A. Miller, S. Wang, N. E. Brasch and D. W. Jacobsen, *Inorg. Chem.*, 2009, **48**, 6615-6622.
17. L. Z. Ouyang, P. Rulis, W. Y. Ching, G. Nardin and L. Randaccio, *Inorg. Chem.*, 2004, **43**, 1235-1241.
18. C. B. Perry, M. A. Fernandes and H. M. Marques, *Acta Crystallogr. Sec. C*, 2004, m165-m167.
19. H. A. Hassanin, M. F. El-Shahat, S. DeBeer, C. A. Smith and N. E. Brasch, *Dalton Trans.*, 2010, **39**, 10626-10630.
20. C. Mannel-Croise and F. Zelder, *Chem. Commun.*, 2011, **47**, 11249-11251.
21. K. L. Brown and S. Peck-Siler, *Inorg. Chem.*, 1988, **27**, 3548-3555.
22. K. L. Brown, J. M. Hakimi, D. M. Nuss, Y. D. Montejano and D. W. Jacobsen, *Inorg. Chem.*, 1984, **23**, 1463-1471.
23. K. L. Brown, J. M. Hakimi and D. W. Jacobsen, *J. Am. Chem. Soc.*, 1984, **106**, 7894-7899.
24. K. L. Brown and J. M. Hakimi, *Inorg. Chem.*, 1984, **23**, 1756-1764.